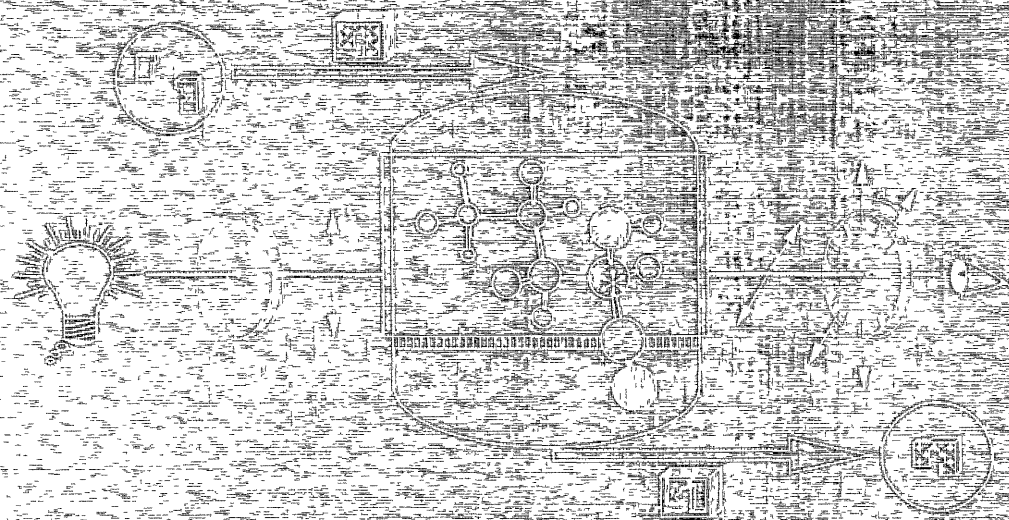# PREPARATION OF
HOMOCHIRAL CYANOHYDRINS
USING AN
ENZYME MEMBRANE REACTOR

BERND BAUER

36

PREPARATION OF HOMOCHIRAL CYANOHYDRINS USING AN ENZYME-MEMBRANE-REACTOR

Acknowledgement

My scientific tutors for this work were:
Prof. Dr.-Ing. H. Strathmann (University of Twente) and
Prof. Dr. Dr. h.c. F. Effenberger (University of Stuttgart)

PREPARATION OF HOMOCHIRAL CYANOHYDRINS
USING AN ENZYME-MEMBRANE-REACTOR

PROEFSCHRIFT

ter verkrijging van
de graad van doctor aan de Universiteit Twente,
op gezag van de rector magnificus,
prof. dr. Th. J. A. Popma,
volgens besluit van het College voor Promoties
in het openbaar te verdedigen
op donderdag 24 oktober 1996 te 13.15 uur.

door

Bernd Uwe Bauer
geboren op 13 september 1958
te Marbach (D)

Dit proefschrift is goedgekeurd door de promotor prof. dr. ing. H. Strathmann en de assistent-promotor dr. ing. M. Wessling.

Preface

Ebenso möchte ich Petra, Sabine, Helga und Peter danken, daß sie mir durch ihre ausgezeichnete Projektarbeit ausreichend Freiräume für diese zusätzliche wissenschaftliche Arbeit schufen. Nur der unermüdliche Einsatz meiner Studenten hat es schließlich ermöglicht, gleichzeitig an so völlig unterschiedlichen Problemen aus der Membran-, Verfahrens- und Biotechnik zu arbeiten. Für ihren Mut und ihre Sorgfalt im Umgang mit Blausäure, sowie für ihren Einsatz auch an Wochenenden danke ich dabei insbesondere Achim, Bernd, Claudia, Ingrid, Martin K., Martin M., Oliver, Rick, Rudi, Siegfried und Silke. Allen zusammen danke ich auch für die schöne Zeit am Fraunhofer.

Mit der vorliegenden Arbeit nimmt eine fast unendliche Geschichte voller Hoffen, Bangen, Streß und Verzicht doch noch ihr Ende. Kraft und Energie durfte ich in dieser Zeit aus meiner Familie schöpfen.

Dabei möchte ich mich besonders bei meiner Frau Irene für Ihre Geduld und unermüdliche Unterstützung in schweren Zeiten mehrfacher Belastung bedanken. Weiterhin danke ich meiner Tochter Britta für die wenigen aber umso schöneren Stunden und die Abwechslung Zuhause.

Zuletzt möchte ich meiner ganzen Familie, insbesondere meinen Eltern für das Vertrauen und Verständnis sowie für die Unterstützung in jeder Phase meiner Ausbildung danken.

Thanks to all of you,

CONTENTS

Chapter

1

GENERAL INTRODUCTION

Synopsis

For many chiral compounds such as pharmaceuticals, drugs, insecticides or pesticides there is an increasing need to produce them in enantiomerically pure form. According to a new recommendation of the 'Food and Drug Administration, USA' a stereochemical identity test will be necessary for the use of racemic pharmacons. Typically, only one enantiomer of a racemic mixture is responsible for the desired effect. Moreover, the other enantiomer has shown in several cases to produce severe toxic effects.

It is expected that 80 % of all chiral compounds will be produced as optically pure substances before the year 2000. Today, the enantiomerically pure agents are predominantly natural products or derivatives thereof. Following from this, an interesting market place is expected for novel methods of asymmetric synthesis or resolution of racemates.

As an example, homochiral cyanohydrins, as an important intermediate for different industries, might be produced through enzymatic stereoselective addition of hydrocyanic acid to carbonyl compounds.

1.1. Introduction

For decades, racemic substances, found in medicines, food additives and pesticides, have been brought onto the market in large quantities without any particular significance being given to their enantiomeric purity. According to a new recommendation by the "Food and Drug Administration" [1], this practice will change in future and a 'stereochemical identity test' will be necessary for the use of racemic and enantiomer-enriched agents in medicines [2]. It is anticipated that this regulation will be extended to other synthetic agents with which human beings come into contact [3]. As for newly approved agents, racemates are only taken account of in exceptional cases where the inactive enantiomer is no longer tolerated as an impurity.

In 1983, approximately 11% of the new chiral pharmaceuticals were brought onto the market as optically pure or enriched compounds. This number increased to 26% between 1983 and 1987 and it is expected that 80% of all chiral agents will be produced as optically pure substances before the year 2000 [4,5]. As summarized in *table 1.1*, in 1992 about 1500 medicines were authorized at the Institute for Medicine at the Federal Ministry for Health, USA. Only about 220 drugs were not on the market. This is also a result of the fact that many agents are now being newly authorized in their enantiomer-pure form.

	Pharmaceutics	Agrochemicals
Total number of compounds	> 1500	~ 700
Optically active compounds	> 600	~ 150
Optically pure compounds	~ 20	~ 60

Table 1.1   *Annual registered homochiral compounds in the pharmaceutical and agrochemical industry [4]*

The recognition of differences in medical effect of the enantiomeric forms will have dramatic consequences for development and future production. A well-known example is thalidomide as shown in *figure 1.1*. While the (R)-enantiomer of thalidomide has a pain-relieving effect and is sold as a somnifacient, the (S)- enantiomer causes serious deformities in unborn children and damages the nervous system of adults. Further examples such as asparagine, limonene, carvone, ethambutole and paclobutrazole are shown in figure 1.1.
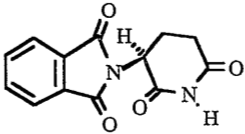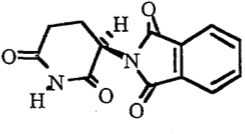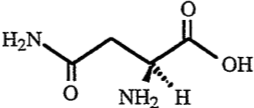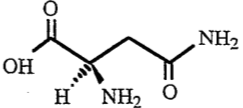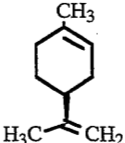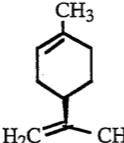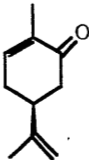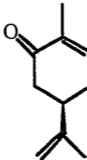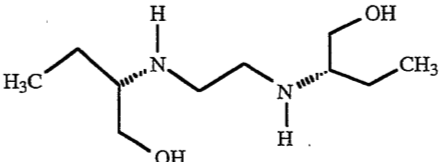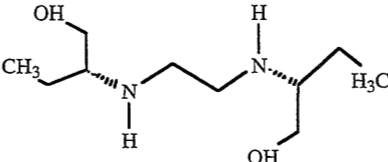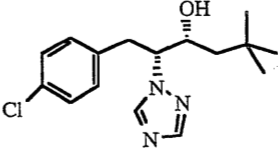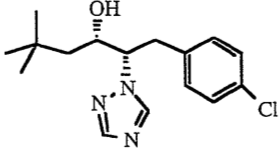
(S)-thalidomide: teratogene	(R)-thalidomide: inactive
(S)-asparagine: bitter	(R)-asparagine: sweet
limonene: lemon taste	limonene: orange taste
(S)-carvone: caraway	(R)-carvone: mint
(S,S)-ethambutole: tuberculostatic	(R,R)-ethambutole: blindness
(2R,3R)-paclobutrazole: fungicide	(2S,3S)-paclobutrazole: plant growth

Figure 1.1 *Industrially important optically active compounds*

1.2. Industrially important chiral compounds

When industrial methods for the production of optically active compounds are considered, the process always refers to the provision of several kilograms of a compound with an optical purity of more than 80 % ee. The enantiomeric excess ee defines the optical purity of a chiral compound or of an enantiomer-enriched compound is given by:

$$\% \ ee \ = \ \frac{[R] - [S]}{[R] + [S]} \cdot 100 \ \% \qquad (1)$$

Here, [R] and [S] are the concentrations of both enantiomers. Chromatographic methods have difficulties to produce the large amounts required on an industrial base. A potential user of chiral compounds has three alternatives to acquire the compound, either by

A)   Purchase of chiral starting compounds from the 'chiral pool'

B)   Separation of racemates
    a)   crystallization of diastereomeric compounds
    b)   direct crystallization
    c)   kinetic resolution of racemates

C)   Asymmetric synthesis based on prochiral compounds
    a)   chemical asymmetric synthesis
    b)   enzymatic asymmetric synthesis

sorbitole	1,87 US-$·kg⁻¹	Ca-pantothenate	17,60 US-$·kg⁻¹
sodiumglutamate	2,20 US-$·kg⁻¹	(-)-carvone	25,30 US-$·kg⁻¹
(+)-limonene	3,30 US-$·kg⁻¹	norephedrine	26,40 US-$·kg⁻¹
L-lysine	3,52 US-$·kg⁻¹	L-threonine	55,00 US-$·kg⁻¹
mannitol	8,25 US-$·kg⁻¹	ephedrine	68,20 US-$·kg⁻¹
ascorbic acid	14,30 US-$·kg⁻¹	L-tryptophan	74,87 US-$·kg⁻¹

Table 1.2   *Homochiral compounds from the chiral pool [6]*

For the 'chiral pool' easily available inexpensive and mostly natural compounds, which can be produced in quantities between 100 tons and 100 ktons annually, are selected. Typical representatives of the chiral pool are shown in *table 1.2*. The α-hydroxycarboxylic acids,

which have usually been produced by fermentation until now, also play an important part in the 'chiral pool'. As an alternative, they may be produced via hydrolysis of homochiral cyanohydrins. The enzymatic synthesis of the homochiral (R)-2-hydroxypentanenitrile will be described in this work.

Various models for the separation of racemates are available. The conventional and most frequently applied industrial process is the crystallization of diastereomer additive compounds. This will always be applied when an 'in-situ' racemization is possible. Racemate resolution by direct crystallization, which in fact must be favored, is only possible when the compounds form an aggregate of crystals with different enantiomers during nucleus formation. For example, this process is applied in (-)-menthol production or in the production of methyldopa where crystallization is induced by the nuclei of optically pure crystals.

Kinetic racemate resolution is based on the property that an enantiomer (R) of a racemate (R/S) can be converted more quickly to a new product. In practical applications, an enantiomer ratio of $E \geq 20$ is required in order to arrive at an optical yield of ee = 98 % with a conversion of $\xi = 60$ %.

$$R \; \underset{k_B}{\overset{k_A}{\rightleftharpoons}} \; A \qquad S \; \underset{}{\overset{}{\rightleftharpoons}} \; B \qquad E = \frac{k_A}{k_B} = \frac{\ln\left(1\text{-}c \; (1\text{+}ee_{(A)})\right)}{\ln\left(1\text{-}c \; (1\text{-}ee_{(B)})\right)}$$

The first substantial work on the kinetic resolution of racemates by means of a stoichiometric, titaniumtartrate-catalyzed chemical epoxidation of allyl alcohols was carried out by Sharpless in 1980 [7,8]. However, more significance can be given to the enzymatic processes on the subject the fundamental work of which was conducted by Whitesides [9] in particular. Based on the prochiral compounds, the chiral center can also be introduced by asymmetric synthesis. In particular, asymmetric reduction, hydroformylation, cycloaddition and phase-transfer-catalysis are the most important chemical methods. Asymmetric synthesis has its industrial origin in the so-called Monsanto process [6] for the production of (L)-dopa by means of a soluble Wilkinson catalyst modified with phosphine ligands. Today, for example, the process is applied in the synthesis of (S)-phenylalanine and in the synthesis of benazaprile on a scale of several hundred kg. Asymmetric biotechnological and particularly enzymatic synthesis contributes to the preparation of homochiral compounds to an ever-increasing extent.

1.3. Chiral compounds from biotechnological processes

Even today, biotechnological processes are still classified as 'new technologies' and industrial application of these processes is accordingly slow. However, considering the market for biologically produced high value products, this classification becomes doubtful. It is obvious that various technical economical processes can be found in the industrial sector. In 1992 more than US-$ 1 thousand million was earned with genetically engineered erythropoetin produced by biotechnological processes after the company Eli-Lilly (USA) was allowed to bring human insulin produced by *Escherichia Coli* onto the market 10 years ago [6]. Since 1992, the Nitto Chemicals Corp. (Japan) has been producing 20 000 tons of acrylamide annually by adding water to acrylnitrile in a bioreactor while applying immobilised *Pseudomonas chloraphis B23* cells [5]. A substrate concentration of 650 g·l^{-1} and a conversion rate < 99% demonstrate excellent space-time yields, resulting in a price of 2,40 US-$·kg^{-1}. In this respect, further 38 industrial production processes with immobilised biocatalysts at a market value of US-$ 900 millions were developed in Japan. In Germany, the most important biotechnical processes using immobilised enzymes include the production of:

- 6-aminopenicillanic acid,
- 7-aminocephalosporine acid,
- palatinose,
- ß-cyclodextrine,
- non-proteinogeneous amino acids,
- as well as L-tryptophan.

As an example, (L)-lysine is an essential amino acid which can affect the nutritional value of certain foodstuffs and fodder due to its limited availability. Nutritional value is doubled by adding just two grams of (L)-lysine to 1000 kg of wheat. (L)-lysine is used today as an additive in fodder for poultry and pigs. It is either produced from sugar by fermentation or from enantiomeric pure (L)-α-amino-ε-caprolactam. In the same way, other enzymatic processes are being or will be installed in industry with the objective of producing chiral molecules. Enzymatic oxidation is applied commmercially for the production of various 1.2 epoxide alkanes and to produce e.g. (S)-naproxen or aryloxypropionate herbicides. Furthermore, the addition of ammonia as well as reductive amination is applied in the production of (L)-amino acids. As early as 1987, 4000 to·year^{-1} of pharmaceutical (L)-aspartic acid with immobilised aspartase having a half-life of 3 years was produced.

1.4.   Scope of work

The objective of this work is the development, reaction engineering characterisation, optimisation and evaluation of a universal process for the industrial production of optically active (R)- and (S)-cyanohydrins [10]. Under the aspect of modern process-integrated environmental protection, the process to be selected should produce a minimum of by-products with maximum energy efficiency and complete recycling of non-converted substrates. From this viewpoint, all methods of racemate resolution would seem difficult to be accepted ad hoc. The disadvantage of the above-mentioned processes for asymmetric synthesis by applying chiral catalysts is that catalyst preparation is very expensive, a recycling of the equimolar catalysts used is usually impossible and the reaction conditions can usually be considered as energy-intensive [11].
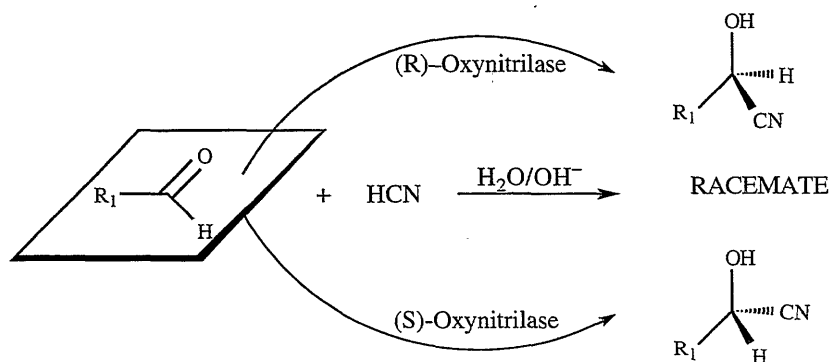
Figure 1.2 *Preparation of homochiral cyanohydrins using (R)- and (S)-oxynitrilase catalyzed addtion of HCN to carbonyl compounds*

It appears that only oxynitrilase-catalysed addition of hydrocyanic acid to carbonyl compounds, as shown in *figure 1.2* can solve the above mentioned problems and can fulfill the required aspects of environmentally benign processing. In aqueous media, the stereoselective enzymatic reaction competes with the non-specific addition of hydrocyanic acid to aldehydes resulting in a racemic mixture of cyanohydrins. This side-reaction can be suppressed in organic media according to the previous work of Effenberger et.al. [12, 13]. As the price per unit of the (R)- and, in particular the (S)-oxynitrilases is very high, an economical process for the production of optically active cyanohydrin can only then be developed when the obtainable cycle number or residence time is sufficiently high [14]. This implies that cyanohydrins should be produced in a continuous process with immobilised enzymes or in an enzyme-membrane reactor. As all cyanohydrins of technical interest have

only little water solubility, the conversion in organic solvents has been chosen as a general problem.

Problems arise (a) concerning the reproducible immobilisation of the oxynitrilases for application in organic media, (b) concerning the choice of a solvent which is also suitable for product treatment, and (c) concerning the development of a process for the racemisation-free separation of products from the reaction mixture. Furthermore, experiments by Jorns [15] showed that all oxynitrilase-catalysed reactions are greatly product-inhibiting. Traditionally, one would solve this by chosing a tubular reactor [16]. In this thesis however, the problem of product-inhibition will be solved by a new process [17]: through continuous product separation by means of a solution-diffusion membrane as shown in *figure 1.3.*, a universal 'process and equipment for enzymatic synthesis' is developed. The applied membrane separation processes are: pervaporation, dialysis and pertraction using tailor-made functional membranes.
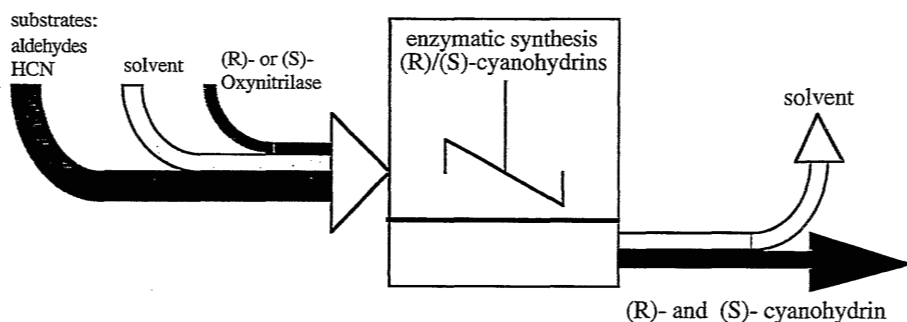
Figure 1.3 *Scope of the thesis: continuous separation of cyanohydrins from an enzyme-membrane reactor using functional membranes [17]*

The concept was proven by enzymatic reaction carried out with two different substrates, two different enzymes and two different methods of product recovery. Fundamentally, there was a distinction made between volatile stable and non-volatile racemating products. Furthermore, the chosen approach distincts enzymes, the kinetic of which suggests a conversion in the stirring-tank reactor, and enzymes, the kinetic of which suggests a conversion in the tubular reactor. Thus, the following systems for the production of homochiral cyanohydrin were selected:

1)   The synthesis of (R)-2-hydroxypentane-nitril describes the (R)-oxynitrilase catalyzed addition of hydrocyanic acid on butanal in the stirring-tank reactor. The product, (R)-butanalcyanohydrin can be evaporated without decomposition and without formation of a

racemate. The product recovery, therefore, occurs via a selective separation of cyanohydrin by means of pervaporation.

2)   The synthesis of (S)-2-hydroxy-2-(3-phenoxyphenyl) acetonitril describes the (S)-oxynitrilase catalyzed addition of hydrocyanic acid on meta-phenoxybenzaldehyde (mpba) in a tubular reactor with laminar flow. The product, (S)-phenoxybenzaldehyde-cyanohydrin (mpbac), cannot be evaporated and forms a racemate upon heating. In this case, the product recovery occurs by means of pertraction.

1.5.   Outline of this thesis

The goal of the thesis is to develop a method for continuous production of homochiral cyanohydrins. Therefore, in chapters 1 and 2, the state-of-the-art in the production of homochiral compounds and especially optically active cyanohydrins is summarized. In order to establish a continuous production process, the following topics have to be clarified:

a)   derivation of the enzyme kinetics

b)   characterization of the enzymes as well as the enzymatic reaction

c)   development of a functional membrane for downstream processing of the products

d)   design of an enzyme-membrane-reactor with integrated product recovery

In chapters 3 and 4 of this thesis, the enzymatic reaction in organic media is described in detail. Investigations on the enzyme-stability, on immobilization procedures and on the influence of the water content on kinetics will be reported.

In chapters 5 and 6, the continuous production of homochiral cyanohydrins with integrated downstream processing using functional solution-diffusion membranes will be described. Both, the development of a pervaporation membrane as well as the design and analysis of the membrane reactor is summarized.

Finally, in chapter 7 an alternative methodology for the production of homochiral compounds using chiral membranes is shown.

List of Symbols

A	species A or compound A
B	species B or compound B
[R]	concentration of (R)-enantiomer [mole·l^{-1}]
[S]	concentration of (S)-enantiomer [mole·l^{-1}]
k_f	forward reaction rate constant [(mol·L^{-3})$^{1-n}$·t^{-1}]
k_r	reverse reaction rate constant [(mol·L^{-3})$^{1-n}$·t^{-1}]
n	order of the reaction
% ee	optical purity; enantiomeric excess [%]
E	enantiomer ratio, dimensionless
ξ	degree of conversion, turnover [%]

References

(1)   FDA, Department of Health and Human Services of the USA
        FDA's Policy Statement for the Development of New Stereoismeric Drugs
        Federal Register, 02. Mai 1992, 57 (22102)

(2)   FDA, Department of Health and Human Services of the USA
        Food and Drug Administration's Statement of Policy: Foods Derived from New Plant Varieties
        Federal Register, 29. Mai 1992, 57 (22984)

(3)   Kessler, D.A.; Taylor, M.R.; Maryanski, J.H.; Flamm, E.L.; Kahl, L.S. (FDA)
        The safety of foods developed by biotechnology
        Science 256, 1747-1832, 26.06.1992

(4)   Stinson, Stephen C.
        Chiral Drugs
        Chem. Eng. News, Sept. 28, 46-79 [1992]

(5)   Stinson, Stephen C.
        Chiral Drugs
        Chem. Eng. News, Oct. 09, 44-74 [1995]

(6)   A.N. Collins, G.N. Sheldrake, J. Crosby
        Chirality in Industry
        John Wiley & Sons, Chichester 1992

(7)   Katsuki, T.; Sharpless, K.B.
        A practical method for asymmetric epoxidation
        J. Am Chem. Soc. 102, 5974 [1980]

(8)   Sharpless, K.B.; Woodard, S.S.
        A practical method for asymmetric epoxidation
        Pure & Appl. Chem. 55, 1823 [1983]

(9)   Whitesides, G.M.; Wong, C.-H.
        Enzyme in der organischen Synthese
        Angewandte Chemie 97, 617-638 [1985]

(10)   Brussee, J.
        Chiral Cyanohydrins - Versatile Building Blocks in Organic Synthesis
        Dissertation, University of Leiden (NL), 1992

(11)   Wandrey, C.
        Fine Chemicals
        Med. Fac. Landbouww. Rijksuniv. Gent 53(4), 1591-1608 [1988]

(12)   Effenberger, F.; Ziegler, T.; Förster, S.
        DEGUSSA AG
        Verfahren zur Herstellung von optisch aktiven Cyanhydrinen
        DE 3 701 383 (28.07.1988)

(13)   Effenberger, F.; Ziegler, T.; Förster, S.
        Enzymkatalysierte Cyanhydrin-Synthese in organischen Lösungsmitteln
        Angew. Chem. 99(5), 491-492 [1987]

(14)   Matson, S.L.; Quinn, J.A.
        Membrane reactors in bioprocessing
        Ann. N.Y. Acad. Sci. 469, 152-165 [1986]

(15)   Schuman-Jorns, M.
        Studies on the kinetics of cyanohydrin synthesis and cleavage by the flavoenzyme oxynitrilase
        Biochim. Biophys. Acta 613, 203-209 [1980]

(16)   Heath, C.A.; Belfort, G.
        Synthetic Membranes in Biotechnology: Realities and Possibilities
        Adv. Biochem. Eng. Biotech., Springer-Verlag Berlin, Vol 47, 45-88 [1992]

(17)   Bauer, B.; Strathmann, H.; Effenberger, F.
        Fraunhofer-Gesellschaft
        Verfahren und Vorrichtung zur enzymatischen Synthese
        DE 40 41 896 C1 (27.12.1990)

(I) CHAPTER *1*

Chapter

2

CHIRAL CYANOHYDRINS

Synopsis

Optically active cyanohydrins are versatile starting materials for the production of a large number of interesting chiral compounds including pharmaceuticals and insecticides. They can be transformed without any racemization by acid-catalyzed hydrolysis into α-hydroxy acids and by hydrogenation with lithium-aluminiumhydride into 1.2-amino alcohols. By the addition of Grignard reagents to the O-protected cyanohydrins and follow-up hydrogenation, 1,2-amino alcohols are gained with very high diastereoselectivity. By O-sulfonylation of (R)- and (S)-cyanohydrins optically active α-sulfonyloxynitriles are obtained. These nitriles react with various nucleophiles by complete inversion of configuration to form various α-substituted carboxylic acid derivatives, α-azido nitriles, α-amino nitriles, α-amino acids etc.

There is little experience in industry in the production of chiral cyanohydrins. Nevertheless, both the resolution of racemates as well as asymmetric synthesis are applied in the production of pharmacons and pyrethroids. Resolution techniques include the separation of diastereomers and kinetic resolution with enzymes or with microorganisms. Enantioselective hydrolysis of cyanohydrin esters, transesterification and transesterification using enol esters catalyzed with lipases have been described in literature. Asymmetric synthesis of cyanohydrins is done by using chiral chemical and enzymatic catalysts. The oxynitrilase catalyzed addition of hydrocyanic acid to carbonyl compounds seems to be the most interesting and environmentally benign processing.

2.1.   Introduction

Cyanohydrins in particular are of great industrial interest as they contain various reaction centres for further racemate-free conversion and they open up various routes to a large variety of chiral compounds. As shown in *figure 2.1*, reaction can procede via the nitrile or the hydroxyl group.

Conversions on the nitrile group may be

- Acid-catalyzed hydrolysis to α-hydroxy carboxylic acids

- Hydrogenation with LiAlH$_4$ to 1.2-amino alcohols

- Addition of a Grignard compound R^1-MgCl to the cyanohydrin protected by Me$_3$SiCl and hydrogenation with NaBH$_4$ to erythro (1R,2S) amino alcohol

    Example: (R)-(-)-noradrenaline, (R)-(-)-adrenaline, (1R,2S)-(-)-ephedrine

Activation and substitution in the hydroxyl group may be

- Conversion with sulfonyl chloride to the activated cyanohydrin

- Inversion of the activated cyanohydrin with potassium acetate to acetylated cyanohydrin

- Inversion with potassium azide in DMF to α-acido nitrile, which can be hydrogenated catalytically by H$_2$/Pd/C to α-amino nitrile and can be converted to α-amino carboxylic acid by hydrolysis.

It is remarkable that both chemical, but also biotechnological processes for the synthesis of cyanohydrin derivatives exist. For example, (1R,2S)-(-)-ephedrine can also be produced by yeast based on a stereo-specific condensation of benzaldehyde with acetaldehyde [1]. Optically active 3-phenoxybenzaldehydecyanohydrin, as a chiral pool in the synthesis of the insecticide Fluvalinat®, is produced by the asymmetric addition of hydrocyanic acid with a cyclic dipeptide cyclo-[D-Phe-D-His] as an inductor [2].
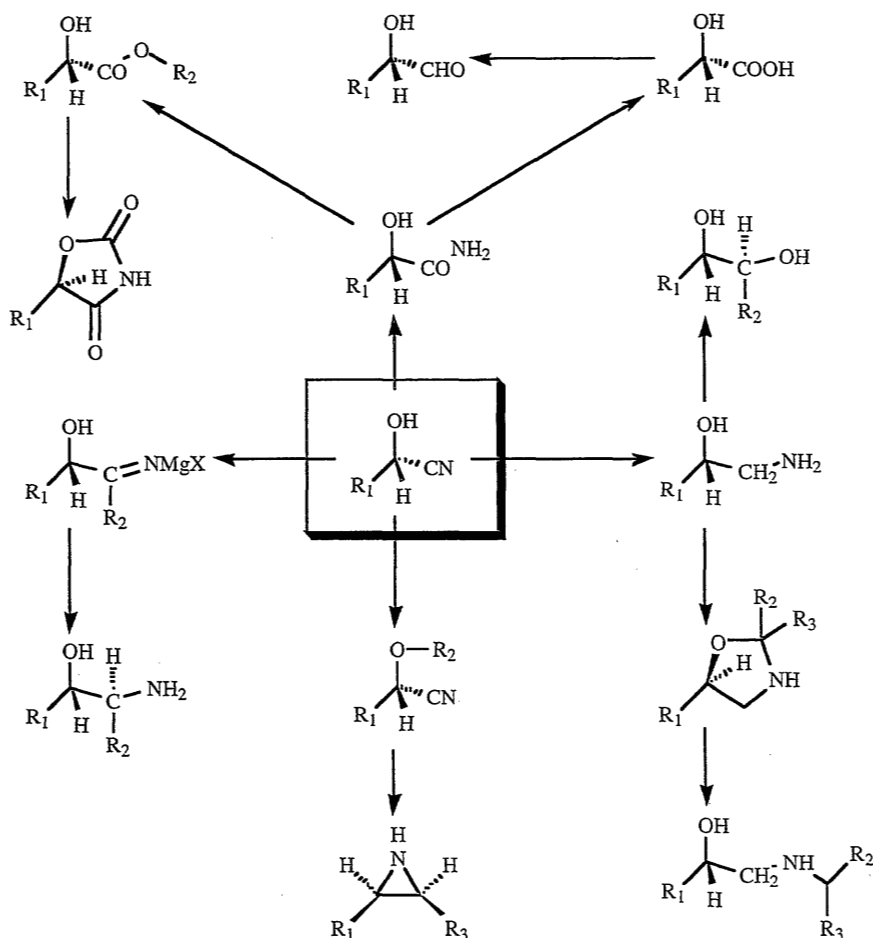
Figure 2.1 *Classes of compounds which can be prepared from cyanohydrins*

2.2. Industrially important cyanohydrins

Cyanohydrins and their homochiral derivatives are widely used in both fine chemicals and agrochemicals. In case of agrochemicals, such as herbicides and insecticides, typically enantiomer-enriched mixtures of both enantiomers are used on an industrial scale. Ultrapure enantiomers are not of interest due to the high production costs. Different from this, in the pharmaceutical industry the cyanohydrins have to be optically pure. In *figure 2.2*, an overview on the most important products based on homochiral cyanohydrins is presented.

OH CH₃ NH CH₃ (structure)	(1R,2S)-(-)- ephedrine; α-sympathomimetic, CNS stimulant (Ephetonin®)
OH COOH (structure)	(R)-α-hydroxyphenylbutyric acid; chiral pool for ACE inhibitors, (Captopril®)
HO OH NH₂ (structure)	noradrenaline; α- and β₂-sympathomimetic (Suprarenin®, Novadral®)
CO–CH₂–CH₃ N CH₃ CH₃ (structure)	propoxyphene; opiate, narcotic effect (Darvon-N®)
OH CH₃ NH CH₃ (structure)	(S)-propanolol; β-adrenoreceptor blocker, (Cardinol®, Bedranol®)
HO OH NH (structure)	(R)-salbutamol; β-adrenoreceptor, for bronchial asthma (Sultanol®)
O NH₂ N O (structure)	pemoline; stimulant for the central nervous system (CNS)
OH HOOC C––H NH₂ (structure)	(R)-GABOB; (R)-γ-amino-β-hydroxybutanoic acid, anti-epilepticum

Figure 2.2 *Important pharmaceuticals prepared from homochiral cyanohydrins*

An industrial enantiomer-pure agent, with an annual production of roughly 1000 tons, is the non-steroidal anti-inflammatory drug (NSAID) (S)-naproxen, an α-arylpropionic acid with a global market of approximately US-$ 650 million [3]. After the European patent expired in 1988, many generica were developed which could since 1993 be produced and sold as so-called O.T.C. (over the counter) products when the US patent also expired. At present (S)-naproxen is produced at a bulk price of US-$ 170 per kg. Not only asymmetric synthesis but also the chromatographic separation of the N,N-bishexylamide derivative are of technical importance. In the same way kinetic racemate resolution with *Bacillus subtilis Thai 1-8/pNAPT-7* is conducted, beginning with a (R,S)-naproxenester [1]:

(R)-naproxenmethylester   (S)-naproxen
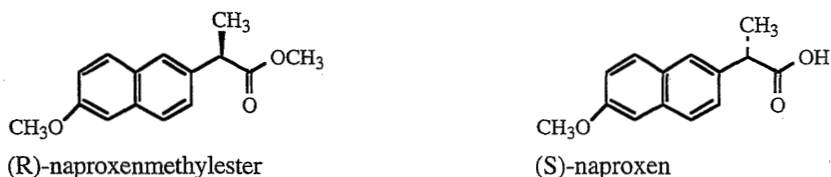
(R)-2-Hydroxy-4-phenylbutyric acid (HPBA) is an important chiral precursor for the production of various angiotensin converting enzymes (ACE) inhibitors with typically (S) 2-amino-4-phenylbutanoic acid groups as biologically important pharmacophores. ACE inhibitors excede, by far, the potential of the antihypertensiva available, such as calcium channel blockers, β-blockers and A2-antagonists. Commercial substances based on (R)-2-HPBA are Cilapril®, Benazepril® and Enalapril®. Various chemical and biotechnological processes are available for the synthesis of (R)-2-HPBA [1].

2.3.   Pyrethroide insecticides

Some of the most effective synthetic insecticides are based on chiral cyanohydrins [4], the most effective and best known of which being deltamethrin. The chemical formula is of deltamethrin is shown in *figure 2.3*.
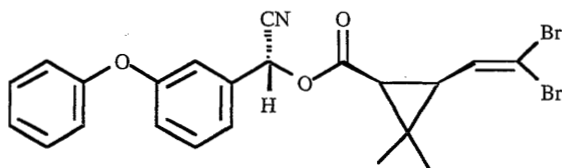
Figure 2.3 *Deltamethrin; best known pyrethroid insecticide; effective against ticks and tested against tsetse flies (Bayticol®)*

The insecticide is synthesized starting from the chiral meta-phenoxy-benzaldehyde cyanohydrin. The enzymatic production of this starting compound will be described in the following chapters as well as a brief overview on the history and competitive production processes [2,4].

The first technically produced synthetic pyrethroide was allethrin which, with its alcohol rethrolon, was very similar to a natural product, allethrolon. The effectiveness of the synthetic pyrethroides depends on the isomeric composition of the product. Both the pyrethrin and the alcohol contain chiral centres resulting in $2^5=32$ isomers. However, only the 1R-,3R- and 4S-isomers have excellent activity. Due to this tests were firstly conducted to convert the enantiomerically pure (1R,trans)-chrysanthemum monocarboxylic acid with the racemic alcohol components. Racemate resolution by crystallisation is applied successfully using a D-(-)-threo-amine and resulting in a 50% mixture of isomers. However, even this product could not overcome the disadvantages of the natural extract, namely instability and environmental effects. Further improvement was obtained by substituting the vinyl gem-dimethyl groups with bromine.

Photostable pyrethroides [5] were finally developed by substituting the alcohol with racemic 3-phenoxybenzaldehyde cyanohydrin, which is sold today either under the name of cypermethrin or deltamethrin, after further concentration by crystallisation. In large-scale technical processes, the acid is produced from (1R,cis)-caronaldehyde by condensation with bromoform and elimination of hydrogen bromide. The racemic cyanohydrin is produced by the Ullmann reaction to phenoxybenzaldehyde followed by the addition of hydrogen cyanide. A subsequent product separation by crystallisation is not practicable on a technical scale so that for the large-scale industrial production of deltamethrin the product cost would be determined by the supply of an optically pure 3-phenoxybenzaldehyde cyanohydrin.

A successful way to racemate resolution was developed by treating the (R,S)-cyanohydrin with (1R,cis)-caronaldehyde to the diastereomeric ketone acetals which can be easily separated by fractionated crystallisation. The (S)-cyanohydrin required is obtained by means of hydrolysis of the appropriate diastereomers [5]. Large-scale industrial production of deltamethrin requires a further process which makes the racemate resolution of the cyanohydrin no longer necessary [6].

For this purpose, a solvent system, in which the desired (1R, αS)-diastereomer of the deltamethrin is poorly soluble, was selected for the last esterification reaction as shown in *figure 2.4*. By adding a weak base an inversion of both the dissolved diastereomers through

an epimerisation at the α-C atom is possible but hydrolysis of the cyano and ester functionalities must be avoided.
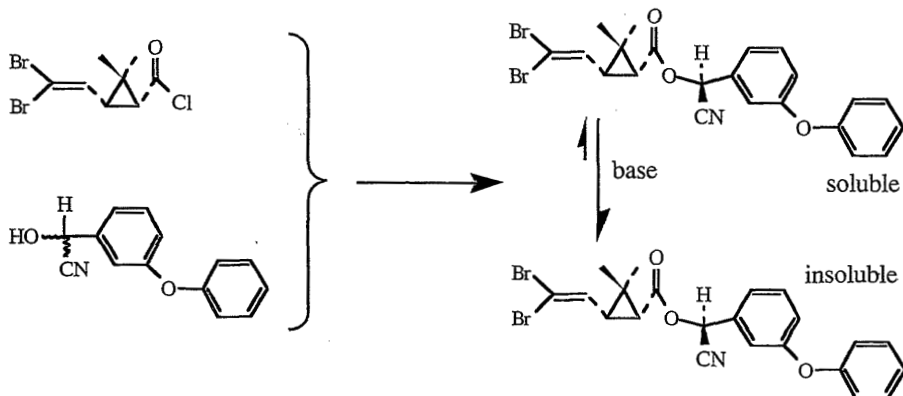
Figure 2.4 *Preparation of (1R, αS)-deltamethrin via esterification and separation through enantioselective crystallization*

During the reaction, pure (αS)-deltamethrin is crystallised out of the solution leading to a lack of this diastereomer in the liquid phase, through which a net conversion of (αR)-diastereomer to (αS)-diastereomer in the solution occurs in order to restore equilibrium. The crystallisation of the desired (αS)-stereoisomer is the driving force for the conversion of (αR) to (αS), which is limited solely by the solubility of the (αS)-diastereomer in the reaction medium. In fact, even in large-scale industrial processes this conversion is almost quantitative.

2.4.   State of the art in cyanohydrin synthesis

The addition of hydrogen cyanide to carbonyl compounds to produce cyanohydrins complies with a specific base catalysis by cyanide ions [7]. Good yields can be obtained by a high concentration of undissociated hydrogen cyanide. High reaction rates can be obtained by a high concentration of cyanide ions. In general, the reaction equilibria are on the product side and donor substituents favour the carbonyl compound rather than the cyanohydrin.

As shown in *figure 2.5*, the nucleophilic addition as rate-determining step, is proportional to the concentration of cyanide ions and therefore dependent on the pH-value due to the

dissociation equilibrium. Relevant production processes are described in the aqueous, organic, and gaseous phase.

$$HCN \quad + \quad H_2O \quad \underset{}{\overset{fast}{\rightleftharpoons}} \quad CN^- \quad + \quad H_3O^+$$
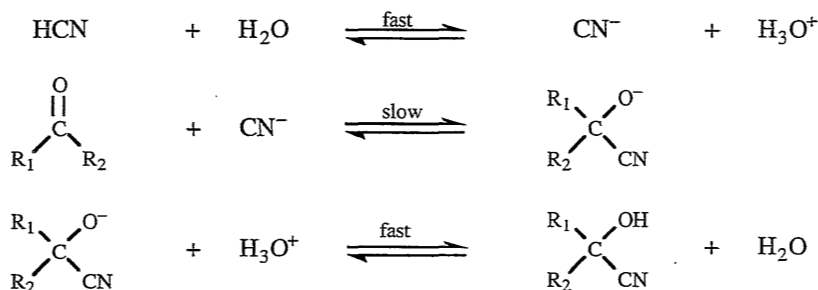
Figure 2.5 *Preparation of cyanohydrin racemates via chemical addition of HCN to carbonyl compounds*

In industry there is little experience in the production of chiral cyanohydrins. Furthermore, also differences exist between the processes for microbial, enzymatic, and chemical racemate resolution and the asymmetric synthesis of cyanohydrins by applying chiral catalysts or enzymes.

2.4.1. Chiral cyanohydrins by means of separation of diastereomers

Elliot [8] describes the separation of the racemic cyanohydrin ethers of 2,4-pentanediol after diastereoselective, ring-opening conversion of aldehydacetale with cyanotrimethylsilane. For analytical purposes, the conversion to chiral norbornyl derivatives and the conversion with chiral MTPA esters according to Mosher [9] are to be discussed.

2.4.2. Chiral cyanohydrins by means of kinetic racemate resolution

Methods of kinetic resolution of racemates, particularly by applying microbial or enzymatic methods mostly based on cyanohydrin esters, have been reported in literature for both the stereoselective forms of esterification and transesterification reactions. In previous publications, most experiments were conducted with the enantioselective hydrolysis [10] of racemic cyanohydrin esters as shown in *figure 2.6*. Ohta [11,12,13] carries out racemate resolutions on various cyanoalkyl acetates using a *Candida Tropicalis* lipase. For 2-hydroxy-

pentanenitrile and 2-hydroxy-2-phenylethanenitrile, Effenberger [14] showed the hydrolytic synthesis of chiral (R)- and (S)-cyanohydrins by the specific application of different lipases of *Candida cylindracea* and *Pseudomonas fluorescens* [15,16,17].
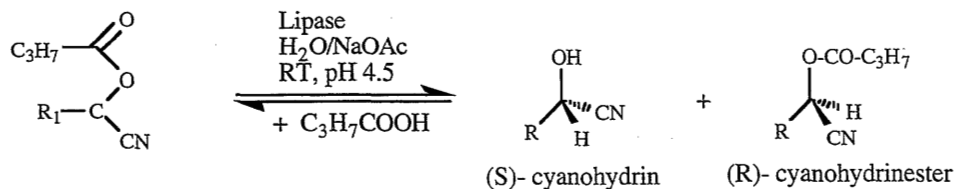
Figure 2.6 *Enzymatic enantioselective hydrolysis of racemic cyanohydrin esters*

Transesterification of cyanohydrin acetates with aliphatic alcohols as shown in *figure 2.7* was described by Bevinakatte [18]. Effenberger [19] tested this reaction with different primary alcohols in various organic solvents. The same selectivities were observed with the above-mentioned lipases.
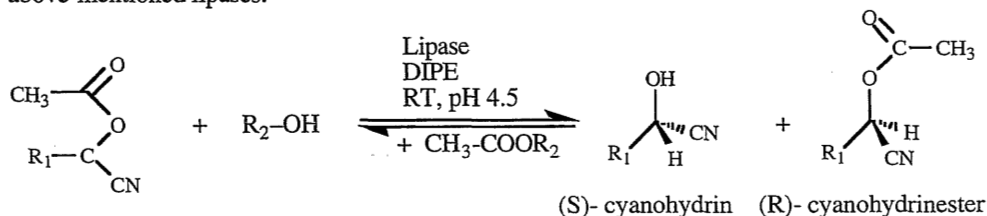
Figure 2.7 *Transesterification of cyanohydrin acetates with aliphatic alcohols*

Irreversible reaction catalyzed by lipases with an enol ester, such as vinyl acetate, is shown in *figure 2.8*. As described by Wong [20,21] this is advantageous because the continuous separation of the evolving acetaldehyde can easily be continued and thus not only a complete shift in equilibrium but also simplified product treatment is achieved.
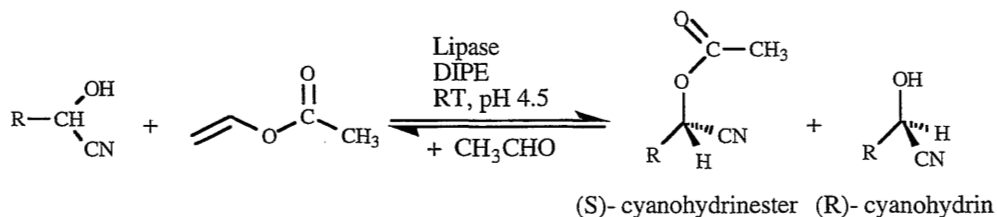
Figure 2.8 *Esterification of cyanohydrins with enol esters such as vinyl acetate*

Effenberger [19] determined the same substrate specifities for all reactions mentioned. Dependent on the substrate the attainable optical yields are frequently very high. The process for kinetic racemate resolution is restricted to the 50% maximum product yield respectively and as a result from this the necessity to racemize the unconverted substrates. As far as technical processes are concerned, further problems with downstream processing occur as, besides the solvent-puffer-enzyme mixture, an equimolar quantity of unconverted substrate must be separated without racemization.

2.4.3. Asymmetric cyanohydrin synthesis by means of chiral catalysts

The application of chiral, base catalysts for the production of optically active cyanohydrins was examined by Bredig [22] in 1912 using the alkaloid quinine. At a later date, other quinine alkaloids, polymers with chiral amino groups such as poly-(S)-isobutylethylenimine were examined. By applying β-cyclodextrin inclusion complexes, a general process could be developed with only moderate optical yields. Finally, better results were obtained with the chiral Lewis acids of various metal complexes with conformation-stable ligands. The most important work, which Inoue [23] began and Danda [24,25] and Jackson [26,27] later elaborated, is based on the use of a chiral, cyclic dipeptide, the cyclo [(S)-phenylalanyl-(S)-histidyl]-dipeptide (syst.: 2 -benzyl -5 (4-imidazole methyl) -3,6-dioxo-piperazine). The process allows a high enantiomeric excess > 90% ee for many substrates, but requires large quantities of catalysts and operates at low temperatures while producing greatly diluted solutions. Therefore, the use of the Inoue catalyst for technical products is very limited. At a temperature of -20°C, the (R)-benzaldehyde cyanohydrin can be synthesized with an enantiomeric excess of 97% at a conversion rate of > 90%. The pyrethroide precursor, the (S)-3-phenoxybenzaldehyde cyanohydrin with an enantiomeric excess of 95%, was produced by Jackson [26] and was patented by Shell Oil [27] for the production of insecticides.
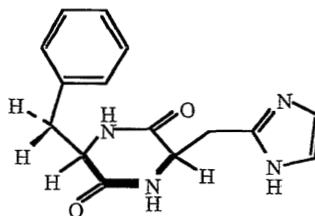
Inoue catalyst: cyclo[(S)-Ala-(S)-His]

Kobayashi [28] showed that enantioselective transcyanidations, based on acetone cyanohydrin, are possible by using these chiral bases. Other chiral Lewis acids such as the (S)-(1,1'-binaphthalene)-2,2'-dioxy titanium dichloride were tested. Through the in-situ conversion of dichlorodiisopropoxy titanium (IV) with (2R,3R)-2,3-O-(1-phenyl-ethylidene)-1,1,1,4-tetraphenyl-1,2,3,4 butantetrol, Narasaka [29] achieved an enantioselective cyanosilylation with Me_3SiCN from aromatic aldehydes with high purity.
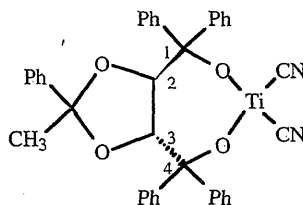
Narasaka catalyst: chiral alkoxytitanium

Other cyanosilylations which require between 20 mole-% and equimolar quantities of the chiral titanium complex have been previously described in publications. Such high quantities can be avoided by conducting the cyanosilylation, according to Elliot [8] with Me_3SiCN by an acetal template of the (2R,4R)-pentanediolacetals in the presence of $TiCl_4$. The non-protected cyanohydrins are obtained after oxidative splitting with pyridinium chlorochromate ($PyH^+ClCrO_3^-$).

2.4.4. Enzyme-catalyzed asymmetric synthesis of cyanohydrins

The only biochemical synthesis known for the production of homochiral cyanohydrins is accomplished through oxynitrilase catalyzed addition of hydrocyanic acid to carbonyl compounds as shown in *figure 2.9* . After Rosenthaler's first observations around 1908 [30], pioneering work was carried out by Becker and Pfeil in 1960 [31,32]. They tested the substrate spectrum of the (R)-oxynitrilase in aqueous media and in 50% ethanol acetate buffer solutions.
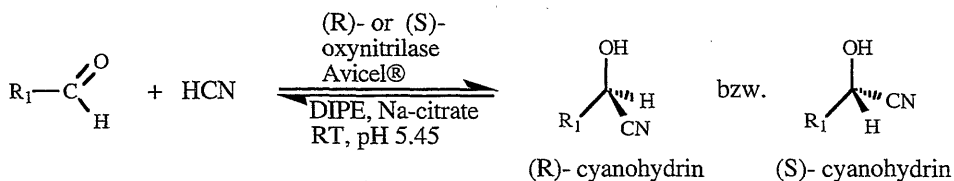
Figure 2.9 *Preparation of cyanohydrins through oxynitrilase-catalyzed addition of hydrogen cyanide to carbonyl compounds*

The substrate specificity of the oxynitrilase was not very high, but then Hörsch [33] could show that on the one hand the (S)-oxynitrilase did not convert any aliphatic substrate and on the other hand, in the organic medium, even the production of aliphatic (R)-ketone cyanohydrin with high optical purity is possible.

After the high synthetic and industrial significance of optically active cyanohydrins was established, particulary in the development of chiral catalysts, enzymatic synthesis was taken up again by various work groups from 1985. As will be described later, the respective patented methods are different from those of Effenberger [34,35], Van der Gen [36,37] and Wandrey [38,39,40] with regard to a maximization of the optical yield, in particular in the choice of the reaction medium. Effenberger suppresses the non-specific spontaneous addition of hydrocyanic acid to the carbonyl compound, for example, by conversion in the organic medium. Wandrey, in contrast, reduces the concentration of cyanide ions by decreasing the pH value. Van der Gen and Brussee work at low temperatures and select an organic-aqueous two-phase system in which the raw extract is inserted in a defatted almond paste. The advantage of this method is the good solubility of the substrate in the organic medium on the one hand and the high stability of the oxynitrilases in the aqueous system on the other hand.

Tert.-butyldimethylsilyl-protected cyanohydrins with a long shelf life as shown in *figure 2.10* are produced by this process and commercialised for the chiral pool :
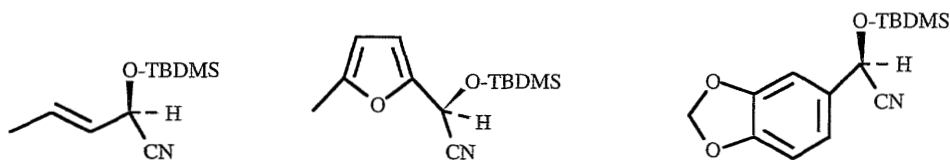
Figure 2.10   *Commercial homochiral cyanohydrins from the chiral pool*

Continuous conversion in an organic media was initiated by Wehtje [41,42]. In contrast to the above-mentioned works, Ognyanov [43] can do without using free hydrocyanic acid or cyanides as in this case acetone cyanohydrin serves as a HCN source as described in *figure 2.11*. In this transcyanidation, catalyzed by oxynitrilase, acetone is generated as a by-product.
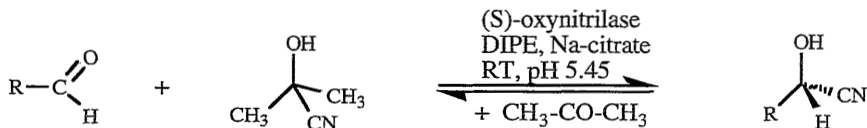
Figure 2.11   *Transesterification of acetone cyanohydrin with aldehydes*

However, the application of the process is restricted to cyanohydrins with small equilibrium constants of formation. Accordingly, the equilibrium conversions or the yields are mostly very small.

2.5. Conclusions

Summarizing this overview on the separation and synthesis of cyanohydrins, it can be concluded that:

• racemate resolution is very important for the production of homochiral cyanohydrins

• racemate resolution is limited to only a few products

• racemate resolution requires further processing of the undesired enantiomer

• asymmetric chemical synthesis can be applied only to a few products and the catalysts are extremely expensive and difficult to recover

• aysmmetric enzymatic synthesis has the potential to produce ultrapure homochiral cyanohydrins

References

(1)   A.N. Collins, G.N. Sheldrake, J. Crosby
        Chirality in industry
        John Wiley & Sons, Chichester 1992

(2)   Naumann, K.
        Synthetic pyrethroid insecticides: chemistry and patents
        Springer-Verlag Berlin Heidelberg 1990

(3)   Stinson, Stephen C.
        Chiral drugs
        Chem. Eng. News, Sept. 28, 46-79 [1992]

(4)   Tombo, G.M.R.; Bellûs, D.
        Chiralität und Pflanzenschutz
        Angew. Chem. 103, 1219-1241 [1991]

(5)   Sanborn, J.R.; Tieman, C.H.
        SHELL OIL COMPANY
        Alpha-aminooxy isovalerate insecticides
        US-Patent 4,537,780 [27.08.1985]

(6)   Hidasi, G.: Székely, I.; Bertók, B.; Zoltan, S.; Nagy, L.; Gajari, A.
        Chinoin Gyogyszer
        Insecticidal composition comprising more than one active ingredient
        PCT/HU86/00004 (16.01.1986)

(7)   March, J.
        Advanced organic chemistry: reactions, mechanisms, and structure
        John Wiley & Sons, New York, 3rd. Ed. 1985

(8)   Elliot, J.D.; Choi, V.M.F.; Johnson, W.S.
        Asymmetric synthesis via acetal templates. 5. Reactions with cyanotrimethylsilane.
        Enantioselective preparation of cyanohydrins and derivatives.
        J. Org. Chem. 48, 2294-2295 [1983]

(9)   Dale, J.A.; Dull, D.L.; Mosher, H.S.
        α-Methoxy-α-trifluoromethylphenylacetic acid, a versatile reagent for the determination of
        enantiomeric composition of alcohols and amines
        J. Organic Chem. 34(9), 2543-2549 [1969]

(10)   Dixon, B.G., Au, A.T.
        Hydrolysis of cyanohydrin esters
        Tetrahedron 42(4), 1123-1126 [1986]

(11)   Ohta, H.; Hiraga, S.; Miyamoto, K.; Tsuchihashi, G.
        Asymmetric hydrolysis of 1-cyanoalkyl acetates
        Agric. Biol. Chem. 52(12), 3023-3027 [1988]

(12)   Ohta, H.; Kimura, Y.; Sugano, Y.
        Kinetic resolution of ketone cyanohydrin acetates with a microbial enzyme
        Tetrahedron Letters 29(52), 6957-6969 [1988]

(13)   Ohta, H.; Kimura, Y.; Sugano, Y., Sugai, Y.
        Enzymatic kinetic resolution of cyanohydrin acetates and its application to the
        synthesis of S-(-)-frontalin
        Tetrahedron 45(17), 5469-5476 [1989]

(14)   Effenberger, F.; Hörsch, B.; Förster, S.; Ziegler, T.
        Enzyme-Catalyzed Synthesis of (S)-Cyanohydrines and Subsequent Hydrolysis to
        (S)-α-Hydroxy-carboxylic Acids
        Tetrahedron Letters 31(9), 1249-1252 [1990]

(15)   Inagaki, M.; Hiratake, J.; Nishioka, T.; Oda, J.
        Lipase-catalyzed kinetic resolution with in situ racemization: one-pot synthesis of optically active
        cyanohydrin acetates from aldehydes
        J. Am. Chem. Soc. 113, 9360-9361 [1991]

(16)   Inagaki, M.; Hatanaka, A.; Mimura, N.; Hiratake, J.; Nishioka, T.; Oda, J.
        One-pot synthesis of optically active cyanohydrins from aldehydes via quinidine-catalyzed
        transhydrocyanation coupled with lipase-catalyzed kinetic resolution in organic solvent
        Bull. Chem. Soc. Jpn. 65, 111-120 [1992]

(17)   Inagaki, M.; Hiratake, J.; Nishioka, T.; Oda, J.
        One-pot synthesis of optically active cyanohydrin acetates from aldehydes via lipase-catalyzed kinetic
        resolution coupled with in situ formation and racemization of cyanohydrins
        J. Org. Chem. 57, 5643-5649 [1992]

(18)   Bevinakatti, H.S.; Banerji, A.A.; Newadkar, R.V.
         Resolution of secondary alcohols using lipase in diisopropyl ether
         J. Org. Chem. 54, 2453-2455 [1989]

(19)   Effenberger, F.; Gutterer, B.; Ziegler, T.; Eckhardt, E.; Aichholz, R.
         Enantioselektive Veresterung racemischer Cyanhydrine und enantioselektive Hydrolyse oder
         Umesterung racemischer Cyanhydrinester mittels Lipasen
         Liebigs Ann. Chem. 47-54 [1991]

(20)   Wang, Y.-F.; Chen, S.-T.; Liu, K.; Wong, C.-H.
         Lipase-catalyzed irreversible transesterification using enol esters: Resolution of cyanohydrins and
         syntheses of ethyl (R)-2-hydroxy-4-phenylbutyrate and (S)-Propanolol
         Tetrahedron Letters 30(15), 1917-1920 [1989]

(21)   Van Almsick, A.; Buddrus, J.; Hönicke-Schmidt, P.; Laumen, K.; Schneider, M.P.
         Enzymatic preparation of optically active cyanohydrin acetates
         J. Chem. Soc., Chem. Commun. 1391-1393 [1989]

(22)   Bredig, G.; Fiske, P.S.
         Durch Katalysatoren bewirkte asymmetrische Synthese
         Biochem. Z. 46,7-23 [1912]

(23)   Asada,S.; Kobayashi, Y.; Inoue, S.
         Asymmetric addition of hydrogen cyanide to aliphatic aldehydes catalyzed by a
         synthetic cyclic peptide, cyclo[(S)-phenylalanyl-(S)-histidyl]
         Makromol. Chem. 186, 1755-1762 [1985]

(24)   Danda, H.; Chino, K.; Murata, T.
         Sumitomo Chemical Company, Ltd.
         Preparing of optically-active cyanohydrins as intermediates for agrochemicals
         JP 63 165 354 (08.07.1988)

(25)   Danda, H.; Nishikawa, H.; Otaka, K.
         Enantioselective autoinduction in the asymmetric hydrocyanation of 3-phenoxybenzaldehyde
         catalyzed by cyclo[(R)-phenylalanyl-(R)-histidyl]
         J. Org. Chem. 56, 6740-6741 [1991]

(26)   Jackson, W.R.; Jayatilake, G.S.; Matthews, B.R.; Wilshire, C.
         Evaluation of some cyclic dipeptides as catalysts for the asymmetric hydrocyanation of aldehydes
         Aust. J. Chem. 41, 203-213 [1988]

(27)   Matthews, B.R.; Jackson, W.R.; Jayatilake, G.S.; Wilshire, C.; Jacobs, H.A.
         Asymmetric hydrocyanation of a range of aromatic and aliphatic aldehydes
         Aust. J. Chem. 41, 1697-1709 [1988]

(28)   Kobayashi, Y.; Hayashi, H.; Miyaji, K.; Inoue, S.
         Asymmetric Transcyanohydrination
         Chem. Lett. 931-934 [1986]

(29)   Narasaka, K.; Yamada, T.; Minamikawa, H.
         The asymmetric hydrocyanation of aldehydes with cyanotrimethylsilane
         promoted by a chiral titanium reagent
         Chem. Lett. 2073-2076 [1987]

(30)   Rosenthaler, L.
         Durch Enzyme bewirkte asymmetrische Synthesen
         Biochemische Zeitschrift 14, 230-253 [1908]

(31)   Becker, W.; Pfeil, E.
         Über das Flavinenzym D-Oxynitrilase
         Biochemische Zeitschrift 346, 301-321 [1966]

(32)   Hustedt, H.-H.; Pfeil, E.
         Zur Kenntnis der Cyanhydrin-Synthese
         Liebigs Ann.Chem. Bd.640, 15-28 [1961]

(33)   Hörsch, B.
         Enzymkatalysierte Synthese von (R)- und (S)-Cyanhydrinen in organischen Lösungsmitteln und
         deren saure Hydrolyse zu optisch aktiven 2-Hydroxycarbonsäuren
         Dissertation, Universität Stuttgart, 1990

(34)   Effenberger, F.; Ziegler, T.; Förster, S.
         DEGUSSA AG
         Verfahren zur Herstellung von optisch aktiven Cyanhydrinen
         US-Patent 4 859 784 (22.08.1989)

(35)   Bauer, B.; Strathmann, H.; Effenberger, F.
         Fraunhofer-Gesellschaft
         Verfahren und Vorrichtung zur enzymatischen Synthese
         DE 40 41 896 C1 (27.12.1990)

(36)   Brussee, J; van der Gen; A.
         Method for preparing optically active cyanohydrin derivatives and their conversion products
         SOLVAY DUPHAR B.V.
         EP 0 322 973 (21.12.1988)

(37)   Brussee, J.
         Chiral Cyanohydrins - Versatile Building Blocks in Organic Synthesis
         Dissertation, University of Leiden (NL), 1992

(38)   Niedermeyer, U.; Kragl, U.; Kula, M.-R.; Wandrey, C.; Makryaleas, K.; Drauz, K.
         KFA Jülich, DEGUSSA AG
         Enzymatisches Verfahren zur Herstellung von optisch aktiven Cyanhydrinen
         EP 0 326 063 (23.01.1989)

(39)   Niedermeyer, U.; Kula, M.-R.
         Enzymkatalysierte Synthese von (S)-Cyanhydrinen
         Angew. Chem. 102(4), 423-425 [1990]

(40)   Niedermeyer, Uwe
         Untersuchungen zur enzymatischen C–C Verknüpfung am Beispiel der chiralen Cyanhydrinbildung
         Dissertation, Universität Düsseldorf, Institut für Enzymtechnologie, 1990

(41)   Wehtje, E.; Adlercreutz, P.; Mattiasson, B.
         Activity and operational stability of immobilized mandelonitrile lyase in methanol/water mixture
         Appl. Microbiol. Biotechnol. 29, 419-425 [1988]

(42)   Wehtje, E.; Adlercreutz, P.; Mattiasson, B.
         Formation of C–C Bonds in Mandelonitrile Lyase in Organic Solvents
         Biotechnology and Bioengineering 36, 39-46 [1990]

(43)   Ognyanov, V.I.; Datcheva, V.K.; Kyler, K.S.
         Preparation of chiral cyanohydrins by an Oxynitrilase-mediated transcyanation
         J. Am. Chem. Soc. 113, 6992-6996 [1991]

Chapter

3

ENZYME KINETICS

Synopsis

A more efficient use of oxynitrilases as biocatalysts for the stereoselective addition of hydrocyanic acid to carbonyl compounds through detailed analysis of enzyme kinetics is made possible. In order to take a choice on the design of an enzyme-membrane reactor, it is necessary to identify the reaction mechanism of the oxynitrilases on a molecular level. It has already been assumed in literature, that the reaction follows an ordered single displacement bisubstrate mechanism. The first step in the condensation reaction is the binding of the aldehyde to the enzyme while release of HCN is the first process in the decomposition reaction. The derivation of mathematical expressions for both ordered and random bisubstrate mechanisms based on the King-Altman formalism is given in the following.

3.1. Introduction

Living cells or enzymes allow a reduction in the heat of activation of a chemical reaction and act accordingly as catalysts, accelerating the reaction in the direction of thermodynamic equilibrium. Hence the specific reaction rate of both the forward reaction and the back reaction is increased to the same proportion [1]. At the end of the 18th century, the first observations were made on this cell-free activity i.e. on enzymatically catalyzed reactions. Around 1830, Robiquet and Boutron [2], as well as Chaland [2] discovered the hydrolysis of amygdalin by bitter almonds. The first specific isolation of an enzyme was carried out by Payen and Persoz [2] in 1833 by means of precipitation of an amylase. However, not until much later, in 1878 was the term 'enzyme' determined by Kühne [2] and finally in 1883 by introducing the ending 'ase' by Duclaux [2] did a nomenclature for enzymes begin. First of all, biochemical engineering of enzymatic processes were based on Henri-Michaelis-Menten (1913) [3] as well as Briggs-Haladane (1925) [3] formalisms for one-substrate reactions. Under the hypothesis of a rapid-equilibrium kinetics, an attempt was made later to describe multi-substrate reactions. By assuming a steady state, Dalziel, Alberty and Hearon [4] were able to deduce better, although awkward relationships. It was only the introduction of a homogeneous and lucid nomenclature by Cleland [5] in 1963 which made possible a description of kinetic mechanisms for multi-substrate reactions under the assumption of a steady state. A kinetic model for allosteric enzymes was estalished by Monod, Wyman and Changeux [6].

3.2. Kinetics of one-substrate reactions

The kinetics of one-substrate reactions is typically described by a relationship which is based on experiments by Henri [6]. Henri determined a reaction rate proportional to substrate concentration by assuming a rapid formation of the enzyme-substrate complex followed by rate-determining resolution of this complex into free enzyme and product.

$$E \;+\; A \;\; \underset{k_{-1}}{\overset{k_1}{\rightleftharpoons}} \;\; EA \;\; \xrightarrow{kp} \;\; E \;+\; P$$

In 1925, these observations were confirmed by Michaelis and Menten [6] in mathematical terms, by which a simple rate equation was developed.

$$\upsilon \; = \; \frac{k_P \cdot [E] \cdot [A]}{K_m + [A]} \qquad (1) \qquad \text{and} \qquad V_{max} = k_P \cdot [E] \qquad (2)$$

In this case, a maximum rate V_{max} was defined by which the so-called Henri-Michaelis-Menten equation [6] can be obtained under the hypothesis of a rapid-equilibrium:

$$\frac{\upsilon}{V_{max}} \; = \; \frac{[A]}{K_m + [A]} \qquad (3) \qquad \text{and} \qquad K_m = \frac{[A] \cdot [E]}{[EA]} \qquad (4)$$

The constant K_m represents the dissociation constant of the enzyme-substrate complex and thus the affinity of the enzyme to the substate. If the rate of product formation is only marginally different from the rate of formation of the enzyme-substrate complex, then rapid equilibrium should not be carried out, but rather a more exact steady-state treatment. This can be achieved in particular by the general rate equation by Briggs and Haldane [3]. In this model, the enzyme-substrate complex is not in equilibrium with the enzyme and the substrate but rather it is assumed that after a short initial phase, the concentration of the enzyme-substrate complex remains unchanged and thus a steady state is obtained. The Briggs and Haldane's model can also be applied to reversible reactions where it represents a complete transfer of the quasi-stationary principle by Bodenstein [2] to enzymatic processes. In this case, the constant K_m represents a dynamic or pseudo-equilibrium constant which represents the relation of the steady-state concentrations to the equilibrium concentrations.

The Henri-Michaelis-Menten relation is therefore an exceptional case of the Briggs-Haldane equation, if the rate of product formation is low compared to the reaction rate constant of the formation of the enzyme-substrate complex. Only when $k_{-1} \gg k_p$, does the K_m represent a dissociation constant of [EA], otherwise, if $k_{-1} \ll k_p$, then K_m is a kinetic constant.

In principle, all processes with enzyme catalysis can be considered as reversible. The rate equations must be extended appropriately.

$$E \; + \; A \; \underset{k_{-1}}{\overset{k_1}{\rightleftharpoons}} \; EA \; \underset{k_{-2}}{\overset{k_2}{\rightleftharpoons}} \; EP \; \underset{k_{-3}}{\overset{k_3}{\rightleftharpoons}} \; E \; + \; P$$
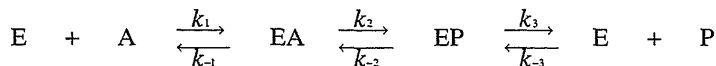
However, in the simplest of cases, only the formation of a central complex, the enzyme-substrate complex ES, is considered.

$$E \; + \; A \; \underset{k_{-1}}{\overset{k_1}{\rightleftharpoons}} \; ES \; \underset{k_{-2}}{\overset{k_2}{\rightleftharpoons}} \; E \; + \; P$$
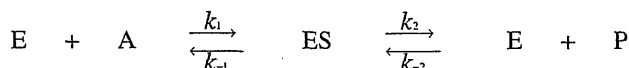
The initial rates for the forward reaction and the reverse reaction result from the relevant Henri-Michealis-Menten equations, by means of which the individual rate constants $k_1...k_{-2}$ can be expressed by [E], V_{max} and K_m. The value of [E] corresponds with the concentration of active centres and, for enzymes with only one active centre per molecule, [E] is equal to the molar concentration of enzymes. However, enzymes with several identical and independent active centres cannot be differentiated from enzymes with only one active centre, as seen from a kinetic viewpoint.

The rate constants $k_2 = V_{max}^+ \cdot [E]^{-1}$ i.e the rate constants for product formation in the forward reaction are also termed 'turnover number' TN or 'molecular activity' k_{cat} and is equal to the maximum rate per 1 mole of enzyme or per 1 mole of active centres if [E] is not expressed as molar enzyme concentration. k_{cat} is equal to the formed mol product per minute and per mol enzyme. The reciprocal value of k_{cat} is equivalent to the time needed to complete a reaction cycle.

definitions:

$$k_{cat} = \frac{V_{max}^+}{[E]} = \frac{\text{mole product}}{\text{min} \cdot \text{mole enzyme}} = \left(\frac{U}{mg}\right) \tag{5}$$

$$1 \text{ U} = 1 \frac{\mu\text{mole product}}{\text{min}} \tag{6}$$

$$1 \text{ kat} = 1 \frac{\text{mole product}}{\text{sec}} \tag{7}$$

In order to carry out a kinetic study of the reaction rate of reversible reactions, it is necessary to know the equilibrium constants.

$$K_{eq} = \frac{[P]_{eq}}{[A]_{eq}} = \frac{V_{max}^+ \cdot K_{m,P}}{V_{max}^- \cdot K_{m,A}} \tag{8}$$

The relation between the kinetic constants and the equilibrium constant is termed Haldane equation. From this it results that a reaction is irreversible on the product side if $K_{m,A}$ becomes small, i.e. at higher affinity of the enzyme for the substrate than affinity of the enzyme for the product. In general, product inhibition is required for reversible reactions but is only observed when $K_{m,P}$ is of the same magnitude as $K_{m,A}$.

3.3. General inhibitions

Inhibitions are usually very unspecifically initiated. They might be induced by conformation changes on the active centre of the enzyme as a result of a change in the environment:

- temperature
- pH value
- ionic strength
- solvent

Typical inhibitors can act as effectors, modulators or regulators. The following inhibitions can be observed:

- product inhibition
- competitive inhibition
- non-competitive inhibition
- partially competitive inhibition
- uncompetitive inhibition
- substrate inhibition

Competitive inhibitors compete for the catalytic centre but are not converted themselves (mainly structural analogues). Typically, the product itself can be a competitive inhibitor. In a kinetic study this effects in particular the law of conservation of mass:

$$[E]_0 = [E] + [EA] + [EI] + ... \tag{9}$$

in which case the inhibition constant is defined as:

$$\frac{\upsilon}{V_{max}^+} = \frac{[A]}{K_{m,A}\left(1 + \frac{[I]}{K_i}\right) + [A]} \tag{10}$$

It can be seen that V_{max} is not influenced by competitve inhibitors but that the apparent $K_{(m,A)}$ is increased. This increase in K_m is the result of the distribution of the enzyme in free enzyme [E] and saturated enzyme [EI]. As inhibitor concentration rises, there is also an increase in the apparent $K_{(m,A)}$. For the oxynitrilase-catalyzed addition of hydrocyanic acid to aldehyde according to Wandrey and Kragl [7], a form of bi-substrate kinetics is asssumed according to an 'ordered bi-uni' mechanism.

$$\frac{v}{V_{max}^{+}} = \frac{[A]}{K_{m,A} + [A]} \cdot \frac{[B]}{K_{m,B} + [B]} \tag{11}$$

According to Jorns [8] the formed cyanohydrin P competes with the aldehyde, i.e. substrate A for the active catalytic centre on the enzyme and accordingly acts as a competitive inhibitor.

$$\frac{v}{V_{max}^{+}} = \frac{[A]}{K_{m,A}\left(1 + \frac{[P]}{K_{i,P}}\right) + [A]} \cdot \frac{[B]}{K_{m,B} + [B]} \tag{12}$$

Non-competitive inhibitors do not compete for the catalytic centre but for the free enzyme and the enzyme-substrate complex at different active centres and, in this way, hinder conversion. V_{max} is typically reduced through non-competitve inhibitors, however, the $K_{m,A}$ value is preserved. In this case there are three inhibition constants to be determined:

$$\frac{v}{V_{max}^{+}} = \frac{[A]}{K_{m,A}\left(1 + \frac{[I]}{K_{i}}\right) + [A]\left(1 + \frac{[I]}{K_{i}}\right)} \tag{13}$$

Partially competitive inhibitors also compete for the enzyme while forming an enzyme-substrate complex [EAI], however, product formation is possible from [EAI]. V_{max} is usually not influenced by a partially competitive inhibition, but the apparent $K_{m,A}$ is increased as a saturated or complexed enzyme, with less affinity to [A] is always present.

$$\frac{v}{V_{max}} = \frac{[A]}{K_{m,A} \cdot \left[\left(1 + \frac{[I]}{K_{i}}\right) \middle/ \left(1 + \frac{[I]}{\alpha \cdot K_{i}}\right)\right] + [A]} \tag{14}$$

Uncompetitive inhibitors compete solely with the enzyme-substrate complex which means that in the first place the substrate can create an active centre for the inhibitor on the enzyme. Both V_{max} and K_A are reduced to the same extent through uncompetitive inhibitors.

$$\frac{v}{V_{max}^{+}} = \frac{[A]}{K_{m,A} + [A]\left(1 + \frac{[I]}{K_{i}}\right)} \tag{15}$$

For the reversed reaction of cyanohydrin synthesis, i.e. for the cleavage of cyanohydrins, inhibition is assumed which is competitive with regard to the aldehyde and uncompetitive with regard to the hydrocyanic acid. The rate equation can be expressed as follows:

$$\frac{\upsilon}{V_{max}^{-}} = \frac{[P]}{K_{m,P} \left(1 + \frac{[A]}{K_{i,A}}\right) + [P] \left(1 + \frac{[B]}{K_{i,B}}\right)} \tag{16}$$

Substrate inhibition occurs particularly with high substrate concentrations and is expressed by a decreasing reaction rate at high concentrations - therefore the formation of a plateau is not observed.

Enzyme activation can be treated in the same way as inhibition.

3.4. Kinetics of bi-substrate reactions

Most enzymes catalyze reactions between two or more substrates while forming two or more products. There are three main categories:

1)   SEQUENTIAL Mechanisms
                      a)-RANDOM mechanisms
                      b)-ORDERED mechanisms

2)   PING-PONG Mechanisms

Furthermore, the number and sequence of the molecules taking part in the reaction are termed. For example, *Ordered Bi Uni* means that two substrates are bonded in an ordered sequence and then a product is released.

3.4.1   Random bi bi mechanisms:

Substrate addition and product release are not subject to a specific sequence, a fact which can be seen in very complex rate equations. Hyperbolic saturation curves are only then obtained when a substrate is actually saturated. However, if product formation is rate-determining then equilibriums, by means of which the differential equations can be solved by algebraic or numerical methods, can be assumed for all previous steps: so-called rapid equilibrium random mechanisms which are expressed by eight formation constants [9].

3.4.2.   Ordered bi bi mechanisms:

The active centre for the second substrate must be prepared by the first substrate by changing the conformation of the enzyme through e.g. influencing the charge distribution via dipol-dipol interactions. In varying the first substrate while keeping the second substrate constant, the saturation curves could take a sigmoid course while a substrate inhibition can occur during variation of the second substrate. If the central complexes only occur in very small concentrations, then this is called a Theorell-Chance-Mechanism. In this respect, the mechanism is simplified as the central complexes can be neglected [10].

3.4.3   Ping pong bi bi mechanism

In this case, after the bonding of a substrate, a product is released, another enzyme form is transformed and the second substrate is converted while forming the second product.

The following reaction sequence in *figure 3.1* shows a typical two-substrate reaction:

$$
\begin{array}{ccccccc}
E & + & A & \underset{k_{-A}}{\overset{k_A}{\rightleftharpoons}} & EA & & \\
+ & & & & + & & \\
B & & & & B & & \\
\end{array}
$$

$$
k_{-B} \uparrow \downarrow k_B \qquad\qquad\qquad k_{-\alpha B} \uparrow \downarrow k_{\alpha B}
$$

$$
EB \quad + \quad A \quad \underset{k_{-\alpha A}}{\overset{k_{\alpha A}}{\rightleftharpoons}} \quad EAB \quad \xrightarrow{k_P} E + P
$$
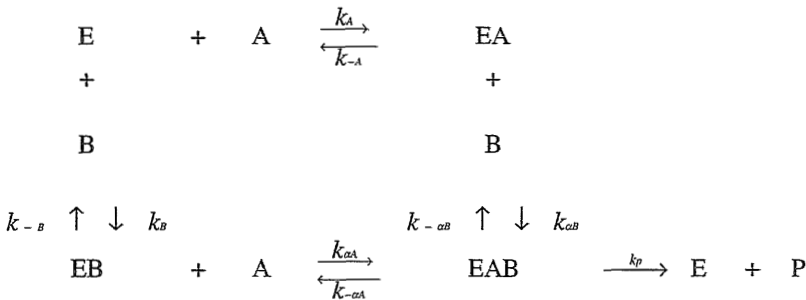
Figure 3.1 *Typical reaction sequence of a two-substrate mechanism*

The intermediate compounds EA, EB and EAB are called transition complexes and the product-forming complex EAB is also termed central complex. Provided that all bonding and dissociation steps are rapid relative to the catalytic step, then the 'rapid equilibrium' assumption can be made. The model describes all RANDOM mechanisms sufficiently accurately, but the 'steady state' assumption must be made for ORDERED mechanisms.

If a reversible product formation reaction is allowed to occur, i.e. that the product is to be considered as a competitive inhibitor, then the relevant rate equations in the presence of P according to the 'rapid equilibrium' assumption can be drawn to:

$$\upsilon = \frac{V_{max}^{+} \cdot [A] \cdot [B]}{\alpha \, K_A \, K_B + \dfrac{\alpha K_A K_B}{K_A} [A] + \alpha \, K_A \, [B] + \dfrac{\alpha K_A K_B}{K_P} [P] + [A] [B]} \qquad (17)$$

As was already seen in the one-substrate reactions, the presence of the product does not influence the V_{max} but does increase the apparent $K_{m,A}$ and $K_{m,B}$. As, the product P requires both the active centres of A and B in a random bi uni reaction, a competitive product inhibition can only be observed under non-saturated conditions of the non-varied co-substrate.

A very lucid nomenclature for the description of multi-substrate reactions was proposed by Cleland [5] in 1963. In this case, the reaction sequences are indicated as arrows and lines. A random bi uni reaction can be expressed by the diagram in *figure 3.2*:
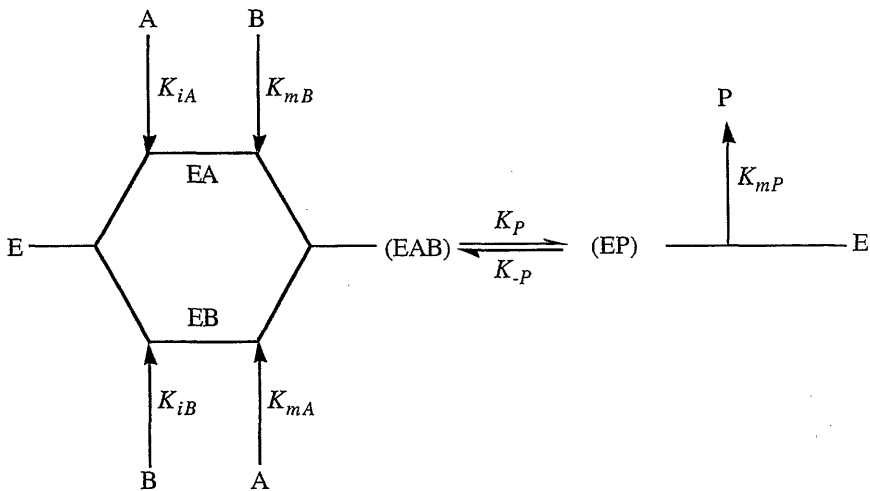
Figure 3.2 *Cleland formalism for description of a random bi uni reaction*

$K_{i,A}$ and $K_{i,B}$ are dissociation constants of A and B from the complexes EA and EB, $K_{m,A}$ and $K_{m,B}$ are the dissociation constants of EA and EB from EAB or EP and are therefore equal to the Michaelis constants of A and B at the saturation of B and A respectively.

By assuming another sequential mechanism, e.g. an ordered bi uni mechanism, the two-substrate reaction in Cleland's nomenclature can be simplified as described in *figure 3.3*.

Figure 3.3 *Cleland formalism for description of an ordered bi uni reaction*

The corresponding reaction sequence can be expressed according to a 'rapid equilibrium' as shown in *figure 3.4*:

Figure 3.4 *Typical reaction sequence of an ordered bi uni mechanism*

The reaction of B to the primary complex EA results in a shift in the equilibrium of the EA formation. From this it can be concluded that the presence of B results in the complete formation of EAB.

$$\upsilon \quad = \frac{V_{max}^+ \cdot [A] \cdot [B]}{K_A\, K_B + K_B\, [A] + [A]\, [B]} \tag{18}$$

By means of the steady state assumption it can be derived that this relation is generally valid when no product inhibition has to be assumed, i.e. for the initial rates and when k_3 or k_p is small relative to the other rate constants, as then $K_{m,A} = 0$. When considering the rate equations, it should be taken into account that this ordered bi uni mechanism represents a limit for the rapid equilibrium assumption and is only to be considered as an exception of a steady state assumption.

3.5. Complete kinetics of bi-substrate reactions

As the derivation of a Michaelis-Menten-relation under steady state conditions leads to complex differential equations, a formal method was derived by E.L.King and C.Altman [11]. In this case, the various occurring enzyme complexes were expressed in the corners of a closed polyhedron and the connecting lines represent the corresponding reactions as shown in *figure 3.5*.
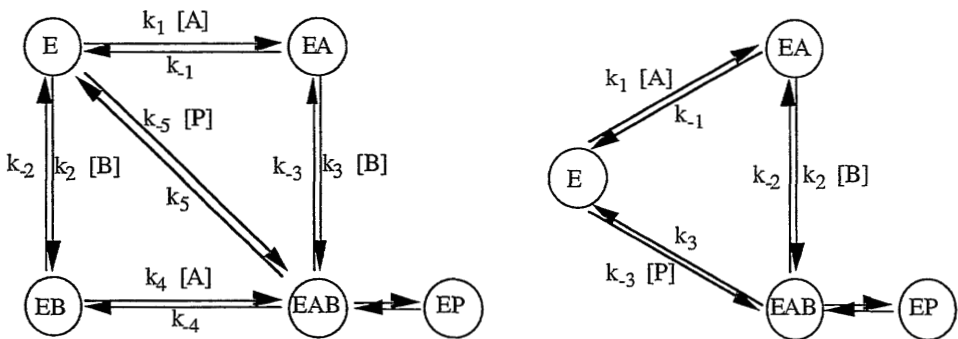
Figure 3.5 *Schematic representation of a random bi uni mechanism and an ordered bi uni mechanism to determine steady-state kinetics according to King Altman.*

According to the King-Altmann method, a rate equation is obtained which is composed from a posititve term of the product of all rate constants of the forward reaction and of all substrates as well as from a negative term of the product of all constants of the reverse reaction in the counter, multiplied by the initial enzyme concentration. As these rate constants are not easily accessible from a kinetic viewpoint, they must ultimately be converted into the so-called kinetic constants K_m and v_{max}. To this end, the denominator must be put into the coefficient form, i.e. all terms with the same concentration terms must be combined. Finally a maximum rate of the forward reaction is defined, $v_{1,max}$, at saturation concentration of all substrates as well as a maximum rate of the reverse reaction $v_{2,max}$, at saturation concentration of the products. Relevant Michaelis constants and rate constants are defined in the same terms [12]. This procedure is described in the appendix A for complete rate equation of an ordered bi uni mechanism. According to Wandrey [7], kinetic analysis of the oxynitrilase catalyzed addition of hydrocyanic acid to carbonyl compounds results in an ordered bi uni mechanism as schematically shown in *figure 3.6*. In this work, both random and ordered kinetics will be compared.
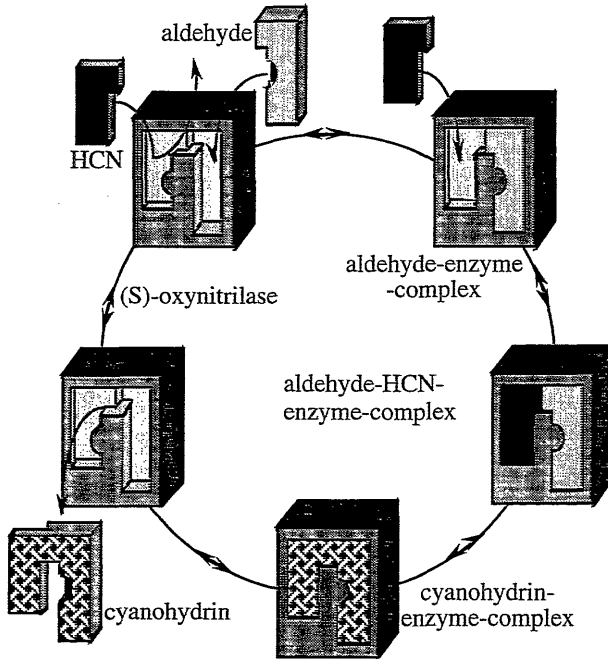
Figure 3.6 *Schematic representation of the reaction sequence of an ordered bi uni mechanism for the formation of cyanohydrins*

Appendix A describes the complete derivation of the rate equations assuming an ordered bi uni mechanism [13]. The complete rate equation of simply inhibited double-substrate kinetics is expressed as follows in equation (19):

$$
\upsilon = \frac{V^{+}_{max}\cdot[A]\,[B] - V^{-}_{max}\,\dfrac{K_{m,B}\cdot K_{i,A}}{K_{m,P}}\,[P]}{K_{m,B}\cdot K_{i,A} + K_{m,B}\cdot[A] + K_{m,A}\cdot[B] + \dfrac{K_{m,A}}{K_{i,P}}\,[B][P] + \dfrac{K_{i,B}\cdot K_{m,A}}{K_{i,P}}\,[P] + [A][B]}
$$

Kinetic treatment of cyanohydrin synthesis according to a random bi uni mechanism is sufficiently accurate, as has already been shown according to the rapid equilibrium model. However, if the decomposition of the central complex was not to be considered as rate-determining, then a steady-state analysis would have to be carried out in this case.

There are many ways in which enzymes can be inactivated and frequently even irreversibly denaturated both during storage or during technical application. This complicates their long-term use in continuous reactors. The causes for enzyme deactivation in aqueous media under non-physiological conditons has been described. For example, possible influences are

impurities caused by proteases (C-N-Hydrolases), microorganisms and auto-oxidants or conformation changes which are caused by the medium and the temperature. As enzymes are also termed polyelectrolytes, the significant influence of the pH value on enzyme stability is obvious. Other important factors of influence are, in particular, mechanical forces through shearing stress and chemically induced conformation changes. These changes in tertiary structure can also be induced by solvation of non-polar groups through organic solvents. The inactivation of enzymes after a reaction of the first order can be expressed mathematically as:

$$\frac{d[E]}{dt} = k_{Des}^{E} \cdot [E] \quad (20) \qquad\qquad t_{1/2} = \frac{\ln 2}{k_{Des}^{E}} \quad (21)$$

To characterize enzyme stability, the half-time or the so-called cycle number, which expresses the quantity of cyanohydrin produced per unit of oxynitrilase used, can be applied. In previous studies by Becker, Pfeil and Kragl the temperature and optimum pH for the (R)-oxynitrilase were determined.

3.6 Conclusions

In chapter 3 the fundamentals of enzyme kinetics are summarized. General inhibitions are described briefly. The complete rate equations for random and ordered bi uni reactions are derived according to King Altman. A kinetic model for oxynitrilase catalyzed addition of hydrocyanic acid to aldehydes is proposed.

List of Symbols

A	species A or substrate A
B	species B or substrate B
E	enzyme
P	species P or product P

I	species I or inhibitor I
EA	binary enzyme-substrate complex
EB	binary enzyme-substrate complex
ES	general enzyme-substrate complex
EAB	tertiary enzyme-substrate complex
EP	binary enzyme-product complex
EI	binary enzyme-inhibitor complex
$[R]$	concentration of (R)-enantiomer [wt.%, $mole \cdot l^{-1}$]
$[S]$	concentration of (S)-enantiomer [wt.%, $mole \cdot l^{-1}$]
$[E]$	free enzyme concentration (concentration of active centres)
$[E]_0$	total enzyme concentration
$[P]_{eq}$	equilibrium product concentration
K_{eq}	reaction equilibrium constant
K_m	Michaelis-Menton constant (half saturation)
$K_{m,A}$	Michaelis half saturation value for the substrate
$K_{(m,A)}$	apparent Michaelis half saturation value for inhibited reactions
$K_{m,P}$	Michaelis half saturation value for the product
K_i	general inhibition constant
$K_{i,A}$	substrate inhibition constant
$K_{i,P}$	product inhibition constant
k_{cat}	molecular acitivity (or turnover number TN) [$U \cdot mg^{-1}$]
k_f	forward reaction rate constant [$(mol \cdot L^{-3})^{1-n} \cdot t^{-1}$]
k_r	reverse reaction rate constant [$(mol \cdot L^{-3})^{1-n} \cdot t^{-1}$]
k_P	product formation rate
$k_1, k_2, \ldots$	elementary forward rate constant
$k_{-1}, k_{-2}, \ldots$	elementary reverse rate constant
k_{Des}^{E}	enzyme deactivation rate constant
n	order of the reaction
$t_{1/2}$	half time (cycle number)
υ	reaction velocity
V_{max}	general maximum reaction velocity
V_{max}^{+}	maximum forward reaction velocity
V_{max}^{-}	maximum reverse reaction velocity
%ee	optical purity; enantiomeric excess [%]
ξ	degree of conversion, turnover [%]

References

(1)   Bailey, J.E., Ollis, D.F.
        Biochemical Engineering Fundamentals
        McGraw-Hill International Editions, 2.nd Ed., 1986

(2)   Bisswanger, Hans
        Theorie und Methoden der Enzymkinetik
        Verlag Chemie, Weinheim 1979

(3)   Lasch, J.
        Enzymkinetik
        VEB Gustav Fischer Verlag Jena, 1987

(4)   Chaplin, M.F.;.Bucke, C.
        Enzyme technology
        Cambridge University Press, Cambridge 1990

(5)   Cleland, W.W.
        The kinetics of enzyme catalyzed reactions with two or more substrates or products
        Biochimica et Biophysica Acta, 67 104-137, [1963]

(6)   Wong, J.Tze-Fei
        Kinetics of enzyme mechanisms
        Academic Press, New York, 1975

(7)   Kragl, U.; Niedermeyer, U.; Kula, M.-R.; Wandrey, C.
        Engineering aspects of enzyme engineering: continuous asymmetric C-C bond formation
        in an enzyme-membrane-reactor
        Ann. N. Y. Acad. Sci. 613, 167-175 [1990]

(8)   Schuman-Jorns, M.
        Studies on the kinetics of cyanohydrin synthesis and cleavage by the flavoenzyme oxynitrilase
        Biochim. Biophys. Acta 613, 203-209 [1980]

(9)   Segel, Irwin H.
        Enzyme kinetics - behavior and analysis of rapid equilibrium and steady state enzyme systems
        John Wiley & Sons, New York 1975

(10)   Petterson, G.
        Kinetic characteristics of the sequential random order two-substrate enzyme mechanism
        Acta chemica scandinavica, 23, 2717-2726, [1969]

(11)   King, E.L., Altmann, C.
        A schematic method of deriving the rate laws for enzyme-catalyzed reactions
        J.Phys.Chem., 60, 1375-1378, [1956]

(12)   Hill, C.M., Waight, R.D.; Bardsley, W.G.
        Does any enzyme follow the Michaelis-Menten equation?
        Molecular & Cellular Biochemistry, 15, 3, 173-178, [1977]

(13)   Ferdinand, W.
        The interpretation of non-hyperbolic rate curves for two-substrate enzymes
        Biochem.J., 98, 278-283 [1966]

Appendix A to Chapter 3

Complete rate equation of an ordered bi uni mechanism according to King-Altman

As the steady-state analysis leads to all kinetic constants for an ordered mechanism, the King-Altman method is specified in detail below:

$$\frac{[E]}{[E]} = \left(k_{-2}\cdot k_{-1} + k_2[B]\cdot k_3 + k_3\cdot k_{-1}\right)\cdot \text{denominator}^{-1}$$

$$\frac{[EAB]}{[E]} = \left(k_1[A]\cdot k_2[B] + k_2[B]\cdot k_{-3}[P] + k_{-3}[P]\cdot k_{-1}\right)\cdot \text{denominator}^{-1}$$

$$\frac{[EA]}{[E]} = \left(k_1[A]\cdot k_{-2} + k_{-3}[P]\cdot k_{-2} + k_3\cdot k_1[A]\right)\cdot \text{denominator}^{-1}$$

$$\upsilon = k_3\,[EAB] - k_{-3}\,[E]\,[P]$$

$$\frac{\upsilon}{[E]} = \frac{\text{numerator (Z)}}{\text{denominator (N)}}$$

$$Z = k_3\cdot\left(k_1[A]\cdot k_2[B]+k_2[B]\cdot k_{-3}[P]+k_{-3}[P]\cdot k_{-1}\right) - k_{-3}\left(k_{-2}\cdot k_{-1}+k_2[B]\cdot k_3+k_3\cdot k_{-1}\right)\cdot[P]$$
$$= k_3\cdot k_1\cdot k_2\,[A]\,[B]+k_3\cdot k_{-3}\cdot k_2[B]\,[P]+k_3\cdot k_{-3}\cdot k_{-1}\,[P]$$
$$\quad - k_{-3}\,k_{-2}\cdot k_{-1}\cdot[P]-k_{-3}\cdot k_3\,k_2[B]\,[P]-k_{-3}\,k_3\cdot k_{-1}\cdot[P]$$

$$N = k_{-2}\cdot k_{-1} + k_3\cdot k_{-1} + k_1\cdot k_2\,[A] + k_1\cdot k_3\cdot[A] + k_2\cdot k_3\,[B] + k_1\cdot k_2\,[A]\,[B]$$
$$\quad + k_2\cdot k_{-3}\,[B]\,[P] + k_{-1}\cdot k_{-3}\,[P] + k_{-2}\cdot k_{-3}[P]$$

$$N = k_{-1}(k_{-2}+k_3\cdot) + k_1\cdot(k_{-2}+k_3\cdot)[A] + k_2\cdot k_3\,[B] + k_1\cdot k_2\,[A]\,[B]$$
$$\quad + k_2\cdot k_{-3}\,[B]\,[P] + k_{-3}\,(k_{-1}+k_{-2})[P]$$

$$\frac{\upsilon}{[E]} = \frac{k_1\cdot k_2\,k_3\cdot[A]\,[B] - k_{-1}\cdot k_{-2}\cdot k_{-3}\,[P]}{k_{-1}(k_{-2}+k_3)+k_1(k_{-2}+k_3)[A]+k_2k_3[B]+k_1k_2[A][B]+k_2k_{-3}[B][P]+k_{-3}(k_{-1}+k_{-2})[P]}$$

After division by the coefficients of [A] [B], the complete rate equation for the inital and reversed reaction is obtained:

$$\frac{\upsilon}{[E]} = \frac{\dfrac{k_1k_2k_3}{k_1k_2}\,[A]\,[B] - \dfrac{k_{-1}k_{-2}k_{-3}}{k_1k_2}\,[P]}{\dfrac{k_{-1}(k_{-2}+k_3)}{k_1k_2}+\dfrac{k_1(k_{-2}+k_3)}{k_1k_2}[A]+\dfrac{k_2k_3}{k_1k_2}[B]+[A][B]+\dfrac{k_2k_{-3}}{k_1k_2}[B][P]+\dfrac{k_{-3}(k_{-1}+k_{-2})}{k_1k_2}[P]}$$

If product inhibition is not allowed to occur and $[P] = 0$, then a simple rate law for the forward reaction is obtained:

$$\frac{\upsilon}{[E]} = \frac{k_3\,[A]\,[B]}{\dfrac{k_{-1}(k_{-2}+k_3)}{k_1 k_2} + \dfrac{k_{-2}+k_3}{k_2}\,[A] + \dfrac{k_3}{k_1}\,[B] + [A][B]}$$

Finally the kinetic constants according to Cleland's rules are to be defined:

$$K_{eq} \equiv \frac{N_1}{N_2} = \frac{k_1 \cdot k_2\, k_3}{k_{-1} \cdot k_{-2} \cdot k_{-3}}$$

$$\frac{V^{+}_{max}}{[E]_t} \equiv \frac{N_1}{C_{AB}} = k_3 \qquad\qquad \frac{V^{-}_{max}}{[E]_t} \equiv \frac{N_2}{C_P} = \frac{k_{-1} \cdot k_{-2} \cdot}{k_{-1} + k_{-2}}$$

$$K_{m,A} \equiv \frac{C_B}{C_{AB}} = \frac{k_3}{k_1} \qquad\qquad K_{i,A} \equiv \frac{C}{C_A} = \frac{k_{-1}}{k_1}$$

$$K_{m,B} \equiv \frac{C_A}{C_{AB}} = \frac{k_{-2} + k_3}{k_2} \qquad\qquad K_{i,B} \equiv \frac{C_P}{C_{BP}} = \frac{k_{-1} + k_{-2}}{k_2}$$

$$K_{m,P} \equiv \frac{C}{C_P} = \frac{k_{-1}}{k_{-3}} \cdot \frac{k_{-2} + k_3}{k_{-1} + k_{-2}} \qquad\qquad K_{i,P} \equiv \frac{C_B}{C_{BP}} = \frac{k_3}{k_{-3}}$$

After substitution, the rate equation for the forward reaction under initial conditions is obtained:

$$\upsilon = \frac{V^{+}_{max} \cdot [A]\,[B]}{K_{i,A} \cdot K_{m,B} + K_{m,B}\,[A] + K_{m,A}\,[B] + [A][B]}$$

in which case $K_{i,A} \cdot K_{m,B} = K_{i,B} \cdot K_{m,A}$ proves to be valid. By means of the steady state assumption, an identical rate equation according to the rapid equilibrium assumption is therefore obtained. As the identity $K_{m,A} = K_{i,A}$ is valid under rapid equilibrium conditions, the rate equation could also have been obtained by dividing into the product of two Michaelis-Menten equations. The advantage of this is that inhibition effects can be treated similar to one-substrate reactions.

$$\upsilon = \frac{V^{+}_{max}\,[A]\,[B]}{\left(K_{m,A}\left(1 + \dfrac{[P]}{K_{i,P}}\right) + [A]\right)\left(K_{m,B} + [B]\right)} - \frac{V^{-}_{max}\,[P]}{K_{m,P}\left(1 + \dfrac{[A]}{K_{i,A}}\right) + [P]\left(1 + \dfrac{[B]}{K_{i,B}}\right)}$$

Two-substrate kinetics for the simply inhibited forward reaction of a one-substrate reaction, with multiple links, according to Michaelis-Menten is then expressed as:

$$\upsilon = \frac{V_{max}^{+}\ [A]\ [B]}{K_{m,A}K_{m,B} + K_{m,B}\ [A] + K_{m,A}\ [B] + \dfrac{K_{m,A}}{K_{i,P}}\ [B][P] + \dfrac{K_{m,A}K_{m,B}}{K_{i,P}}\ [P] + [A][B]}$$

One advantage of the steady state condition is the fact that the rate constants of the elementary reaction can be attributed to the kinetic constants. The complete rate equation can be obtained from the coefficient equation by means of relevant substitution.

$$\upsilon = \frac{V_{max}^{+}\cdot[A]\ [B]\ -\ \dfrac{V_{max}^{+}}{K_{eq}}\ [P]}{K_{m,B}\cdot K_{i,A} + \dfrac{K_{i,B}\cdot K_{m,A}}{K_{i,P}}\ [P] + K_{m,A}\cdot[B] + K_{m,B}\cdot[A] + \dfrac{K_{m,A}}{K_{i,P}}\ [B][P] + [A][B]}$$

By applying the Haldane ratio $K_{i,A}\cdot K_{m,B}\cdot K_{i,P} = K_{i,B}\cdot K_{m,A}\cdot K_{m,P}$, the following is obtained:

$$\upsilon = \frac{V_{max}^{+}\cdot[A]\ [B] - V_{max}^{-}\ \dfrac{K_{m,B}\cdot K_{i,A}}{K_{m,P}}\ [P]}{K_{m,B}\cdot K_{i,A} + K_{m,B}\cdot[A] + K_{m,A}\cdot[B] + \dfrac{K_{m,A}}{K_{i,P}}\ [B][P] + \dfrac{K_{i,B}\cdot K_{m,A}}{K_{i,P}}\ [P] + [A][B]}$$

The individual rate constants result for the kinetic constants as follows:

$$k_1 = \frac{V_{max}^{+}}{[E]_t}\ K_{m,A}$$

$$k_{-1} = \frac{V_{max}^{+}}{[E]_t}\ \left(\frac{K_{i,A}}{K_{m,A}}\right)$$

$$k_2 = \frac{V_{max}^{+}}{[E]_t}\ \left(\frac{K_{m,A} - 1}{K_{m,A}\ K_{m,B} - K_{m,A}\ K_{i,B}}\right)$$

$$k_{-2} = \frac{V_{max}^{+}}{[E]_t}\ \left(\frac{K_{m,B} - K_{i,B}\ K_{m,A}}{K_{m,A}\ K_{i,B} - K_{m,A}\ K_{m,B}}\right)$$

$$k_3 = \frac{V_{max}^{+}}{[E]_t}$$

$$k_{-3} = \frac{V_{max}^{+}}{[E]_t}\ \left(\frac{1}{K_{i,P}}\right)$$

Chapter

4

OXYNITRILASES

Synopsis

Immobilized biocatalysts, e.g. oxynitrilases adsorbed on Avicel®, represent a particularly complex area of heterogeneous catalysis involving fundamental and technical disciplines. The relevant criteria for applications are technical or technological feasibility and cost. Therefore, a kinetic characterization of the overall system is required. This should include the impact of byproducts and inhibitions on enantiomeric excess and reaction rate. However, the mathematical equations relating the fundamental physical parameters to the properties of interest become very complex unless the influence of the carrier itself, the distribution of substrates or diffusion limitations are neglegible. For these reasons, a pragmatic characterization of the oxynitrilases is derivated. Kinetic constants are calculated assuming an ordered-bi-uni mechanism. Computer simulation and parameter identification is done on basis of ordered and random mechanisms.

It could be shown, that the reaction is preferably carried out in organic media of low hydrophilicity. The stability of the enzymes is at a maximum in non-polar ethers such as di-iso-propylether or di-n-pentylether. Immobilization of the enzyme through adsorption on microcrystalline cellulose is necessary in order to keep the enzyme stable. In this case, the enantiomeric excess for the production of homochiral cyanohydrins increases with decreasing total amount of water. A sensitive aspect in catalyst preparation results from the removal of sorbed water and oxygen.

In agreement with literature data, the mechanism of the oxynitrilase-catalyzed formation of cyanohydrins is following an ordered-bi-uni mechanism. All relevant kinetic parameters are calculated from the Lineweaver-Burk plots and are identified via computer simulation.

4.1. Introduction

In various previous studies, particularly in the works of Effenberger [1,2], Hörsch [3], Brussee [4] and Niedermeyer [5] the substrate specificity of the (R)- and (S)-oxynitrilases were screened and the essential reaction conditions were determined. The enzymes catalyzes the specific addition of hydrocyanic acid to carbonyl compounds as shown in *figure 4.1*.
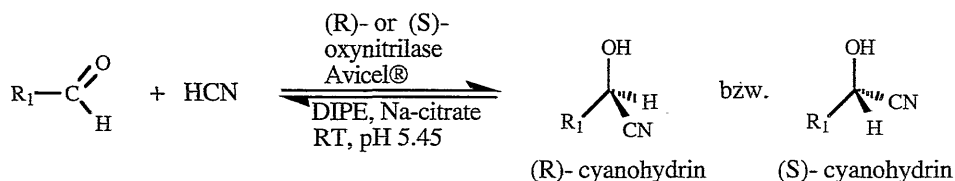
Figure 4.1 *Preparation of homochiral cyanohydrins through (R)- or (S)-oxynitrilase catalyzed addition of hydrocyanic acid to carbonyl compounds*

The advantages of the organic reaction medium become significant in cases where the substrates exhibit poor solubility in aqueous media and where the equilibrium constants of the cyanohydrin formation based on hydrated aldehyde are substantially greater than those in the organic medium. As summarized in *table 4.1*, the enantiomeric excess for the formation of homochiral cyanohydrins is typically much higher in organic media whereas the yields are similar in low-water conditions. However, the reaction rates are lower in organic media.

substrate	solvent...H₂O / ethanol			solvent...ethylacetate / Avicel		
	time [h]	yield [%]	ee [%]	time [h]	yield [%]	ee [%]
benzaldehyde	1	99	86	2.5	95	99
3-phenoxybenzaldehyde	5	99	10,5	192	99	98
butyraldehyde	2	75	69	4.5	75	96

Table 4.1 *Experimental batch results according to Effenberger [1] on the (R)-oxynitrilase catalyzed formation of homochiral cyanohydrins*

Considering the additional aspect of different downstream processing for volatile and non-volatile products, the (R)- and (S)-oxynitrilase catalysed addition of hydrocyanic acid to butyraldehyde and 3-phenoxybenzaldehyde was chosen as the model systems to be investigated in this work. Moreover both compounds are commercially important as a chiral C_4-pool and for the production of various insecticides and pharmaceutics.

4.1.1. (R)-Oxynitrilase

In 1908, Rosenthaler [6] described, for the first time, the enzyme (R)-oxynitrilase [E.C.4.1.2.10] from *Prunus amygdalus amara* as a component of the enzyme complex emulsin. Amygdalin, from which benzaldehyde and hydrocyanic acid is released in several stages, is considered as a physiological substrate. The (R)-oxynitrilase contains flavine-adenine-dinucleotide (FAD) as a prosthetic group and completely loses its activity during the splitting of this co-factor. In general, forms of the oxynitrilase can be found in plants of the *Rosaceae* species such as *Prunoideae* and *Maloideae*, i.e. in cherries, peaches, apricots, almonds, plums and apples. The (R)-oxynitrilase always occurs in various, mostly four isoforms [4]. Effenberger [2] (Institute for Organic Chemistry at the University of Stuttgart) isolated and purified the enzyme from defatted bitter almonds according to the methods described by Becker and Pfeil [7,8] in their publications and also by means of affinity chromatography by Hochuli [9]. By subsequently applying ultrafiltration, the solution is treated and an enzyme concentrate with $A_{vol} = 2500...3200$ U·ml^{-1} is produced. Approximately 75 mg of oxynitrilase with a specific activity of $A_{spec} = 100$ U·mg^{-1} can be produced from 100 g of defatted almond meal. In later studies, enzyme purification was simplified distinctly with the result that preparations with a specific activity of $A_{spec} = 70$ U·mg^{-1} were made available at a marginal cost of US-$ 47,-- per 1000 U. The effect of enzyme purification on the specific activity of the (R)-enzyme and the total yield are summarized in *table 4.2*.

(R)-oxynitrilase: 57 - 59 kDa
1.1 (meq FAD) · (meq protein)$^{-1}$
$pK_i = 4.0$
production costs 47,-- US-$ · 1000 U^{-1}

reference	specific activity A_{spec}	yield ξ
van der Gen & Brussee [10]	100 U · mg^{-1}	800 mg · kg^{-1} almond meal
Kruse & Brussee [11]	86 U · mg^{-1}	4000 mg · kg^{-1} bitter almonds
Wandrey & Kragl [12]	527 U · mg^{-1}	750 mg · kg^{-1} bitter almonds
Effenberger & Förster [1]	100 U · mg^{-1}	200 mg · kg^{-1} bitter almonds

Table 4.2 *Specific activity and yield of similar (R)-oxynitrilases isolated and purified according to different references*

4.1.2. (S)-Oxynitrilase

The enzyme (S)-oxynitrilase [E.C.4.1.2.1] from Sorghum bicolor was described and characterized by Conn [13,14,15,16] for the first time in 1961. The S-oxynitrilase can be isolated from various cyanogen plants of the species *Sorghum, Ximenia americana* or *Sambucus nigra* such as flax or millet. In this case the physiological substrate is acetone cyanohydrin or 4-hydroxy-benzaldehydecyanohydrin respectively. The enzyme, from sorghum seedlings cultivated in darkness, was also isolated and purified by Effenberger [2] according to methods already published and, depending on the composition, three isoforms on average could be determined [17]. According to studies conducted by Brussee [4], the kinetic constants of the iso-enzyme are mostly only marginally different so that chromatographic separation for preparative compositions does not seem necessary. After salting-out chromatography on Sepharose 4B [18], a specific activity of $A_{spec} = 70$ U·mg^{-1} is obtained, which can be increased to 112 U·mg^{-1} under loss of activity by means of further hydrophobic chromatography on phenyl sepharose. By means of subsequent ultrafiltration the solution is treated and an enzyme concentrate with $A_{vol} = 3250...4000$ U·ml^{-1} is produced. According to Hörsch [3], the enantiomeric excess, which can be achieved by the less active oxynitrilase, are much higher. In this way, by using benzaldehyde as a substrate with a 112 U·mg^{-1} preparation, an enantiomeric excess of 78 % ee can be obtained, whereas an optical purity of 93 % ee can be obtained with a 70 U·mg^{-1} preparation. The difference in quality can be explained by a loss of subunits during chromatography on phenyl sepharose. (S)-Oxynitrilase was made available at a marginal cost of US-\$ 400,-- per 1000 U. The effect of enzyme purification on the specific activity of the (S)-enzyme and the total yield are summarized in *table 4.3*.

reference	specific activity	yield	MW
van der Gen & Brussee [10]	1.5 U · mg^{-1}	30 mg · kg^{-1} Hirse	95 kDa
Wandrey & Kragl [12]	190 U · mg^{-1}	20 mg · kg^{-1} Hirse	124 kDa
Effenberger & Förster [1]	112 U · mg^{-1}	17 mg · kg^{-1} Hirse	120 kDa

Table 4.3   *Specific activity and yield of similar (S)-oxynitrilases isolated and purified according to different references*

The pH optimum of the oxynitrilase with regard to its specific activity shows a distinct maximum at pH 6. As the kinetics of racemization is proportional to the pH value, pH 5.4 was determined a priori as a point of operation.

4.2. Experiments

The performance of all experimental works was determined by the toxicity of hydrocyanic acid. In the study ' Health Aspects of Chemical and Biological Weapons' by the World Health Organisation (WHO), the Ict_{50} with 1 $g \cdot min^{-1} \cdot m^{-3}$ or the fatal quantity for percutane application is specified at $LD_{50} = 1$ $mg \cdot kg^{-1}$. Due to safety reasons, both stationary and mobile Compur-Monitox HCN detectors were used. The capacity of the laboratory fume chamber was doubled to 1.400 $l \cdot h^{-1} \cdot m^{-2}$ and separated from the central waste air plant.

HCN conc. [ppm]	Effect on human being
0,5 - 2	smell threshold
10	maximum tolerable concentration
90	highly dangerous to life
180 - 270	lethal

Table 4.4 *Tolerance values for contact with hydrocyanic acid*

The legislation permits operations with HCN only in the laboratory fume chamber with a performance of > 1.200 $m^3 \cdot h^{-1}$. Since the hydrocyanic acid is resorbed through oral and physical contact, protective clothing and gloves are vital. Moreover, an HCN-detector is applied. This equipment indicates that HCN concentration of air is above 1 ppm and gives up a 10 ppm acute warning signal.
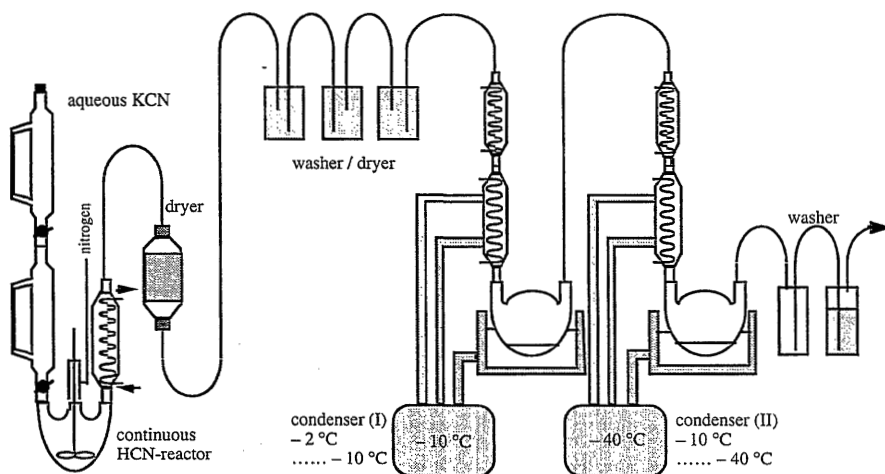
Figure 4.2 *Laboratory mini plant for the preparation of liquid hydrocyanic acid*

Since HCN has a propensity to store exothermal decomposition reactions, the production is continually conducted and accompanied in a separate experimental layout. In *figure 4.2*, the laboratory mini plant for continuous and on-line preparation of liquid hydrocyanic acid is shown. HCN is produced according to standard methods through addition of aqueous potassium cyanide to concentrated 80 w/w sulfuric acid. The reaction mixture is stirred and the HCN produced is removed with nitrogen. After drying, the gas is recovered in a two-staged condenser.

Experiments on Enzyme Kinetics [19.20]

The microcrystalline cellulose Avicel® swells up during a one-hour stirring process in a citrate buffer (0,045 M Na-citrate buffer, pH 5,4) and is pressed dry. Buffer-saturated di-iso-propylether, DIPE, (34ml) is degassed by vacuum in an ultrasonic bath. The reactor is rinsed und degassed with argon, Avicel® is inserted and 500 U enzyme is added in drops. Then the remaining solvents, butanal (3.61 g in 10 ml DIPE) and HCN (5 ml) are added. After closing the reactor, argon pressure for sampling is produced. The batch or recycle reactor for kinetic investigations is shown in *figure 4.3*.

a heat exchanger
b reaction vessel
c stirrer
d sampling valve
e peristaltic pump
f polarimeter and photometer
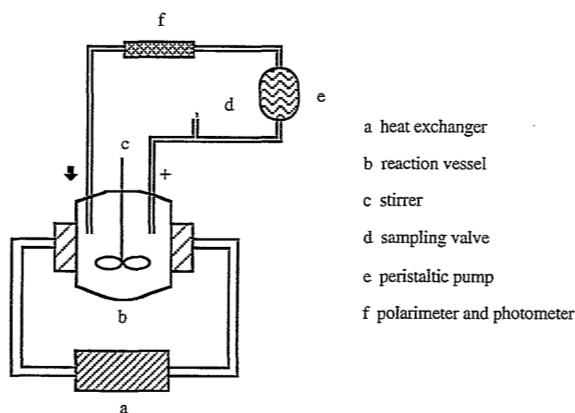
Figure 4.3 *Experimental set-up for characterization of enzyme kinetics*

Conditioning of the Avicel®

The Avicel® is stirred in a 0,054 M sodiumcitrate buffer solution. Following this, the fluid is filtered by a paper filter with a membrane pump and the cellulose is gently pressed out with the plunger of a disposable injection. An appropriate quantity of enzyme solution is dropped onto this carrier and placed in the receiver vessel of a micro-concentrator. The choice of membrane depends on the desired degree of dryness and the specified molecular

weight of the enzyme. The micro-concentrator is put together and the contents centrifugated at 5000 U·min^{-1} for twenty minutes. After centrifugation, the receiver vessel is turned, placed on the filtrate container with the concentrate container and counter-centrifugated for five minutes at 5000 U·min^{-1}. Now the Avicel® is almost completely in the concentration vessel. The results of typical batch reference experiments are shown in *table 4.5*. New enzyme batches are characterized in terms of yield and enantiomeric excess at reference conditions. Especially at high substrate concentrations, differences in the enzyme activity can easily be seen. Furthermore, a standard activity test is carried out.

concentration [mole · l^{-1}]	temperature [°C]	yield [%]	ee-value [%]
0,2	20	93,0	98,2
0,2	30	88,9	96,8
1,0	20	81,1	93,5
2,0	20	87,8	53,1
5,0	20	88,7	37,6

Table 4.5 *Yield and optical purity of (R)-2-hydroxypentanenitrile as a function of the butanal concentration and the temperature*

Standard activity test of Oxynitrilases

(1150 ml-x-ml) buffer solution and (x ml) enzyme solution with 50 ml benzaldehyde are placed in layers in an Eppendorf cap, 50 ml hydrocyanic acid solution are added 1 : 1 and the reaction is started by shaking vigorously. The reaction mixture is then fed into a L = 1 dm polarimeter micro-cell and the increase in the amount of rotation α_D^{20} is observed. After five minutes, the specific activity is calculated for the amount of rotation.

$$A_{spec} = \frac{\alpha_D^{20} \cdot 5 \cdot X}{1000 \cdot L} \quad \left[\frac{U}{ml}\right] \tag{1}$$

1 U forms 1.0 µmole·min^{-1} benzaldehyde and HCN from benzaldehyde cyanohydrin (at 25°C).

4.3. Enzymatic reactions in organic media

In the synthesis of optically active cyanohydrins with the enzyme (R)- or (S)-oxynitrilase in aqueous or water-ethanol systems, only moderate optical yields could be obtained at unbuffered pH values [21,22]. This is caused by the non-stereoselective chemical addition of hydrocyanic acid to aldehyde which occurs in competition to the enzyme-catalyzed reaction and results in a racemic mixture of cyanohydrins. This non-specific addition of hydrocyanic acid can be suppressed in organic solvents as described later. Generally speaking, there are three reasons for using an organic solvent [23,24]:

- higher solubility of the reactants
- suppression of unwanted side reactions
- easier product recovery and purification

However, organic solvents have a deactivation effect on many enzymes and, for this reason, their use is limited [25,26,27,28]. If an enzyme is placed in a non-polar solvent, then dispersion of the hydrophobic part in the interior begins, i.e. the conformation of the enzyme is reorganised. In extreme cases, the active center of the enzyme can be considered as 'upside down'. It generally applies that the deactivation effect is all the more pronounced, the greater the polarity and the hydrophobicity of the solvent is. Hydrophobicity is expressed by decadic logarithms of the partition coefficient log P of the solvent in a standardised octanol/water two-phase system as shown in *table 4.6*.

solvent	log P	water solubility
ethanol	- 0,24	soluble
acetone	- 0,23	soluble
ethylacetate	0,68	3,30
diethylether	0,85	
tert.-butylmethylether	1,21	2,54
diisopropylether	1,90	0,57
dibutylether	2,90	
dipentylether	3,90	
decane	5,60	

Table 4.6 *Partition coefficients for commonly used organic solvents*

With increasing log P value, the solubility of water in the organic solvent decreases. For simple molecules log P values are known or can be calculated from group contribution constants. For complicated or unknown molecules the partition coefficient can be determined by measuring the equilibrium concentration of the solute in both phases [29]:

$$\log P = \frac{[\text{solute}]^{\text{octanol}}}{[\text{solute}]^{\text{water}}} \qquad (2)$$

A more detailed correlation between water content, enzyme activity and the partition coefficient of a solvent can be drawn from the three-dimensional Hildebrand solubility parameter approach. Laane [30,23] have shown, that the dipole-dipole interactions as well as the capacity to form hydrogen bridges are the most important attractive forces to modifiy the enzyme activity.

Different from lipases, oxynitrilases are neither stable in the dry state nor in completely dehydrated solvents. A minimum quantity of water seems to be absolutely necessary for the functioning of the oxyntrilases in organic solvents. It will be shown later, that at least a monolayer of water should protect the enzyme from denaturation. If they are to be used in unpolar solvents, then they must be put in a stabilised form, e.g. immobilized on Avicel® in the reaction system [31]. The influence of water content of the solvent is shown in *figure 4.4.*
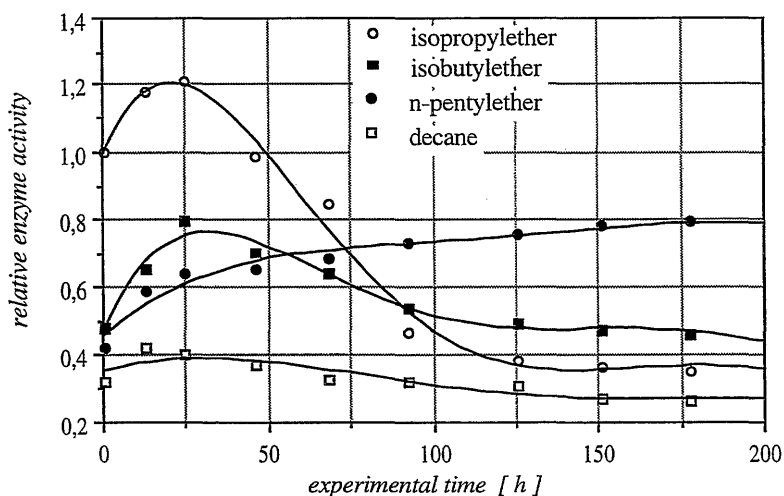
Figure 4.4 *Specific activity of the (R)-oxynitrilase in different organic solvents used in this study. Data are drawn from exposure experiments*

(R)-oxynitrilase, immobilized on Avicel® according to standard methods was exposed to buffer-saturated organic solvents. In figure 4.4, it could be shown, that for diethyl-, diisopropyl- and dibutylether having a partition coeffient log P < 3 the specific activity of the oxynitrilase passes a maximum and finally decreases with time. Life-time of the oxynitrilase in more hydrophilic solvents seems to be limited. The group of solvents having a partition coefficient log P > 3 yields in higher stability of the oxynitrilase. In general, aprotic solvents such as ethers promote higher activities. Hydrocarbons, such as decane result in inacceptable low activities of the enzyme. Nevertheless, di-iso-propylether was chosen for further investigations, because of limited ability to build up peroxides. The solubility of water in diiospropylether at 25°C is, according to Mattiasson, roughly 0.41 vol% or 0.57 wt% and increases with the substrate concentration so that a 0.2M reaction solution absorbs 0.75 vol% or 1.04 wt%. This is a further reason for decreasing optical purity with increasing substrate concentrations as shown in table 4.5.

4.3.1.   Stability of (R)- and (S)-Oxynitrilases

The stability of the oxynitrilases was already examined in previous studies by Wandrey [12] and Seely [16], in dependence on external variables such as pH value and temperature.

pH-value (0.045m citrate-buffer)
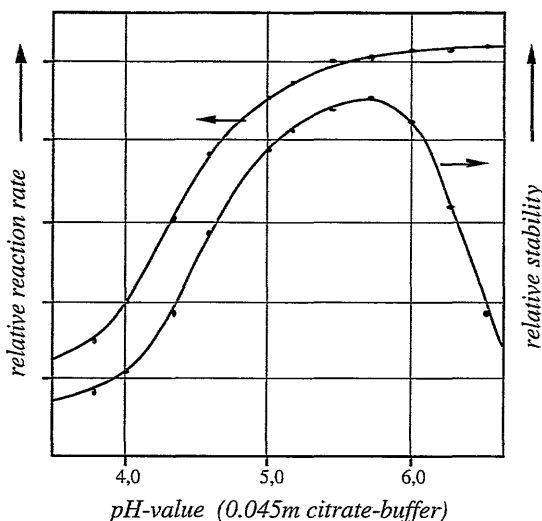
Figure 4.5   *pH Optimum of the (S)-oxynitrilase according to Seely [16]*
       Data were confirmed by Wandrey, Kula and coworkers [12]

Increasing activity with a rise in pH value as shown in *figure 4.5*, with a maximum between $5 < \text{pH} < 7$, was discovered to coincide with the chemical reaction for both the (R)- and (S)-oxynitrilases. The cyanohydrin synthesis exhibits positive activation energy in which case the temperature dependence of the chemical reaction is more pronounced, therefore favouring operation at lower temperatures. In experiments it could be shown, that the enantiomeric excess decreases with increasing temperature. However, at 40°C and 35°C for the (R)- and (S)-oxynitrilase respectively, denaturation of the enzyme is observed.

Within the framework of this study other solvents as shown in *figure 4.4*, different methods of immobilization as well as the impact of water content are to be tested and the stability of the oxynitrilases are to be quantified. To this end, the stability was measured in static and dynamic experiments using exposure experiments, e.g. *figure 4.4*, and experiments using a continuous recycle bioreactor as shown in *figure 4.5*. In case of recycle bioreactor experiments, the oxynitrilase buffer solution is pumped through a reaction tube, and the amount of optical rotation is measured as a function of time.
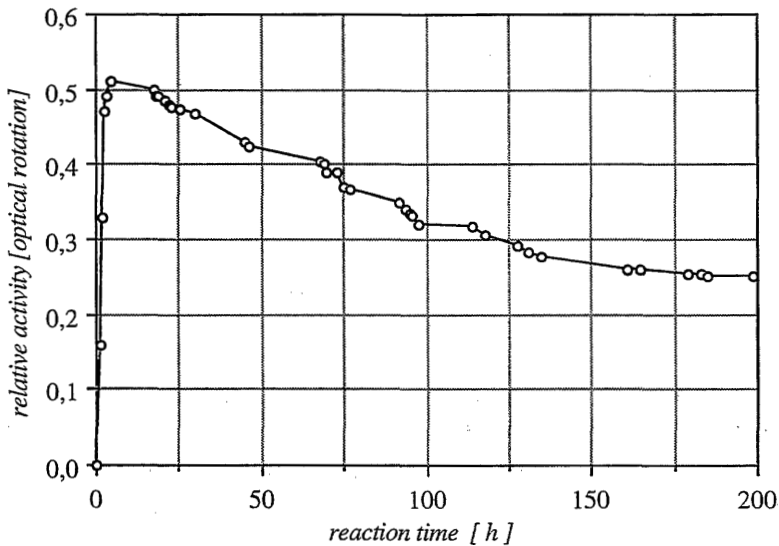
Figure 4.6 *Stability of the (R)-oxynitrilase measured in 0.5 m reaction media (di-iso-propylether, butanal, HCN) in a laminar flow tubular reactor*

Generally, reduced relative activity proportional to solvent concentration with regard to the buffer solution was determined. According to studies by Jorns [32], there is an increase in the stability of the oxynitrilases when pH value rises. Under the experimental standard

conditions of pH 5.4, the half-life period of the (R)-oxynitrilase was found to be greater than 400 hours and that of the (S)-oxynitrilase roughly 242 hours. However, the addition of co-solvents affects the stability of the (R)-enzyme in particular. The carbonyl compound also seems to affect the stability of the oxynitrilases. No stability-reducing effect, caused by HCN, could be determined. Moreover, it could be shown in the bioreactor experiments, that the enzyme can completely be regenerated through a rinse with hydrocyanic acid.
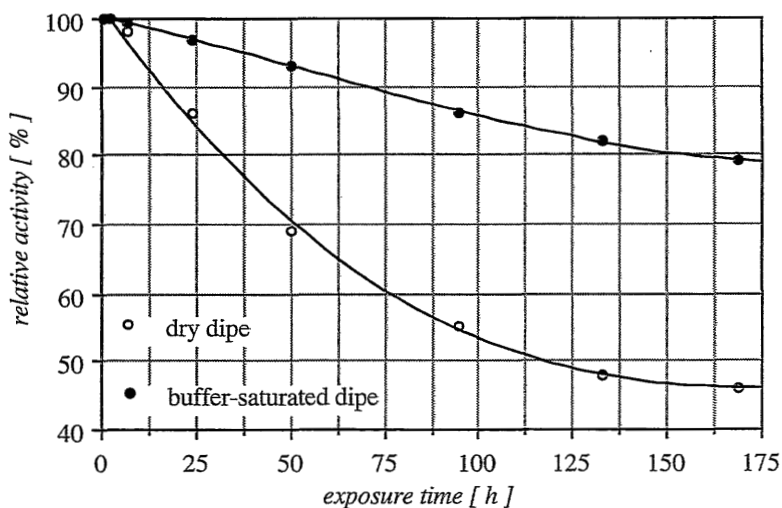
Figure 4.7 *Stability of the (R)-oxynitrilase in 0.5 m solution of the substrates in buffer-saturated di-iso-propylether and dry di-iso-propylether*

The most sensitive parameter on the enzyme stability is the content of water in the diisopropylether. A quantification of the effect will be discussed later. In figure 4.7, the results of a comparative experiment using dry and buffer saturated diisopropylether is shown. Organic solvents of low log P-value tends to desiccate the enzyme. Resulting from this, denaturation is observed. The best stabilities are observed in general by using buffer saturated media with a low amount of total water.

In the following it will be shown, that the amount of bound or dissolved water in the reaction mixture can be adjusted through post-treatment of the immobilization material.

4.3.2. Immobilisation of (R)- and (S)-Oxynitrilases

Immobilisation of the enzymes on carriers is urgently required for the large-scale technical application of bioprocesses. This is due to a higher long-term stability and a better retention of the enzymes in the reactors. In this case though, the stability obtained must be compared with losses during immobilisation. In adsorption processes, these types of losses are typically low and frequently negligible while fluctuations in ionic potential, concentration, temperature, or excessively strong shear cause a desorption of the carrier.

With respect to oxynitrilases, the following methods have already been described in publications:

adsorptive bonding: AVICEL® microcrystalline cellulose (1.35-1.43 $m^2 \cdot g^{-1}$); [1]

ECTEOLA® cellulose [5]

DEAE cellulose ® [5]

Sepharose® 4B [1]

Celite® (Ø 65 µm, 3.0 $m^2 \cdot g^{-1}$) [1]

lyotropic liquid crystals [33]

covalent bonding: Eupergit C250L® [3]

VA-Epoxy® [3]

200Å Silicagel (Ø 41 µm, 300 $m^2 \cdot g^{-1}$) [33]

controlled pore glass (CPG; 7.4 $m^2 \cdot g^{-1}$) [33]

Avicel® is a regenerated cellulose with a polymerisation degree of 500-2000. The fibrous tertiary structure is statistically oriented through hydrogen bridges by means of which a granular microcrystalline product with a very open hydrophilic network is obtained. DEAE® is more strongly basic and is frequently used to immobilise enzymes with neutral or weakly acidic isoelectric point. Ecteola®-cellulose represents a reaction product of epichlorohydrin, triethanolamine and cellulose. Sepharose® represents a macroporous ion-exchange resin on the basis of cross-linked agarose gel.

Despite the high cost of Eupergit® C, tentative immobilisation experiments were conducted. Eupergit® C is a bead co-polymer of methacrylic amide, N.N'-methylene-bis-methacrylic amide and oxirane groups supporting monomers such as glycidylmethacrylate and allyl-glycidyl ether. The macroporous, spherical material C250L with a content of reactive oxirane groups of > 200 meq·g^{-1} was chosen as a carrier for the experiments. Immobilisation in

citrate buffer solution proved suitable. After washing, carrier activity of 140 U·g^{-1} could be determined in a standard test.

The enantioselective, oxynitrilase-catalyzed reaction is in competition with the non-specific chemical addition of hydrocyanic acid during cyanohydrin formation. For this reason, in the immobilisation on Avicel®, it is important that the water content of the carrier must be set at a reproducible level. A definition of the water content of the carrier should be achieved by centrifugation, by freeze-drying and by previous complete drying and re-moistening [34].

In initial approaches, the (R)-oxynitrilase was put onto the Avicel® by means of ammonium sulfate precipitation and freeze-drying after filtration. In the lyophilisation process, the swollen Avicel® is frozen firstly at -78°C and then the water is sublimated in a high vacuum. This step is termed primary drying, and ends at a water content of roughly 30%. During subsequent secondary drying, the residual water content can be minimised by increasing temperature to 25°C. The experiments showed that the (R)-oxynitrilase was completely denatured after secondary drying. In order to avoid conformational changes during freezing, the cooling process was firstly set at 0°C and then crystallisation was induced by means of spontaneous cooling down to -78°C. Enzyme-kinetic experiments on samples, prepared in this way and then defrosted, showed no change with regard to their specific activity. Becker [8] stated that the drying process of the (R)-oxynitrilase is accompanied by a splitting of small quantities of FAD. As it was expected this splitting was not to occur until during the secondary drying process, so that the drying process was stopped at a sampling temperature of 10°C. The residual water content still amounted to 60-65% with regard to the weighed quantity of Avicel®. With regard to the standard test, the specific activity is reduced to roughly 45% by primary drying. These kinds of pretreated carriers have a specific activity of $A_{spec} = 100$ U per 1 g Avicel®.

4.4. Chemical synthesis and racemization

The racemization of homochiral cyanohydrins as a reversed cleavage reaction of enzyme-catalyzed synthesis could be observed by a decrease in the optical purity of the products during storage or at long reaction times [36]. The H-atom which is bonded to the asymmetric C-atom of the α-hydroxynitrile is acidic due to the strong electron-drawing effect of the nitrile group and therefore can easily be split off by bases [35]. The reaction equilibrium depends strongly on the structure of the carbonyl compound, in which case steric and

electronic factors play an important role. If the dissociation of HCN in diisopropylether is disregarded, then the rate of the chemical sythesis is proportional to the concentration of cyanide ions and, therefore, proportional to the pH value and the water concentration in the organic media.

$$HCN \;+\; H_2O \;\; \underset{}{\overset{K}{\rightleftharpoons}} \;\; H_3O^+ \;+\; CN^-$$

The hydrocyanic acid, with a pK_S-value of 9.31, can be considered as a very weak acid.

$$K_S^{HCN} = K \cdot [H_2O] = \frac{[CN^-] \cdot [H_3O^+]}{[HCN]} \tag{3}$$

$$v_C^+ = k_C^1 \cdot [CN^-] \cdot [A] \tag{4}$$

$$v_C^+ = k_C^1 \cdot \frac{K_S^{HCN}}{K_w} \cdot [HCN] \cdot [OH^-] \cdot [A] \tag{5}$$

The general rate equation must be extended as both the hydrocyanic acid and the carbonyl components are completely soluble in diisopropylether but the water necessary for the protolysis reaction can only be concentrated to a saturation limit of 0.86 wt.%.

$$v_C^+ = k_C^1 \cdot \frac{K_{eq}^{HCN}}{K_w} \cdot [HCN] \cdot [OH^-] \cdot [H_2O] \cdot [A] \tag{6}$$

The following applies for the reversed reaction:

$$v_C^- = k_C^{-1} \cdot \frac{K_{eq}^{HCN}}{K_w} \cdot [OH^-] \cdot [H_2O] \cdot [(R/S)\text{-}P] \tag{7}$$

Equations No. (6) and (7) can be considered as fundamental equations for describing the influence of reaction conditions on the enantiomeric excess. In this rate equation for non-enzymatic synthesis, the possibilities, in principle, for the suppression of the non-selective chemical addition of hydrocyanic acid become evident.

- Reduction in water concentration: synthesis in aprotic, organic solvent under anhydrous conditions (Effenberger).

- Reduction in base concentration: synthesis in aqueous, buffered media at low pH values (Wandrey).

•   Reduction of the dissociation constants of HCN: synthesis in solvents with a low
     dielectric constant (DK<10) (Brussee)

With respect to the formation of acetone cyanohydrin, Hustedt and Pfeil [7] observed that
the addition reaction can be completely suppressed in anhydrous media such as acetronitrile
or chloroform. However, it could be shown that just traces of water were sufficient to start
the reaction. In the first approximation, the transfer to a solvent system with 1 wt.% water
caused the same deceleration of chemical synthesis as the reduction in pH value from 5.25 to
3.25. Principal differences result additionally from the different solubility of substrates and
products. Nevertheless, the influence of pH value on enzyme-catalyzed synthesis as well as
the stability optimum of the respective oxynitrilases remain negligible. As it was not possible
to carry out successful conversions with native oxynitrilases, the treatment of a form of
kinetics corresponding to heterogeneous catalysis is required for a complete description of
the individual kinetic constants. Such a description is unsuitable for the use of a non-inert
carrier such as Avicel ® which exhibits a pronounced sorption capacity for both water and
the cyanohydrin formed. Due to this, various framework parameters were kept constant and
the individual constants for the apparent rate constants were calculated for the present
experiments.

At constant pH-value and constant water content, equations No. (6) and (7) can be
simplified through the introduction of the apparent forward and reverse rate constant of the
chemical reaction k_C. The application of equations (8) and (9) is therefore limited to buffered
systems with water content which is defined and constant with time.

$$\upsilon_C^+ \quad = \quad k_C^+ \cdot [HCN] \cdot [A] \tag{8}$$

$$\upsilon_C^- \quad = \quad k_C^- \cdot [(R/S)\text{-}P] \tag{9}$$

In *table 4.7* the measured reaction rate constants are summarized as a function of the total
water content of the reaction mixture. It can be demonstrated, that the rate constant of the
non-specific chemical formation of cyanohydrins can be decreased by a factor of appr.
50.000 or 60.000 while decreasing the water content from 10 %v/v to 0,99 %v/v or
0,01 %v/v respectively. This is done by modification of the solvent, the enzyme and the
Avicel® post-treatment. As a conclusion of experiments shown in *table 4.7*, the optimal
post-treatment results in a 0.99 %v/v of water. Because the pH-value was kept constant, the
apparent rate constant could be normalized by dividing with the water content. In this case,
for Avicel® preparations all rate constants remain in the same order of magnitude. It can be
seen, that the hydrophobic Celite® carrier results in lower chemical reaction rates. An
activating effect at the surface of the hydrophilic Avicel® is expected to occur.

Table 4.7 *Reaction rate constants for the chemical addition of 1.9m of hydrocyanic acid and 0.5m butanal in di-iso-propylether at pH 5.4 (A_{spez} = 100 $U \cdot g^{-1}$)*

enzyme preparation	water content	$k_C^+ \left[\dfrac{1}{\text{mole} \cdot \text{h}}\right]$	$\dfrac{k_C^+}{[\text{H}_2\text{O}]}\left[\dfrac{\text{l}^2}{\text{mole}^2 \cdot \text{h}}\right]$
100 $g \cdot l^{-1}$ Avicel, dry, pressing buffer saturated dipe (pH 5.4)	10-11 % v/v	$3900 \cdot 10^{-5}$	$669 \cdot 10^{-5}$
100 $g \cdot l^{-1}$ Avicel, centrifuge buffer saturated dipe (pH 5.4)	8.8 % v/v	$2100 \cdot 10^{-5}$	$430 \cdot 10^{-5}$
100 $g \cdot l^{-1}$ Avicel, dry + 100 $\mu l \cdot g^{-1}$ buffer buffer saturated dipe (pH 5.4)	1.84 % v/v	$320 \cdot 10^{-5}$	$313 \cdot 10^{-5}$
100 $g \cdot l^{-1}$ Avicel, dry + 32 $\mu l \cdot g^{-1}$ buffer buffer saturated dipe (pH 5.4)	1.18 % v/v	$101 \cdot 10^{-5}$	$154 \cdot 10^{-5}$
100 $g \cdot l^{-1}$ Avicel, dry + 100 $\mu l \cdot g^{-1}$ buffer, dry dipe	0.99 % v/v	$79 \cdot 10^{-5}$	$143 \cdot 10^{-5}$
25 $g \cdot l^{-1}$ Celite + 100 $\mu l / g$ buffer buffer saturated dipe (pH 5.4)	1.11 % v/v	$13 \cdot 10^{-5}$	$21 \cdot 10^{-5}$
no Avicel, no enzyme, buffer saturated dipe (pH 5.4)	0.87 % v/v	$2.2 \cdot 10^{-5}$	$5 \cdot 10^{-5}$
no Avicel, no enzyme, dry dipe (pH 5.4)	< 0.01 % v/v	$0.63 \cdot 10^{-6}$	——

The reproducibility of the outline conditions, particularly the water content, is of great importance for precise kinetic experiments. When the water content of the carrier is related to the quantity of Avicel® used, then a swelling of 105....115 wt.% for various operators is obtained after pressing. Through the centrifugation process described above, no substantial quantities of water could be removed with loss of enzymes. However, the fact that the various water contents level out at 88±3 wt.% proves to be an advantage. Even if carrier activity is increased to 100 $U \cdot g^{-1}$, in contrast to the standard composition of 60 $U \cdot g^{-1}$, then approximately 8 wt.% water is additionally introduced through the carrier into the water-saturated phase at an enzyme concentration of 10 $U \cdot ml^{-1}$. As these water molecules are

bonded to the Avicel® by sorption, no simple relation between the total water content and the rate of chemical addition can be determined. Due to this, the rate constants for the reduced rate law of the second order were measured in dependence on the catalyst preparations at compositions of 0.2m, 0.5m and 1.0m and the arithmetic mean was compared respectively.
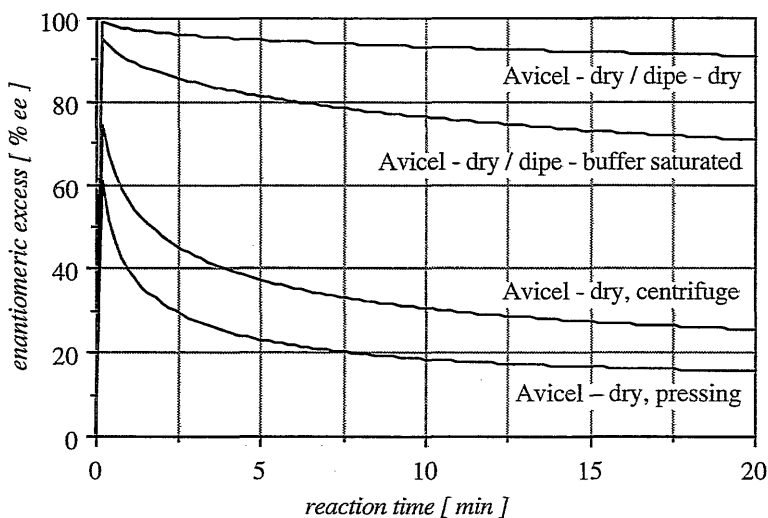
Figure 4.8 Numerical simulation of the influence of water-content on enantiomeric excess with time for the (R)-oxynitrilase

A comparison of the rate constants in *table 4.7* shows that non-stereoselective chemical addition to the racemate in an anhydrous medium can be completely suppressed. Applying dry Avicel® in a buffer-saturated di-iso-propylether at low pH-values, the proportion of the chemical reaction can also be neglected. By simulation as shown in *figure 4.8*, it was shown that in a carrier-free, buffer-saturated medium both racemization and chemical reaction can be neglected. A decrease in the enantiomeric excess, starting from homochiral cyanohydrins as shown in *figure 4.8.* indicates the reversibility of the reaction. This effect is of importance for either long reaction times with low enzyme concentrations or during storage of wet cyanohydrins.

However, by further increasing the water content, if e.g. a two-phase system is formed by adding the swollen carrier, then the rate constant k_C^+ increases proportionally to the water

content [37]. The only exception is the synthetic carrier Celite® which produces distinctly reduced rate constants. If the k_C^+ is related to the water content, then no constant value results showing that the proportionalities do not correlate solely with the molar fraction on water in the reaction system. Wehtje [27,28] could show that a better agreement can be obtained by inclusion of the surface of the heterogeneous three-phase system diisopropylether–carrier–water. In this case, the best results were also obtained with hydrophobic carriers and the rate of spontaneous addition with Celite® was still linearly dependent on carrier content. In general, it can be determined that, in the presence of hydrophilic Avicel®, the relative rate constant $k_C^+/[H_2O]$ is increased.

The molar fraction on water in the reaction system occurs in dependence on catalyst preparation from the sorbed proportion of the carrier, on the concentration of the enzyme concentrate and on the dissolved proportion in the diisopropylether. As long-term stability of the oxynitrilases does only occur in a non-hygroscopic medium, i.e. with completely hydrated enzymes, only buffer-saturated media can be used. In this way, the total water content can be minimized only by using minimum carrier quantities and enzyme solutions with maximum concentration. By using undiluted enzyme concentrates, a water content of 1.18 vol% and a $k_C^+ = 101 \cdot 10^{-5}$ $l \cdot mol^{-1} \cdot h^{-1}$ can be achieved. In this case, however, the distribution of the enzyme on the carrier is hardly reproducible so that finally a more diluted enzyme solution and therefore an increased water content of 1.84 vol% and a $k_C^+ = 320 \cdot 10^{-5}$ $l \cdot mol^{-1} \cdot h^{-1}$ must be accepted. The thus increased unspecific formation of racemic cyanohydrin is not quite so evident, as, according to Wehtje, the rate of the enzymatic reaction is also proportional to the water concentration and will not reach a maximum until the organic phase is completely saturated.

As a consequence for the preparative production of optically active cyanohydrins, the quantity of enzyme must be subsequently chosen so that the rate of the enzymatic synthesis must exceed the chemical synthesis by the factor of at least 100. The condition is fulfilled by the standard composition while the enzyme concentration cannot be reduced further without reducing the optical yield. As the competition between enzymatic and chemical synthesis is valid for both the forward and the reversed reactions, the proportion of the non-stereoselective chemical reaction can easily be seen by means of the racemization of the cyanohydrins.

4.5. Enzyme-kinetic characterisation of the oxynitrilase-catalysed cyanohydrin synthesis

A kinetic characterisation of the enzymatic cyanohydrin synthesis has to be carried out in order to obtain a data basis of the assessment of attainable space-time yields. Different conventional bioreactors have to be compared with the novel enzyme-membrane reactor with selective product recovery. As has already been described, a sequential ordered bi uni mechanism can be used as a basis. The determination of kinetic constants was conducted on the basis of time-activity curves. To this end, the concentration of derivatised (R)- and (S)-cyanohydrins as a function of time was determined by chromatography with the assistance of chiral β-cyclodextrin capillary columns after continuous sampling. It was not possible to carry out a continuous photometric or polarimetric determination of concentration and optical yield with sufficient accuracy. Both methods were mostly used as an in-line control of the GC measurements. In this case, problems are caused in particular by the poor transmission co-efficient of the diisopropylether. During substrate concentration variation, all other parameters were kept constant. In this case, no variation in temperature took place as at temperatures above 20°C, losses by evaporation due to the high partial vapour pressure cannot be ruled out. Simultaneously, a constant argon pressure of 100 mbar was installed above the reaction mixture. The excess pressure was applied as both delivery pressure during sampling and as a rapid indication of leakages with the aid of a hydrocyanic acid sensor. The stirring velocity was specified as constant at 450 min^{-1} and preliminary studies showed that a minimum number of revolutions of 200 min^{-1} can be considered necessary for reproducible measurements.

As the heterogeneous reaction system can also be considered as a two-phase system, then diffusion limitations are to be expected in an inadequately mixed system. The initial rates as shown in *figure 4.9* and *figure 4.10.* for different butanal and hydrocyanic acid concentrations respectively were determined by non-linear regression and subsequent mean value formation. Steady-state ordered bi uni kinetics were applied as a base for the evaluation of K_m and K_i values. In this case, the kinetic constants were firstly determined from the reciprocal primary and secondary diagrams and verified for various activity curves by parameter identification [19].The reproducibility of the measurements is sufficient as long as post-treatment of the enzyme and the carrier, degassing of the stirred cell and purification of the aldehyde are perfect. Already traces of butyric acid, resulting from the oxidation of the aldehyde, yield in a strong inhibition of the enzymatic reaction.
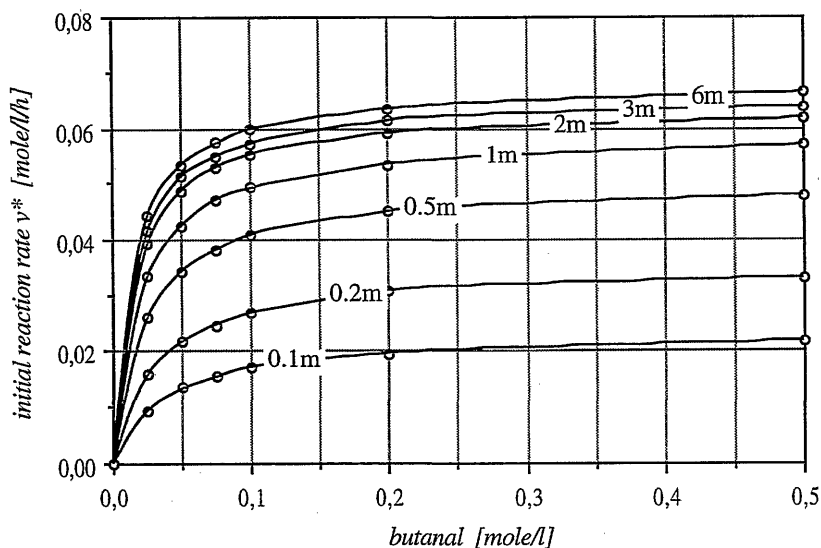
Figure 4.9 *Initial rate kinetics of (R)-oxynitrilase catalyzed addition of hydrocyanic acid to different concentrations of butanal*
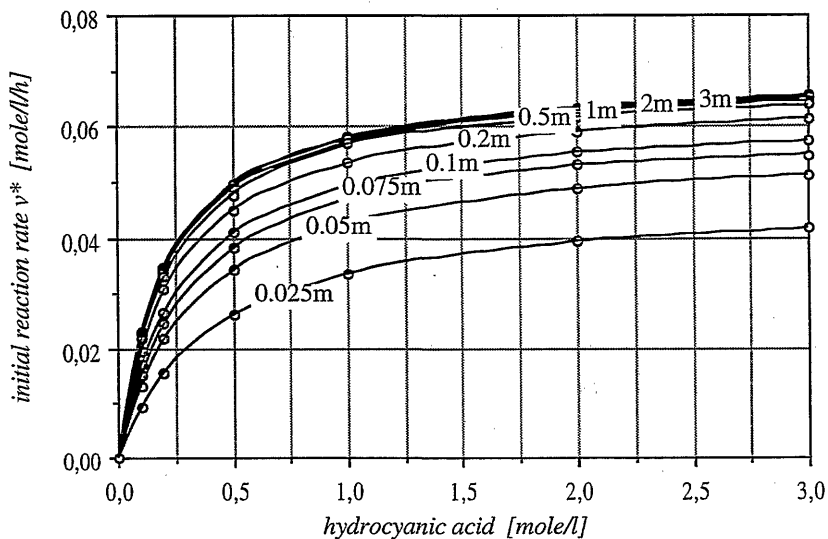
Figure 4.10 *Initial rate kinetics of (R)-oxynitrilase catalyzed addition of different concentrations of hydrocyanic acid to butanal*

The initial rates obtained produced approximately linear relationships in the reciprocal diagrams. For this purpose, the complete rate equation for the forward reaction under initial conditions at $[P] \to 0$ was simplified.

$$\upsilon = \frac{V_{max}^{+}\,[A]\,[B] - V_{max}^{-}\,\dfrac{K_{m,B}\cdot K_{i,A}}{K_{m,P}}\,[P]}{K_{m,B}\cdot K_{i,A} + K_{m,B}\cdot[A] + K_{m,A}\cdot[B] + \dfrac{K_{m,A}}{K_{i,P}}\,[B][P] + \dfrac{K_{i,B}\cdot K_{m,A}}{K_{i,P}}\,[P] + [A][B]}$$

The reversed reaction can be disregarded for the dependence of the initial rate on the initial concentration of [A] and [B] of the ordered bi uni reaction.

$$\frac{\upsilon}{V_{max}^{+}} = \frac{[A]}{\dfrac{K_{m,B}\cdot K_{i,A}}{[B]} + \dfrac{K_{i,B}\cdot K_{m,A}}{K_{i,P}}\dfrac{[P]}{[B]} + K_{m,A} + K_{m,B}\cdot\dfrac{[A]}{[B]} + \dfrac{K_{m,A}}{K_{i,P}}[P] + [A]}$$

$$\frac{\upsilon}{V_{max}^{+}} = \frac{[B]}{\dfrac{K_{m,B}\cdot K_{i,A}}{[A]} + K_{m,B} + K_{m,A}\dfrac{[B]}{[A]} + \dfrac{K_{m,A}}{K_{i,P}}\dfrac{[B][P]}{[A]} + \dfrac{K_{i,B}\cdot K_{m,A}}{K_{i,P}}\dfrac{[P]}{[A]} + [B]}$$

It becomes evident again that the product [P] acts as a competitive inhibitor over the entire concentration range. Through saturation of [B], the apparent V_{max}^{*} becomes V_{max}, however, the dependence of $K_{m,A}$ on [P] remains.

$$\frac{\upsilon}{V_{max}^{+}} = \frac{[A]}{K_{m,A}\left(1 + \dfrac{K_{i,A}}{K_{m,A}}\dfrac{K_{m,B}}{[B]} + \dfrac{K_{i,B}}{K_{i,P}}\dfrac{[P]}{[B]} + \dfrac{[P]}{K_{i,P}}\right) + [A]\left(1 + \dfrac{K_{m,B}}{[B]}\right)}$$

$$\frac{\upsilon}{V_{max}^{+}} = \frac{[B]}{K_{m,B} + \left(1 + \dfrac{K_{i,A}}{[A]} + \dfrac{K_{i,A}\cdot[P]}{K_{m,P}\,[A]}\right) + [B]\left(1 + \dfrac{K_{m,A}}{[A]} + \dfrac{K_{m,A}}{K_{i,P}}\dfrac{[P]}{[A]}\right)}$$

The determination of kinetic parameters was carried out by non-linear regression by using numerical methods such as Runge-Kutta. $K_{m,A}$, $K_{m,B}$, $K_{i,A}$ and $K_{i,B}$ must be preserved from the Lineweaver-Burks plots [19] in the absence of the product [P]. $K_{m,P}$ and $K_{i,P}$ are determined by the secondary diagram during product inhibition. The constants $K_{i,A}$ and $K_{i,P}$ are equivalent to the real dissociation constants.

$$\frac{1}{\upsilon} = \frac{1}{V_{max}^{+}}\left(1 + \frac{K_{m,B}}{[B]}\right) + \frac{K_{m,A}}{V_{max}^{+}}\left(1 + \frac{K_{i,A}}{K_{m,A}}\frac{K_{m,B}}{[B]} + \frac{K_{i,B}}{K_{i,P}}\frac{[P]}{[B]} + \frac{[P]}{K_{i,P}}\right)\frac{1}{[A]}$$

$$\frac{1}{\upsilon} = \frac{1}{V_{max}^{+}}\left(1 + \frac{K_{m,A}}{[A]} + \frac{K_{m,A}}{K_{i,P}}\frac{[P]}{[A]}\right) + \frac{K_{m,B}}{V_{max}^{+}}\left(1 + \frac{K_{i,A}}{[A]} + \frac{K_{i,A}\cdot[P]}{K_{m,P}\,[A]}\right)\cdot\frac{1}{[B]}$$

In the absence of the product ([P] = 0) the reciprocal diagrams can be simplified as follows:

$$\frac{1}{\upsilon} = \frac{1}{V_{max}^{+}}\left(1 + \frac{K_{m,B}}{[B]}\right) + \frac{K_{m,A}}{V_{max}^{+}}\left(1 + \frac{K_{i,B}}{K_{i,P}}\frac{K_{m,P}}{[B]}\right)\frac{1}{[A]}$$

$$\frac{1}{\upsilon} = \frac{1}{V_{max}^{+}}\left(1 + \frac{K_{m,A}}{[A]}\right) + \frac{K_{m,B}}{V_{max}^{+}}\left(1 + \frac{K_{i,A}}{[A]}\right)\frac{1}{[B]}$$

From the Lineweaver-Burks diagrams for butanal and for hydrocyanic acid, the secondary diagrams were formed and V_{max}^{+}, $K_{m,A}$, $K_{m,B}$ as well as $K_{i,A}$ were calculated. The resulting linear equations showed good agreement at a regression coefficient of $r^2 > 0.98$.

$$\frac{1}{V_{max}^{*}} = \frac{1}{V_{max}^{+}} + \frac{K_{m,B}}{V_{max}^{+}}\frac{1}{[B]} = 14.293 + 0.169\,[B]^{-1}$$

$$\left(\frac{K_{m,A}}{V_{max}^{+}}\right)^{*} = \frac{K_{m,A}}{V_{max}^{+}} + \frac{K_{i,A}\cdot K_{m,B}}{V_{max}^{+}}\frac{1}{[B]} = 2.842 + 0.1443\,[B]^{-1}$$

From this linear equation, the kinetic constants for the (R)-oxynitrilase catalyzed addition of hydrocyanic acid to butanal can be calculated as summarized in *table 4.8.*

Table 4.8 *Characterisation of (R)-oxynitrilase catalyzed addition of hydrocyanic acid to butanal. Kinetic constants were obained from Lineweaver-Burks plots and the corresponding secondary diagrams using numerical non-linear Runge-Kutta procedure.*

maximum reaction rate	V_{max}^{+}	$= 69.9\,\frac{meq}{l\cdot min}$
Michaelis-Menten constant	$K_{m,A}$	$= 11.9\,\frac{meq}{l}$
Michaelis-Menten constant	$K_{m,B}$	$= 198.9\,\frac{meq}{l}$
Inhibition constant	$K_{i,A}$	$= 50.8\,\frac{meq}{l}$
apparent inhibition constant	$K_{i,B}^{*}$	$= 849.7\,\frac{meq}{l}$
specific activity	A_{spez}^{+}	$= 489.9\,\frac{U}{mg}$
molecular activity	k_{cat}	$= 27917\,\frac{U}{\mu mol}$
catalytic efficiency	$\left(\frac{k_{cat}}{K_{m,A}}\right)$	$= 2350\,\frac{1}{min\cdot meq}$

$*A_{spez}^{E} = 70\,\frac{U}{mg}$, $\overline{M_w} = 57$ kDa

The molecular activity k_{cat} is frequently termed, turnover number (TN), and is equivalent to a rate constant for product formation. The apparent inhibition constant of hydrocyanic acid expresses the relationship of product inhibition and is defined by $K_{i,B}^* = K_{i,B} \cdot K_{m,P} \cdot (K_{i,P})^{-1}$.

It could be shown that the (R)-oxynitrilase exhibits an excellent affinity to butanal, but that the affinity with regard to hydrocyanic acid is very low. In general, inhibition by hydrocyanic acid seems to be negligible. The specific activity of the reaction of butanal with hydrocyanic acid in an organic medium is roughly seven times quicker that the reaction of benzaldehyde with hydrocyanic acid under standard conditions. The specific activity of 490 U·mg^{-1} is equivalent to a maximum product formation rate of 2,88 g per hour and mg of enzyme. At a typical enzyme concentration of 10 U·ml^{-1}, a maximum 4,19 mole·l^{-1}·h^{-1} or 416 g·l^{-1}·h^{-1} of butanal cyanohydrin is formed. The specific activity of the reaction would be increased to 3688 U·mg^{-1}, if a highly purified (R)-oxynitrilase with $A_{spez}^E = 527$ U·mg^{-1} according to Kragl [12] is used.
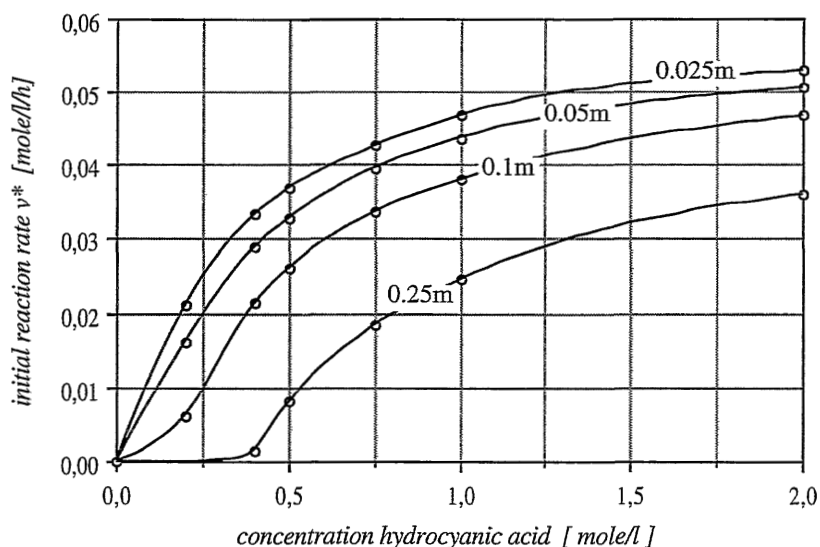
Figure 4.11   *Product inhibition of (R)-2-hydroxypentanenitrile on (R)-oxynitrilase catalyzed addition of hydrocyanic acid to butanal*

It was not possible to determine the constants $K_{m,P}$ and $K_{i,P}$ during product formation with sufficient accuracy, by graphical means from *figure 4.11*. The sensitivity of the reciprocal Lineweaver-Burks diagram could not be fulfilled satisfactorily through gas-chromatographic

sample analysis. In this case, only non-linear numerical methods were applied. However, Kragl's experiments show that the (S)-enantiomer of the cyanohydrin has a non inhibiting effect on the (R)-oxynitrilase.

In order to rule out systematic errors, for example, by sampling or diffusion limitations on the Avicel® cellulose and deduce non-stationary effects due to the decreasing organic volume caused by sampling, further series of measurements were carried out, in which one substrate was respectively submitted as saturated. The enzyme in diisopropylether together with the hydrocyanic acid was submitted and the reaction was started by injecting butanal in a closed auto-sampler vial. This procedure has the advantage that errors as a result of loss by evaporation during the addition of hydrocyanic acid can be ruled out. After exactly three minutes, the reaction was stopped by injecting the derivatisation reagent and the mixture was analysed.
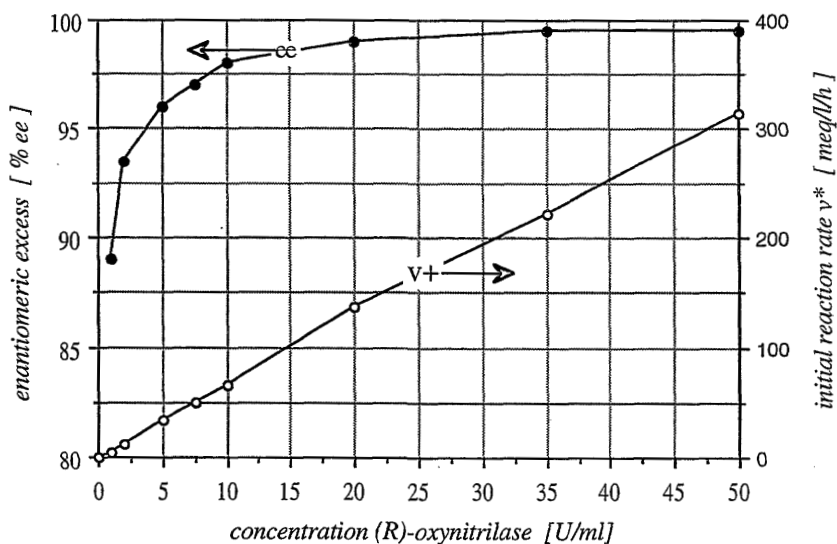
Figure 4.12   *Influence of the concentration of (R)-oxynitrilase on initial reaction rate and on optical purity of the product*

At saturation with regard to the butanal with 4 M of solution and with regard to the hydrocyanic acid with 6 M of solution for V_{max}^{+}, $K_{m,A}$ and $K_{m,B}$ deviations $< 5\%$ resulted in a relation to the above-mentioned kinetic constants. Moreover, between $0 < [E]_0 <$

50 U·ml^{-1}, a strongly linear dependence of the maximum rate, as shown in *figure 4.12* on enzyme concentration could be confirmed.

The competition for chemical reaction can also be considered in dependence on enzyme concentration. This is expressed by a decreasing optical yield with sinking enzyme concentration. An increased water content on the carrier, caused by the enzyme preparation, accelerates, as already explained, both the chemical and the enzymatic reaction. In this way, the product formation rate V_{max}^{+} can be controlled while maintaining a sufficiently high optical purity caused by the increase in enzyme concentration. The kinetic constants $K_{m,A}$, $K_{m,B}$, $K_{i,A}$, $K_{i,B}$, $K_{m,P}$ und $K_{i,P}$ remain uninfluenced by the water content of the reaction mixture. The above results were obtained with a defined and reproducible water content, however can be transferred with the exception of the specific activity A_{spez}^{+} to the reaction conditions which are further discussed in the following.

4.5.1. Interactions of inhibitors with the substrate

In the experimental determination of yield-time diagrams, sigmoid curves were frequently found [42]. First it was speculated whether this is due to a systematic error based on time-function elements in sampling and sample treatment. In double reciprocal application, non-linear functions result. Such a deviation from the usual Michaelis-Menten kinetics can be based on experimental artefacts such as aggregation, ionic effects or similar factors. If these possibilities are to be ruled out, then the presence of substrate inhibition or activation, of allosteric effects or of a random mechanism must be examined. However, a qualitative analysis of the kinetics observed showed that the course of the curve can be explained respectively by the interaction of an inhibitor with the substrate as shown in *figure 4.13*.

$$
\begin{array}{cccccc}
E & + & A & \underset{k_{-A}}{\overset{k_{A}}{\rightleftharpoons}} & EA & \\
 & & + & & + & \\
 & & I & & B & \\
 & & k_{-I} \uparrow \downarrow k_{I} & & k_{-\alpha B} \uparrow \downarrow k_{\alpha B} & \\
EAI & \underset{k_{-AI}}{\overset{k_{AI}}{\rightleftharpoons}} & A \cdot I & & EAB & \overset{k_{P}}{\longrightarrow} \quad E \quad + \quad P
\end{array}
$$
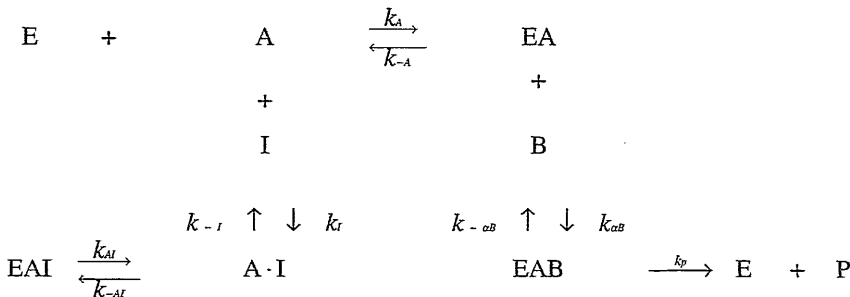
Figure 4.13   *Typical reaction sequence for inhibition of the substrate*

One phenomenon is the reaction of the aldehyde with traces of atmospheric oxygen to carboxylic acid and the well-known resulting inhibition. By the specific addition of organic acids, i.e. by adding butyric acid, the effect of sigmoid activity curves can easily be intensified as demonstrated in *figure 4.14*.

The presence of atmospheric oxygen in the reaction mixture is based on the use of Avicel® as a carrier for the oxynitrilases. The microcrystalline cellulose is also an excellent sorbent for oxygen. By vacuum drying and aeration with argon, an oxygen-free atmosphere suitable for reproducible kinetic experiments can be produced in the reaction mixture.
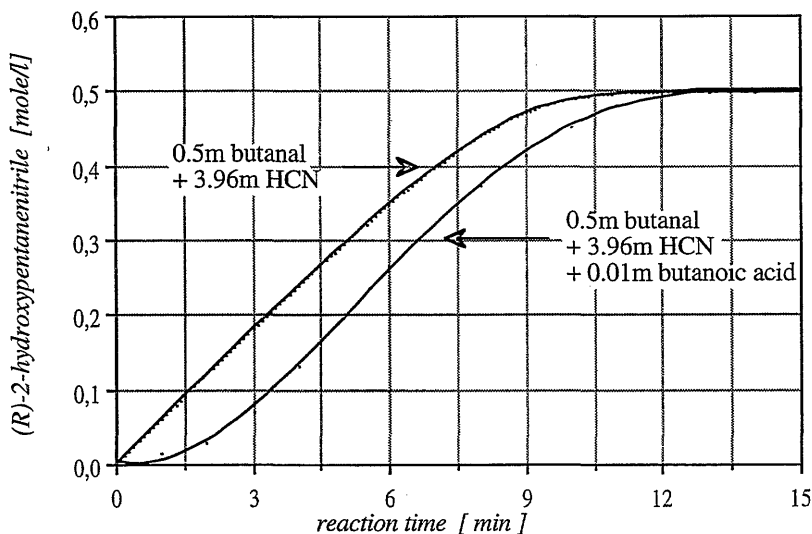
Figure 4.14   *Sigmoide reaction curve for product inhibition*

4.5.2.   Identification of kinetic constants

For the modelling of cyanohydrin synthesis, the simplified model of reversible bi-substrate kinetics random bi uni was firstly specified.

$$E \quad + \quad A \quad \underset{}{\xrightleftharpoons{K_1}} \quad [EA] \qquad K_1 = \frac{[E]\,[A]}{[EA]}$$

$$E \quad + \quad B \quad \underset{}{\xrightleftharpoons{K_2}} \quad [EB] \qquad K_2 = \frac{[E]\,[B]}{[EB]}$$

$$[EA] \quad + \quad B \quad \underset{}{\xrightleftharpoons{K_{12}}} \quad [EAB] \qquad K_{12} = \frac{[EA][B]}{[EAB]}$$

$$[EB] \quad + \quad A \quad \underset{}{\xrightleftharpoons{K_{21}}} \quad [EAB] \qquad K_{21} = \frac{[EB][A]}{[EAB]}$$

$$[EAB] \quad \underset{}{\xrightleftharpoons{k_3^+\,/\,k_3^-}} \quad P \quad + \quad E$$
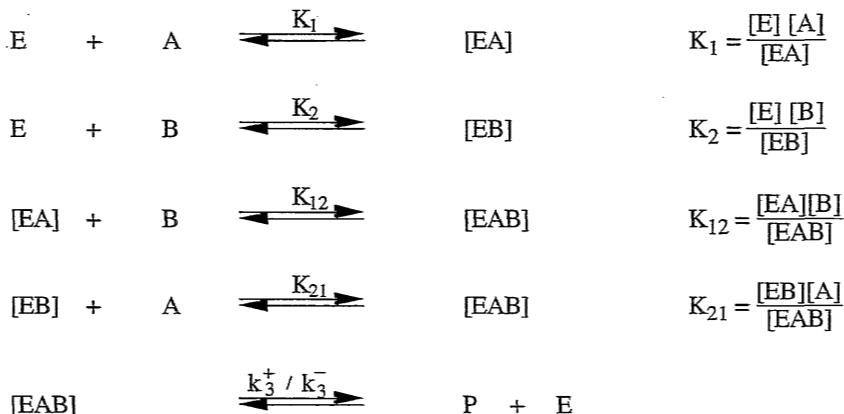
The result of the linkage of the relationships of K_{12} and K_{21} is:

$$\frac{[A]\cdot[B]\cdot[E]}{[EAB[} = k_1\cdot k_{12} = k_2\cdot k_{21}$$

The rate equation can be expressed by means of a rapid equilibrium assumption as follows:

$$\upsilon^E \quad = \left[\frac{d(R)\text{-}P}{dt}\right]^E = k_3^+\cdot[EAB] - k_3^-\cdot[(R)\text{-}P]\cdot[E]$$

By means of the equation of the conservation of mass, a linkage to $[E]_0$ is obtained:

$$[E]_0 \quad = [E] + [EA] + [EB] + [EAB]$$

$$[E]_0 \quad = [E] + \frac{[E]\cdot[A]}{k_1} + \frac{[E]\cdot[B]}{k_2} + \frac{[E]\cdot[A]\,[B]}{k_1\cdot k_{12}}$$

$$[E]_0 \quad = [E]\left(1 + \frac{[A]}{k_1} + \frac{[B]}{k_2} + \frac{[A][B]}{k_1\cdot k_{12}}\right) = [E]\left(\frac{k_1\cdot k_{12} + k_{12}\cdot[A] + k_{21}\cdot[B] + [A][B]}{k_1\cdot k_{12}}\right)$$

$$\upsilon \quad = [E]\left(\frac{k_3^+\cdot[A][B]}{k_1 k_{12}} - k_3^-\cdot[(R)\text{-}P]\right)$$

$$\upsilon \quad = [E]_0 \frac{k_3^+\cdot[A][B] - k_3^-\cdot k_1\cdot k_{12}\cdot[(R)\text{-}P]}{k_1\cdot k_{12} + k_{12}\cdot[A] + k_{21}\cdot[B] + [A][B]}$$

$$\upsilon \quad = \frac{V_{max}^+\cdot[A]\,[B] - V_{max}^-\cdot k_1 k_{12}\,[(R)\text{-}P]}{k_1 k_{12} + k_{12}\cdot[A] + k_{21}\cdot[B] + [A][B]}$$

The enzymatic stereoselective reaction is in competition to the chemical undifferentiated addition of hydrocyanic acid to aldehyde.

$$[A] \quad + \quad [B] \quad \xrightleftharpoons{k_C^+ / k_C^-} \quad [(R)\text{-}P] \quad + \quad [(S)\text{-}P]$$

$$\upsilon^C \quad = \left[\frac{d(R)\text{-}P}{dt}\right]^C = \left[\frac{d(S)\text{-}P}{dt}\right]^C = k_C^+ \cdot [A] \cdot [B] - k_C^- \cdot [P]$$

Finally four differential equations for mass equilibrium result from the derivation of the kinetic equations.

$$\frac{d(R)\text{-}P}{dt} = \left[\frac{d(R)\text{-}P}{dt}\right]^E + \left[\frac{d(R)\text{-}P}{dt}\right]^C$$

$$\frac{d(S)\text{-}P}{dt} = \left[\frac{d(S)\text{-}P}{dt}\right]^C$$

$$\frac{dA}{dt} = \left[\frac{dA}{dt}\right]^E + \left[\frac{dA}{dt}\right]^C$$

$$\frac{dB}{dt} = \left[\frac{dB}{dt}\right]^E + \left[\frac{dB}{dt}\right]^C$$
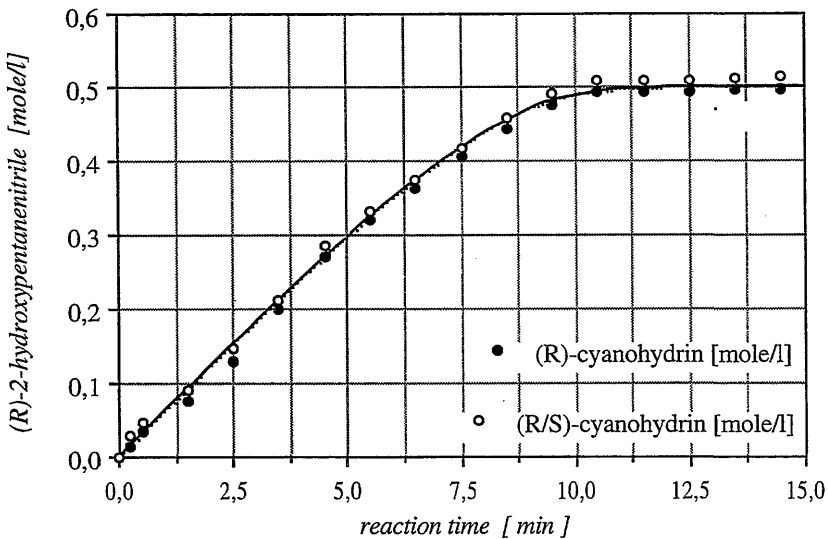
Figure 4.15   *Comparison of experimental data with parameter identification assuming random bi uni mechanism (initial value $[A]^0 = 0.512 \frac{mol}{l}$ and $[B]^0 = 1.0507 \frac{mol}{l}$)*

Then this model was tested in the simulation language ACSL (Mitchell & Gauthier, USA) by VAX/VMS (Digital Equipment, USA) and was later translated into the simulation language SIMUL_R. Parameter adjustment was carried out by means of a non-linear numerical optimisation as shown in *figure 4.15*.

Chemical reaction was both considered and disregarded for the parameter identification shown in *figure 4.15*. By assuming simple reversible bi-substrate kinetics in the lower concentration areas, at $0 < [A] < 0.5$ M this parameter identification resulted in a good correlation with the time-activity curves measured. However, a negative deviation from the simulation was observed for high substrate concentrations. To a certain extent, this deviation could also be explained by experimental errors. At high substrate concentrations only reduced concentrations have an effect with regard to the enzymatic reaction as a result of the distribution coefficients between the organic and the aqueous phase.

Table 4.9   *Characterisation of (R)-oxynitrilase catalyzed addition of hydrocyanic acid to butanal. Kinetic constants were obained from parameter identification based on a random bi uni mechanism.*

parameter	dimension	incl. chemical reaction	without chem. reaction	comments
V_{max}^+	$\dfrac{meq}{l \cdot min}$	61.2	67.7	$V_{max}^+ = k_3^+ \cdot [E]_t$
V_{max}^-	$\dfrac{meq}{l \cdot min}$	0.78	0.8003	$V_{max}^+ = k_3^- \cdot [E]_t$
K_1	$\dfrac{meq}{l}$	30	37.4	$K_{i,A}$
K_{12}	$\dfrac{meq}{l}$	1.47	1.72	$K_{m,B}$
K_{21}	$\dfrac{meq}{l}$	38.9	48.8	$K_{m,A}$
k_C^+	$\dfrac{1}{mole \cdot min}$	0.00710	–	chemical addition
k_C^-	min^{-1}	0.0000167	–	chemical cleavage

According to studies by Jorns [32], a random uni bi or a random bi uni mechanism produces no linear Lineweaver plots, unless a substrate is present in a clearly saturated form. In order to judge the deviations which occur, the model was extended to a steady state ordered bi uni mechanism as is described above. The results from computer parameter identification are shown in *figure 4.10*.

Table 4.10 *Comparison of random bi uni and ordered bi uni mechanism for (R)-oxynitrilase catalyzed addition of hydrocyanic acid to butanal*

mechanism		random bi uni		ordered bi uni		
concentration		0.5M	0.5 M	1.0 M	0.5 M	0.2 M
method		graphical	identified	identified	identified	identified
V_{max}^+	$\left(\frac{meq}{l \cdot min}\right)$	69,09	61,2	62,7	57,1	36,4
V_{max}^-	$\left(\frac{meq}{l \cdot min}\right)$	0,145	0,78	0,0841	0,0826	0,0726
$K_{m,A}$	$\left(\frac{meq}{l}\right)$	53,39	38,9	14,3	24,7	9,63
$K_{m,B}$	$\left(\frac{meq}{l}\right)$	0,0813	1,47	0,0870	0,0857	0,0766
$K_{m,P}$	$\left(\frac{meq}{l}\right)$	0,0561	–	0,0905	0,0918	0,0947
$K_{i,A}$	$\left(\frac{meq}{l}\right)$	0,0999	30,1	0,0841	0,0827	0,0727
$K_{i,B}$	$\left(\frac{meq}{l}\right)$	–	–	0,0917	0,0917	0,0916
$K_{i,R}$	$\left(\frac{meq}{l}\right)$	0,8236	–	0,1018	0,1002	0,1015
k_C^+	$\left(\frac{1}{mole \cdot min}\right)$	1,793e-5	7,10e-3	9,59e-3	4,82e-3	3,823e-5
k_C^-	(min^{-1})	6,727e-6	1,67e-5	0,175e-3	0,388e-3	4,937e-6

For this model, the region of validity is extended to the entire, experimentally tested concentration area between $0 < [A] < 2M$ of both substrates. Conversions at higher substrate concentrations are possible in principle, but no kinetic analysis can be conducted due to the rapid reaction times and due to the marginally reproducible water content of the

swollen Avicel® cellulose. Up to an aldehyde concentration of approx. 2m, the water content of the organic phase can be considered as almost constant. With further increasing aldehyde and hydrocyanic acid concentrations, the solubility of water in the organic phase also increases. This is expressed by a decreasing optical purity, as at a pH value of 5.6, the chemical non-selective addition can be no longer neglected.

In order to additionally assess the fundamental reaction mechanism and to examine the identified kinetics, a classic evaluation according to the Lineweaver-Burk primary and secondary diagrams was carried out. Also in this case, good agreement with a steady-state ordered bi uni mechanism could be achieved. The kinetic constants were determined from the initial rates by means of a non-linear regression with a simplex algorithm with the aid of SYSTAT ® (Systat Inc., Evanston, USA). A comparison of parameter identification and experimental data is presented in *figure 4.15*.
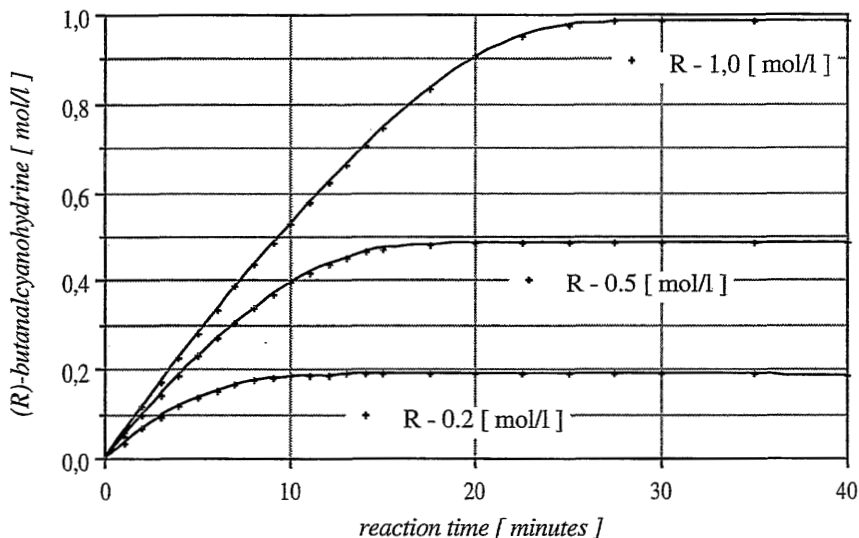
Figure 4.16   *Comparison of experimental data with parameter identification assuming an ordered bi uni model*

The equilibrium of cyanohydrin synthesis for aliphatic aldehydes is almost completely on the product side. The equilibrium constants decrease as molecular weight of the aliphatic residue increases. The following equilibrium constants of formation can be found for the addition of hydrocyanic acid to non-hydrated aldehydes [45].

formaldehyde	$K_B = 1.09 \cdot 10^{-9}$ mol$\cdot$l^{-1}
acetaldehyde	$K_B = 2.74 \cdot 10^{-5}$ mol$\cdot$l^{-1}
acetone	$K_B = 7.16 \cdot 10^{-2}$ mol$\cdot$l^{-1}
benzaldehyde	$K_B = 5.14 \cdot 10^{-3}$ mol$\cdot$l^{-1}
p-methylbenzaldehyde	$K_B = 9.62 \cdot 10^{-3}$ mol$\cdot$l^{-1}
p-hydroxybenzaldehyde	$K_B = 3.62 \cdot 10^{-2}$ mol$\cdot$l^{-1}

From the Hammett relation, established by Niedermeyer [5], a formation constant comparable to the unsubstituted benzaldehyde can be expected for m-phenoxybenzaldehyde. The formation constants increase with rising temperatures, i.e. the reaction equilibrium is shifted in the direction of the substrate. Parallel to the equilibrium constants, there is the tendency towards racemization of the chiral cyanohydrins [43].

Deviations of the apparent equilibrium constant, calculated from the relationship of the kinetic constants, can also be partly based on the distribution equilibrium between the organic and the aqueous phase. According to Wehtje [28], HCN has, in the system DIPE/H$_2$O, a distribution coefficient of approx. = 1. In contrast, benzaldehyde, for example, with a distribution coefficient of 66 is more in the organic phase. The product, i.e. the cyanohydrine can be considered as polar, and becomes concentrated in the aqueous phase. Resulting from this a low distibution coefficient, which has a negative influence on both the equilibrium constant and the apparent rate constant of the enzymatic reaction, is obtained for butanal cyanohydrin.

4.5.3. Comparison of the models and the kinetic constants with previous publications

Similar experiments as reported for the (R)-oxynitrilase and butanal were carried out for the (S)-oxynitrilase and meta-phenoxybenzaldehyde as a typical substrate useful in the synthesis of pyrethroids. In order to limit the amount of experimental data, both complete kinetics, chiral gas chromatography and modelling are not included in this chapter. *Table (I).4.11* will summarize all kinetic data, important for selection of an appropriate bioreactor. An ordered-bi-uni mechanism has to be applied in order to compare results of batch and continuous results.

Both substrates of this thesis have not been described in literature. Kinetic data are reported by work groups of Wandrey [12] for (R)-oxynitrilase and Kula [44] for (S)-oxynitrilase. Typically, only aromatic aldehydes are used. Wandrey concentrated on the natural substrate benzaldehyde according to the work done by Becker and Pfleil [8]. Kinetic data obtained from benzaldehyde correspond with the reaction rate and reaction constants at standard conditions.

Table 4.11 *Comparison of (R)-oxynitrilase and (S)-oxynitrilase catalysed addition of hydrocyanic acid to butanal. The data are compared to those obtained from literature.*

enzyme		(R)-oxynitrilase		(S)-oxynitrilase	
concentration		butanal	benzaldehyde	m-phenoxy-benzaldehyde	p-hydroxy-benzaldehyde
reference		this work	Wandrey et.al.	this work	Kula et.al.
V_{max}^+	$\left(\dfrac{meq}{l\cdot min}\right)$	69	1.002	50,20	84
V_{max}^-	$\left(\dfrac{meq}{l\cdot min}\right)$	0,145	143	4,80	26,6
A_{spez}^+	$\left(\dfrac{U}{mg\ protein}\right)$	2.415	527*	187	153
K_{cat}^+	$\left(\dfrac{U}{\mu mole}\right)$	137.655	31.620	22.440	18.972
$\dfrac{K_{cat}}{K_{m,A}}$	$\left(\dfrac{1}{min\cdot meq}\right)$	2.597	68.739	369	31.101
$K_{m,A}$	$\left(\dfrac{meq}{l}\right)$	53	0,46	60,69	0,61
$K_{m,B}$	$\left(\dfrac{meq}{l}\right)$	0,0813	711	52,11	264
$K_{m,P}$	$\left(\dfrac{meq}{l}\right)$	0,0561	1,05	115,8	1,74
$K_{i,A}$	$\left(\dfrac{meq}{l}\right)$	0,0999	0,37	50,92	0,32
$K_{i,B}$	$\left(\dfrac{meq}{l}\right)$	–	72,5	92,64	17,3
$K_{i,R}$	$\left(\dfrac{meq}{l}\right)$	0,8236	7,19	86,39	1,7
k_C^+	$\left(\dfrac{1}{mole\cdot min}\right)$	1,793e-5	1,452e-2	5,77e-4	
k_C^-	$\left(min^{-1}\right)$	6,727e-6	5,136e-5	1,743e-6	

Particularly in the presence of competitive inhibitors, the expression of the so-called catalytic effectiveness $\frac{K_{cat}}{K_{m,A}}$ as a relevant parameter is helpful. In general, higher space-time yields can be expected when catalytic effectivness is increased.

Enzymes used by Wandrey [12] and Kula [44] were of higher purity and by this the specific activity was rather high. However, for any practical application enzyme losses during purification and improved space-time yields due to higher catalyst purity have to be compared. Therefore, Brussee [10] recommends using an almond meal which is not purified according the Becker and Pfeil [7] procedure followed by affinity chromatography.

4.6. Conclusions

In this chapter, the complete enzyme-kinetics in organic media of the (R)-oxynitrilase catalyzed addition of hydrocyanic acid to butanal is described. Furthermore, the same data are measured for the (S)-oxynitrilase catalyzed addition of hydrocyanic acid to 3-phenoxybenzaldehyde and summarized in a table.

First of all, the stability of the enzyme in various organic solvents was investigated. Further experiments such as immobilization on microcrystalline cellulose and kinetics were carried out in diisopropylether as the best solvent. A detailed analysis on the influence of the water content on the reaction rate and on the enantiomeric excess is described. The characterization of enzyme kinetics is based on standard conditions using the solvent diisopropylether and a Avicel® for a immobilization material.

The kinetics were calculated on the basis of initial rate equations and from parameter identification experiments. It can be shown, that the kinetics of both enzymes fit perfectly with an ordered bi-uni mechanism.

List of Symbols

A	substrate A (aldehyde)
B	substrate B (hydrocyanic acid)
E	enzyme (oxynitrilase)
P	product P (cyanohydrin)
I	inhibitor I (e.g. butyric acid)
EA	binary enzyme-substrate complex
EB	binary enzyme-substrate complex
EAB	tertiary enzyme-substrate complex
EP	binary enzyme-product complex
EI	binary enzyme-inhibitor complex
$[CN^-]$	concentration of cyanide ions
$[H_3O^+]$	concentration of protons (pH-value]
$[HCN]$	concentration of hydrocyanic acid
$[A]$	concentration of the aldehyde
$[P]$	concentration of the cyanohydrin
$[(R/S)\text{-}P]$	concentration of the racemic cyanohydrin
$[R]$	concentration of (R)-enantiomer [wt.%, mole·l^{-1}]
$[S]$	concentration of (S)-enantiomer [wt.%, mole·l^{-1}]
$[E]$	free enzyme concentration (concentration of active centres)
$[E]_0$	total enzyme concentration
$[P]_{eq}$	equilibrium product concentration
K_{eq}	reaction equilibrium constant
K_m	Michaelis-Menton constant (half saturation)
$K_{m,A}$	Michaelis half saturation value for the substrate
$K_{(m,A)}$	apparent Michaelis half saturation value for inhibited reactions
$K_{m,P}$	Michaelis half saturation value for the product
K_i	general inhibition constant
$K_{i,A}$	substrate inhibition constant
$K_{i,P}$	product inhibition constant
K_S^{HCN}	apparent HCN dissociation constant $K_S^{HCN} = K_{eq}^{HCN} \cdot [H_2O]$
K_{eq}^{HCN}	HCN equilibrium dissociation constant
K_W	dissociation product of water
A_{spec}	specific acitivity of the enzyme [U · mg^{-1}]
A_{vol}	specific volumetric acitivity of the enzyme solution [U · ml^{-1}]
k_{cat}	molecular acitivity (or turnover number TN) [U·mg^{-1}]

k_f forward reaction rate constant $[(mol \cdot L^{-3})^{1-n} \cdot t^{-1}]$

k_r reverse reaction rate constant $[(mol \cdot L^{-3})^{1-n} \cdot t^{-1}]$

k_P product formation rate

k_C^1 forward rate constant of the non-specific chemical reaction

k_C^{-1} reverse rate constant of the non-specific chemical reaction

$k_1, k_2, \ldots$ elementary forward rate constant

$k_{-1}, k_{-2}, \ldots$ elementary reverse rate constant

k_{Des}^E enzyme deactivation rate constant

n order of the reaction

$t_{1/2}$ half time (cycle number)

υ reaction velocity

υ_C^+ forward velocity of the chemical reaction

υ_C^- reverse velocity of the chemical reaction

V_{max} general maximum reaction velocity

V_{max}^* apparent maximum reaction velocity

V_{max}^+ maximum forward reaction velocity

V_{max}^- maximum reverse reaction velocity

%ee   optical purity; enantiomeric excess [%]

ξ degree of conversion, turnover [%]

References

[1]   Effenberger, F.; Ziegler, T.; Förster, S.
Enzymkatalysierte Cyanhydrin-Synthese in organischen Lösungsmitteln
Angew. Chem. 99(5), 491-492 [1987]

[2]   Effenberger, F.
(R)- and (S)-Cyanohydrins - Their Enzymatic Synthesis and their Reactions
in: 'Microbial Reagents in Organic Synthesis', Ed. Stefano Servi
NATO ASI Series C, Vol. 381, 25-33, Kluwer Academic Publishers, 1992

[3]   Hörsch, B.
Enzymkatalysierte Synthese von (R)- und (S)-Cyanhydrinen in organischen Lösungsmitteln
und deren saure Hydrolyse zu optisch aktiven 2-Hydroxycarbonsäuren
Dissertation, Universität Stuttgart, 1990

[4]   Brussee, J.
Chiral Cyanohydrins - Versatile Building Blocks in Organic Synthesis
Dissertation, University of Leiden (NL), 1992

[5]   Niedermeyer, Uwe
        Untersuchungen zur enzymatischen C–C Verknüpfung am Beispiel der chiralen Cyanhydrinbildung
        Dissertation, Universität Düsseldorf, Institut für Enzymtechnologie, 1990

[6]   Rosenthaler, L.
        Durch Enzyme bewirkte asymmetrische Synthesen
        Biochemische Zeitschrift 14, 230-253 [1908]

[7]   Hustedt, H.-H.; Pfeil, E.
        Zur Kenntnis der Cyanhydrin-Synthese
        Liebigs Ann.Chem. Bd.640, 15-28 [1961]

[8]   Becker, W.; Pfeil, E.
        Über das Flavinenzym D-Oxynitrilase
        Biochemische Zeitschrift 346, 301-321 [1966]

[9]   Hochuli, E.
        Reinigung der D-Oxynitrilase aus Mandeln mit Hilfe der Affinitäts-Chromatographie
        Helv. Chim. Acta 66(2), 489-493 [1983]

[10]   Zandbergen, P.; van der Linden, J.; Brussee, J.; van der Gen, A.
        Synthesis of optically active cyanohydrins using almond meal
        Synth. Commun. 21(12&13), 1387-1391 [1991]

[11]   Brussee, J.; Loos, W.T.; Kruse, C.G.; van der Gen, A.
        Synthesis of optically active silyl protected cyanohydrins
        Tetrahedron 46(3), 979-986 [1990]

[12]   Kragl, U.; Niedermeyer, U.; Kula, M.-R.; Wandrey, C.
        Engineering aspects of enzyme engineering
        Continuous asymmetric C–C bond formation in an enzmye-membrane-reactor
        Ann. N.Y. Acad. Sci. 613, 167-175 [1990]

[13]   Bové, C.; Conn, E.E.
        Metabolism of Aromatic Compounds in Higher Plants
        J. Biol. Chem. 236(1), 207-210 [1961]

[14]   Xu, L.-L.; Singh, B.K.; Conn, E.E.
        Purification and characterization of acetone cyanohydrin lyase from *linum usitatissimum*
        Arch. Biochem. Biophys.. 263(2), 256-263 [1988]

[15]   Selmar, D.; Lieberei, R.; Biehl, B.; Conn, E.E.
        α-Hydroxynitrile lyase in Hevea brasiliensis and its significance for rapid cyanogenesis
        Physiologia Plantarum 75, 97-101 [1989]

[16]   Seely, M.K.; Criddle, R.S.; Conn, E.E.
        The Metabolism of Aromatic Compounds in Higher Plants
        J. Biol. Chem. 241(19), 4457-4462 [1966]

[17]   Smitskamp-Wilms, E.; Brussee, J.; van der Gen, A.; van Scharrenburg, G..; Sloothaak, J.
        Hydroxynitrile lyase from almond and sorghum as biocatalysts
        Recl. Trav. Chim. Pays-Bas 110(5), 209-215 [1991]

[18]   Reay, P.F.; Conn, E.E.
        The purification and properties of a uridine diphosphate glucose:
        Aldehyde cyanohydrin β-glucosyltransferase from sorghum seedlings
        J. Biol. Chem. 249(18), 5826-5830 [1974]

[19] Lee, H.-J.; Wilson, I.B.
Enzymatic parameters: measurement of V and Km
Biochimica et Biophysica Acta 242, 519-522 [1971]

[20] Clapés, P.; Mata-Alvarez, J.; García-Antón, J.M.; Reig, F.; Valencia, G.
Application of a Recycle Reactor to obtain kinetic data from progress curves
in immobilized-enzyme-catalyzed reactions
Biotech. Appl. Biochem. 11, 483-491 (1989)

[21] Niedermeyer, U.; Kragl, U.; Kula, M.-R.; Wandrey, C.; Makryaleas, K.; Drauz, K.
KFA Jülich, DEGUSSA AG
Enzymatisches Verfahren zur Herstellung von optisch aktiven Cyanhydrinen
EP 0 326 063 (23.01.1989)

[22] Effenberger, F.; Ziegler, Th.; Förster, S.
Degussa AG
Verfahren zur Herstellung von optisch aktiven Cyanhydrinen
DE 37 01 383 (28.07.1988)

[23] Laane, C.; Tramper, J.; Lilly, M.D.
Biocatalysis in Organic Media
Studies in Organic Chemistry 29, Elsevier Sci. Publishers 1987

[24] Brink, L.E.S.; Tramper, J.; Luyben, K.Ch.A.M.; Van`t Riet, K.
Biocatalysis in organic media
Enzyme Microb. Technol., 10, 736-743, [1988]

[25] Butler, Larry G.
Enzymes in Non-Aqueous Solvents
Enzyme Microb. Technol., 1, 253-259, [1979]

[26] Larreta-Garde, V.; Xu, Z.F.; Biton, J.; Thomas, D.
Stability of enzymes in low water activity media
in Biocatalysis in organic media (eds: C.Lanne, J.Tramper, M.D.Lilly)
Elsevier, Amsterdam, 247-252, [1987]

[27] Wehtje, E.; Adlercreutz, P.; Mattiasson, B.
Activity and operational stability of immobilized mandelonitrile lyase in methanol/water mixture
Appl. Microbiol. Biotechnol. 29, 419-425 [1988]

[28] Wehtje, E.; Adlercreutz, P.; Mattiasson, B.
Formation of C–C Bonds in Mandelonitrile Lyase in Organic Solvents
Biotechnology and Bioengineering 36, 39-46 [1990]

[29] Halling, P. J.
Solvent selection for biocatalysis in mainly organic systems:
predictions of effects on equilibrium position
Biotechnology and Bioengineering, 35, 691-701, [1990]

[30] Laane, C.; Boeren, S.; Vos, K.; Veeger, C.
Rules for Optimization of Biocatalysis in Organic Solvents
Biotechnology and Bioengineering, 30, 81-87, [1987]

[31] Klibanov, A.M, Cambou, B.
Enzymatic production of optically active compounds in biphasic aqueous-organic systems
Methods in Enzymology (ed: K.Mosbach), 136, 117-137, [1987]

[32] Jorns, M. Schuman
Studies on the kinetics of cyanohydrin synthesis and cleavage by the flavoenzyme oxynitrilase
Biochim. Biophys. Acta 613, 203-209 [1980]

[33]   Miethe, P.; Jansen, I.; Niedermeyer, U.; Kragl, U.; Kula, M.-R.; Wandrey, C.;
        Mohr, K.-H.; Meyer, H.-W.
        Continuous Synthesis of (R)-(+)-Benzaldehydecyanohydrin using
        (R)-Oxynitrilase in Lyotropic Liquid Crystal
        Biocatalysis 1991

[34]   Pikal, M.J. (Eli Lilly & Co.)
        Freeze-Drying of Proteins
        Bio-Pharm 3(8), 18-27 [1990]

[35]   Ching, W.-M.; Kallen, R.G.
        Mechanism of Carbanion Addition to Carbonyl Compounds. Equilibria and Kinetics of
        Substituted Cyanohydrin Cleavage and Formation in Aqueous Solution. Substituted
        Cyanohydrin Proton Dissociation Constants
        J. Am. Chem. Soc. 100(19), 6119-6124 [1978]

[36]   Corcoran, R.C.; Ma, J.
        Stereochemical dependence of the rate of cyanohydrin reversion
        Tetrahedron Letters 32(45), 6513-6516 [1991]

[37]   Eggers, D. K.; Blanch, H. W.; Prausnitz, J. M.
        Extractive catalysis: solvent effects on equilibria of enzymatic reactions in two-phase systems
        Enzyme Microb. Technol., 11, 84-89, [1989]

[38]   Carrea, G.; Riva, S.; Bovara, R.; Pasta, P.
        Enzymatic oxidoreduction of steroids in two-phase systems: effects of organic solvents
        on enzyme kinetics and evaluation of the performance of different reactors
        Enzyme Microb. Technol., 1-4, [1988]

[39]   Bailey, J.E., Ollis, D.F.
        Biochemical Engineering Fundamentals
        McGraw-Hill International Editions, 2.nd Ed., 1986

[40]   Julia, S.; Sans, J.M.
        Resolution of racemic modifications by gas-liquid chromatography via the
        separation of diastereoisomeric esters. VII. Cyanohydrins
        J. Chrom. Sci. 17, 651-655 [1979]

[41]   König, W.A.; Francke, W.; Benecke, I.
        Gas Chromatographic Enantiomer Separation of Chiral Alcohols
        Journal of Chromatography, 239, 227-231, [1982]

[42]   Ferdinand, W.
        The interpretation of non-hyperbolic rate curves for two-substrate enzymes
        Biochem.J., 98, 278-283 [1966]

[43]   Klein, D.P.; Gladysz, J.A.
        Activation of organic carbonyl compounds by Lewis acids: Relative reactivities of σ and π
        adducts toward nucleophiles and implications for enantioselective addition reactions
        J. Am. Chem. Soc. 114, 8710-8711 [1992]

[44]   Niedermeyer, U.; Kula, M.-R.
        Enzymkatalysierte Synthese von (S)-Cyanhydrinen
        Angew. Chem. 102(4), 423-425 [1990]

[45]   Jammot, J.; Pascal, R.; Commeyras, A.
        The influence of borate buffers on the hydration rate of cyanohydrins: evidence for an
        intramolecular mechansim
        J. Chem. Soc. Perkin Trans. 2, 157-162 [1990]

Chapter

5

FUNCTIONAL
SOLUTION DIFFUSION MEMBRANES

Synopsis

Dense polymer membranes are widely used in reverse osmosis, gas separation and pervaporation. The transport properties such as flux and selectivity are described using the solution-diffusion model. Membrane selectivities are given either by different solubilities or moreover by differences in the diffusivity of the penetrant molecules. As long as the polymer selectivity merely has to intensify the evaporation selectivity, the overall performance of a membrane is mostly sufficient for practical applications. However, in case the membrane selectivity is contradictory to evaporation, overall selectivities of commercial polymer membranes are rather poor.

Both the selective recovery of cyanohydrins from an enzyme-membrane-reactor, as well as the separation of low volatile aldehydes from a reaction mixture are not suited with the use of polymeric solution-diffusion membranes. However, through introduction of functional groups into the polymer, the selectivities can be improved via preferential sorption of either the cyanohydrin or the aldehyde. It could be demonstrated that thin-film ion-exchange membranes will result in sufficient selectivities. Cation-exchange membranes such as sulfonated poly(styrene-co-isoprene) enable a selective recovery of the cyanohydrin. In general, selectivities depend on the counter-ion and are high for the potassium ion. Anion-exchange membranes such as quaternized polyphenylenoxide enable the selective removal of aldehydes from the reaction mixture via reversible formation of bisulfite complexes.

5.1. Introduction

In chapters 5, 6 and 7 of this thesis dense polymer membranes will be considered. The permeation through dense membranes and the separation of gaseous and liquid mixtures occurs according the solution-diffusion mechanism [1] as shown in *figure 5.1*. At the feed side of the membrane, molecules of component i dissolve in the polymer phase and thermodynamic equilibrium exists between the molecules sorbed in the membrane and molecules in the feed phase [2,3]. The same is valid for the equilibrium at the permeate side of the membrane. The chemical potential at the permeate side is lower than that at the feed side. This driving force causes diffusional mass transport through the polymer matrix. The feed may be a mixture of gases, vapors or liquids and the mixtures can be separated due to different affinities of the permeant to the polymer material and different mobilities inside the matrix.
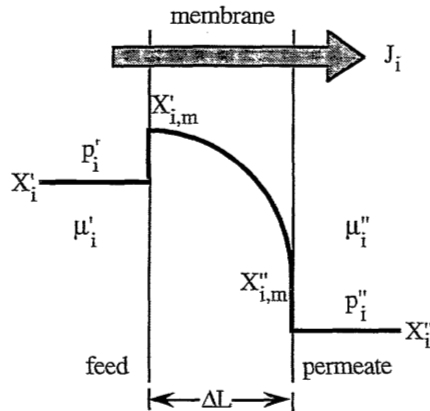
Figure 5.1 *Schematic drawing of mass transport through solution-diffusion membranes*

In this chapter, the development of a membrane to remove the cyanohydrin product from a multicomponent liquid mixture will be demonstrated. The membranes can be applied to a pervaporation as well as to a pertraction process [4,5]. The permeation and separation properties will be characterized in a pervaporation process. The membranes will be later used in the enzyme-membrane reactor as described in chapter 6. There, the membranes will be used in both processes.

5.2. Background

5.2.1. Mass transport according to solution diffusion model

The mass transport models described in literature [7,8,9] represent an adequate theoretical framework to quantify permeation of molecules through solution diffusion membranes. Petropoulos [6] presumes that a permeating molecule under the driving force of a chemical potential gradient diffuses with constant velocities u(z) against the frictional force exerted by the polymer matrix. This presumption is comparable to the Stokes Law of friction.

$$v(z) = -u_i^m \frac{d\mu_i}{dz} \tag{1}$$

The flux through the membrane at a given cross-section in the place (z) results from the concentration c_i^m and the velocity rate v(z).

$$J_i = c_i^m \cdot v(z) = -c_i^m \cdot u_i^m \frac{d\mu_i}{dz} \tag{2}$$

Corresponding to Fick's Law, the assumption of Meares [10] leads to the result that the flux of a component i through a membrane must be equal to the product from concentration, c_i^m, mobility, u_i^m, and driving force, $(d\mu_i \cdot dz^{-1})$. The chemical potential written in terms of fugacities and using Einstein's Law of Diffusion, $D_i^{m,T} = u_i^m \cdot R\,T$, a thermodynamic diffusion coefficient can be defined as well as the solubility which is the ratio of the concentration in the membrane and the gas fugacity.

$$J_i = -c_i^m \cdot u_i^m \cdot R\,T \frac{d\ln(f_i/f_i^0)}{dz} = -D_i^{m,T} \cdot \frac{c_i^m}{f_i} \cdot \frac{df_i}{dz} = -D_i^{m,T} \cdot S_0 \cdot \frac{df_i}{dz} \tag{3}$$

The thermodynamic diffusion coefficient is only to a small extent concentration-dependent in a non-ideal system, and can be considered as a constant across the membrane. This is closely related with the Fickian diffusion coefficient pertaining to the concentration dependency of the activity coefficients. Equation (3) can be further developed into:

$$J_i = -c_i^m \cdot D_i^{m,T} \frac{d\ln(f_i/f_i^0)}{dz} = -c \cdot D_i^{m,T} \cdot \frac{\partial \ln a_i}{\partial \ln x_i} \cdot \frac{dx_i}{dz} \tag{4}$$

The integration of the general transport equation in relation to membrane thickness demands a singular correlation of the acitivtiy coefficients,γ_i, with the fugacities,f_i. Thus, the fugacity

in an actual mixture is expressed as the function of the fugacity of the pure components at standardized pressure.

$$J_i = -D_i^{m,T} \cdot \frac{c_i}{\gamma_i \, x_i \, f_i^0} \cdot \frac{df_i}{dz} = -\frac{c_i \cdot D_i^{m,T}}{f_i^0} \cdot \frac{1}{\gamma_i} \cdot \frac{df_i}{dz} \tag{5}$$

As the penetrant alters the polymer matrix by swelling, the thermodynamic diffusion coefficient can no longer be considered constant [11]. In such non-ideal systems, $D_i^{m,T}$ is, therefore, frequently expressed as an empirical mathematical relation related to the concentration of the penetrant. The concentration-dependent sorption coefficients can be described by the Flory-Huggins [12] thermodynamics, in which the activity of a penetrant i in the membrane is given by the volume fraction Φ_i in the membrane and the interaction parameter χ_{ip}. The interaction parameter assumes a large numeric value if the interaction energy of the penetrant and the polymer are small.

$$\ln a_i = \ln \Phi_i + \left(1 - \frac{\Phi_i}{\Phi_p}\right)\Phi_p + \chi_{ip} \cdot \Phi_p^2 \tag{6}$$

The Flory-Huggins interaction-parameter χ_{ip} can be expressed by the solubility parameters. Likewise, the evaluation of the diffusion rate can be improved by determining the self-diffusion coefficients and by calculating the actual diffusivity all of which adheres to a modified Maxwell-Stefan equation.

The molecular models on the diffusion of permeands are based on a change in place of molecules through the cooperative movement of polymer segments. According to Meares [8], the activation energy of diffusion can correlate to the jump length λ, the kinetic diameter of the permeand σ, and the cohesion energy e_A.

$$E_D = \frac{\pi}{4} \cdot \sigma^2 \cdot \lambda \cdot N_A \cdot e_A \tag{7}$$

According to the free volume model of Fujita [1], the cumulative free volume of the polymer matrix is accessible for the diffusion of molecules. Vrentas and Duda [13,14] have revised this model by introducing more molecular details. They established a correlation of the diffusion coefficients with intrinsic constants describing the material, like cumulative free volumes, critical free volume for a diffusional jump, and the interaction energy between the polymer and the permeand.

5.2.2.   Pervaporation

Pervaporation is characterized by the occurence of phase transition of the feed phase within the membrane module. The fluid phase (') is brought into contact with the feed side of the membrane.The molecules permeate through the membrane according to their gradient in the chemcial potential, and are desorbed at the permeate side (") into the vapor phase. The mass transport can be characterized in three subphases [2,3,15]:

1)   Sorption of the permeating molecules from the feed solution into the adjoining interior membrane surface at the feed side

2)   Diffusion of the sorbed molecules through the membrane

3)   Desorption from the interior membrane surface at the permeate side during evaporation into the permeate gas phase.

The first step can hardly be affected in practical application by the expression that the separation problem and the feed solution are fixed through the feed fugacity f_i' of component i. Membrane preparation and the material selection have strong impact on step 2 of the mass transport process. With the given fugacity f_i'' at the permeate side the third step, desorption into the permeate, allows influencing of the driving forces. Regarding desorption, three methods are available, namely, vacuum pervaporation, purge gas pervaporation, and thermopervaporation. In all cases, the driving force is described by the difference in the feed side fugacity in condensed phase, and by the permeate side fugacity in vapor phase. A thermodynamic consideration of mass transport was done by Gudernatsch [16].

The fugacity f_i of a component i in condensed phase is defined with reference pressure in relation to the fugacity of the pure component f_i^0.

$$ f_i \; = \; \gamma_i \cdot x_i \cdot f_i^0 \qquad\qquad \varphi_i^S = \frac{f_i^S}{p_i^S} \qquad\qquad (7) $$

With the introduction of a fugacity coefficient φ_i^S, the fugacity of the pure component can be expressed for saturation when the Poynting correction is applied.

$$ f_i^0 = \varphi_i^S \cdot p_i^S \cdot \exp\left[\int_{p_i^S}^{p} \frac{v_i^M}{RT} \, dp \right] \qquad\qquad (8) $$

According to Gudernatsch [16], the conditions of pervaporation can dismiss the Poynting correction and can be set for unassociated fluids, $\varphi_i^S \approx 1$. Thus, the fugacity in a condensed phase is maintained:

$$f_i = \gamma_i \cdot x_i \cdot p_i^S \tag{9}$$

In encountered assumptions, the fugacity in an uncondensed phase also simplifies itself.

$$f_i = x_i \cdot p \tag{10}$$

The transport equation for pervaporation can thus be expressed in the dependence of the fugacity difference.

$$J_i = \frac{P_i}{\Delta z} \cdot (f_i^{'} - f_i^{''}) = P_i \cdot \frac{1}{\Delta z} \cdot (\gamma_i^{'} \cdot x_i^{'} \cdot p_i^S - x_i^{''} \cdot p^{''}) \tag{11}$$

In vacuum pervaporation, or generally, when $f_i^{''} \to 0$, the conditions on the permeate side can be disregarded and equation (11) simplifies to (12):

$$J_i = P_i \cdot \frac{1}{\Delta z} \cdot \gamma_i^{'} \cdot x_i^{'} \cdot p_i^S \tag{12}$$

5.2.3.   Pertraction

Pertraction differs from pervaporation in that the desorption does not occur in the vapor phase, but instead in a condensed phase [5,17]. Pertraction must also be distinguished from dialysis. A process is termed dialysis when both feed and permeate sides of the membrane are in contact with the same solvent. However, the process is considered a pertraction when the solvents on feed and permeat sides differ. This has the advantage that such an additional extractive effect can be observed when solvents selection occurs. Mass transport once again is described by the solution diffusion model according to equation (13):

$$J_i = \frac{P_i}{\Delta z} \cdot (f_i^{'} - f_i^{''}) = P_i \cdot \frac{1}{\Delta z} \cdot p_i^S \cdot (\gamma_i^{'} \cdot x_i^{'} - \gamma_i^{''} \cdot x_i^{''}) \tag{13}$$

5.2.4. Definition of Selectivities

To judge the efficiency of a solution diffusion process [18], not only the flux or the permeability of a component i are important, but also the separation efficiency must be

sufficiently high. In the simplest case, this can be expressed as the ratio of the permeability to the separable components i and j, called the ideal selectivity.

$$S^*_{i,j} = \frac{P^*_i}{P^*_j} \tag{14}$$

The statement of the enrichment factors β_i, or the separation factors $\alpha_{i,j}$, is favored for the design of a complete plant, or rather for comparing membranes under process conditions:

$$\alpha_{i,j} = \left(\frac{x''_i}{x'_i}\right) \cdot \left(\frac{x'_i}{x''_j}\right) \tag{15}$$

In this case x'_i and x'_j or x''_i and x''_j are the molar fractions of the components i and j in the feed or permeate mixture. The enrichment factor β_i occurs from the molar fractions x'_i and x''_i of a component i in the external phases.

$$\beta_i = \left(\frac{x''_i}{x'_i}\right) \tag{16}$$

For a binary system, the separation factor $\alpha_{i,j}$ can be defined as a function of the actual selectivitiy $S_{i,j}$. Clearly, the separation factor in the pervaporation is not only a function of the membrane selectivity, but is also a function of the activity coefficients, the saturation vapor pressure, and the permeate gas pressure.

$$\alpha_{i,j} = S_{i,j} \cdot \frac{x'_i}{x'_j} \cdot \frac{\gamma'_j \cdot x'_j \cdot p^S_j - x''_j \cdot p''}{\gamma'_i \cdot x'_i \cdot p^S_i - x''_i \cdot p''} \approx S_{i,j} \cdot \frac{\gamma'_j \cdot p^S_j}{\gamma'_i \cdot p^S_i} \tag{17}$$

According to equation (17) and work published by Wijmans [7,19], the overall separation factor of pervaporation $\alpha_{i,j}$ can be expressed as a thermodynamic separation factor $\alpha^{evap}_{i,j}$ based on vapor-liquid equilibrium and a membrane selectivity $\alpha^m_{i,j}$ based on the solution-diffusion selectivity.

$$\alpha_{i,j} = \alpha^{evap}_{i,j} \cdot \alpha^m_{i,j} \tag{18}$$

5.3. Problem definition

5.3.1. Membrane development

As already mentioned, the oxynitrilase-catalyzed addition of hydrocyanic acid to carbonyl compounds carried out in organic medium is limited to a technical scale by a slow reaction kinetic, incomplete conversion, and finally through complicated processing of the pure cyanohydrin in order to avoid further racemization.

The aim of the thesis [20] is to overcome these limitations by designing a continuous enzyme membrane reactor where the product, the cyanohydrins, are selectively removed from the reaction mixture through a functional solution diffusion membrane by means of pervaporation or pertraction. The concept is shown in *figure 5.2*.
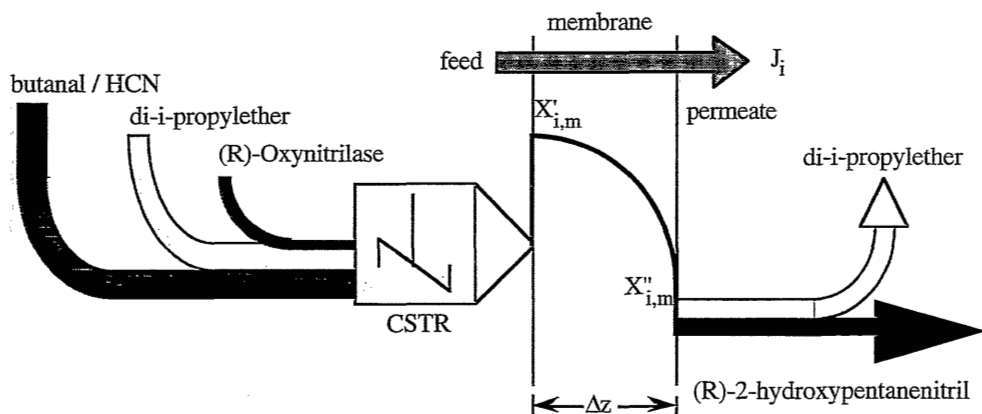
Figure 5.2 *Schematic drawing of the basic principle of a solution diffusion enzyme membrane reactor for the continuous production of homochiral cyanohydrins*

The multi-component mixture in the reaction vessel can be separated by selectively transferring them into the membrane permeate phase without either decomposition or racemization. Within the framework of this work, the enzymatic synthesis of (R)-2-hydroxypentanenitrile based on butanal, is examined as an exemplary reaction mixture. Further processing of the products is carried out through pervaporation. The experiments are carried out with quarternary mixtures consisting of a solvent (di-iso-propylether), substrate (butanal, hydrocyanic acid) and product (cyanohydrin). Furthermore, the catalyst (oxynitrilase), which is adsorptively immobilized to Avicel®, as well as small quantities of

water and buffer substances are present in the solution. The physical properties of all components of the solution are listed in *table 5.1*.

Table 5.1 *Physical properties of the compounds investigated*

property	ether (DIPE)	HCN	butanal	2-hydroxy-pentanenitrile
molecular weight [Da]	102.18	27.03	72.11	99.14
boiling point [°C]	68	26	75	230 [1]
kinetic diameter [Å]	6.16	3.98	5.27	5.57
vapor pressure 25 °C [mbar]	198	992	149	0.9 [2]
enthalpy vaporizat. [kJ·mole^{-1}]	31,957	25,233		
dielectric constant	3,95	114	10,78	
polarity [debye]	1.21	2.98	2.72	3.81

(1) acc. Wagner relation   (2) acc. Joback group contribution method

In a second example of this work, the selective removal of a residual, non-volatile substrate is considered. For non-volatile compounds, as well as compounds which decompose or even racemize during vaporization, pertraction must be applied to the membrane separation process. For this purpose the enzymatic synthesis of (S)-2-hydroxy-2-(phenoxy)-phenylacetonitrile out of meta-phenoxybenzaldehyde is examined as a model mixture for pertraction. This will be described in detail in chapter 6.

The same type of membrane can principally be applied to both processes. The requested membrane should fulfill a series of requirements, such as:

• solvent stability
• selectively permeable for the product
• impermeable for the substrates and the solvent
• complete rejection of enzyme, carriers and buffer salts.

5.3.2. Process optimization

The pervaporative separation of products, however, does not only require special property membranes, but also previously unknown requirements based on the design of the process. Until now, pervaporation was exclusively applied to the separation of high volatile compounds from a mixture of highly volatile compounds. Technically applied pervaporation

separations are limited today by the realizable downstream pressure. Therefore, in known applications, as a rule, the boiling point of the penetrant molecule does not exceed appr. 130 °C. Otherwise, the liquids are regarded to have such a low vapor pressure that removal by pervaporation is not possible.

The saturation vapor pressue of butanalcyanohydrin should be known in order to define, whether the desorption of permeands could represent the rate-determining step in the pervaporation of low volatile compounds. Since butanalcyanohydrin decomposes at atmospheric pressure below the boiling point, no known value for the temperature range of interest exists. According the Joback group contribution method [21], a boiling point of T_S (p = 1atm) = 208,8 °C is calculated. The saturation vapor pressure in the range of 20...35 °C is sustained by extrapolating the data from known literature.
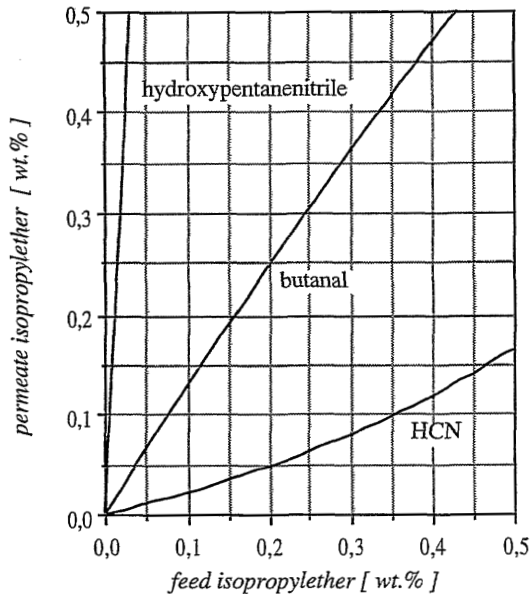
Figure 5.3 *Calculated McCabe-Thiele diagrams for binary systems of*
(a) isopropylether/ hydrocyanic acid, (b) isopropylether/ butanal
and (c) isopropylether/ cyanohydrin

The saturation vapor pressure at 30 and 35 °C is calculated with 1,12 and 1,49 mbar respectively. This indicates, that in considering the pressure drop in the permeate, in the support plate, as well as in the substructure of the membrane the separation process might be controlled by the permeate pressure, since the thermodynamic liquid/vapor equlibrium is reached [22]. In this range of measurements, the maintained selectivities and permeabilities

are very difficult to reproduce. Accordingly, one must carefully observe the permeate pressure and temperature during the course of the experiments . How similar the permeate pressure is with the saturation vapor pressure also indicates the pervaporation results, which show, that the selectivity of a butanalcyanohydrin selective membrane might drop at a decrease in feed temperature from 30 °C to 20 °C.

From the McCabe-Thiele diagrams in *figure 5.3*, which are calculated by using the UNIFAC group contribution method, the importance of the membrane selectivity compared to the evaporation selectivity becomes obvious. The figure shows the equilibrium compositions of the ether in binary mixtures with the cyanohydrin, butanal and HCN. For the HCN mixture, the ether weight fraction is lower in the vapor phase than in the liquid phase. The volume fractions of the butanal are almost equal in the liquid and the vapor phase. For the cyanohydrin, the ether will be always enriched in the vapor phase. A membrane selectively separating the cyanohydrin from the diisopropylether has to completely overcome the evaporation selectivity in order to become cyanohydrin selective [23].
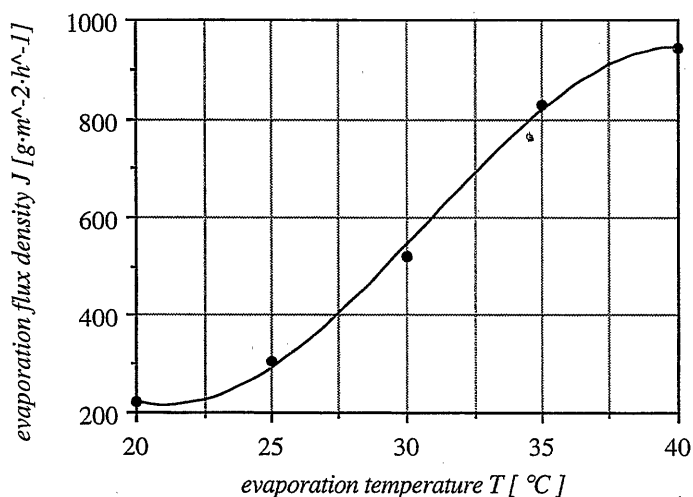
Figure 5.4 *Influence of temperature on the evaporation rate from an non-stirred, unruffled vapor/liquid surface of the cyanohydrin*

To check whether an evaporation of the cyanohydrin is possible at all without any membrane resistance, a control experiment was performed at various temperatures. A vacuum was applied to the cyanohydrin and the vapors were condensed in a cold trap. The measured evaporation fluxes are plotted as a function of the temperature in *figure 5.4*. It is assumed

that the fluxes reported in this figure will be the maximum fluxes since a membrane would be an additional resistance resulting in a decreasing flux. At the experimental temperature of 30 °C, a vapor pressure of 0,75 mbar could be obtained at a maximum evaporation rate of 600 $g \cdot m^{-2} \cdot h^{-1}$.

5.4. Experiments

The experimental setup of *figure 5.5* was proven to be solvent stable as well as explosion profed. The stirred test cell from Duran® glassware was later on used in enzyme membrane reactor experiments.
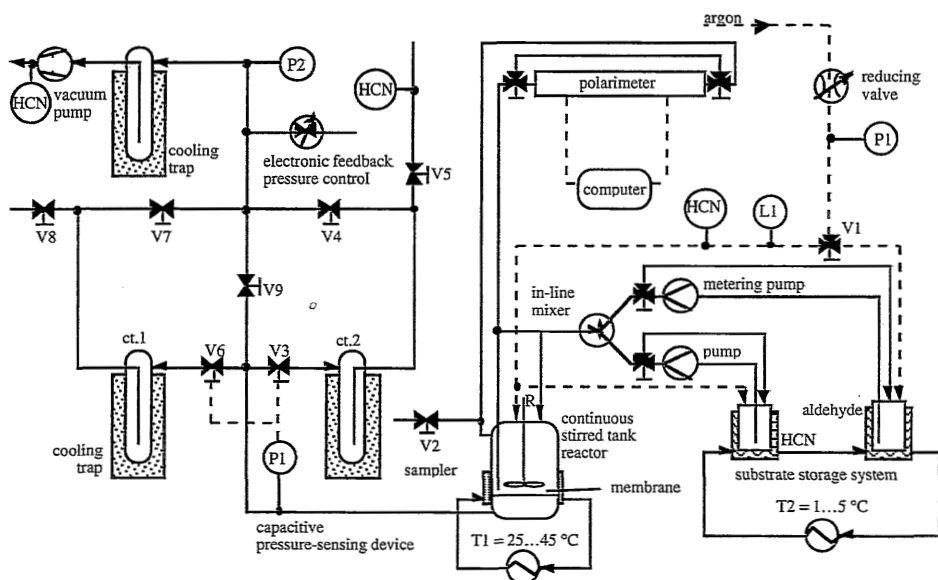
Figure 5.5 *Experimental set-up for the continuous characterization of pervaporation membranes as a function of feed composition, temperature and permeate pressure*

The experimental equipment permits a continuous characterization of the feed composition, as well as an automated replacement of the components separated via pervaporation. In order to avoid any oxidation of the aldehyde, the whole system is subjected to an argon inert gas pressure. The stirred tank reactor is equipped with a flat sheet membrane of Ø(90mm) in diameter.

To ensure a constant temperature over the whole cell, as well as a constant temperature gradient along the membrane, the support plate of the cell is indirectly heated as shown in *figure 5.6a*. To handle toxic substances, the cold trap shown in *figure 5.6b* should have a pressure-stable flat flange system, which allows a contact-free change as well as a reproducible weighing of the permeates.
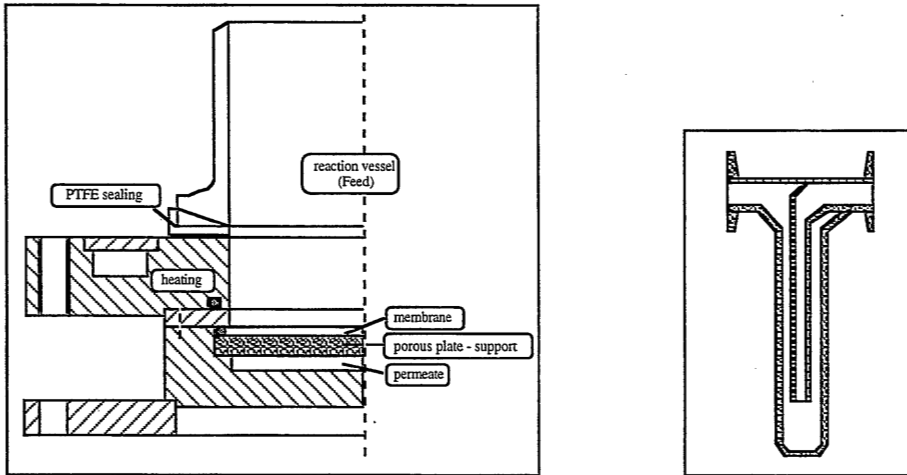
Figure 5.6 *Detail of the experimental set-up for the characterization of membranes*
a) membrane temperature control (b) cooling trap for sampling HCN

In membrane separation processes, concentration polarization often occurs. Due to selective transport, one of the components is depleted in the boundary layer at the membrane surface. The other components are enriched and the established concentration gradients in the boundary layer influence the separation performance of the membrane. Experiments in well-stirred cells are generally required to decrease the boundary layer thickness and to minimize possible concentration polarization effects. Concentration polarization and boundary layer effects could be identified as shown in *figure 5.7.* for pervaporation experiments with a hydrophilic ion-exchange membrane and a model mixture out of 80 w/w di-iso-propylether, 15 w/w 2-hydroxypentanenitrile, and 5 w/w butanal.

It is apparent from *figure 5.7*, that a significant transport limitation due to the boundary layer exists at small stirring velocities . However, because of generally low fluxes in non-supported thick membranes, no significant influence on the selectivity could be measured. The composition of the permeates is approximately constant for all stirring velocities. In the succeeding bioreactor experiments described in chapter 6, thin film composite membranes were installed at flux densities 20 times higher compared to these experiments. In this case,

at stirring velocities smaller than 300 upm, both the cyanohydrin flux and the separation factor decreases.
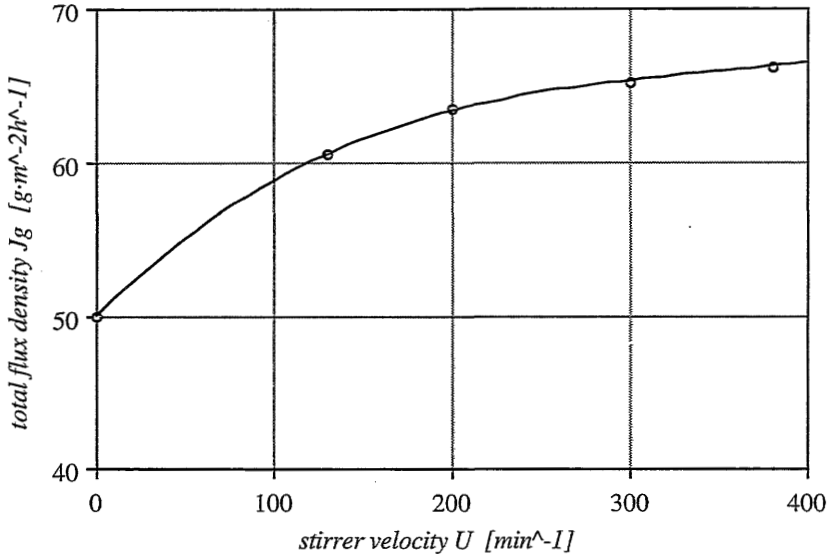
Figure 5.7 *Characterization of concentration polarization phenomena*
Influence of the flux density on the stirring velocity during pervaporation

5.5. Results and discussion

5.5.1. General aspects of material selection

In order to separate the low volatile cyanohydrin, 2-hydroxypentanenitrile with a boiling point of about 210 °C from the substrates hydrocyanic acid and butanal and from the solvent diisoproylether with boiling points of 26 °C, 75 °C and 68 °C respectively, the required membrane must show good membrane selectivities. Furthermore, in order to overcome the accompanying evaporation selectivity α_{evap}, the permeate partial pressure of the product has to be as low as possible. This is achieved in the experimental set-up by condensating the permeands in liquid nitrogen. Then the permeation selectivity $\alpha_{i,j}$ in this particular case, results into a product of the evaporation $\alpha_{i,j}^{evap}$ and the membrane selectivity $\alpha_{i,j}^{m}$.

$$\alpha_{i,j} = \alpha_{i,j}^{evap} \cdot \alpha_{i,j}^{m} \tag{19}$$

For the solution diffusion membranes, the membrane selectivity equals the product of the sorption selectivity $\alpha_{i,j}^S$ and the diffusion selectivity $\alpha_{i,j}^D$.

$$\alpha_{i,j}^m = \alpha_{i,j}^S \cdot \alpha_{i,j}^D \tag{20}$$

In the present separation problem of molecularly similar compounds, a sufficient membrane selectivity can only be obtained by preferential sorption assuming similar diffusivities. A sorption-controlled permeation is achieved through a sufficiently strong interaction of the permeating compounds with e.g. functional groups of the membrane polymer. The extend of a preferential sorption of cyanohydrins through a functional membrane, therefore, relies on the particular interaction of the penetrant and the polymer matrix. As a further requirement for the membrane, the polymer penetrant interaction should work on the broad family of cyanohydrins.

The development of a suitable membrane can be approached through theoretical pre-considerations. The concept of solubility parameters [24,25] refers to work of Hildebrand and Scott [26]. The fundamental relationship of this model postulates a correlation between the cohesion energy e_A, namely, to the potential energy of a condensed phase per unit volume and to the relative solubility, namely, to the solubility paramter δ of a component.

$$\delta \equiv \sqrt{\frac{E^o}{S^m}} = \sqrt{e_A} \tag{21}$$

The mixing of a penetrant in a polymer membrane matrix can further be treated according to the historical approaches of van Laar, Scatchard and Hildebrand [27,28] by quantifying the energy of mixing of two components as:

$$\Delta_m U_v = (x_A \cdot S_A^m + x_B \cdot S_B^m) \cdot \Phi_A \cdot \Phi_B \cdot A_{AB} \tag{22}$$

The term A_{AB} is marked as an exchange energy density, and represents a value for the internal cohesive strength between the molecules. Consequently, it combines with the heat of vaporization to the cohesion energy.

$$A_{AB} = \left(\sqrt{\frac{E_A^o}{S_A^m}} - \sqrt{\frac{E_B^o}{S_B^m}} \right)^2 = (\delta_A - \delta_B)^2 \tag{23}$$

Thus, the Hildebrand-Scatchard relationship is finally obtained for the energy of mixing, which corresponds to the Gibb's free enthalpy of mixing for regular solutions. For non-ideal solutions, the Gibbs enthalpy must be expanded by the excess entropy.

$$\Delta_m U_v = (x_A \cdot S_A^m + x_B \cdot S_B^m) \cdot \Phi_A \cdot \Phi_B \cdot (\delta_A - \delta_B)^2 \qquad (24)$$

The smaller the heat of mixing, the more stable a solution or mixture is. Therefore, from the Hildebrand-Scatchard relationship it can be concluded that compounds with similar solubility parameters mix well. Three different interactions contribute to the cohesion energy:

- dispersion energy E_d
- dipole-dipole-interaction energy E_p
- hydrogen bonding energy E_h

Thus, the solubility parameters can be analyzed into three components as shown in *table 5.2*:

$$\delta^2 = \delta_d^2 + \delta_p^2 + \delta_h^2 \qquad (25)$$

For illustration one can depict the three-dimensional solubility parameters [29] in a spatial coordinate system. The miscibility of two components can then be determined from the distance of two spots in the spatial diagram.

$$\Delta = \sqrt{(\delta_A^d - \delta_B^d)^2 + (\delta_A^p - \delta_B^p)^2 + (\delta_A^h - \delta_B^h)^2} \qquad (26)$$

Table 5.2 *Solubility parameters of the compounds investigated*

property	ether (DIPE)	HCN	butanal	2-hydroxy-pentanenitrile
kinetic diameter [Å]	6.16	3.98	5.27	5.57
polarity [debye]	1.21	2.98	2.72	3.81
δ (H)	1.5		9.6	24.7
δ (P)	4.7		8.9	15.2
δ (D)	13.61		13.1	11.1
$\delta \Sigma$	4.4	24.7	18.6	31.0

Solubility parameters can be determined experimentally from sorption and osmotic pressure experiments and a number of chemicals are tabulated. For unknown compounds, solubility parameters can be estimated using group contribution methods. The values listed in *table 5.2.* were taken from Barton. In the following three subsections, membrane material selection and development will be described: in a first screening experiment uncharged polymers differing in hydrophilicity will be characterized. Thereafter, ion-exchange membranes will be studied. First anion-exchange and then different cation-exchange membranes will be discussed.

5.5.2 Pervaporation with hydrophilic membranes

An initial membrane screening was performed to investigate the influence of material characteristics on permeability and selectivity. The experiments were carried out with pure components of butanal and 2-hydroxypentanenitrile. The results are tabulated in *table 5.3*. The hydrophilic character of the membranes increases from top to bottom. Hydrophobic membranes, such as polydimethylsiloxane (PDMS), are highly selective for the non-polar components, such as diisopropylether and butanal. For the cyanohydrin, the best selectivities can be found with hydrophilic solution diffusion membranes such as polyvinylalcohol and collagene. A cyclodextrin membrane [30,31] showed the best properties: the preparation of these membranes will be described in chapter 7.

Table 5.3 *Permeability and selectivity of pure components of 2-hydroxypentanenitrile and butanal in different hydrophilic polymers*

polymer film	thickness [μm]	normalized flux density $J_N \cdot 10^3$ [$g \cdot m^{-1} \cdot h^{-1}$]		ideal selectivity $S\left(\dfrac{J_{cyano}}{J_{but}}\right)$
		butanal	2-hydroxy-pentanenitrile	
polydimethylsiloxane (Wacker Dehäsiv 930)	5	75	2.05	0.027
polyetheretherketon (ICI Stabar K 200)	50	1.5	0.12	0.08
polyether-block-amide (Atochem PEBA 4033)	20	4,71	0.16	0.34
cellulose regenerate (Fa. Wolff, Walsrode)	22	3.1	3.2	1.03
collagene / g.d.a. (Fa. Naturin - Colli)	20	0.71	1.13	1.59
polyvinylalcohol / e.c.h. (Aldrich)	2.5	0.138	0.289	2.09
β-cyclodextrin / m.d.i. (Chinoin Ltd.)	8	4.2	13.6	3.24

The membranes have to separate a multi-component mixture and therefore permeation experiments with a representative mixture must be performed. A ternary system was chosen consisting of the solvent, substrate, and product with a reactor-typical composition of

solvent: 80 % w/w   di-iso-propylether
substrate: 5 % w/w   butanal
product: 15 % w/w   2-hydroxypentanenitrile

As experimental conditions, a stirring rate of 350 upm, a temperature of 30 °C, and a permeate pressure of 0,1 mbar is provided in advance. To determine the enrichment factors, the permeate was analyzed by using gas-chromatography. In order to avoid thermal decomposition of the cyanohydrin in the GC column, a protective derivatization reaction via either silylation or acetylation was carried out.

Table 5.4 *Enrichment factor and flux density obtained from actual pervaporation experiments of a standard model mixture in hydrophilic polymers*

polymer film	enrichment factor $\beta_i = \left(\dfrac{x''_i}{x'_i}\right)$ in % w/w			flux density
	butanal	di-iso-propyl-ether	2-hydroxy-pentanenitrile	J_G [$g \cdot m^{-2} \cdot h^{-1}$]
GFT 1361 D (Deutsche Carbone)	1,0	0,88	1,40	0,83
Poly-L-lactide (acc. chapter 7)	2,40	0,71	2,07	8,65
β-cyclodextrin / m.d.i. $OH/_{NCO} = 3,5$	3,20	0,55	2,67	116
β-CD-co-DMCD / m.d.i. $OH/_{NCO} = 1,5$	2,20	0,26	4,53	52,1

The results from *table 5.4* proves the better selectivities of the cyclodextrin membranes relative to the commercial hydrophilic membranes prepared from polyvinylalcohol. Furthermore, the 15 µm cyclodextrin membrane has a 50-fold higher flux than the commercial < 2 µm thin film composite membrane of GFT. The two cyclodextrin membranes differ in hydrophilicity as determined by the number of hydroxyl groups per monomer unit. In this case, however, the selectivity of the more hydrophilic non-modified β-cyclodextrin membrane is lower than the selectivity obained from less hydrophilic dimethylated β-cyclodextrin.

The hydrophilic membranes favor butanalcyanohydrin permeation, but they cannot be considered for practical applications because of their small fluxes and their limited long term

stability in the reaction mixture. Further improvements in terms of selectivity are expected to be obtained with hydrophilic ion-exchange membranes.

5.5.3. Pervaporation with anion-exchange membranes

Commercial anion-exchange membranes

Most of the commercial anion-exchange membranes did not show sufficient chemical stability in organic solvents. Only a few membranes were stable enough to be characterized. Membranes obtained from Pall RAI Corporation were tested with various counter ions such as sulfate, chloride, citrate, and sulfite. All membranes listed in *table 5.5* showed a cyanohydrin and aldehyde enrichment. However, the required enrichments could not be met by the commercial membranes.

Table 5.5 *Enrichment factor and flux density obtained from actual pervaporation experiments through commercial anion-exchange membranes*

polymer film	enrichment factor $\beta_i = \left(\dfrac{x_i''}{x_i}\right)$ in % w/w			flux density
	butanal	di-iso-propyl-ether	2-hydroxy-pentanenitrile	J_G [$g{\cdot}m^{-2}{\cdot}h^{-1}$]
RAI 4030 - sulfate (Pall RAI Corp.)	2,20	0,53	3,13	3,45
RAI 1030 - chloride (Pall RAI Corp.)	1,60	0,80	1,87	30,9
RAI 1030 - sulfate (Pall RAI Corp.)	1,60	0,43	3,87	22,9
RAI 1030 - citrate (Pall RAI Corp.)	1,40	0,32	4,47	9,48
RAI 1030 - sulfite (Pall RAI Corp.)	6,86	0,59	1,23	25,3

It could be seen from *table 5.5*, that the counter ion will greatly influence the separation characteristics of charged membranes. In case of the thin film, non-reinforced membrane type 1030, the enrichment factor increases with increasing valence of the counter ion. This

effect from chloride (I) to sulfate (II) and finally to citrate (III) might be attributed to a reversible crosslinking reaction. The most interesting effect, however, results from a direct comparison of the sulfate SO_4^{2-} and the sulfite ion SO_3^{2-}. In case of the sulfite counter ion, the aldehyde enrichment factor is strongly increasing. It will be shown later, that the sulfite counter ion is facilitating the transport of aldehydes in general.

A further improvement of the membrane performance can only be achieved by synthesizing new anion-exchange membranes. This will be described in the following two subsections. To improve solvent stability of the membranes, the polymer backbone has to be completely crosslinked. The final morphology should consist of a 3-dimensional network. Homogeneous membranes are therefore required and various chemical modifications of halomethylated polysulphone, copolymers of poly(4-vinylpyridine), copolymers of poly(vinylimidazole) and halogenated polyphenylenoxide are easily accesible, in synthetic terms, for the production of homogeneous anion-exchange films.

Poly(4-vinly pyridine) based membranes

Anion-exchange membranes were prepared from poly(4-vinyl-pyridine) with methyliodide and dibenzylchloride [32] resulting in a network as shown in *figure 5.9*. The membranes showed promissing results, however, the reproducibility was bad. Therefore, no further systematic experiments were carried out.
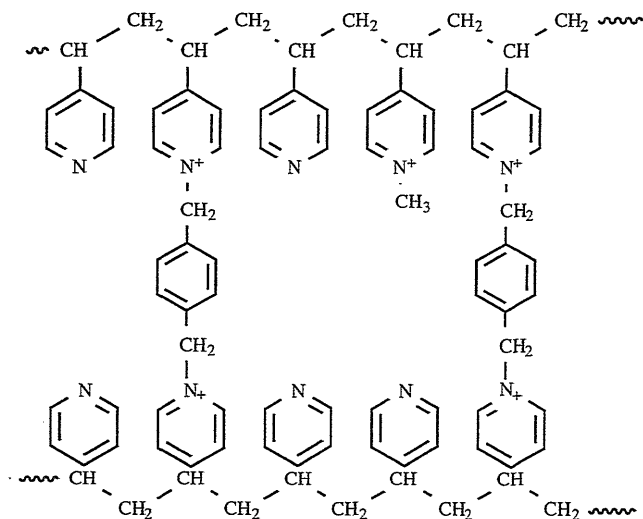
Figure 5.9 *Anion-exchange membrane prepared from poly(4-vinyl-pyridine), methyliodide and dibenzylchloride*

The insufficient reproduciblity results from the fact that the crosslinking reaction occurs very slowly with bifunctional compounds. This is confirmed by reactive dialkyl-compounds like α,ω-dibromoalkanes. But a very rapid mono-quarternization coupled with reversible formation of a polymeric gel occurs. The resulting viscosity increase hinders the second quarternization leading to a limited reproducibility in the formation of the network. Similar viscosity effects are described for polyelectrolytes in solution.

Polyphenyleneoxide based membranes

Alternatively, homogeneous anion-exchange membranes based on polyphenylenoxide were examined. The introduction of functional groups follows through a reaction with bromine, which can be introduced into aromatic polymers via electrophilic and radical reactions as shown in *figure 5.10*.
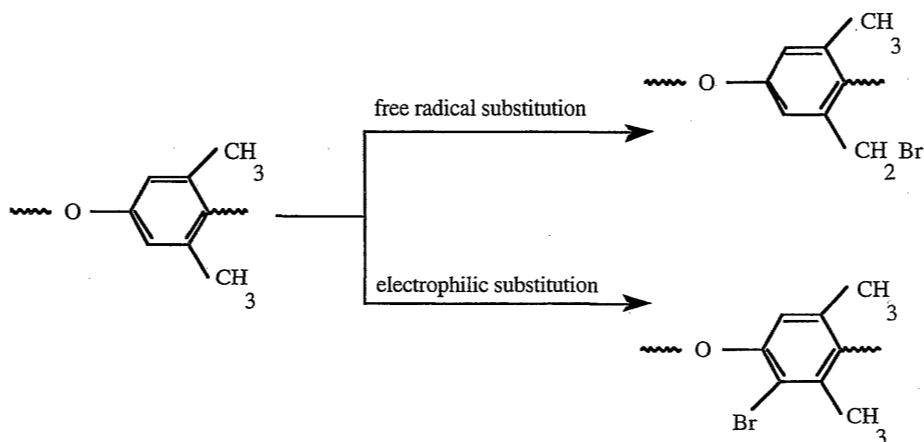
Figure 5.10   *Electrophilic and radical substitution of PPO with bromine*

The bromination is desired to occur on the methyl group but not on the phenylene ring. The reaction can be shifted into this direction according to Malon [33]. The degree of substitution of the membrane was adjusted to 3,75 meq·g^{-1}. The degree of substitution was determined from ^{1}H-NMR. The conversion with 1.4-bis-(dimethylamino)butane [TMBDA] resulted in a completely crosslinked anion-exchange membrane as shown in *figure 5.11*.
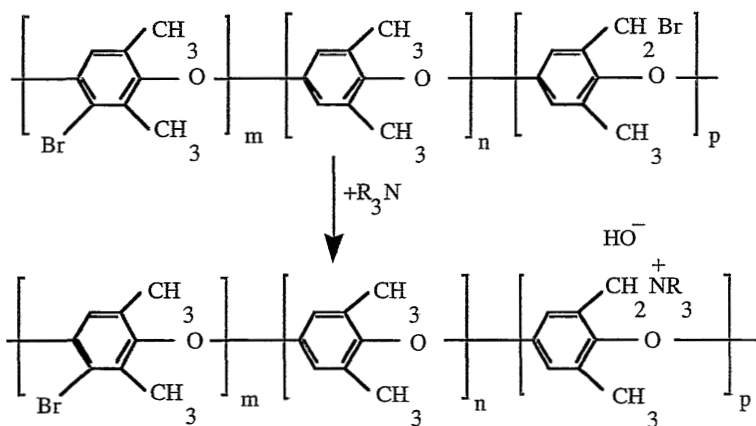
Figure 5.11 *Quaternization of brominated polyphenyleneoxide*

Fluxes and selectivities of these membranes were determined as a function of operation temperature and permeate pressure. The feed liquid was the multi-component mixture as described earlier consisting of solvent, substrate, and product. *Figure 5.12.* shows that the flux increases with increasing temperature by about an order of magnitude due to an increase in driving force and polymer permeability. Often in pervaporation the selectivity increases with decreasing temperature, however, in this case, a significant improvement in selectivity can be obtained with increasing temperature. Probably, this is due to a higher driving force at higher temperatures minimizing the effect of mass transport limitation at low temperatures as has been already seen in *figure 5.4.*

Figure 5.13 shows the effect of permeate pressure on the separation factor as obtained from the multi-component mixture [22,23]. The selectivity for cyanohydrin over the diisopropylether is a strong function of the permeate pressure as hypothesized earlier. The separation factor for the butanal hardly changes over the pressure range studied (p < 20 mbar) because its partial vapor pressure is much lower than the saturation vapor pressure. However, the cyanohydrin selectivity drops from about 9 at very low permeate pressure to below 1 at higher pressures. The selectivity even changes from cyanohydrin selective to ether selective. The developed membrane showed excellent properties and will later be used in chapter 6.
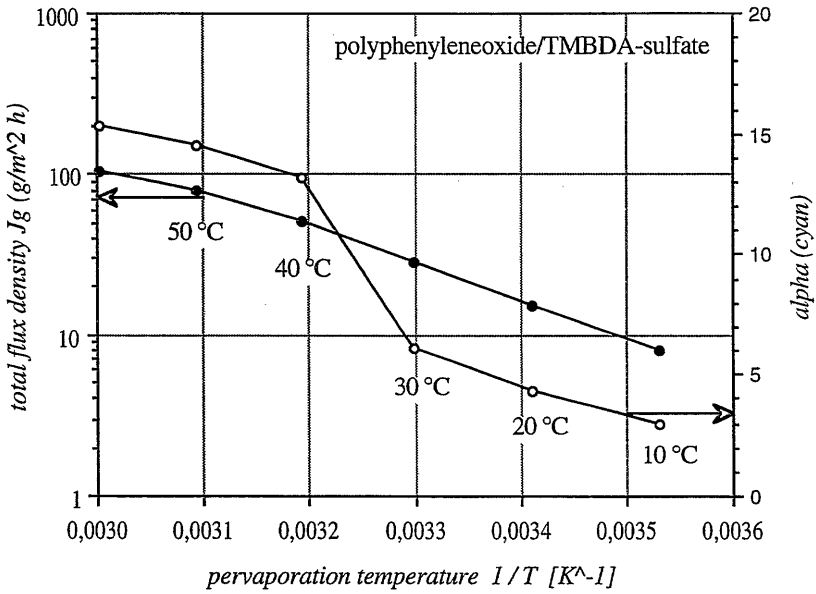
Figure 5.12   *Influence of pervaporation temperature on flux density and separation factor α for a PPO anion-exchange membrane*
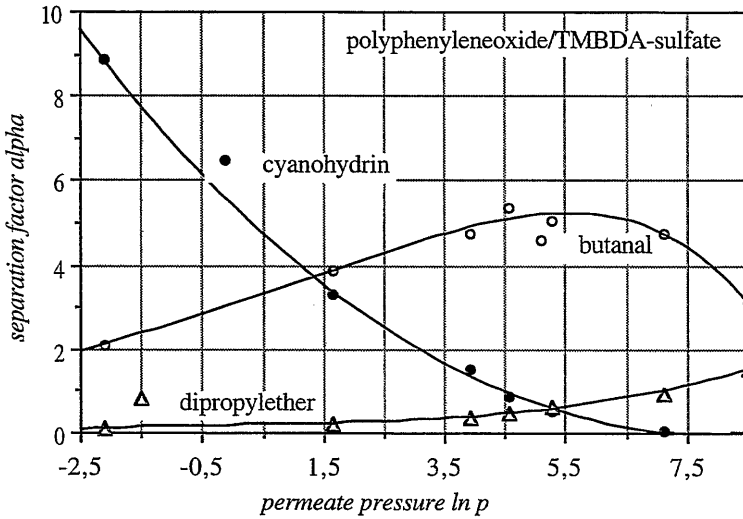
Figure 5.13   *Influence of permeate pressure on the separation factor α for a PPO anion-exchange membrane*

Anion-exchange membranes for the aldehyde removal

One option to operate the process of enzymatic production of homochiral products is a plug flow tubular reactor with subsequent processing of the products. The separation can be either a pervaporation or a pertraction process. In chapter 6, the removal of a small amount of aldehyde from a mixture of aldehyde, cyanohydrin, and solvent is required. Experiments with anion-exchange membranes have shown that the butanal / di-isopropylether selectivity strongly depends on the conditioning of the membranes. A very different transport behavior can be found when the counter ion was sulfate or sulfite. The results for a Pall anion-exchange membrane are shown in *figure 5.15* and *figure 5.16*.

●	cyanohydrin / di-iso-propylether
○	cyanohydrin / butanal

y-axis: cyanohydrin permeate conc. [% w/w]

x-axis: butanalcyanohydrin feed concentration [% w/w]
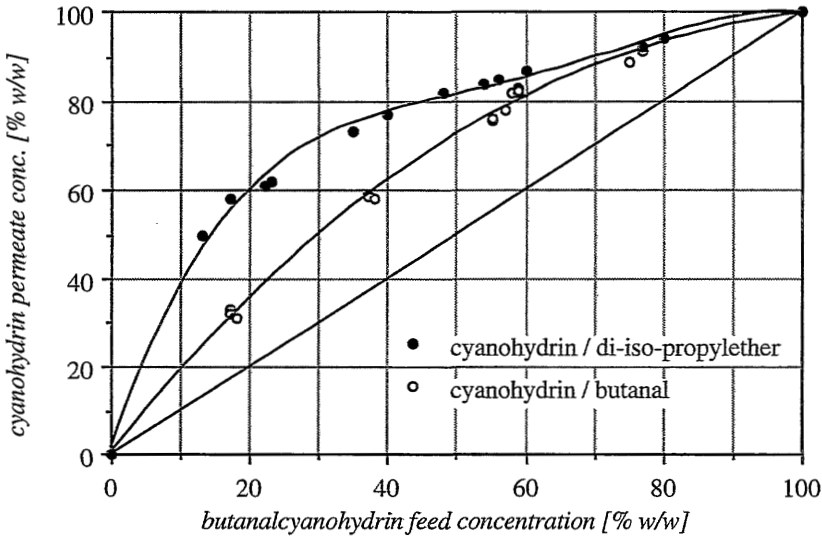
Figure 5.15   *Binary McCabe-Thiele diagram related to an anion-exchange membrane from Pall RAI type 1030–$SO_4{}^{2-}$ with sulfate counter ions*
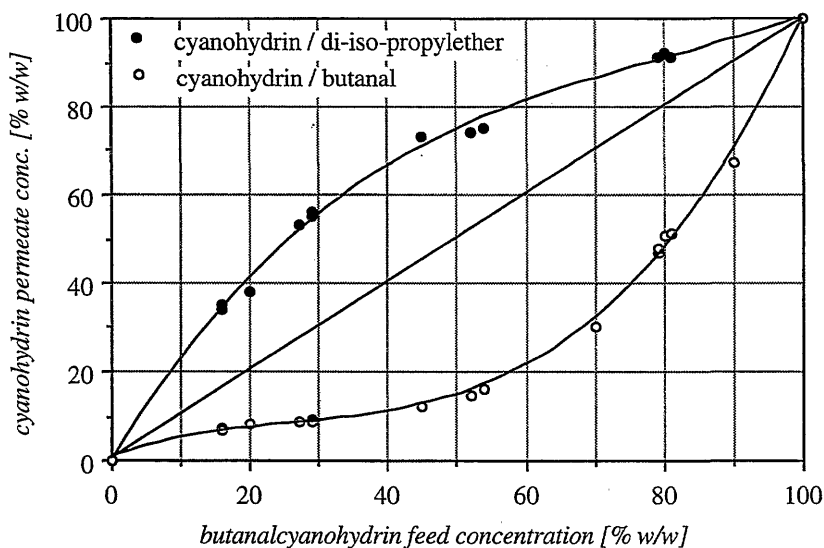
Figure 5.16   *Binary McCabe-Thiele diagram related to an anion-exchange membrane from Pall RAI type 1030–HSO₃⁻ with sulfite counter ions*

Figure 5.15 and *figure 5.16* show, that the selectivity of the membrane related to the binary system of cyanohydrin and di-isopropylether is not influenced while changing the counter ion from sulfate to the hydrogensulfite. However, the selectivity of the second binary system consisting of cyanohydrin and butanal will reverse from the sulfate to the hydrogensulfite. Through the complete concentration range, the Pall RAI type 1030–SO₄²⁻ membrane is selective towards the cyanohydrin. The 1030–HSO₃⁻ with hydrogensulfite counter ions on the other hand will enrich the aldehyde starting from binary mixtures with the cyanohydrin. *Figure 5.17* and *figure 5.18* demonstrate, that this is due to an alteration of the partial flux density of the aldehyde component. The sulfate counter ion results in an approximately linear dependence of the cyanohydrin and butanal fluxes with the feed composition. Exchanging the sulfate with hydrogensulfite ions results in an generally increased butanal flux density, which is approximately constant between 0,25…1,0 meq of butanal in the feed. At rather low butanal concentrations, the partial flux density is dropping sharply to low values.
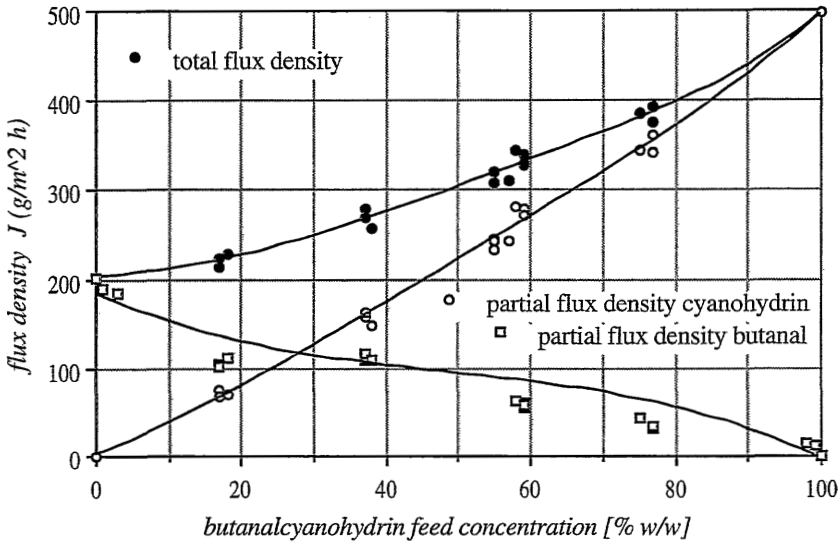
Figure 5.17   *Flux of the cyanohydrin and the aldehyde through an anion-exhange membrane from Pall RAI type 1030–SO_4^{2-} with sulfate counter ions*
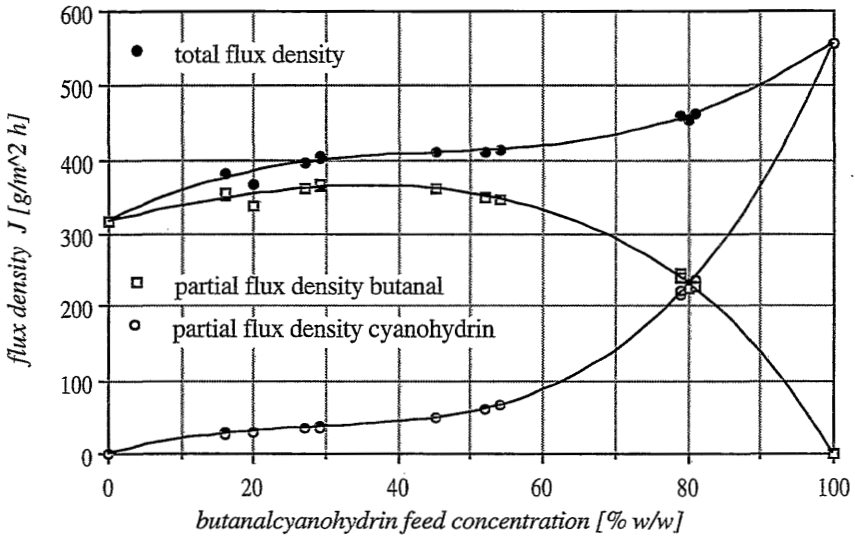
Figure 5.18   *Flux of the cyanohydrin and the aldehyde through an anion-exhange membrane from Pall RAI type 1030–HSO_3^- with sulfite counter ions*

Aldehydes, in this case the butanal, strongly react with bisulfite by the reversible formation of hydroxyalkanesulfonates [34] which represent the conjugated base of a strong acid as shown in *figure 5.14*. It can be hypothesized that a facilitated tranport or a coupled transport through counter ions of hydroxyalkanesulfonates can occur in the conditioned anion-exchange membrane [35]. In this case, the aldehyde can permeate according to different mechanisms:

-     through a rapid and reversible hopping mechanism on the bisulfite counter ions of the anion-exchange groups

-     or through facilitated diffusion of completely dissociated adducts.
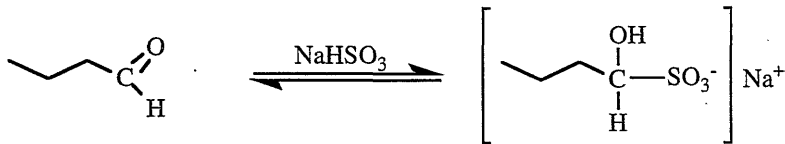
Figure 5.14   *Formation of bisulfite adducts from sodium hydrogensulfite and form sodium bisulfite in alkaline solutions*

A differentiation of the mechanisms should be possible on either the binding constants of the bisulfite adducts, or on the influence of the kinetic radius and the molecular weight on diffusion.

5.5.4 Pervaporation through cation-exchange membranes

General material screening

The cation-exchange membranes used, again, have to be chemically stable in the reaction mixture. Commercial electrodialysis membranes contain a reinforcing non-woven material from e.g. polyvinylchloride which dissolves in di-isopropylether. Therefore, one is limited to use either electrolysis membranes, such as Nafion® and Flemion®, or non-reinforced electrodialysis membranes, typically produced by using plasma grafting techniques such as the Pall-RAI and the Solvay-Morgane membranes. Typically these membranes have a higher film thickness because mechanical stability is obtained solely through the polymer itself. Therefore, fluxes are expected to be very low. In this case it would not be possible to transfer pervaporation experiments to an enzyme membrane reactor consisting of the same stirred test cell.

Table 5.6 *Enrichment factor and flux density obtained from actual pervaporation experiments through commercial cation-exchange membranes*

polymer film	enrichment factor $\beta_i = \left(\dfrac{x_i''}{x_i'} \right)$ in % w/w			flux density
	butanal	di-iso-propyl-ether	2-hydroxy-pentanenitrile	J_G [$g \cdot m^{-2} \cdot h^{-1}$]
PRP (Solvay Morgane)	1,20	1,04	0,73	727
Flemion® – 900 / COOH (Asahi Glass)	0,80	1,19	0,06	121,2
Flemion® – 900 / SO$_3$H (Asahi Glass)	2,00	0,79	1,80	9,92
NAFION® 117-H$^+$ (DuPont)	2,80	0,66	2,20	43,2
NAFION® 117-K$^+$ (DuPont)	1,60	0,41	3,93	9,81
RAI 1010-H$^+$ (Pall RAI Corp.)	2,00	0,91	1,13	29,9
RAI 1010-K$^+$ (Pall RAI Corp.)	1,80	0,78	1,93	20,6
RAI 5010.M-H$^+$ (Pall RAI Corp.)	1,20	1,06	0,60	8,16
RAI 5010.L-H$^+$ (Pall RAI Corp.)	1,40	1,01	0,80	22,6
RAI 5010.L-K$^+$ (Pall RAI Corp.)	1,20	0,96	1,13	11,2
sulfonated PEEK-0.65 24µm (ICI Victrex)	2,20	0,42	3,73	174
sulfonated PEEKK-0.88 15µm (Hoechst Ultrapek)	1,40	0,31	4,53	273
sulfonated PEK-1.05 12µm (BASF Ultrapek)	1,20	0,23	5,07	186

In a preliminary screening, solvent stable membranes were compared relative to their permeability and their selectivities. Data presented in *table 5.6* are drawn from experiments by using the standard mixture containing 15 w/w cyanohydrin and 5 w/w butanal in diisopropylether. Comparing the results on Flemion® membranes, it can be stated that strong acid sulfonic acid groups have much stronger interaction to the cyanohydrin than weakly acid carboxylic acid groups. Both membranes were specifically tailored by Asahi Glass Corporation using the same perfluorinated polymer matrix.

Furthermore, it can be concluded, that interpolymer membranes generally exhibit lower selectivities. This might be due to a permeation of hydrophobic organic solvents through the inert regions of the polymer matrix.

Homogeneous cation-exchange membranes are available through e.g. DuPont. The Nafion® membrane is the most intensively described charged polymer structure. Nafion® shows the best selectivities of all commercial membranes. However, fluxes are much too low.

The best results were found on membranes based on sulfonated Ultrapek®, which is a thermoplastic polyetherketone. Originally, we developed the membrane for electrodialysis purposes. In order to obtain solvent stability, the degree of sulfonation was lowered. Comparing the three commercial polymers polyetheretherketone (PEEK, Victrex®), polyetheretherketoneketone (PEEKK, Hostatec®) and polyetherketoneketone (PEKEKK, Ultrapek®) one can see, that with an increasing ratio of polyketone segments in the polymer, the degree of sulfonation to a solvent stable membrane can be increased. Following from an higher ion-exchange capacity, the selectivity of the membranes increases with increasing ratio of polyketone segments in the thermoplast.

For application in aqueous media, these polymers were sulfonated up to 1,45 meq·g^{-1} for Victrex®, 1,60 meq·g^{-1} for Hostatec® and 1,68 meq·g^{-1} for Ultrapek®. Solvent stable membranes are obtained at a maximum degree of sulfonation of 0,65 meq·g^{-1} for Victrex®, 0,88 meq·g^{-1} for Hostatec® and 1,05 meq·g^{-1} for Ultrapek®. For processing of thin films, the polymeric sulfonic acids –SO$_3$H can still be extruded and calandered above 280 °C .

However, all attempts to introduce well defined crosslinking of the sulfonated polymers failed. Crosslinking through radical reactions always yield in chain transfer and a reduction of the molecular weight. Therefore, higher degree of sulfonation and higher density of functional groups could not be realized for the separation of cyanohydrins.

Pervaporation on Nafion® 117

The permeation rate as well as the equilibrium sorption was determined for Nafion® 117 with different counter ions [36]. To calculate the equilibrium sorption as a function of the counter ion, an average density of $\rho = 2,1$ g·cm^{-3} was assumed. The results of the solubility experiments are presented in *table 5.7*.

Table 5.7 *Solubility of the liquids in Nafion® 117 at room temperature*

sorption [g·100 g^{-1}]	butanal	butanal-cyanohydrin	di-iso-propyl-ether	water
H$^+$	25,47	18,81	25,81	17,5
Na$^+$	20,62	18,78	13,14	13,91
K$^+$	8,3	18,89	8,37	9,68
Cs$^+$	9,2	4,86	6,96	5

The results of the solubility for Nafion® clearly show a strong dependence of the solubility on the counter ion. The adjustment of the optimal interaction with respect to the separation problem could therefore occur for example via a variation of the counter ions of the sulfonic acid group.

Table 5.8 Physicochemical properties of different counter ions in Nafion® 117

counter ion	ion-radius [Å]	hydration-radius [Å]	hydration-enthalpy [kJ · mol^{-1}]	electro-negativity
H$^+$			-708	2.20
Li$^+$	0.68	3.40	-499	0.97
Na$^+$	0.97	2.76	-390	1.01
K$^+$	1.33	2.32	-306	0.91
Rb$^+$	1.47	2.28	-281	0.89
Cs$^+$	1.67	2.28	-248	0.86

The acidic strength, or the interaction energy of the negative charge, depends on the degree of dissociation of the sulfonic acid and increases as a function of the counter ion in the following order:

$$H^+ \quad < \quad Li^+ \quad < \quad Na^+ \quad < \quad K^+ \quad < \quad Rb^+ \quad < \quad Cs^+$$
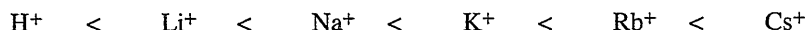
The trend of decreasing solubility from H^+ over Na^+ and K^+ to Cs^+ is clear for all substances with the exeption of butanalcyanohydrin. This phenomenon can be related to the structure of the Nafion® membrane: interconnected clusters are formed by the sulfonic acid groups the diameters of which change in the presence of different counter ions. Furthermore, the sorption capacity also depends on the concentration of the counter ions which in turn depends on the number of the fixed ions (expressed in the ion-exchange capacity as equivalent weight grams of membrane per eq of charge) [37].

Table 5.9 shows the calculated sorption selectivities for the three different binary selectivities. It is remarkable that the Nafion material hardly shows any sorption selectivity. Which in fact appears to contradict the earlier described concepts of material selection assuming that selectivity is determined by solubility. However, later in this section, experimental data for homogeneous hydrophilic polymers show that the solubility is the separation determining parameter and we ascribe the low sorption selectivity to the heterogeneous morphology of Nafion having hydrophilic clusters embedded in the hydrophobic polymer.

Table 5.9 *Ideal solubility selectivity of the pure liquids in Nafion® 117 at room temperature*

selectivity	$\alpha^{id}_{Sorp} \left(\dfrac{butanal}{cyanohydrin} \right)$	$\alpha^{id}_{Sorp} \left(\dfrac{butanal}{ether} \right)$	$\alpha^{id}_{Sorp} \left(\dfrac{cyanohydrin}{ether} \right)$
H+	1,35	0,98	0,73
Na+	1,09	1,57	1,43
K+	0,44	0,99	2,26
Cs+	1,89	1,32	0,69

The measured permeation rates at different counter ions are presented in *table 5.10* averaged from several measurements. With potassium as the counter ion, Nafion® membrane exhibits

the highest permeabilities for the separation of low volatile butanalcyanohydrin. Butanal as a substrate reaches only its second lowest flux in the K+-form. For application pervaporation in the enzyme membrane reactor, the measured permeabilities indicate that butanal substrate would be favored in permeating the membrane.

Table 5.10 *Permeation rate of the probes in Nafion® 117 at room temperature*

flux density [g·m^{-2}·h^{-1}]	butanal	butanal-cyanohydrin	di-iso-propyl-ether	water
H+	678,2	19,8	49,7	489,6
Na+	353,5	13,9	14,3	709,5
K+	136,7	68,3	8,9	139
Cs+	16,6	4,6	43	44,6

Typically, the pervaporation selectivity is higher than the sorption selectivity in hydrophilic membranes. These can be confirmed in many experiments by Néel [3], who published data on the influence of counter ion binding on pervaporation selectivity in charged membranes.

Table 5.11 *Ideal separation factor α of the probes in Nafion® 117.*

selectivity	$\alpha^{id}_{perm}\left(\dfrac{butanal}{cyanohydrin}\right)$	$\alpha^{id}_{perm}\left(\dfrac{butanal}{ether}\right)$	$\alpha^{id}_{perm}\left(\dfrac{cyanohydrin}{ether}\right)$
H+	34,25	13,65	0,39
Na+	25,43	24,72	0,97
K+	2,00	15,36	7,67
Cs+	3,61	0,39	0,11

Table 5.10 and *table 5.11* show that the transmembrane flux as well as the selectivity of the cyanohydrin over the ether are very low and the Nafion was therefore dismissed as a potential membrane for the enzyme reactor application.

Crosslinked Poly(styrene-co-isoprene)-sulfonic acid

A novel membrane should combine the optimal properties of the homogeneous thin film polyetherketone membranes with the solvent stability of the Nafion® membrane. This can only be achieved through a homogeneous network of sulfonic acid groups.

For this purpose, a commercial poly(styrene-co-isoprene) with a higher amount of 3.4-isoprene subunits is sulfonated and the pre-polymer was kindly synthesized on a contract basis at the Fraunhofer-Institute. The final, water soluble sulfonated polymer, having an ion-exchange capacity of 1,88 meq·g^{-1} was further crosslinked via subsequent in-situ hydrosilylation. Procedures for crosslinking of unsaturated, 3.4-isoprene moities containing styrene-isoprene copolymers are developed within the thesis of Kerres [38] at the Fraunhofer-Institute as shown in *figure 5.19*.
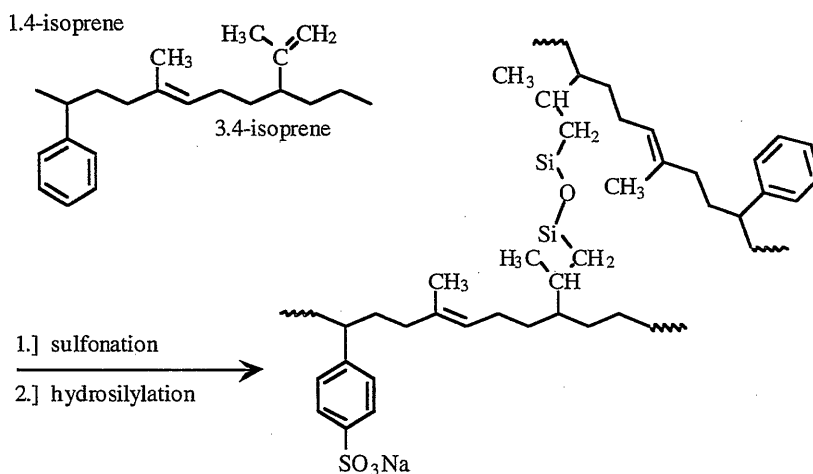
Figure 5.19   *Molecular formula of poly(styrene-co-isoprene)-sulfonic acid crosslinked via hydrosilylation*

The resulting membranes are colorless and transparent. The film forming properties are excellent and sorption experiments were carried out on polymer films with different counter ions in the polymer matrix. *Figure 5.20* shows a decrease in absolute sorption of the di-isopropylether and the butanal with decreasing electronegativity of the counter ion. The solubility of cyanohydrin increases significantly and results in change in solubility selectivity. For potassium and caesium the material is cyanohydrin selective.
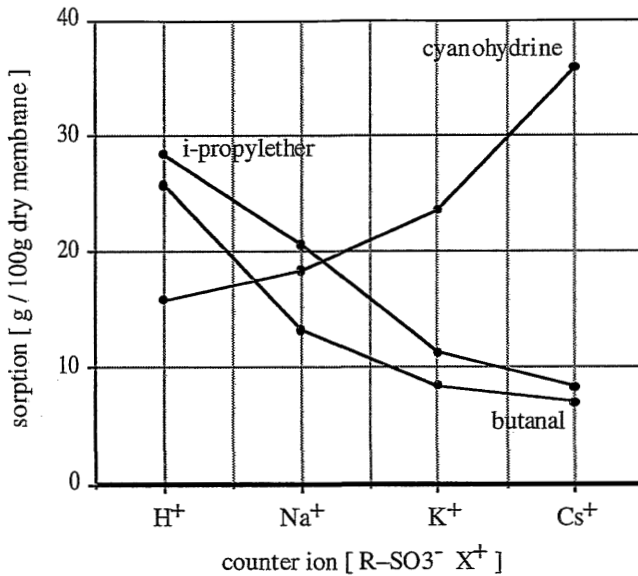
Figure 5.20   *Sorption capacity of the sulfonated poly(styrene-co-isoprene)*
membrane for the solvent, the substrate, and the product

For application in pervaporation, the membranes were prepared as a composite structure on top of an aluminum microfiltration membrane. The selection of the support material was based on the requirements of solvent stability and maximum surface porosity. Within the experiments it could be seen, however, that the aluminum support was sensitive towards an attack of excess hydrocyanic acid. Therefore, reactor experiments were carried out by using a polymeric support material from PALL Ultipore polyamide 6.6 microfiltration membranes. This support structure is stable at cyanohydrin concentrations below 50 w/w in the feed. At higher concentrations, a tremendous swelling is observed.

From *figure 5.20* the influence of the total permeation on the counter ion can again be recognized. Contrary to the Nafion® membrane, the sorption selectivity predominates the cyanohydrin permeation selectivity. The tailor-made functional membrane based on sulfonated poly(styrene-co-isoprene) results in enrichment factors between $\beta_{Permeation} = 4...9,5$ depending on the counter-ion [39].
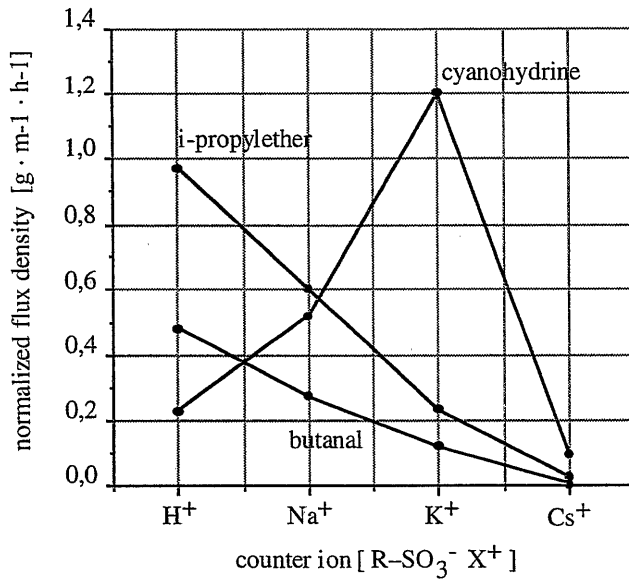
Figure 5.20   *Normalized flux density of the sulfonated poly(styrene-co-isoprene) membrane for the solvent, the substrate, and the product*

The permeability for the butanal and the di-isopropylether decreases as the solubility does from the proton to caesium ion. For the proton, sodium, and potassium ion the permeabilty of the cyanohydrin increases as the sorption does. Only the permeability through a Cs^+ membrane does not follow the trend of solubility and decreases dramatically.

The selection of counter ions determines the acid strength of the sulfonic acid group, and the interaction energy with the penetrant. As given in *table 5.13*, the sorption selectivity rises in the series $H^+ < Li^+ < Na^+ < K^+ < Cs^+$ in contradiction with the permeation selectivity which shows a maximum for potassium. This points to a strong interaction of the fixed ions to the penetrants, particularly to a too high stability constant of the permeand-carrier complex within the membrane resulting in a diffusion limitation [40].

Any change in the counter ion of the membrane will also modify the polymer morphology. This is due to a varying electronegativity of the different counter ions, which influences the energy of binding and the distance of the counter ions to the fixed sulfonic acid groups. An increase of the acidic strength of the sulfonic acids groups results from the proton H^+ through the sodium Na^+ to the caesium Cs^+.

Within the first main group of the alkali metals, the hydration number decreases in the same direction as from Li^+ to Cs^+, followed by a densification of the polymer network. Therefore, different chemical interactions of different interaction lengths between the penetrants and the functional groups have to be considered. Sometimes, a complete exclusion of the penetrants from regions with high interactions will result.

A similar phenomenon called membrane poisoning is desribed in literature for the permeation of large organic anions through anion-exchange membranes. The large caesium cation is characterized by the smallest hydration diameter. This can also be seen from a contraction of the membrane during exchange of counter ions. According to the Lewis theory on acid base strength, the sulfonic acid group has the highest acidity with the Cs^+ counter ion. Furthermore, the interaction between protic and aprotic dipolar penetrants is at a maximum. Non-polar permeands, however, can still migrate through the hydrophobic regions of the matrix. The permeation rates of non-polare compounds are typically low, due to the dense morphology of the material.

These interpretations are based in single-component permeation experiments. But the general features can also be observed for binary mixtures as shown in *figures 5.22 and 23*. In general all membranes act against the vapor liquid equilibrium (indicated by distillation). In the proton form, the membrane in proton form is still butanal and ether selective over the whole concentration range. However, potassium and caesium form is cyanohydrin selective over the whole concentration range. The maximum in permeability selectivity can also be found in the McCabe-Thiele diagrams. From the single-component sorption diagrams, the Cs^+ line could be expected to shift even more to higher cyanohydrin concentrations in the permeate phase. However, the values for membranes in Cs^+ form fall between the data for the potassium and sodium form. This trend is in agreement with the predictions from the single-component permeation experiments [41].
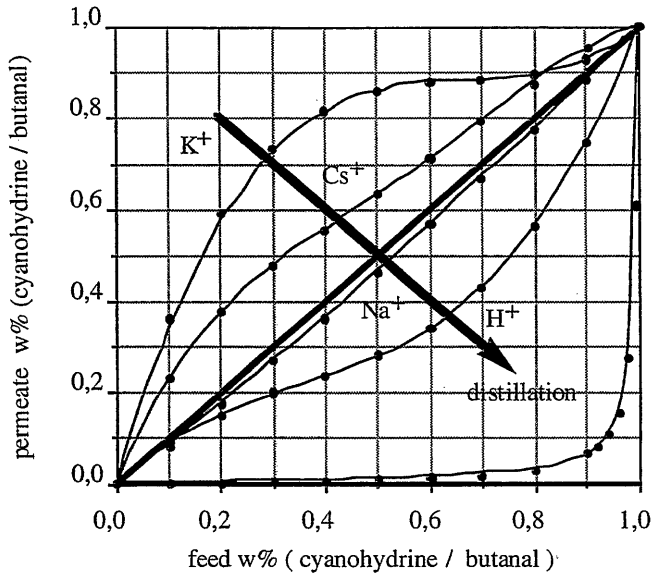
Figure 5.22   *Mc.Cabe-Thiele diagram of the PSIS membrane for the binary system of the substrate and the product*
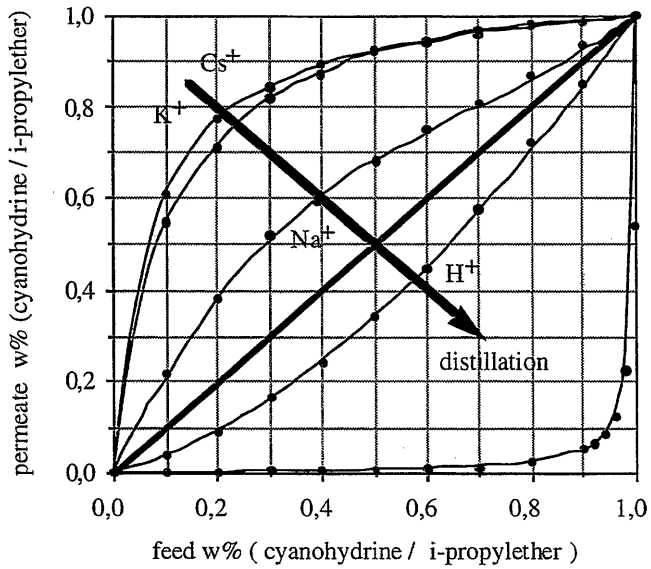
Figure 5.23   *Mc.Cabe-Thiele diagram of the PSIS membrane for the binary system of the product and the solvent*

The results from sorption experiments might be supported by solubility parameters for the permeants and the membrane. The data presented in *table 5.13* show, that differences in the dispersion interaction term δ_D for the permeands are negligible. Major differences in the parameters [42] of the permeants occur from the hydrogen bonding energy δ_H and from dipole-dipole interactions δ_P. The strong dipole of the cyanohydrin molecule along the C–CN bond, is the reason for such a high dipole-dipole interaction parameter. As an effect of the strong dipole of the cyanohydrin, a dynamic immobilization at positively or negatively charged functional groups in the membrane can occur.

Table 5.12 *Solubility parameters for the permeands and the polymers*

	δh	δP	δD		δ total
di-iso-propylether	1.5	4.7	13.6	1	4.4
butanal	9.6	8.9	13.1		18.6
2-hydroxypentanenitrile	24.7	15.2	11.1		31.0
polydimethylsiloxane	4.7	0.1	15.9		16.6
sulfonated polysulfone	11.9	14.7	17.4		25.7
Nafion® 117	polymer matrix				20.67*
	ion cluster				34.19*
RAI 1010					32.0*

The cation-exchange polymers, on the other hand, also show significant high solubility parameters. The total value of homogeneous sulfonated polysulfon, sulfonated polystyrene interpolymers (RAI 1010) and sulfonated poly(tetrafluoroethylen-perfluorovinylether) are $\delta_{total} = 26$, 32 and 34 respectively. The corresponding value for the cyanohydrin is $\delta_{total} = 31$.

The overall solubility parameter of these cation-exchange membranes will change upon exchange of the counter ion. This effect was described by Yeo [33] for both Nafion and radiation grafted membranes from Pall RAI. Within the 1. group of alkali metals from Li^+ to K^+, the solubility paramter of the RAI membrane increases. This effect is in agreement with the results in this work. Yeo gave an explanation for the change in solvent uptake from less polar solvents to aprotic dipolar solvents and finally to protic polar solvents while changing the counter-ion in the above mentioned order. The ideal solubilitiy of the sulfonated poly(styrene-co-isoprene) membrane corresponds perfectly with this model. The sorption of less polar butanal, $\delta_{total} = 18.6$, and di-iso-propylether, $\delta_{total} = 4.4$ decreases, the

sorption of 2-hydroxypentanenitrile $\delta_{total} = 31.0$ increases with increasing solubility parameter due to an exchange of counter ions.

The effect of enhanced solubility due to specific dipole-dipole interactions can also be related with the abnormal behavior of the permeation rates. According to work described by Metayer [40], the strong exchange capacity of an ion-exchange membrane can result in a 'reaction specifity' which will determine the selectivity of the membrane [44]. This reaction specifity is proportional to the stability of complexes between the fixed ion of the membrane, the sulfonic acid groups and the permeand, the cyanohydrin. The complex formation constants vica versa is depending on the strength dipole-dipole interaction energies. From the permeation simulation of Metayer [40] one can conclude, that facilitated transport or even a more rapid permeation of permeands arises only in case that the stability constants of the dipole pairs are neither too low nor too high.

Therefore, the separation effect is based on a preferential sorption of the permeants in the membrane.

5.5. Conclusions

In chapter 5 of this work, the development of a tailor-made functional membrane for the selective separation of cyanohydrins from the reaction broth of an enzyme membrane reactor using pervaporation is described. The separation problem is complicated through the physical properties of the individual components of the mixture. Generally, the low volatile cyanohydrins tend to decompose or in case of homochiral cyanohydrins tend to racemize upon heat treatment. Therefore, low temperatures and mild separation conditions are required for processing of the solutions. The substrates and the solvent on the other side are highly volatile compounds, the product has a low volatility. Therefore, the membrane selectivity has to be very high to counteract the evaporation selectivity.

It can be summarized, that hydrophilic functional membranes are generally requested for the removal of cyanohydrins. Sufficient results in terms of selectivity and permeation rate with hydrophilic membranes were obtained from a β-cyclodextrin-polyurethane copolymer membrane. Better results, however, are obtained with charged membranes. Anion-exchange membranes, prepared from brominated polyphenylenoxide exhibit good selctivities for the cyanohydrin in case of sulfate counter ion. In contrast, the selectivity reverses towards the

aldehyde by an exchange of the counter ion with the hydrogensulfite. Facilitated diffusion of the aldehyde via reversible formation of bisulfite complexes might occur in this case.

For cation-exchange membranes, the best results concerning the separation of cyanohydrins are observed. Reasonable selectivities as well as high permeation rates are found with sulfonated polyetherketones. However, the stability of those membranes within the whole concentration range of the organic solvents was limited. Therefore, a crosslinked cation-exchange membrane was developed. Formation of the 3-dimensional network occured via hydrosilylation of a sulfonated poly(styrene-co-isoprene) elastomer. The film forming properties of the material is excellent. For different counter ions of the membrane, different selectivities and permeation rates were found. The highest sorption selectivity was observed from the caesium Cs^+ counter ion. The highest permeation selectivity was found for the potassium K^+ counter ion. This effect can be attributed to a preferential sorption of the cyanohydrin as described using solubility parameters.

List of Symbols

a_i	activity of component i
A_{AB}	exchange energy density
c	concentration
D	diffusivity
$D_i^{m,T}$	thermodynamic diffusion coefficient
e_A	cohesion energy density
E_A	activation energy
E_D	activation energy of diffusion
E^o	potential energy of a condensed phase per unit volume
f_i	fugacity of component i
J_i	mass transfer or permeation rate
J_N	normalized flux density
K_S	sorption coefficient
L	membrane thickness
N_A	Avogradro's constant
p	total pressure

p_i	partial pressure of component i
p_i^S	saturation vapour pressure of species i
P_i	permeability coefficient of species i
R	gas constant
$S_{i,j}^*$	ideal permeation selectivity
$S_{i,j}$	permeation selectivity
S_0	solubility coefficient
S^m	relative solubility
$\Delta_m U_v$	energy of mixing
T	temperature
$\alpha_{i,j}^0$	ideal selectivity
u_i^m	absolute mobility of species i in the membrane
v	permeation velocity of species i
x_i	mole fraction of species i
z	coordinate in direction of transport

Greek Letters:

$\alpha_{i,j}$	separation factor
$\alpha_{i,j}^{evap}$	destillation separation factor
$\alpha_{i,j}^m$	solution-diffusion membrane separation factor
β_i	enrichment factor
δ	solubility paramter
δ_d	dispersion energy parameter
δ_p	dipole-dipole-parameter
δ_h	hydrogen bonding parameter
γ_i	activity coefficient
λ	jump length,
φ_i^S	fugacity coefficient
Φ_i	volume fraction of species i
Φ_p	volume fraction of species i in the polymer
χ_{ip}	Flory-Huggins interaction-parameter
σ	kinetic diameter
σ^2	penetrant cross section
μ	chemical potential
ξ	degree of conversion, turnover

Subscripts and Superscripts:

'	value in the feed stream
' '	value in the permeate stream
0	standard reference state
*	ideal case
i	species i
m	membrane
T	temperature

Abbreviations:

Avicel®	microcrystalline cellulose, FMC Corporation, type PH-101
β-CD	β-cyclodextrin
DIPE	di-iso-propylether
HCN	hydrocyanic acid
mdi	methylene-bis-diphenylisocyanate
PDMS	polydimethylsiloxane
PEEK	polyetheretherketone
PSIS	poly(styrene-co-isoprene)sulfonic acid
SPEEK	sulfonated polyetheretherketone
PPO	polyphenyleneoxide
TMBDA	1.4-bis-(dimethylamino)butane

References

[1] Fujita, H.
Diffusion in polymer-diluent systems
Fortschr. Hochpolym.-Forschung 3, 1-47 [1961]

[2] Böddeker, K.W.
Pervaporation durch Membranen und ihre Anwendung zur Trennung von Flüssiggemischen
Fortschrittsbericht VDI-Reihe 3, Nr. 129, VDI-Verlag Düsseldorf 1986

[3] Néel, J.M.
Pervaporation: fundamentals and practice
Makromol. Chem., Makromol. Symp. 70/71, 327-339 [1993]

[4] Acharya, H.R.; Stern, S.A.; Liu, Z.Z.; Cabasso, I.
Separation of liquid benzene/cyclohexane mixtures by perstraction and pervaporation
J. Membrane Sci. 37, 205-232 [1988]

[5] Lee, L.T.C.; Ho, W.S.; Liu, K.-J.
Allied Chemical Corporation
Membranlösungsmittelextraktionsverfahren
DE 2 364 679 [27.12.1973]

[6] Petropoulos, H.H.
Membranes with non-homogeneous sorption properties
Adv. Polymer Sci. 64, 85-134

[7] Wijmans, J.G.; Baker, R.W.
The solution diffusion model: a review
J. Membrane Sci. 107, 1-21, [1995]

[8] Meares, P.
Transport through polymer membranes from liquid phase
Ber. Bunsenges. Phys. Chem. 83, 342-351 [1979]

[9] Okada, T.; Matsuura, T.
Theoretical and experimental study of pervaporation on the basis of pore flow mechanism
in: 'Proceedings of the sixth international conference on pervaporation
processes in the chemical industry', Ed. R. Bakish
Bakish Materials Corporation, Englewood, 1992, 137-152

[10] Meares, P.
Separation by membrane, synthetic membranes; science, engineering and applications.
NATO ASI Series, Series C:
Mathematical and Physical Sciences, Vol. 181, 155 [1983]

[11] Fujita, H.
Organic vapors above the glass transition temperature
in: 'Diffusion in Polymers', Ed. J. Crank, G.S. Park
Academic Press, New York, 1968

[12] Flory, P.J.
Principles in polymer chemistry
Cornell University Press, Ithaca, New York, 1953

[13] Vrentas, J.S.; Duda, J.L.
Diffusion in polymer-solvent systems. I. Reexamination of the free-volume theory
J. Polym. Sci., Polym. Phys. 15, 403 [1977]

[14] Vrentas, J.S.; Vrentas, C.M.; Duda, J.L.
Comparison of free-volume theories
Polymer J. 25(1), 99-101 [1993]

[15] Bell, C.-M.
Untersuchungen zum Permeationsverhalten von Lösungsmitteln und deren Gemische
in Membranen aus elastischen und glasartigen Polymeren
Dissertation, Universität Stuttgart 1987

[16] Gudernatsch, W.-N.
Integration des pervaporativen Produktaustrags in die Fermentation von organischen Lösungsmitteln
Dissertation Universität Stuttgart, 1989

[17] Boyadzhiev, L.
Liquid pertraction or liquid membranes - state of the art
Separation Sci. Tech. 25(3), 187-205 [1990]

[18] Böddeker, K.W.
      Terminology in Pervaporation
      European Society of Membrane Science and Technology (ESMST), 1989

[19] Wijmans, J.G.; Baker, R.W.
      A simple predictive treatment of the permeation process in pervaporation
      J. Membrane Sci. 79(1), 101-114, [1993]

[20] Bauer, B.; Strathmann, H.; Effenberger, F.
      Verfahren und Vorrichtung zur enzymatischen Synthese
      Fraunhofer-Gesellschaft
      DE 40 41 896 C1 (27.12.1990)

[21] Reid,Prausnitz,Poling
      The properties of gases and liquids
      Mac Graw-Hill, 4.Auflage

[22] Shelden, R.A-; Thompson, E.V.
      Dependence of diffusive permeation rates and selectivities on upstream and downstream pressures
      III. Membrane selectivity and implications for separation processes
      J. Membrane Sci. 4, 115-127 [1978]

[23] Neel, J.; Nguyen, Q.T.; Clement, R.; Lin, D.J.
      Influence of downstream pressure on the pervaporation of water-tetrahydrofuran mixtures
      through a regenerated cellulose membrane (Cuprophan)
      J. Membrane Sci. 27, 217-232 [1986]

[24] Barton, A.F.M.
      CRC Handbook of solubility parameters and other cohesion parameters
      CRC Press, Inc., Boca Raton, USA, 1985

[25] Hansen, C.M.
      The universality of the solubility parameter
      I&EC Prod. Res. Dev. 8(1), 2-11 [1969]

[26] Hildebrand, J.H.; Scott, R.L.
      Regular Solutions
      Prentice Hall, Englewood Cliffs, N.J. 1962

[27] Hildebrand, J.H.; Scott, R.L.
      Solubility of non-electrolytes
      Reinhold, New York, 3rd. Ed., 1950

[28] Hildebrand, J.H.; Prausnitz, J.M.; Scott, R.L.
      Regular and related solutions
      Van Norstrand-Reinhold, Princeton, N.J. 1970

[29] Hansen, C.M.
      Three dimensional solubility parameter and solvent diffusion coefficient
      Danish Technical Press, Copenhagen 1967

[30] Miyata, T.; Iwamoto, T.; Uragami, T.
      Characteristics of permeation and separation for propanol isomers through
      poly(vinylalcohol) membranes containing cyclodextrin
      J. Appl. Polymer Sci. 51, 2007-2014 [1994]

[31] Yamasaki, A.; Iwatsubo, T.; Masuoka, T.; Mizoguchi, K.
      Pervaporation of ethanol/water through a poly(vinylalcohol)/cyclodextrin membrane
      J. Membrane Sci. 89, 111-117 [1994]

[32]   Gudernatsch, W.; Krumbholz, Ch.; Strathmann, H.
       Development of an anion-exchange membrane with improved permeability for
       organic acids of high molecular weight
       Desalination 79, 249 [1990]

[33]   Malon, R.F.; Zampini, A.
       Crosslinked polyphenyleneoxide gas separation membranes
       Monsanto Co.
       US-Patent 4,530,703 (23.07.1985)

[34]   Betterton, E.A.; Erel, Y.; Hoffmann, M.R.
       Aldehyde-bisulfite adducts: prediction of some of their thermodynamic and kinetic properties
       Environ. Sci. Technol. 22, 92-99 [1988]

[35]   Igawa, M.; Fukushi, Y.; Hayashita, T.; Hoffmann, M.R.
       Selective transport of aldehydes across an anion-exchange membrane
       Ind. Eng. Chem. Res. 29(5), 857-861 [1990]

[36]   Cabasso, I.; Liu, Z.Z.
       The permselectivity of ion-exchange membranes for non- electrolyte liquid mixtures
       I.Seperation of alcohol/water mixtures with NAFION hollow fibers
       J.Membrane Sci. 24 [1985] 101-119

[37]   Hsu, W.Y.; Gierke, T.D.
       Ion transport and clustering in NAFION perfluorinated membranes
       J.Membrane Sci. 13 [1983] 307-326

[38]   Kerres, Jochen
       Synthese und Charakterisierung von vernetzten Blockcopolymeren aus
       Polyhydrogensiloxanen und ungesättigte Seitengruppen enthaltenden Styrol-Copolymeren
       Dissertation, Universität Stuttgart, 1991

[39]   Cabasso, I.
       The permselectivity of ion-exchange membranes for non-electrolyte liquid mixtures
       II.The effect of counterions
       J. Membrane Sci. 28 [1986] 109-122

[40]   Métayer, M.; Langevin, D.; El Mahi, B.; Pincoche, M.
       Facilitated extraction and facilitated transport of non-ionic permeants through ion-exchange
       membranes: influence of the stability of the permeant/carrier complexes
       J. Membrane Sci. 61, 191-213 [1991]

[41]   Wenzlaff, A.; Böddeker, K.W.; Hattenbach, K.
       Pervaporation of water-ethanol through ion-exchange membranes
       J. Membrane Sci. 22, 333-344 [1985]

[42]   Jonquières, A.; Roizard, D.; Lochon, P.
       Use of empirical polarity parameters to describe polymer/liquid interactions:
       correlation of polymer swelling with solvent polarity in binary and ternary systems
       J. Appl. Polymer Sci. 54, 1673-1684 [1994]

[43]   Yeo, R.S.; Chan, S.F.; Lee, J.
       Swelling behavior of Nafion® and radiation-grafted cation-exchange membranes
       J. Membrane Sci. 9, 273-283 [1981]

[44]   Brun, J.P.; Larchet, C.; Melet, R.; Balvestre, G.
       Modelling of the pervaporation of binary mixtures through moderately swelling,
       non-reacting membranes
       J. Membrane Sci. 23, 257-283 [1985]

Chapter

6

ENZYME-MEMBRANE REACTOR

Synopsis

The large-scale (R)- or (S)-oxynitrilase catalyzed addition of hydrocyanic acid to carbonyl compounds might be done either in batch or in continuous bioreactors. High marginal costs for isolation and purification of the enzymes from almonds or sorghum respectively make it necessary to achieve maximum specific productivities. Both, the specific productivity and the space-time-yield of an enzymatic reaction can be optimized by the choice of an appropriate continuous bioreactor.

As already shown in chapter 4, the K_m-values of the cyanohydrin synthesis are small, so that the reaction rate is in the V_{max}^*-range already at low substrate concentrations. Therefore, the enzymatic synthesis of (R)-2-hydroxypentanenitrile is carried out in a stirred tank reactor. Build-up of the inhibiting products is avoided by continuous removal of the cyanohydrin. Product recovery is done via pervaporation using selective membranes from potassium poly(styrene-co-isoprene)sulfonate. The partial pressure of the low volatile cyanohydrin is decreased using water as an entrainer. During 500 hours, a space-time-yield of 3,8 mole$\cdot$l^{-1}$\cdot$h^{-1} at an enationmeric excess of >95 % ee was achieved.

The shear sensitivity of the (S)-oxynitrilase, on the other hand, does not allow the use of an stirred tank reactor. Even though, the enzymatic reaction is slow, the degree of conversion is high because the reaction equilibrium is almost completely on the product side. Therefore, the synthesis of (S)-2-hydroxy-2-(3-phenoxy-phenyl) acetonitrile is carried out in a laminar flow tubular reactor. The residual aldehyde is removed from the product via pertraction using a quaternized polyphenyleneoxide bisulfite membrane. In a long-term experiment, a space-time-yield of 0,442 mole$\cdot$l^{-1}$\cdot$h^{-1} at an enationmeric excess of >96 % ee was achieved.

6.1. Introduction

6.1.1. General introduction

To achieve high space-time yields and a high turnover in the application of enzymatic reactions, a continuous process design is required [1]. For native as well as for immobilized enzymes, this can be carried out in so-called continuous stirred-tank reactors (CSTR), tubular reactor with plug flow (PFR) or membrane reactors (EMR) as shown in *figure 6.1* [2]. There are various procedures available for the immobilization of the enzyme. Covalent or adsorptive bonding on a fixed carrier, the intermolecular cross-linking of the enyzmes with the help of multi-functional reagents, and also the encapsulation of the enzymes are of technical importance. The kind of immobilization, the design of the enzyme reactors, and finally, the selection of an appropriate reactor are the key elements of a biotechnological process [3]
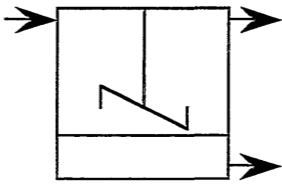
(a) CSTR
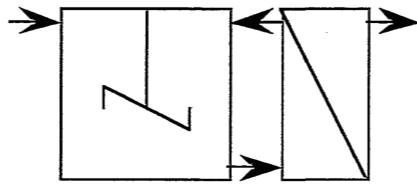
(b) CSTR with external filtration unit
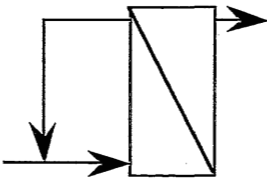
(c) Loop reactor
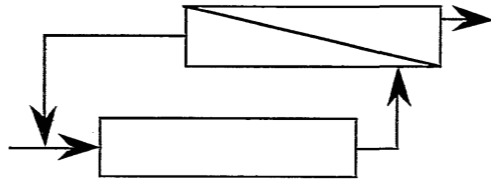
(d) PFR with external filtration unit

Figure 6.1 *Technical bioreactor design: (a) continuous stirred tank reactor,*
(b) continuous stirred tank reactor with external filtration unit,
(c) loop-type bubble column, (d) tubular plug flow reactor

The interaction of all these factors is not straightforward and the design of a new process requires detailed optimization of each part separately, of the parts in respect to each other and finally as a complete concept. This thesis has described in the previous chapters the optimization of the enzymatic reaction to produce homochiral cyanohydrins and the development of membranes removing the reaction product from the reaction liquid. In this part, the integration of reaction and separation into an enzyme membrane reactor will be described [4,5]. The focus will be on the integration of reaction kinetics and reactor design with separation and separation process design.

6.1.2. Choice of Reactor

The selection of a suitable type of reactor can be related to the kind of enzyme-kinetic inhibition observed. Generally, substrate-inhibited reactions perform better in CSTR whereas product-inhibited reactions are advantageous in the batch reactor or in PFR. An essential parameter in the examination is the relation of the substrate concentration $[A]_0$ in the feed and the accompanying K_m-value of the enzyme. For the large substrate concentration on the total range of reaction relative to the Michaelis-Menton constants, no significant difference between a CSTR and a PFR exists [6]. The case is approximately fulfilled for the cyanohydrin synthesis, since the measured K_m-values are generally small. Thus, it is possible to perform a reactor design on the basis of both kinetic data characterized for enzymatic reaction and on practical aspects of product processing.

The influence of the retention time on the conversion is strictly proportional to the enyzme concentration in the reactor. Howaldt [2] derived that the ratio $[E]_{CSTR}/[E]_{PFR} = \tau_{CSTR}/\tau_{PFR}$ are valid for the compared valuations. In principle a continuous stirred-tank reactor is appropriate in combination with a selective product recovery, since constantly small product concentrations exist in continuous operation. However, the substrate also approaches constantly its entry concentration.

The ideal continuous stirred tank reactor

The simplest type of a reactor is the stirring-tank, which is suitable for media of higher viscosity and immobilized biocatalysts of low activity [7]. For the batch reactor the degree of conversion ξ as a function of time might be obtained through the integration of the rate equation. For the continuous reactor, in an ideal stirring-tank reactor, the reaction mass flows continually through the reactor. Due to perfect mixing, no temperature or

concentration profiles exist in the reactor vessel. Therefore, the concentration in the tank must be equal to the outlet concentration:

$$\frac{d\,[A]}{d\,t} = \frac{Q_V\,(\,[A]_{0,in} - [A]\,)}{V_R} + \upsilon* \tag{1}$$

The mass balance of component A is given by [A] the concentration in the reactor, $[A]_{0,in}$ the concentration at the inlet, Q_V from the volume flow, V_R from the reactor volume, and of the reaction rate $\upsilon*$. The degree of conversion ξ related to the reaction of A $\rightarrow$ B is determined by the residence time τ, as the relation of the reactor volume V_R and the volume flow Q_V, the reaction rate in the outlet υ_{out}^* and the substrate concentration $[A]_{0,in}$ at the inlet.

$$\xi = \frac{\upsilon_{out}^* \cdot \tau}{[A]_{0,in}} \qquad \text{with} \qquad \tau = \frac{V_R}{Q_V} \tag{2}$$

The above mentioned relationship allows the determination of the necessary residence time τ for a desired conversion. Since in the CSTR conditions and concentrations for the outlet are constantly present, that is e.g. low substrate concentrations and high product concentrations, the stirring-tank reactors are preferably applied, if the kinetics of the enyzmatic reaction shows a distinct substrate inhibition. In the presence of product inhibition a tubular reactor is desired. The selection of the suitable reactors depends, however, also on the average conversion, since enzymatic reactions follow a zero-order reaction in the substrate saturation range ($[A] \gg K_{m,A}$), whereas they follow a first-order reaction at low stubstrate concentrations. For higher reaction orders a PFR is generally favourable over a CSTR. The conversion in the tube reactor with laminar flow profile is constantly smaller than in the plug flow reactor, however, shear stress in the LFR is smaller. The advantages in process engineering of a CSTR, like the simpler balance of an enzyme deactivation, can be overcome in product-inhibited reactions through application of a cascade of stirring-tank reactors.

From the kinetic data for the (R)-oxynitrilase, the continuous stirred-tank can be characterized as an ideal reactor type. The allowed high starting concentration of the substrates $[A]_{0,in}$ at the inlet firstly results in a high space-time yield. The ideal and complete mixing of the substrates as well as a turbulent flow of the immobilized enzyme leads to minimal transport limitations.

In contrast, the expected space-time yields for the (S)-oxynitrilase is smaller. The slow reaction kinetic causes a high retention time in the reactor. Simultaneously, the reaction encounters a strong inhibition through both the substrate and the product. An improvement of space-time yields in the application of a cascade of CSTRs does not seem advantageous due to the high shear sensitivity of the adsorptively immobilized enzyme.

6.1.3. State-of-the-art of enzyme membrane reactors

Enyzme membrane reactors [8] are mostly utilized for continuous processes with native enzymes. Ultrafiltration membranes retain the enzyme in the reaction vessel, however are permeable for substrate, solvent and product [3]. In a subsequent step, the product must be separated from solvent and substrate the latter being fed back to the reactor. The ultra-filtration membranes usually applied [9] can, therefore, be installed in the form of flat or hollow fiber membranes. Sometimes, the enzymes are additionally immobilized on the feed side surfaces of the membranes, so that the dynamics of the reaction along with the enzyme kinetics is especially dependent on the transport limitations [10]. Such enzyme membrane reactors are successfully applied industrially, for instance, for the resolution of amino acids, like (L)-methionine, (L)-valine, or (L)-phenylalanine by using an aminoacylase starting from an acetylaminoacid. Furthermore, the addition of ammonia to fumaric acid resulting in (L)-asparaginic acid by using aspartase, as well as the subsequent decarboxylation to (L)-alanine, and the addition of water to the (L)-malic acid using a fumarase, are applied for a long time in the industrial enzyme reaction technology.

In the technical application of enzyme membrane reactors the problems frequently result from mass transport limitations, concentration polarization, and fouling due to higher protein concentrations through the make-up of new enyzmes. An interference of the enzymatic reaction, due to limitations in forward and backward mass transport of the corresponding substrate or product, is particularly described in diffusively operated membrane reactors. Examples are given by Flaschel [3], in which the enzyme is encapsulated in the lumen of a dialysis membrane [11]. This reactor configurations offer advantages, if the shear sensitive catalysts, like animal cells, for instance, are applied. A satisfactory improvement and increased productivity is observed in convectively operated reactors. Most of the concentration polarization appearing in dead-end filtration through a concentration excess increase of the retentate can further be reduced in the cross-flow technique. Mostly through fouling, the tendency of porous membranes to form an organic biofilm under filtration conditions can be comprehended. Experiments through membrane modification, for instance, through the production of hydrophilic, or even charged surfaces for improving the filtration performance, have so far led to only gradual improvements of long-term stability of transmembrane flux density [2]. In an improved process design, for instance, through back-flushing, pulsatile flows, mechanically abrasive cleansing, or ultrasonic energy, but more particularly through cyclical washing with chemical and enzymatic additives and detergents, a satisfactory constant membrane-separating performance could be attained. If the circulation flow rate of a convectively operated UF-membrane reactor is large relative to the substrate dosage, such a reactor can be described as a continuous stirred tank reactor.

Matson [12] suggested a modification of conventional membrane reactors for the multi-phase membrane bioreactor for the enyzmatic resolution of racemates. Thus, the enzyme is encapsulated in a hydrophilic membrane, the hydrophobic substrate is dissolved into an organic feed liquid, and the more hydrophilic product leaves the membrane reactor module in an aqueous permeate phase. Strictly seen, these arrangements describes the first continuous enzymatic synthesis with selective product recovery. The selectivity, in this case, however not induced through the membrane, but instead through the distribution coefficient of the reaction partner in the organic and aqueous phase.

6.2. The Solution-Diffusion Bioreactor Concept

(R)-oxynitrilase (EC 4.1.2.10) and (S)-oxynitrilase (EC 4.1.2.11) catalyze the formation of (R)- and (S)-cyanohydrins out of a greater multitude of aldehydes or ketones in the presence of HCN. The advanced conversion of these optically pure cyanhydrins without any further racemization into α-hydroxycarboxylic acids, α-amino alcohols and pyrethroid insecticides is widely known in scientific literature [13,14,15].

As described, the enantioselective enzymatic reaction competes with the non-stereospecific chemical addition of hydrogen cyanide on the carbonyl compound. This undesired side reaction can either be supressed through shifting of pH-values or through an enzymatic conversion in an organic medium. The unlimited solubility of the carbonyl compounds is a further advantage of the organic medium, since now also aromatic aldehydes, higher aliphatic, and heterocyclic aldehydes and ketones can be transformed. Therefore, besides a higher reaction rate and better optical yields, also higher substrate concentrations and improved space-time yields are achieved.

The practical application of these enzymatic syntheses face a number of engineering and economical problems:

a)   The profitability of the process is determined exclusively through the maximum cycle quantity or turnover of the enzyme. On the one hand, this depends on the enzyme stability, and on the other hand, however, more importantly on the quality of the immobilization. The latter is mainly concerned with exactly how the enzyme remains in the reaction vessel. The adsorptive immobilization of the enzyme on Avicel® is reversible and very sensitive to changes of the ionic potential of the solution.

b)   The oxynitrilase-catalyzed conversion experiences a competitive inhibition through the carbonyl component, particularly the aldehyde, and through the product, particularly the cyanohydrin.

c)   The products cannot be removed by distillation nor by chromatography without further racemization. This makes an isolation of products very costly and often impossible. The distillation residue contains aside from cyanohydrin also buffer salts, which are very costly, for instance, and are separated from a cyanohydrin through an extraction or ion exchange.

d)   The optical yields are, in principle, very good, but the reaction towards the equilibrium conversion is frequently very low.

e)   In the operation mode with an organic medium, the typical problems of disposal of organic waste has to be addressed.

The task of a new bioreactor [16] shall, therefore, be a rapid and complete attainment of an enantiomeric pure product in which the cyanohydrin shall be directly removed from the reactor. The bioreactor concept was proven with two different substrates, two different enzymes and two different methods of product recovery. Fundamentally, there was a distinction made between volatile stable and non-volatile racemating products. Beyond that there was a distinction made between enzymes, the reaction kinetics of which suggests a conversion in the stirring-tank reactor, and enzymes, the reaction kinetics of which suggests a conversion in the tubular reactor. Thus, the following substrate selection was met for the production of homochiral cyanohydrin:

1)   The synthesis of (R)-2-hydroxypentane-nitrile describes the (R)-oxynitrilase catalyzed addition of hydrocyanic acid on butanal in the stirring-tank reactor. The product, (R)-butanalcyanohydrin can be in general evaporated without thermal decomposition and formation of a racemate. The product recovery from a stirred reactor, therefore, occurs via a selective separation of cyanohydrin, by means of pervaporation.

2)   The synthesis of (S)-2-hydroxy-2-(3-phenoxyphenyl) acetonitrile describes the (S)-oxynitrilase catalyzed addition of hydrocyanic acid on meta-phenoxybenzaldehyde (mpba) in a laminar flow tubular reactor. The product, (S)-meta-phenoxybenzaldehydecyanohydrin (mpbac), cannot be evaporated and forms a racemate upon heat treatment. The product recovery occurs, therefore, by means of pertraction.

6.3. Product recovery by pervaporation

6.3.1. Mass transport and separation process performance

Vacuum pervaporation

The cyanohydrin, (R)-2-hydroxypentane-nitrile, shall be synthesized in the pervaporation membrane reactor. The cyanohydrin represents, however, a low-volatile compound with the lowest saturation vapor pressure of all compounds present in the reaction mixture (see *table 6.1.*). Since the driving forces are small, the selectivities of the installed membranes must be high. The results of a screening on a suitable solution-diffusion membrane, described in Chapter 5, clearly demonstrates that cation-exchange membranes are suitable for the selective removal of 2-hydroxypentanenitrile. The best selectivities and permeation rates are obtained from a crosslinked and sulfonated membrane prepared from poly(styrene-co-isoprene). These will be applied in the following.

	di-iso-propyl-ether	HCN	butanal	2-hydroxypentane nitrile
M_W [g·mol^{-1}]	102.18	27.03	72.11	99.14
bp [°C]	68	26	75	230 [2]
d_m [Å]	6.16	3.98	5.27	5.57
p_S [mbar] [1]	198	992	149	0.9
Polarity [D]	1.21	2.98	2.72	3.81

[1]   acc. Wagner relationship   [2]   acc. Joback group contribution method

Table 6.1   *Physical properties of the solvent, the substrates and the product [17,18]*

In chapter 5, the characterization of the PSIS membrane is described in terms of pure component selectivities and permeabilities. Concerning practical applications, a description of the actual performance under process conditions is required. The characterization of membranes using vacuum pervaporation occurs typically with a very low, negligible activity on the permeate side. This is attained by condensation of the permeants in liquid nitrogen. For $f_i'' \rightarrow 0$ the proportionality between the permeation rate, partial flux density J_i of a component as well as its driving force [19,20] is expressed by:

$$J_i \;=\; P_i \;\cdot\; \frac{1}{\Delta z} \;\cdot\; \gamma_i' \;\cdot\; x_i' \;\cdot\; p_i^S \tag{3}$$

Therefore, one must certainly keep in mind, that the permeability of the membrane must be regarded as an intrinsic constant only in pure component systems. However, it is a variable in realistic systems. Through the sorption of co-permeants, the polymer matrix alters which can be seen in a concentration-dependent swelling. Furthermore, diffusion coefficients for pure components change also in the presence of other permeants.
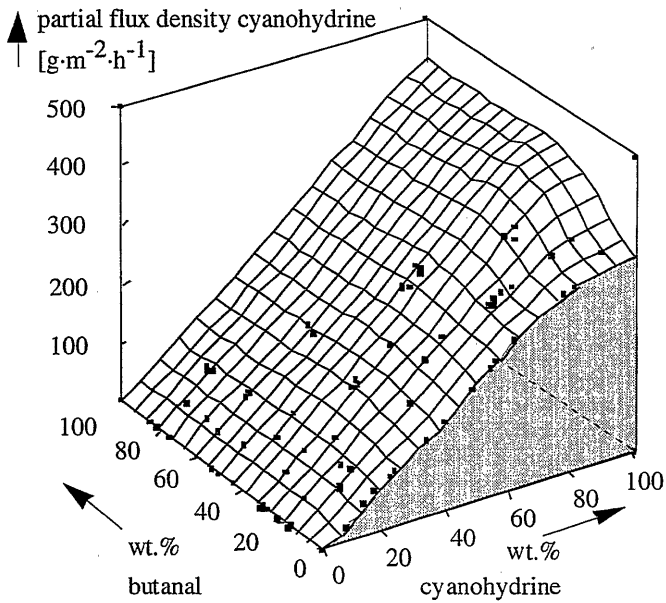
Figure 6.2 *Partial flux density of the cyanohydrin as a function of the 3-dimensional composition of the feed solution*

Especially in functional membranes with stronger interactions between the permeant and the membrane matrix, coupled flux of the individual species must be presumed and the permeabilty P of a component i depends on a large number of parameters.

$$P_i \;=\; f\,(c_i',\, c_j',\, c_k',\, \ldots\ldots;\ a_i'',\, a_j'',\, a_k'',\, \ldots\ldots \ldots L,\, T,\, p'',\, Re\ etc.) \tag{4}$$

Error

An error occurred while processing this page. See the system log for more details.

cyanohydrin in the feed solution. Due to the copermeation of butanal, the total permeation rate through the membrane increases strongly with increasing cyanohydrin concentrations. Through the whole concentration range, the rejection of the solvent is sufficient.

The physical properties of the reaction partner do not only influence the design of the membranes but also the process design. The low vapor pressure of the cyanohydrin requires for the pervaporation, that the permeate pressure be $p'' < 0,1$ mbar, since the permeation selectivity $\alpha_{i,j}$ can then be expressed as a product of evaporation selectivity $\alpha_{i,j}^{evap}$ and the membrane selectivity $\alpha_{i,j}^{m}$. The pressure dependency shown in *figure 6.4* of the transmembrane flux and the partial flux indicates, that the actual selectivity of permeation and the enrichment factor concerning the separation of low volatile compounds decrease with increasing permeate pressure until the partial flux density of the cyanohydrin finally is reduced to zero favoring the partial flux density of di-iso-propylether and butanal.

Figure 6.4 *Partial flux density as a function of downstream pressure for permeation of solvent, substrate and product through poly(styrene-co-isoprene)sulfonic acid*

In view of the temperature dependency of the partial flux density, as shown in *figure 6.5* one recognizes that the selectivity of the membranes increases with increasing temperature. In other words, the activation energy related to cyanohydrin permeation is increased over the remaining co-permeants. Consequently, a maximum enrichment factor for the product can be obtained with a maximum temperature and minimum permeate presssure.
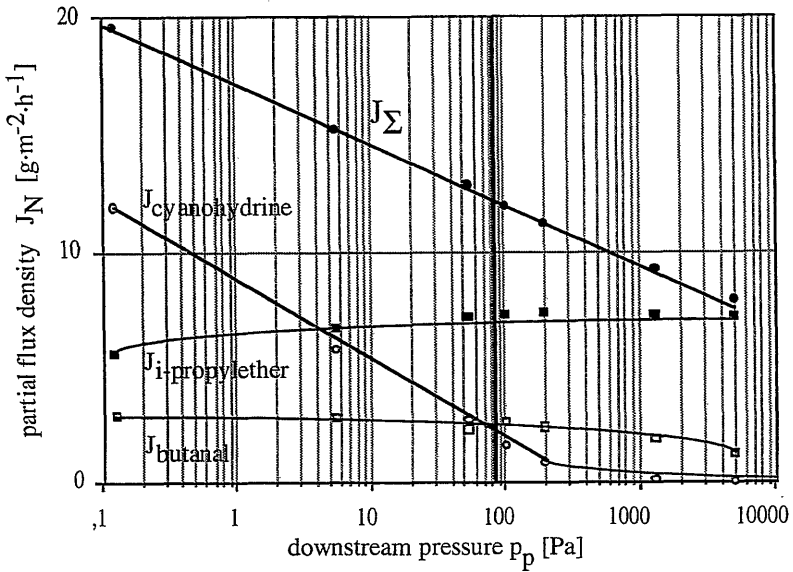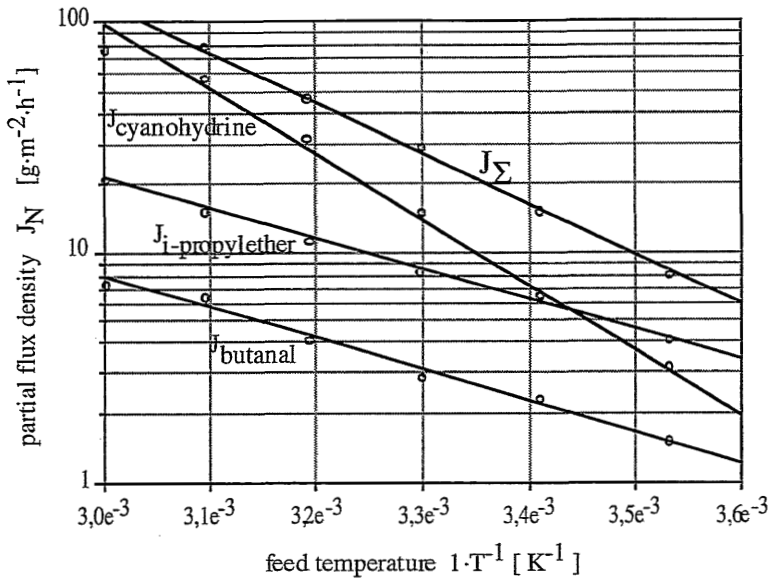
Figure 6.5 *Partial flux density as a function of feed temperature for the permeation of solvent, substrates and product through poly(styrene-co-isoprene)sulfonic acid*

Due to a limited temperature stability of the enzyme, a stirring-tank reactor with an integrated pervaporation membrane has only a limited application range. Another process option is to spatially separate the stirring-tank and the separation unit in order to set the pervaporation on a high temperature level. However, this also means additional investment and operational costs. Heat exchangers had to be added further into supplementary enzyme rejection through ultrafiltration as well as equipment for the condensation of the hydrocyanic acid. Consequently, the temperature was thus limited at a maximum of 35°C, and further optimization was carried out by minimizing the permeate pressure.

Entrainer pervaporation

Two possibilities exist to minimize the permeate pressure: (a) by increasing the vacuum pump performance or by (b) utilizing a side effect of co-permeation in pervaporation termed 'entrainer pervaporation'. Since the SPIS-membranes described in chapter 5 not only demonstrate a high selectivity towards the cyanohydrin, the membranes are also permeable

for water and hydrocyanic acid. The water or hydrocyanic acid co-permeation reduces the cyanohydrin vapor pressure relative to the downstream pressure since the permeate pressure is calculated as the sum of all the partial vapor pressure on the permeate side. This phenomenon will be described in more detail below.

During initial pervaporation experiments it was found that the available excess water from imperfect post-treatment of the Avicel® during immobilization of the oxynitrilases is dissolved in the liquor, specifically, in the di-iso-propylether. This physically dissolved water portion of the feed is recovered in the first condensates of the pervaporation experiment. In case that dehydration of the solvent continues and further water from the Avicel® dissolves in the solvent, this removal of the hydration water of the enzyme would cause an irreversible denaturation and must be avoided in any case. Therefore, continuous addition of water would solve this problem.

In the initial phases of pervaporation with the removal of the hydration water, overproportionally high initial flux was observed which was interpreted as an entrainer effect. Hence, addition of water to the reaction mixture would have two benefits: it would prevent denaturation and increase the driving force by decreasing the cyanohydrin partial permeate pressure. However, the dosage of water has to be adjusted to the amount of selective removal of water through the membranes. Otherwise, the non-specific chemical reaction would take place and the enantiomeric excess of the product will decrease.

To quantify the latter effect, pervaporation experiments with different water concentrations were carried out. A clear increase of the total flux with increasing water content can be found in *figure 6.5*. Due to the enrichment of the water in the permeate phase separation will occur in the permeate after condensation and most of that condensate is an aqueous phase.

The organic and water phase was analyzed separately regarding the cyanohydrin concentration. Cyanohydrin fluxes can be calculated then for the aqueous and organic phase and they are shown in *figure 6.6*.
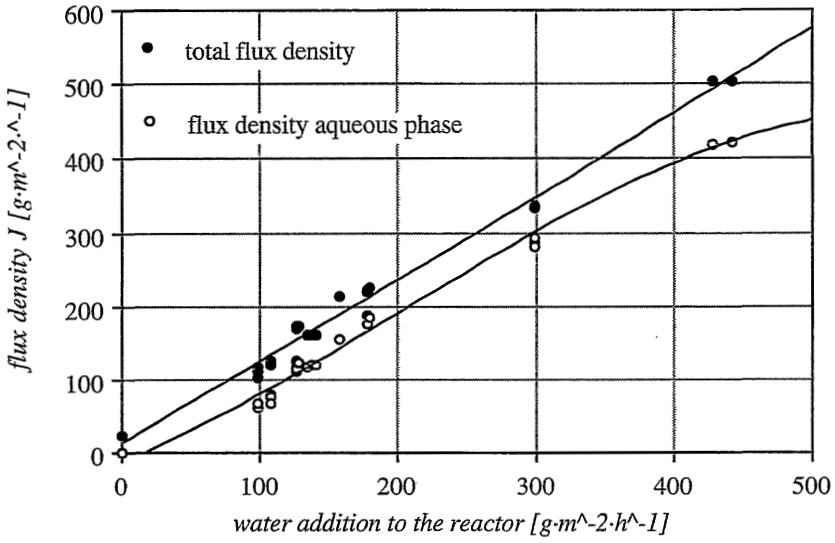
Figure 6.5 *Total flux density and partial flux density of the aqueous phase as a function of added water per effective membrane area*
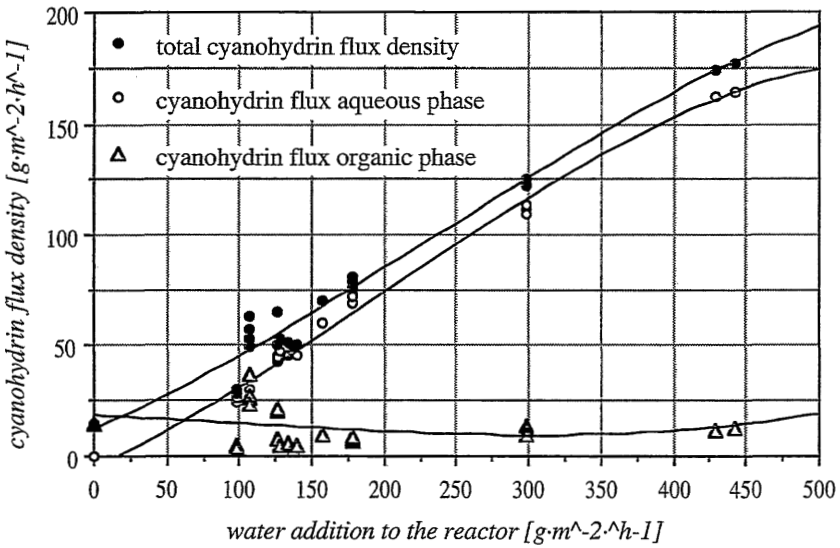
Figure 6.6 *Cyanohydrin flux density in both aqueous and organic phase as a function of added water per effective membrane area*

The addition of the organic and aqueous cyanohydrin fluxes gives the total flux which is compared to the total transmembrane flux in *figure 6.7*. In all figures the entrainer effect is clearly found. Hence, the stability of the enzyme as well as an increase in driving force can be guaranteed.
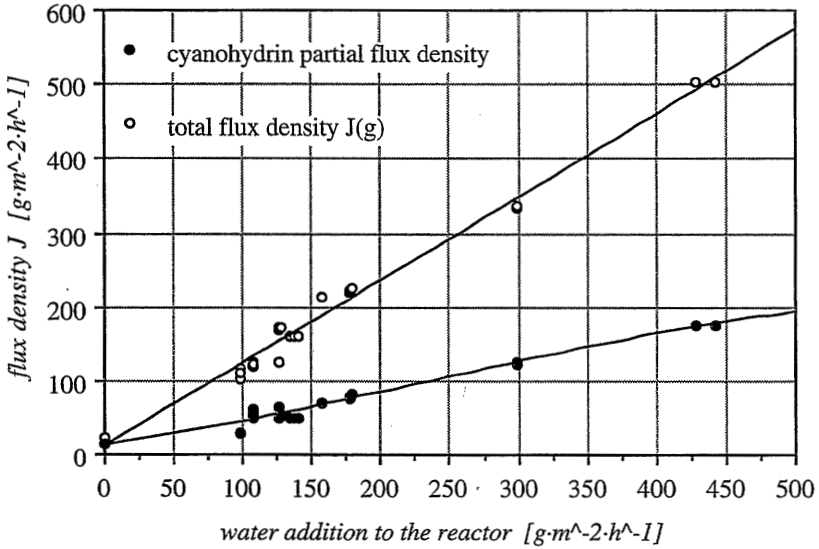
Figure 6.7 *Total flux density and partial flux density of the cyanohydrin as a function of added water per effective membrane area*

The hydrocyanic acid can also act as an entrainer. In the presence of hydrocyanic acid at 30°C, constant and stable selectivities and transmembrane flux densities were measured up to a permeate pressure of 20 mbar. Therefore, also hydrocyanic acid represents an ideal co-substrate for a entrainer pervaporation. The hydrocyanic acid can thus simultaneously accelerate the reaction kinetics, shift the reaction equilibrium to the product side, and accelerate the recovery of cyanohydrin in an entrainer effect. Due to experimental problems while using large amounts of hydrocyanic acid on a laboratory scale, these experiments were not proved in detail within a long-term run.

For practical realization, a process must be designed which allows condensation of the permeate at ambient pressures, specifically behind the vacuum pump. Liquid piston pumps,

dry-piston pumps, or membrane vacuum pumps are suitable for this. In this work , due to security reasons, such an arrangement could not be carried out in continuous processes.

Therefore, only entrainer pervaporation using make-up water represents a feasible technical process design. From the pre-examinations it could be proven, that the desired dosage of water influences the enzymatic reaction only slightly. Therefore, care must be taken so that no water from the Avicel® is sorbed. In the state of a continuing physical saturation of the di-iso-propylether with water just as with the hydration shell of the Avicel®, the enzymes stabilized accordingly. Through this continuous addition of water as an entrainer, the permeate pressure then increased to 10 mbar with constant cyanohydrin flux relative to the organic components in the two-phased condensate. A cost analysis [21] accounting for the additional operational costs demanded by the entrainer pervaporation was not carried out.

6.3.2. Pervaporation-Bioreactor

As already mentioned, the K_m values of the (R)-oxynitrilase-catalyzed cyanhydrin synthesis are small enough to conduct the reaction at a small substrate concentration in the V_{max} -range. Consequently, the continuous synthesis in the organic medium was carried out in a stirred tank reactor coupled with in-line product separation as shown in *figure 6.8.*
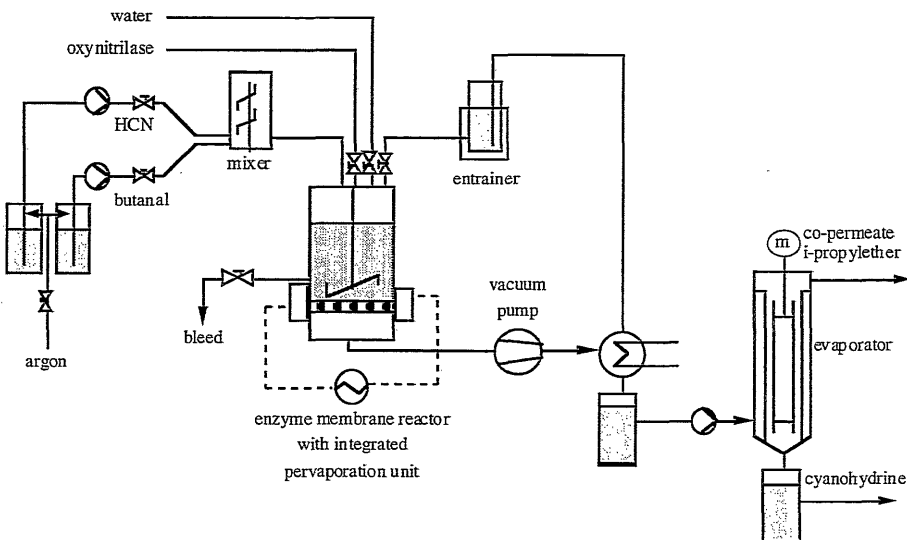

Figure 6.8 *Experimental setup of a continuous stirred tank reactor coupled with selective cyanohydrin recovery using pervaporation*

Continuous cyanohydrin syntheses were conducted previously by Wandrey [15,20]. The application of the synthesis in the aqueous medium is limited to a few soluble substrates. The experiments on cyanohydrin synthesis of Wandrey were carried out by using a stirred tank reactor, whereas the enzymes are retained through a solvent resistant ultrafiltration membrane from Berghof type BM 500. The authors achieved constant reaction conditions for a period of 19 hours with a 10 cm^3 stirred ultrafiltration cell prepared from polytetrafluoroethylene. With a residence time of 3.8 minutes, and with ultrapure (R)-oxynitrilase, a conversion of the substrates of 93 % was achieved at a space-time-yield of approximately 0,74 mole·l^{-1}·h^{-1}. A comparison of the results of the (R)-oxynitrilase with the data reported for the (S)-oxynitrilase shows that the reaction rate is much slower under the same conditions. The maximum space-time-yield reported for 4-hydroxybenzaldehyde was approximately 0,016 mole·l^{-1}·h^{-1}. All experiments, done by Wandrey, were carried out with native enzymes in case of (R)-oxynitrilase and immobilized catalysts in case of the (S)-oxynitrilase. The further product processing should to be carried out by using extraction and distillation.

As an alternative, the scope of this work is to separate the products through a non-porous, tailor-made solution-diffusion membrane. The reactions were carried out in an experimental arrangement as shown in *figure 6.8*. In order to transfer the enzyme kinetics described in chapter 4 for the design of a novel bioreactor, the experimental conditions were kept constant. For pervaporation experiments, the standard conditions were set at a temperature of T = 25°C, a downstream pressure of p" = 15 mbar and substrate concentrations of c(butanal) = 2 mole·l^{-1}; c(HCN) = 4 mole·l^{-1} in di-iso-propylether as a solvent. The total volume of the stirred tank reactor was V_R = 450 ml, corresponding with a maximum load of 55 g of hydrocyanic acid.

In a series of experiments, the general reaction conditions had to be optimized in order to reach a stationary state. The most sensitive element of the bioreactor is the enzyme itself. Kinetics of the (R)-oxynitrilase are strongly influenced by the concentrations of the substrates and the products, which are described by the initial rate equation. A rough optimization was done through spreadsheet simulations.

All substrates were added slowly with the use of precise metering pumps. This is essential to avoid destabilization of the reaction. However, the enzyme stability and activity is also greatly influenced by either contaminations, like carboxylic acids and, furthermore, by the water content. These aspects are not covered by the detailed analysis of the reaction rates.
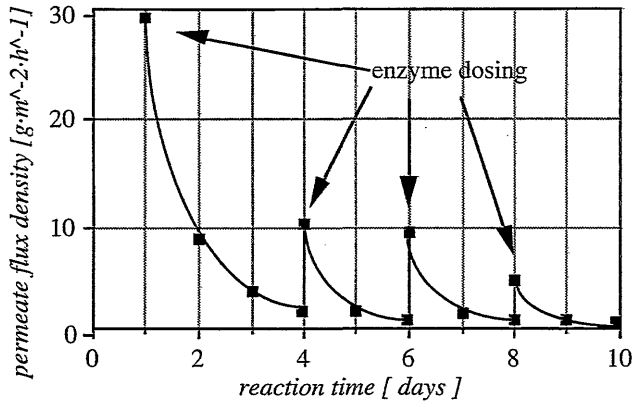
Figure 6.9 *Example of an instationary bioreactor experiment for the synthesis of (R)-2-hydroxypentanenitrile from butanal*
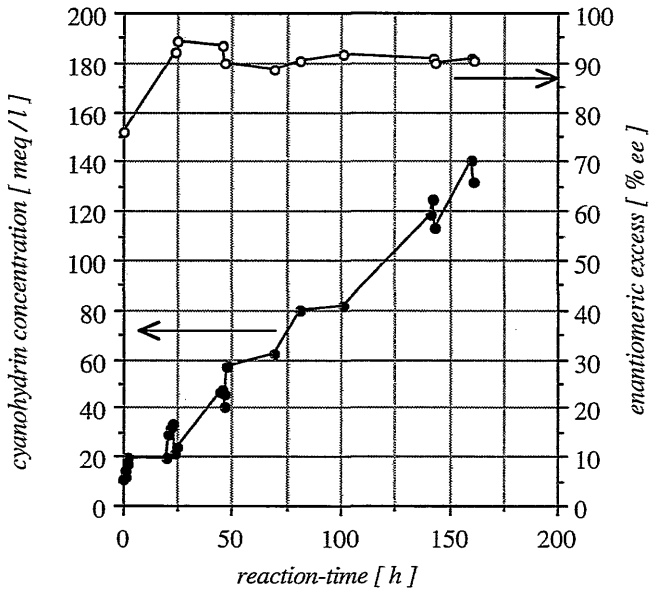
Figure 6.10 *Initial phase of the synthesis of (R)-2-hydroxypentanenitrile from butanal in a continuous stirred tank reactor.*

In the very first experiments, shown in *figure 6.9*, the water was removed from the first hydration sphere of the enzyme through pervaporation by using hydrophilic membranes,

which results in an immediate denaturation. Therefore, the deactivation of the enzyme is compensated through batch-wise dosage of oxynitrilase-loaded Avicel®. As described in chapter 4, the Avicel® functions as a support material for the enzyme as well as a buffer for the water necessary to keep the enzyme stable. Due to precise dosage of the pervaporation entrainer water, the denaturation of the enzymes could be avoided.

During the initial phase of the reactor experiments, a steep increase in the cyanohydrin concentration was typically observed as shown in *figure 6.10*. Simulation of the reaction clearly shows, that the downstream processing of the cyanohydrins during pervaporation should not be done before a stationary increase in the product concentration is measured. Therefore, all experiments were carried out in such a way, that the enzymatic reaction was completed up to the equilibrium concentrations, before the pervaporation loop was started. For the (R)-oxynitrilase catalyzed addition of HCN to butanal under standard conditions the reaction equilibrium was reached within 20...30 minutes.
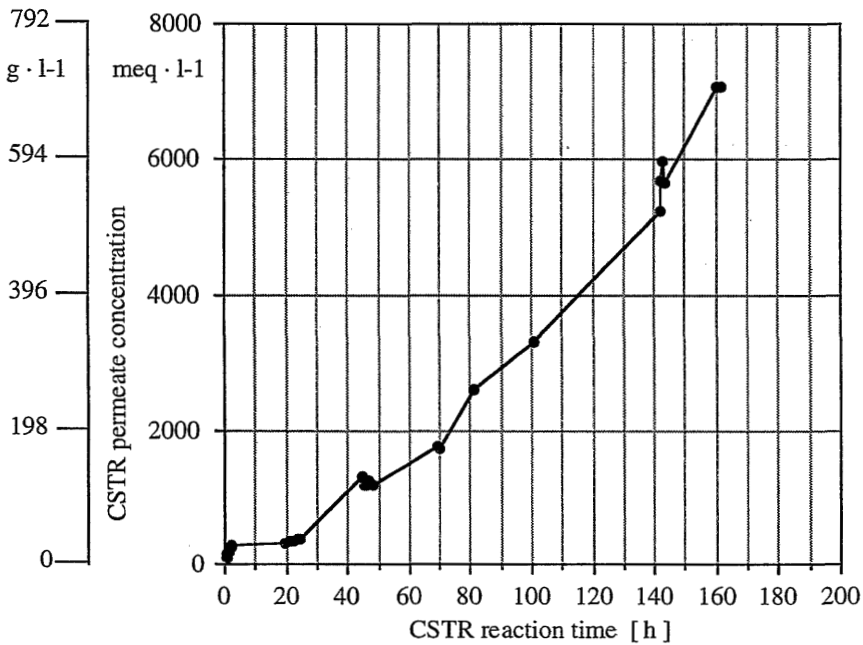
Figure 6.11   *Concentration of the cyanohydrin in the permeate of the stirred tank reactor during initial phase of the experiment*

In the course of the enzymatic reaction, the products removed by the pervaporation unit are replaced by adding substrates to the feed solution. In such a way, the reaction could be kept

constant. Essential information necessary for the adjustment of the substrate dosing rate is obtained from enzyme kinetics described in Chapter 4. The membrane area available for the separation of the cyanohydrin is given by the size of the reactor. It was constant for all experiments in this work. Therefore, the only way to keep the concentrations in the reactor constant is through the adjustment of the dosing rate and the concentration of the catalyst. The formation of by-products was not observed.

The results shown in *figure 6.11* are drawn from an experiment with the goal of keeping constantly 100 meq·l^{-1} of the cyanohydrin in the reaction mixture. The dosage of substrates to the feed results in an immediate increase of the feed concentration and finally to a rather high concentration of the cyanohydrin in the permeate. However, it was impossible to reach a stationary state. From *figure 6.10* it is obvious, that the enantiomeric excess of the produced cyanohydrin is always about 90 % ee. Optical purity of the product seems to be sufficient for succeeding practical applications of the cyanohydrins. The enantiomeric excess does not diminish under the reaction conditions of the stirred tank reactor.

Within a certain concentration range, the enzyme membrane reactor stabilizes its dynamic behaviour. This is due to the fact that an increase in production rate is compensated by an increase in transmembrane flux. The increase in flux reduces the product concentration in the reaction liquid, which in turn reduces the effect of product inhibition. By starting the reaction within the proper concentration range, the reaction will be stable. Nevertheless, the system has to be stabilized through proper dosage of the substrates before minimal fluctuations can be equilibrated through the dynamic reaction system.

The situation, however, is complicated due to a non-linear relationship between membrane permeation rates and feed concentrations. A complete experimental approach to achieve stationary concentrations is more or less impossible. This is especially due to a certain delay of the response of the system relative to small changes in the actual reaction conditions such as concentrations.

Based on enzyme kinetics, described in chapter 4, the simulation of a reactor experiment was done, assuming a linear relationship between infinitesimal small segments of the three dimensional characterization plot of the membrane shown in *figure 6.2 and 6.3*. The combination of simulation data of in-line polarimetry and on-line chiral gas chromatography allows the development of the concentrations in the reactor to be predicted. These data are used to adjust the metering pumps of the substrate dosing equipment. The results of an optimized long-term enzyme-membrane reactor experiment are illustrated in *figure 6.12*.
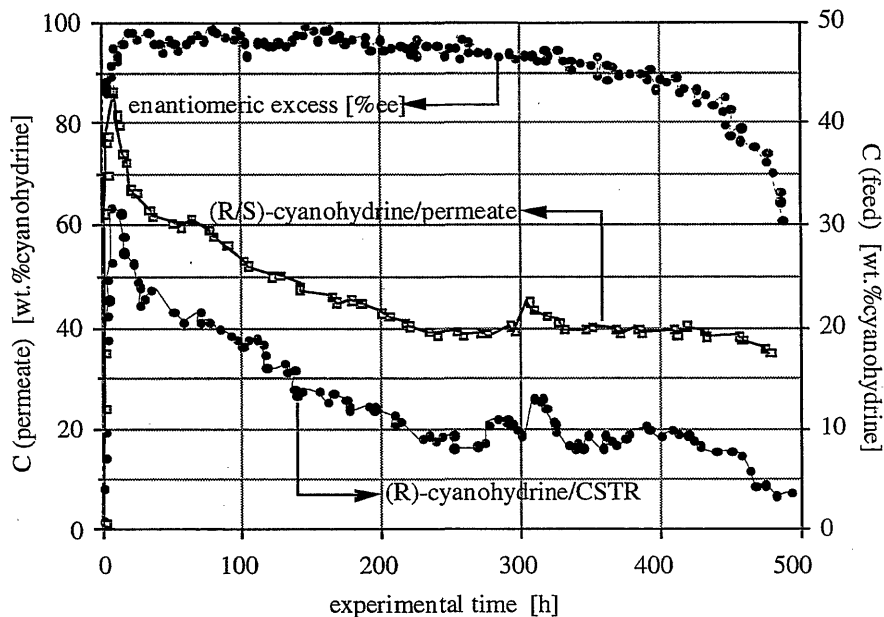
Figure 6.12   *Performance of a continuous stirred tank reactor. Long-term experiment of 21 days for the production of (R)-2-hydroxypentane-nitrile from butanal and hydrocyanic acid*

The long-term experiment of 21 days of *figure 6.12* for the production of (R)-2-hydroxy-pentanenitrile from butanal and hydrocyanic acid was carried out by using the completely automated continuous stirred tank reactor described in *figure 6.8*. During the experimental time problems occurred especially through insufficient availability of hydrocyanic acid which had to be synthesized in parallel in a second reactor. Consumption of HCN was in the order of magnitude of 40 g $\cdot h^{-1}$ in the inital period of the long-term run.

From *figure 6.12* and *table 6.3* it can be deduced, that the optical purities of the produced (R)-2-hydroxypentanenitrile is excellent. The enzyme deactivation rate can be kept below 1.7 % per day. This results in a small decrease in the optical purity of the products after approximately 300 hours of operation. In the final period of the long-term run, the enantiomeric excess declines rapidly after 450 hours. This phenomenon could be overcome through continuous dosing of active enzymes.

Table 6.3 *Summary of the results from a continuous stirred tank enzyme membrane reactor using PSIS membrane for product recovery*

enzyme	(R)-oxynitrilase
specific enzyme activity	$137 \ U \cdot mg^{-1}$
butanal	$2.0 \ mole \cdot l^{-1}$
HCN	$3.9 \ mole \cdot l^{-1}$
solvent	di-iso-propylether
reactor volume	$450 \ cm^3$
average degree of conversion	55 %
average CSTR concentration	14 wt.%
average permeate concentration	62 wt.%
optical purity	$\geq 95 \ \%$ ee
enzyme deactivation rate	$1.7 \ \% \cdot d^{-1}$
space-time yield	$3.8 \ mole \cdot l^{-1} \cdot h^{-1}$

Nevertheless, the reaction was perfectly controlled by gas chromatography, the time for reaching a stationary state took more than 100 hours. The first rapid change in the enzyme activity is due to the slow equilibration of the water hydration sphere of the enzymes. Water removed from the reactor through pervaporation was re-added batchwise to the reaction mixture. The average CSTR concentration of the cyanohydrin was 14 wt.% which correponds with an average turnover of 55 %. Resulting from this, the average permeate concentration was typically 62 wt.% of cyanohydrin in di-iso-propylether.

The most important result from the long-term experiment concerns the efficiency of the process. The space-time-yield of the enzymatic synthesis in organic media in a continuous stirred tank reactor coupled with selective removal of the inhibiting product, (R)-2-hydroxycyanohydrin, is approximately $3,8 \ mole \cdot l^{-1} \cdot h^{-1}$. This result has to be compared with $1,65 \ mole \cdot l^{-1} \cdot h^{-1}$ of the cyanohydrin achieved from the same reaction mixture in a tubular reactor with laminar flow without selective product removal.

Pressure driven enzyme-membrane reactors have appeared in previous publications. This concept is used by Wandrey for the preparation of cyanohydrins. Within a comparative experiment in a continous-stirred ultrafiltration tank reactor in aqueous media, retaining the native enzymes with a porous membrane, a a space-time-yield of only $0,242 \ mole \cdot l^{-1} \cdot h^{-1}$ was achieved.

It is clearly demonstrated, that the enzymatic synthesis in organic media generally results in much higher space-time-yields. As long as the enzyme stability and activity in organic media can be controlled through the reaction conditions, synthesis in aqueous media will never compete. The use of selective product removal with tailor-made functional membranes prepared from crosslinked, sulfonated poly(styrene-co-isoprene) enables maximum space-time-yields to be achieved. An enzyme-membrane reactor with selective product removal seems to be the only synthetic route to overcome limitations due to substrate and product inhibition.

6.4. Product Recovery through Pertraction

6.4.1. Mass transport and separation process performance

The pertraction process

In pertraction [23,24], a homogeneous polymeric membrane has contact with the feed on one side and an extractant liquid on the permeate side. The basic principle of pertraction is illustrated in *figure 6.13*. In the case of product recovery from the oxynitrilase membrane reactor, the feed solution consists of the reaction mixture containing low volatile cyanohydrins. Typically the extractant liquid is an organic solvent with excellent solubility characteristics for the cyanohydrin. In order to facilitate the regeneration of this extractant liquid through rectification, the heat of vaporization should preferably be small. The membrane, separating the feed from the permeate can either be porous or non-porous but should avoid any penetration of both liquids [25,26].

The driving force of the separation once again is a difference in chemical potential of the components in the feed and in the extractant liquid. This gradient is due to a difference in the activity coefficients of a component i in the individual liquids. Through careful selection of the extractant on the permeate side, large differences in chemical potential can be installed across the membrane [27,28,29].
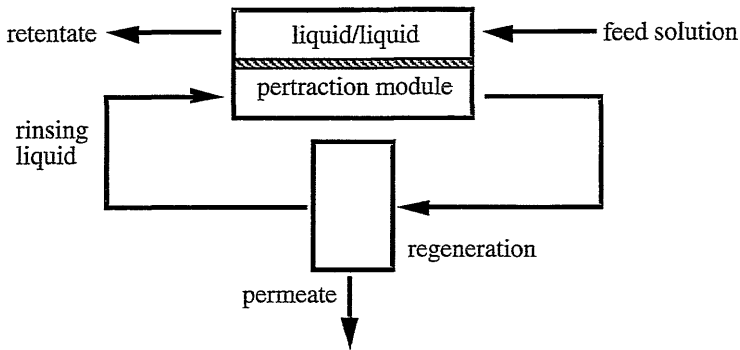
Figure 6.13   *Schematic drawing of the basic principle of pertraction*

As shown in *figure 6.14*, the most important presumption for the process is given by a sufficient solubility of the permeant in the membrane. The membrane in fact acts also as a spatially immobilized extractant.

Concentration polarization

In *figure 6.14* the transport resistances of the overall separation process are indicated. Besides the permeation resistance of the membrane, the boundary layers on both the feed and the permeate side have to be considered. In conventional solution-diffusion processes, the resistance of the membrane is generally dominant. An exception might be found for the removal of trace organics from water. In pertraction, however, the resistance of the permeate boundary layer has to be considered for interpretation of permeation data.

In order to reduce the boundary layer thickness on the feed side, the crossflow velocity of the feed solution can be enhanced. Due to the fact that pervaporation shows concentration polarization only on the feed side, the solution-diffusion membranes developed in chapter 5 are designed with a selective non-porous top-layer and a microporous support structure on the permeate side. In pertraction, this support structure would result in an exceptionally strong polarization concentration [30].
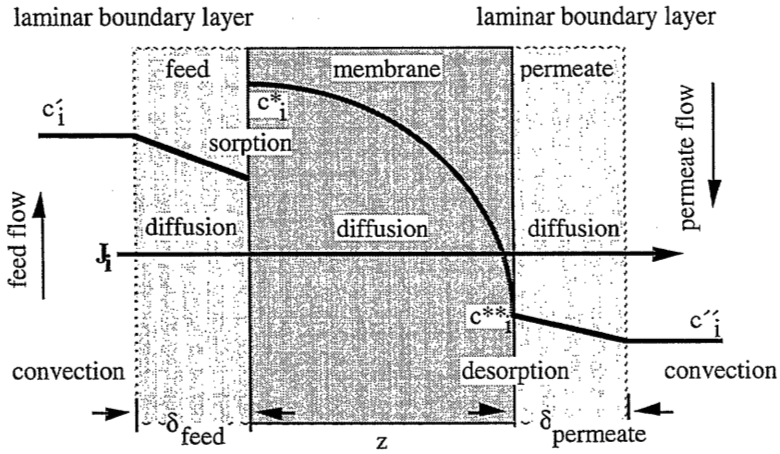
Figure 6.14   *Schematic drawing of the basic principle of pertraction*

From concentration polarization considerations it can be concluded that special, non-reinforced, non-supported membranes have to be developed. Such membranes can either be produced from polymer films of sufficient thickness or can be produced as a thin film membrane with an integrated non-woven support. Both techniques were applied in this work. In order to supply sufficient operational security, the membranes used in the final reactor experiments were reinforced with a 25 μm woven material from polyester.
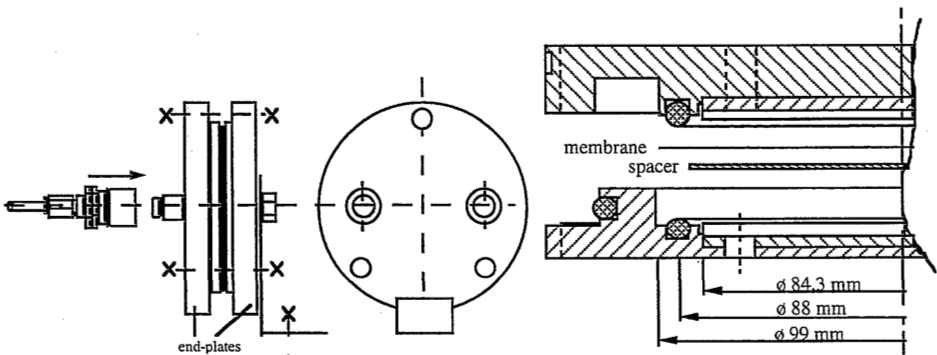
Figure 6.15   *Schematic drawing of the pertraction test cell DPD 90*

The flat sheet membranes were fitted into a test cell developed by Amafilter as shown in *figure 6.15*. The cell is stable in organic solvents and consists of two baffled feed and permeate flow channels. Turbulence was calculated to occur at flow velocities of 0,5 m·s⁻¹

assuming a rectangular geometry and a hydraulic diameter of 4,2 mm. The membrane is fixed between support plates of PTFE.

The complete pertraction unit, as shown in *figure 6.16* was completely automated. Furthermore, all electrical installations were explosion-proof in order to allow the handling of large amounts of di-iso-propylether. The set-up can be divided into the feed-loop, permeate-loop and regeneration-loop of the extractant liquid. For processing of the extractant, a thin film evaporator is used for rectification and recovery of the solvent. The permeants are collected in the residue of the vaporizer. The permeation rate was calculated on-line through gravimetric analysis of the residue. The heating jacket of the destillate and condensate of the evaporator are coupled through a heat exchanger. The condensation heat is recovered for evaporation with a heat pump having an efficiency of 70 %.
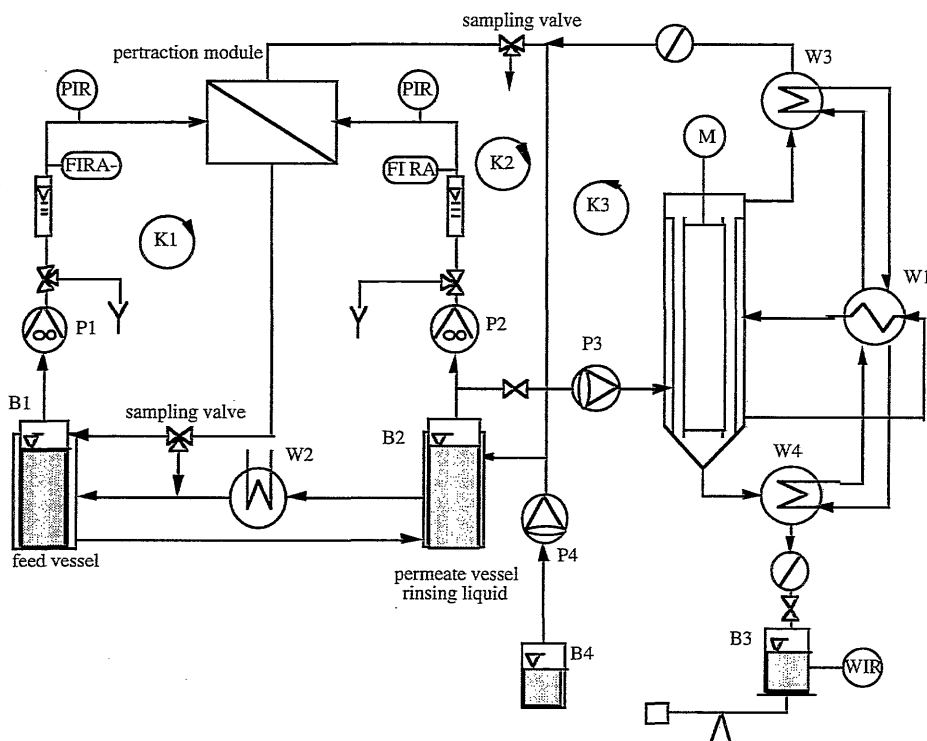
Figure 6.16   *Schematic drawing of the automated, explosion-proof and solvent stable liquid/liquid pertration laboratory set-up*

During the experiments, a dynamic control of all valves and pumps was guaranteed by a MacIntosh computer using the software Workbench from Strawberry Tree Inc. This is important for protection of the membrane in order to equalize the pressure on the feed and permeate side. Furthermore, the software is used for data collection and automatic calculation of the permeation rate.

Reference Experiments on the Separation of Octanol from Water

For the characterization of the pertraction set-up, reference experiments on the removal of low volatile organics were carried out [31]. As a model system, a non-toxic mixture, composed of a saturated aqueous solution of octantol was chosen. The solubility of octanol in water is approximately 0,072 v/v at 25 °C.
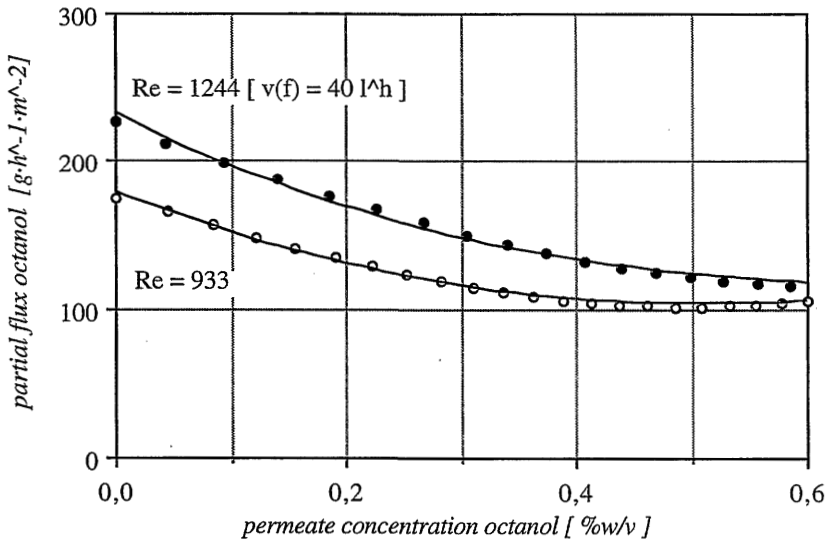
Figure 6.17   *Permeation rate of octanol from saturated octanol/water mixtures as a function of the octanol permeate concentration*

The membrane used within this series of experiments was a 100 μm film from polydimethyl-siloxane. As an extractant liquid, ethanol was chosen. All experiments were carried out at room temperature. The thin film evaporator was set to a temperature of 80 °C. Within this series of experiments, the components in the bottom of the evaporator were not recycled.

Through variation of the crossflow velocity of the permeate as shown in the *figure 6.17*, the optimum separation conditions relative to mass transfer in the pertraction test cell should be determined. The maximum flow velocity in an individual chamber was limited to about $40...70$ $l \cdot h^{-1}$ which corresponds to a crossflow velocity of about 0,3 $m \cdot s^{-1}$ and a Reynolds-Number of 1244. The limitation has to be made due to insufficient mechanical properties of the membranes. For a saturated solution of octanol in water, the permeation rate of octanol is about $170...230$ $g \cdot h^{-1} \cdot m^{-2}$. The influence of flow velocity on permetion rate was much stronger for more diluted solutions. In general, the basic principle of pertraction could be demonstrated in this first series of experiments.

From various membrane processes, such as electrodialysis [32], it is known, that a further reduction of the boundary layers can be achieved through the use of selected spacer materials as turbulence promoters as shown in the *figure 6.18*.
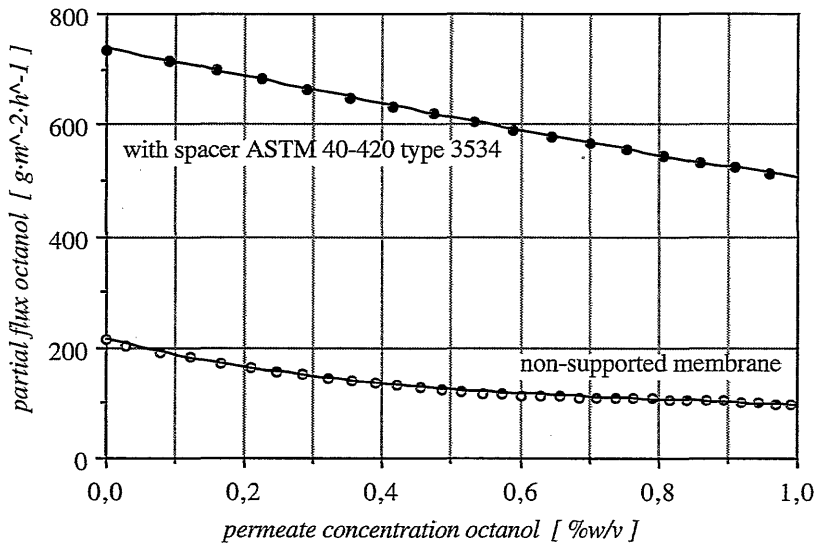
Figure 6.18   *Permeation rate of octanol from saturated octanol/water mixtures using non-supported membranes with and without a turbulence promoter on the feed side of the membrane*

The positive effect of a turbulence promoter on the feed side of the cross-flow cell is clearly shown in *figure 6.18*. The crossflow velocity of both experiments corresponds to a Reynolds Number of Re=622, calculated for an empty feed and permeate channel. The

octanol permeation rate increases by a factor of 4 to an approximate transmembrane flux of 550 to 750 $g \cdot m^{-2} \cdot h^{-1}$. In further experiments, the spacer was installed on the permeate side and on both the feed and permeate side of the membrane. However, the permerate spacer did not improve mass transfer. This indicates, that the separation is limited due to a concentration polarization on the feed side. Desorption from the non-porous non-supported membrane is not limiting. This might change with different extractants. In this case where ethanol is used, perfect solubility for both water and octanol is given. If the solubility of solvent and solute in the extractant is not given, concentration polarization on the permeate side is likely to occur.

Further experiments on pertraction were carried out installing a non-supported membrane combined with a turbulence promotor on the feed side.

Comparison of pervaporation versus pertraction in the removal of octanol from water

For a final comparison of the results on the separation of the low volatile octanol from water, mass transport through membranes of polydimethylsiloxane was compared for different process conditions. In the same test cell, pervaporation and pertraction experiments were carried out. The process conditions on the feed were identical. However, desorption of the permeants was different in both methods.
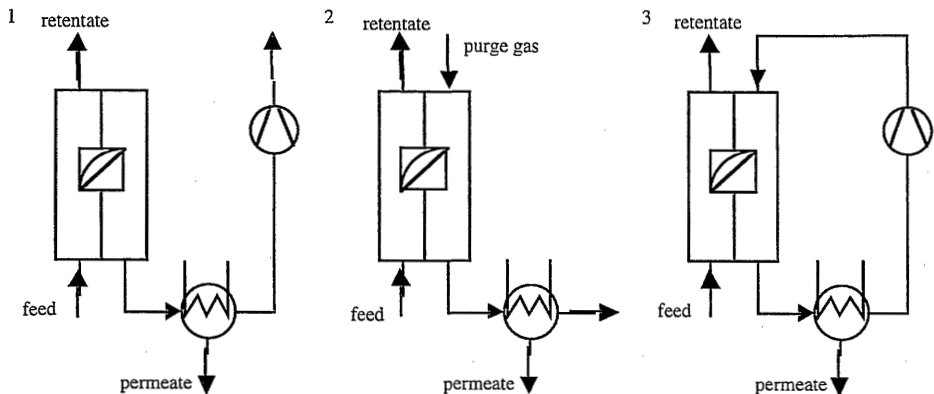
Figure 6.19   *Basic principle of (a) vacuum pervaporation (b) purge gas pervaporaion and (c) pertraction*

The basic principle of vacuum pervaporation, purge gas pervaporation [33] and pertraction is illustrated in *figure 6.19*. Applying the solution-diffusion model, major differences of all the three methods result from the third step of desorption of the permeants. The driving force for the separation results from a gradient in the chemical potential of the permeants. In vacuum pervaporation, this difference is installed through a reduction of the partial vapor pressure of the permeants at a low downstream pressure. The permeate is separated through condensation in liquid nitrogen. The permeate pressure must be below the saturation vapor pressure. Therefore, the separation of the low volatile organic permeants is always limited because of limitations concerning high vacuum plants.

In purge gas pevaporation, the partial pressure drop is installed by an inert purge gas such as nitrogen. A maximum driving force can be easily realized by sufficiently high purge gas flow rates. The permeants have to be condensed typically from high volume flow of gas containing low loading of the permeants. One disadvantage of purge gas pervaporation, is that the processing of the permeate is costly because the condensers have to be very large. Therefore, this method typically is applied for the removal of low volatile trace compounds, e.g. aroma compounds from aqueous solutions.

As an alternative, pertraction combines the advantages of both pervaporation modes. The driving force is easily realized, especially by proper selection of the extractant. The processing of the permeants is less expensive, due to the possibility of hybrid processes, e.g. the comination with a thin film vaporizer.

The results, shown in *figure 6.20*, are obtained from a 100 µm polymeric film of polydimethylsiloxane. The feed flow rate was about 0,3 m·s^{-1}. Vacuum pervaporation was conducted at a downstream pressure of less than 0,01 mbar. In purge gas pervaporation, the gas flow velocity was varied in the range of 0,1...5,0 m·s^{-1}. As reported by Nii, a flow rate of 0,1 m·s^{-1} was defined to be sufficient . Preliminary tests indicate, that a minimum flow velocity of 0,4 m·s^{-1} is recommended. Higher flow rates will not result in a further increase of the permeation rate, but will complicate the complete condensation of the permeants.

It can be seen from *figure 6.20*, that the octanol permeation rate increases significantly from vacuum pervaporation with 24,8 g·m^{-2}·h^{-1}, to purge gas pervaporation with 39,1 g·m^{-2}·h^{-1}, and finally to pertraction with 202,3 g·m^{-2}·h^{-1} relative to octanol. The difference between both pervaporation modes results from a better desorption of the octanol and from an infinite low downstream vapor pressure of the permeants.

For pertraction, further aspects have to be considered. Once again it can be confirmed, that a turbulence promoter on the feed side of the membrane will enhance the permeation rate from

202,3 $g \cdot m^{-2} \cdot h^{-1}$ to 715,8 $g \cdot m^{-2} \cdot h^{-1}$. The most important question, however, stems from the differences of purge gas pervaporation and pertraction. In cases where that both methods apply an activity of the permeant of $a_i \rightarrow 0$, permeation rates are expected to be equal. From a thermodynamic point of view, no differences in the driving force can occur if the permeate term is assumed to be neglegible. In this case, only the permeability of the membranes as well as the thickness of the membrane might differ. Probably the thickness of the membrane will change due to different concentration profiles. However, major differences might be due to a plastizication of the membrane by the extractant, ethanol in this case. The back migration of the ethanol was neglegible relative to the permeation of octanol, but a sorption of ethanol was observed from swelling of the membrane. Therefore, permeabilities in pertraction cannot be compared with permeabilities of the same membrane in pervaporation.
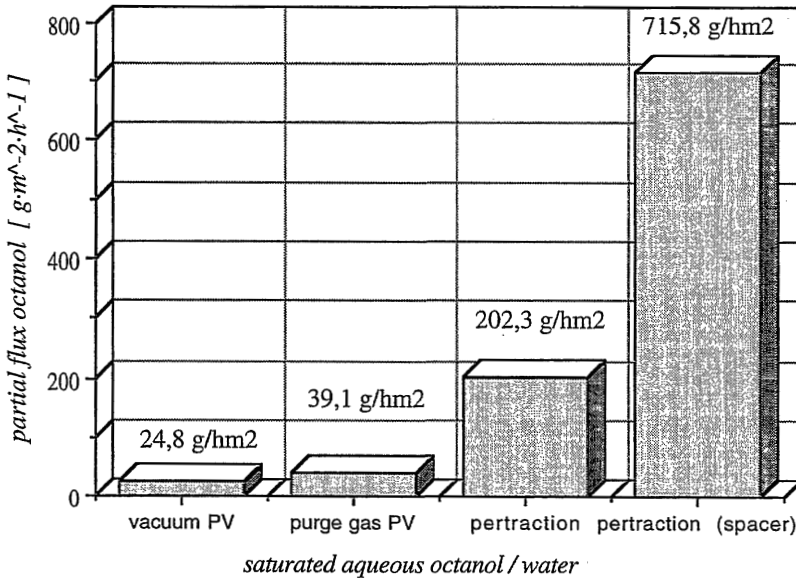
Figure 6.20 *Separation of octanol from an saturated aqueous solution using of (a) vacuum pervaporation (b) purge gas pervaporaion and (c) pertraction with and without a spacer in the feed channel*

In the following part of this work, purge gas pervaporation is not applied for the removal of low volatile cyanohydrins, because complete condensation of hydrocyanic acid cannot be guaranteed. Therefore, vacuum pervaporation, entrainer pervaporation and pertraction are considered to be feasible for technical processes.

Cyanohydrin removal by pertraction

The results described for the model system were transferred to a feasibility study on the pertractive recovery of the cyanohydrin from a model solution. The membrane used in this feasibility study was a commercial cation-exchange membrane from Pall RAI type 1010, which is a plasma grafted sulfonated film of polyethylene. The cation-exchange membrane was applied in two different modifications. As reported in the previous chapter, the selectivity of these membranes can be altered through an exchange of the counter ions. Therefore, the membrane type $1010/SO_3$-H^+ and type $1010/SO_3$-K^+ were included in the screening. The model mixture for the pertraction experiments consists of a solution which corresponds with the composition of the final product of an enzyme-membrane reactor. This solution is composed of a non-volatile cyanohydrin, 0,80 mole·l^{-1} 2-Hydroxy-2-(3-phenoxyphenyl) acetonitril, and the substrate, 0,20 mole·l^{-1} meta-Phenoxybenzaldehyd.
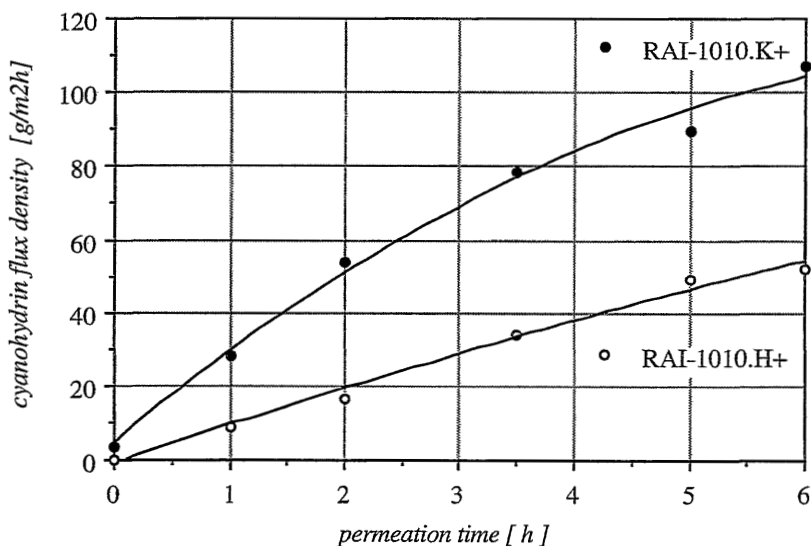
Figure 6.21   *Removal of (S)-2-Hydroxy-2-(3-phenoxyphenyl) acetonitril from the model mixture using pertraction through cation-exchange membranes using pertraction*

As shown in *figure 6.21* the permeation rate in pertraction experiments increases with time. This might be due to a slow plastization of the cation-exchange membrane. The final fluxes, however, were much higher than data obtained from pervaporation experiments. In

pervaporation, as demonstrated in table (I).5.6, the maximum fluxes obtained from the permeation of low-volatile 2-hydroxypentanenitrile were 29,9 and 20,6 $g \cdot m^{-2} \cdot h^{-1}$ for the Pall RAI type 1010/SO3-H$^+$ and -K$^+$, respectively. In pertraction, using methylenchloride as an extractant, the fluxes of non-volatile 2-Hydroxy-2-(3-phenoxyphenyl) increased slowly to 57,2 and 108,7 $g \cdot m^{-2} \cdot h^{-1}$ for the H$^+$ and the K$^+$ respecitively. Once again, it can be confirmed that the permeation of the phenoxybenzaldehydcyanohydrin is much higher in pertraction compared to the permeation of the much smaller molecule of 2-hydroxypentane-nitrile in pervaporation.

The further processing of the product might be done through rectification. Since a large amount of solvent must be evaporated in this case, methylenchloride was chosen for the extractant. Problems during the use of methylenchloride result from a back-migration into the reactor. Other solvents with lower diffusivity through the membrane were not recommended due to their high heat of vaporization. As a consequence, supercritical carbondioxide or solvents having a boiling point about room temperature, such as hydrocyanic acid, are recommended for future experiments.

6.4.2. Pertraction bioreactor

The pertraction bioreactor concept

As an example for the application of a pertraction bioreactor with product removal through functional membranes, the synthesis of non-volatile (S)-2-hydroxy-2-(3-phenoxy-phenyl) acetonitril was investigated. The reaction kinetics of the (S)-oxynitrilase catalyzed addition of hydrocyanic acid to 3-phenoxy-benzaldehyde are described in chapter 4 of this work [34].

From the calculation of the kinetic constants it is obvious, that the reaction encounters a strong inhibition through the substrate during the slow start-up period. The overall kinetics is very slow. Therefore, the expected space-time yields for the (S)-oxynitrilase are small. From this, a tubular reactor appears to be the prefered reactor type. The extremely small reaction rate causes a maximum residence time of the substrates which can not be realized in stirred tank reactors on a laboratory scale. Using a tubular reactor with laminar flow, these requirements can be fulfilled by a sufficient reaction length of the tube, or by a minimum flow rate. Nevertheless, maximum conversion can be realized as deduced from calculations of the reaction equilibrium.

A further problem using the (S)-oxynitrilase arises from the shear sensitivity of the enzyme. According to Brussee [14], high shear stress of the enzyme results in the loss of subunits and by this results in a decreasing activity. Also from this point of view, the use of a stirred tank reactor is not recommended. Low shear stress for the (S)-oxynitrilase can be established in the laminar operating regime of a tubular reactor.
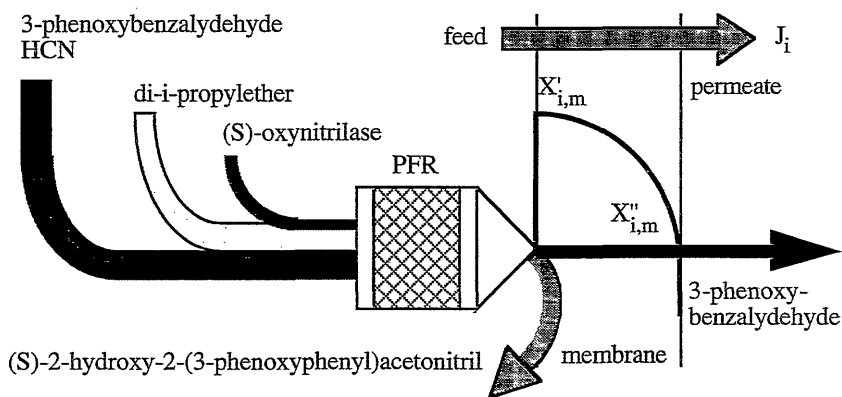
Figure 6.22   *Schematic drawing on the basic principle of the enzymatic synthesis of (S)-2-Hydroxy-2-(3-phenoxyphenyl) acetonitril using an tubular reactor with laminar flow. Final processing of the reaction mixtue is done using pertraction.*

The above mentioned restrictions on enzymatic synthesis have led to a modified concept as shown in *figure 6.22*. The (S)-oxynitrilase catalyzed addition of hydrocyanic acid to meta-phenoxybenzaldehyde is carried out in a continuous tubular reactor with laminar flow. The enzyme is immobilized in the tube reactor in the form of a fixed bed. The product solution leaving the reactor is continuously fed to the pertraction unit. In further processing of the products using liquid/liquid pertraction, the residual aldehyde separates from the homochiral phenoxybenzaldehyde through tailor-made anion-exchange membranes.

From enzyme kinetics, the enzyme concentration in the reactor as well as the length of the reaction tube were simulated. The goal of this calculation was to achieve an outlet concentration from the bioreactor of approximately 0,90 mole·l^{-1} 2-hydroxy-2-(3-phenoxy-phenyl)acetonitrile, and 0,10 mole·l^{-1} meta-phenoxybenzaldehyde. The hydrocyanic acid dosing was carried out in large quantities.

Batch production of homochiral 2-Hydroxy-2-(3-phenoxy-phenyl)acetonitril

From (S)-oxynitrilase catalyzed reactions with the 3-phenoxybenzaldehyde (mpba) substrate, a concentration of 1,0 mol·l⁻¹ mpba and 4,0 mol·l⁻¹ HCN was found to be suitable. As an example, the kinetics of the enzymatic reaction, using 100 U (S)-oxynitrilase·g⁻¹ AVICEL® corresponding to 20 U·ml⁻¹ of the enzyme are given in *figure 6.23*. The enantiomeric excess in batch reactions of the 3-phenoxybenzaldehyde typically was about 95…98 % ee. The maximum yield at equilibrium conditions is about 90 %.
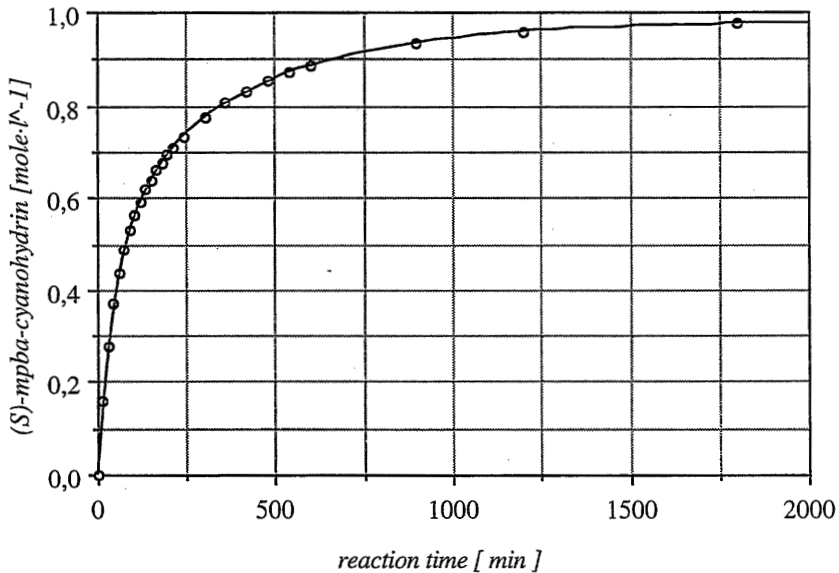
Figure 6.23   *Degree of conversion as a function of reaction time for the (S) oxynitrilase catalyzed reaction of 3-phenoxybenzaldehyde.*

In (S)-oxynitrilase catalyzed batch reactions, the optical purity of the products strongly depends on the amount of enzyme used. Since the reaction is very slow and furthermore strongly inhibited by carboxylic acids, the enzymatic reaction has to compete with the chemical non-stereoselective additon of HCN. In batch reactions, the formation of carboxylic acids via oxidation of trace amounts of the aldehyde is difficult to control. This is due to the fact, that degassing of solvents and Avicel® in batch experiments cannot be perfect in practice. The micropores of the microcrystalline cellulose are excellent sorbents for oxygen. To overcome these problems in tubular reactors, a simple inert gas rinse with argon is sufficient.

In batch experiments, an initial space-time-yield was found to be 0,3 mole·l⁻¹·h⁻¹. At best conditions, using 50 U·ml⁻¹ enzyme or 150 U·mg⁻¹ of Avicel® respectively, a turnover of 95 % was achieved in an experimental time of 72 hours. The enzyme concentration in this case can be calculated to 30 U·meq⁻¹ meta-phenoxybenzaldehyde. An economical production of homochiral (S)-cyanohydrins seems not to be feasible, due to the extremely cost-intensive enzymes consumed in batch experiments.

Design of the reaction tube

Based on results from the enzymatic reaction in batch reactors, a tubular reactor with laminar flow was designed. The fixation of the enzyme was accomplished in a tube with three distinct zones. For immobilizing the (S)-oxynitrilase, buffer swollen Avicel®, Avicel® immobilized with enzymes and finally again buffer swollen Avicel® were pumped into the tube. The experimental set-up was degassed using argon. Through variation of the flow velocity, the residence time of the substrates in the tube is adjusted. Results of these experiments are summarized in *table 6.5*.

Table 6.5   *Space-time-yield for the production of 2-Hydroxy-2-(3-phenoxy-phenyl)acetonitril in a tubular reactor with laminar flow (V_{tube}= 20 ml; C_{mpba} = 1,15 mole·l⁻¹; C_{HCN} = 4,05 mole·l⁻¹; 100 U·meq⁻¹)*

residence time [min]	yield [%]	space-time yield [meq·l⁻¹·h⁻¹]	enantiomeric excess [%]
800	95,0	81,93	98,1
600	93,6	107,6	> 99
400	90,2	155,6	> 99
200	79,3	273,6	> 99
120	61,9	355,9	94,7

The goal of the pertraction reactor in this case is not to maximize the degree of conversion of the products, but to maximize the space-time-yields or volumetric conversion rates of the enzymatic reaction. Unreacted substrates will be further separated and recycled by pertraction.

The yield as a function of the residence time demonstrates, that the turnover in a tubular reactor is higher than in a stirred tank reactor. With increasing flow velocity, or decreasing residence time, the space-time yield of the product inhibited reaction increases. From a practical point of view, there are limitations due the limited availability of pulsation-free pumps and due to back-diffusion effects at flow velocities which are too low. Furthermore, the enantiomeric excess at a residence time below 120 hours for the given enzyme loading is not tolerable. For the given capacity of the reaction tube and for the given loading of the Avicel®, a residence time of about 200 minutes seems to be best. Following from this, a turnover of 79 % of the cyanohydrin can be achieved.

However, further experiments using the tubular reactor demonstrate, that with increasing concentration of the oxynitrilase, the reaction time decreases. Comparative reactions using 200 $U \cdot meq^{-1}$ mpba instead of 100 $U \cdot meq^{-1}$ result in a space-time-yield of 304 $meq \cdot l^{-1} \cdot h^{-1}$ at an average turnover of 88 %. From these data also the final conditions for long-term experiments in the tubular reactor with laminar flow were drawn.

Selection of the membrane

The anion-exchange membranes used in these experiments are described in chapter 5. Before their use in pertraction, the membranes have to be conditioned in aqueous sodium hydrogen-sulfite. In this case, the aldehyde is selectively removed through the reversible formation of bisulfite complexes. The physical properties of the substrates, the product and the solvent are shown in *table 6.6*. The table indicates, that a separation of both the cyanohydrin and the aldehyde is difficult using conventional methods. A separation of the components via distillation is impossible due to the thermal sensitivity of the cyanohydrin. In case of the industrial production of the racemic cyanohydrin, the residual aldehyde is removed through extraction with aqueous sodiumbisulfite solutions. However, large-scale formation of the bisulfite complexes is not accepted in homochiral cyanohydrins, due to a decrease of the enantiomeric excess.

For extracting of the phenoxybenzaldehyde, methylenchloride was chosen as the extrant liquid. The back-diffusion of methylenchloride into the feed solution in this case is not of interest, because the product is further purified by evaporating the solvent. Regarding the toxicity of methylenchloride on the enzymatic reaction, it is important to carefully remove the residual solvent from the substrate.

Table 6.6   *Physical properties of the compounds investigated*

property	di-iso-propyl-ether	HCN	3-phenoxy-benzaldehyde	2-hydroxy-2-(3-phenoxy-phenyl)acetonitril
molecular weight [Da]	102.18	27.03	198,22	225,25
boiling point [°C]	68	26	melting 13°C	decomposition
kinetic diameter [Å]	6.16	3.98	5,89	6,02
vapor pressure 25 °C [mbar]	198	992	–	–
enthalpy vaporizat. [kJ·mole^{-1}]	31,957	25,233	–	–
dielectric constant	3,95	114	–	–
polarity [debye]	1.21	2.98	2,01	3,77

Within the series of bioreactor experiments, a 10 μm tailor-made functional membrane based on tetramethylbutanediamine quarternized polyphenylenoxide (PPO-TMBDA$^+$ –HSO$_3^-$) is used. The membrane properties are described in detail in chapter 5. Starting from a model mixture composed of 0,90 mole·l^{-1} 2-hydroxy-2-(3-phenoxy-phenyl) acetonitrile and 0,10 mole·l^{-1} meta-phenoxybenzaldehyde, the permeation rate for the aldehyde corresponds to 853 g·m^{-2}·h^{-1} and for the cyanohydrin to 166 g·m^{-2}·h^{-1}. The selectivity $\alpha_{i,j}$ is not of any practical use in pertraction, because the permeate concentration always is kept to a minimum by regeneration through distillation of the extractant.

Tubular enzyme membrane reactor combined with a continuous pertraction and regeneration machine

A completely automatic production / separation laboratory unit was installed for the continuous synthesis of homochiral meta-phenoxybenzaldehydcyanohydrins. The product of the enzymatic reaction is an important precursor for industrially produced pyrethroid insecticide. As already mentioned in previous chapters, the reaction is carried out in an tubular reactor with laminar flow as shown in *figure 6.24*. The experimental set-up is operated under a controlled atmosphere of argon. By this means, any loss of hydrocyanic acid due to evaporation can be avoided, furthermore, oxidation of the aldehyde due to

oxygen from air is excluded. The reaction is controlled by in-line polarimetrie, in-line photometrie and on-line gas chromatrographie.
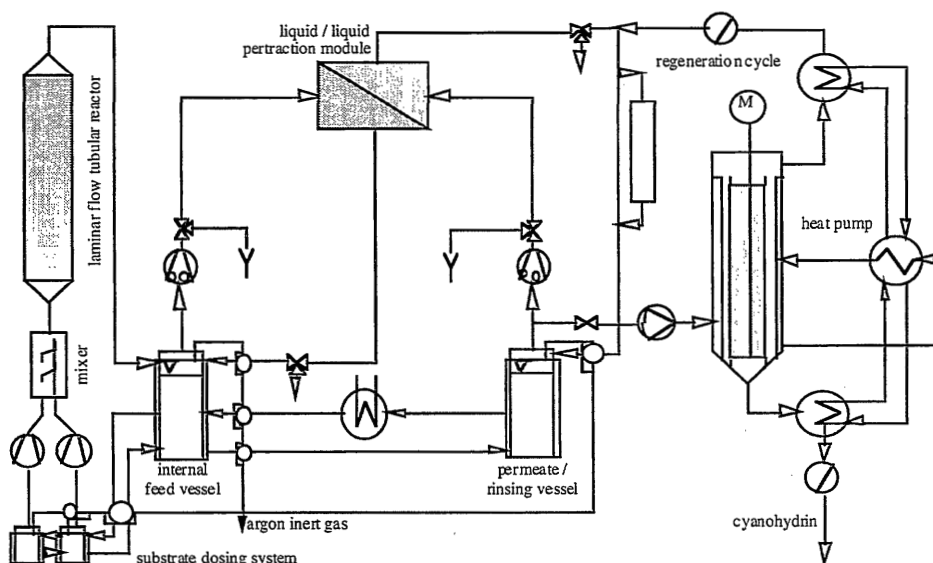
Figure 6.24   *Tubular reactor with laminar flow coupled with a pertraction and a regeneration unit used for the (S) oxynitrilase catalyzed reaction of 3-phenoxybenzaldehyde in diisopropylether .*

A high reproducibility of the space-time-yield requires an accurate purification of the aldehyde through distillation. Furthermore, the diisopropylether must be purified by chromatography at α-aluminiumoxide. Otherwise the formation of carboxylic acids may inhibit the enzymatic reaction. Different from the (R)-oxynitrilase, the saturation of the solvent with water results in a lower enantiomeric excess. The water, bound to the 3-zones of Avicel® in the reaction tube stabilizes the (S)-oxynitrilase sufficiently.

The tubular reactor with laminar flow is characterized as follows:

- volume of the empty tube $Vt_{ube} = 40$ cm^3
- volume of the fixed bed $V_{Avicel} = 30$ cm^3
- active volume of the reactor $V_{reactor} = 15$ cm^3

The (S)-oxynitrilase used for the experiments was prepared according standard procedures described in chapter 4. The purity of the enzyme was improved in the meantime, so that specific productivity is further improved.

- specific activity   200 $U \cdot g^{-1}$ Avicel®
- concentration of the enzyme $C_{oxynitrilase} = 133\ U \cdot ml^{-1}$
                                      $C_{oxynitrilase} = 1{,}91$ mg $proteine \cdot ml^{-1}$
- buffer concentration $C_{phosphate} = 0.05\ mole \cdot l^{-1}$
- pH-value of the buffer   pH = 5.4
- deactivation rate of the enzyme $\lambda = 2.8\ \% \cdot d^{-1}$

The results obtained at the outlet of the tubular reactor are summarized in *table 6.7*. Due to an improved immobilization of the enzyme, the residence time can be reduced from 200 minutes to about 150 minutes.

Table 6.7   *Summary of the results from an continuous tubular reactor with laminar flow for the preparation of homochiral meta-phenoxy-benzaldehydcyanohydrins using (S)-oxynitrilase catalysed addition of HCN to meta-phenoxybenzaldehyde*

enzyme	(S)-oxynitrilase
3-phenoxybenzaldehyde	$C_{PBA\ [1]} = 1{,}15\ mole \cdot l^{-1}$ at 20°C
hydrocyanic acid	$C_{HCN\ [2]} = 4{,}05\ mole \cdot l^{-1}$ at 5 °C
reaction temperature	23 °C
residence time	$\tau = 150$ minutes
average degree of conversion	88,5 %
optical purity	$\geq 97\ \%$ ee
enzyme deactivation rate	2,8 $\% \cdot d^{-1}$
specific productivity	2,655 $\mu mole \cdot U^{-1} \cdot h^{-1}$
space-time yield	0,443 $mole \cdot l^{-1} \cdot h^{-1} = 2390\ g \cdot l^{-1} \cdot d^{-1}$

The results of the enzymatic synthesis of (S)-2-hydroxy-2-(3-phenoxy-phenyl) acetonitril summarized in *table 6.7* represents data obtained in an experiment of 906 hours in total. All data in the table are calculated from the best experimental results between the third and the fourth period of the run after the initial start-up where the reaction tube is conditioned.

Between the individual periods, the reactor had to be shut down because of the limitations in the availability of hydrocyanic acid. Furthermore, on weekends, only an internal loop of hydrocyanic acid solutions was operated, without reaction. After conditioning with a 4 molar solution of hydrocyanic acid in diisopropylether on weekends, the acitivity of the enzyme always was enhanced as shown in *figure 6.25*.
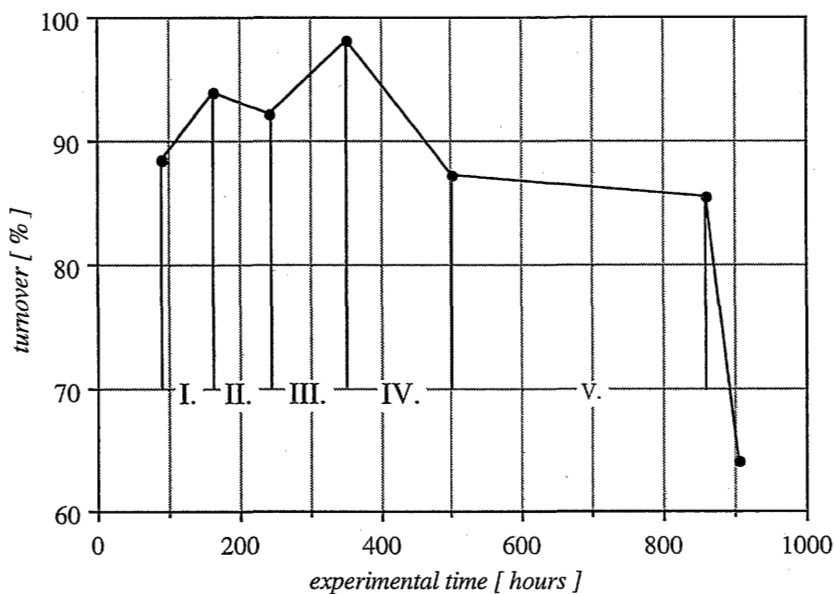
Figure 6.25   *Plot of the reaction yield versus experimental time of a long-term experiment for the enzymatic production of 3-phenoxybenzaldehyde-cyanohydrin using a tubular reactor.*

After the fifth period of reaction, the weekend operation was done only by pumping the substrates in an internal loop through the reaction tube. This circulation results in a more or less complete deactivation of the enzyme. The turnover dropped steeply down to 64 % and finally to 32 % after two additional days of operation. However, the enantiomeric excess was excellent during all the five periods of experiments. A loss of optical activity was observed not before the loss of enzyme activity after the fifth period.

The results from the continuous production in a tubular reactor indicate that the choice of the reactor was perfect in terms of enzyme stability as well as in terms of operational stability. The optical yields, and the turnover are sufficiently high for any practical application of the

product. The space-time-yields of the (S)-2-hydroxy-2-(3-phenoxy-phenyl) acetonitril are about 0,443 mole·l^{-1}·h^{-1} which corresponds to 2,39 kg·l^{-1}·d^{-1}.

The outlet solution of the tubular reactor still contains residual concentrations of unreacted aldehyde in a solution of the cyanohydrin in diisopropylether. From the economical point of view, it is not attractive to recycle the aldehyde into the reactor. However, from the application point of view, it can not be accepted, that the homochiral cyanhydrin is contaminated with an oxidation sensitive aldehyde. Therefore, further processing of the product is required. This can be accomplished through chromatographic means, or through liquid/liquid extraction with aqueous solutions of bisulfite. Since the cyanohydrin is partially soluble in water, extraction impossible. Furthermore, the cyanohydrins tends to racemize during processing.

As an alternative, pertraction using tailored-made anion-exchange membranes can be applied. The polyphenylenoxide membrane described in chaper 5 was used with the hydrogensulfite as a counter ion which enables reversible binding of the aldehyde. The membrane rejects the cyanohydrin, and enables the permeation of the aldehyde. By this means, pertraction combines the advantage of extraction and a selective barrier material.

A further advantage arises from the fact, that the unreacted aldehyde is recovered completely. This will improve the technical attractiveness of the process. In this experiment, however, the aldehyde was only separated and further concentrated by subsequent evaporation.

From *table 6.8* it can be seen, that the continuous separation of the aldehyde was possible with sufficient regeneration of the purge liquid. The aldehyde in the bottom of the thin film evaporator did not show any oxidation by-products. A complete removal of the aldehyde from the feed solution, however, was not possible in laboratory scale because the membrane area used for the separation was too small. However, the basic principle of the separation is clearly demonstrated.

The cyanohydrin product leaving the tubular reactor is purified in the retentate of the pertraction. After final processing of the solution, the diisopropylether is removed by distillation. The (S)-2-hydroxy-2-(3-phenoxy-phenyl) acetonitril is further concentrated to a 85 wt.% solution in diisopropylether. The enantiomeric excess of this concentrate was kept stable through processing at a level of 96 % ee.

Table 6.8   *Summary of the results from the processing of the product solution using liquid/liquid pertraction through anion-exchange membranes.*

inlet concentration	$C_{mpba} = 0,14$ mole·l^{-1} at 20°C
	$C_{cyan} = 1,01$ mole·l^{-1} at 20°C
outlet concentration	$C_{cyan} = 0,97$ mole·l^{-1} at 20°C
start-up time	after 39 hours of reaction time
extractant liquid	hexane
crossflow-velocity feed	$0,15$ m·s^{-1}
crossflow-velocity permeate	$0,23$ m·s^{-1}
regeneration flow rate	800 ml·h^{-1}
bottom product flow rate of evaporator	16 ml·h^{-1}
bottom aldehyde concentration	$C_{mpba} = 0,35$ mole·l^{-1}
condensate (top) aldehyde concentration	$C_{mpba} < 0,01$ meq·l^{-1}

6.5. Conclusions

The goal of this chapter was to demonstrate the basic principle of an enzyme membrane reactor for the production of homochiral cyanohydrins. Within the work, two different enzymes, the (R)- and (S)-oxynitrilase were used for the production of a low-volatile cyanohydrin, the (R)-2-hydroxypentane-nitrile, and a non-volatile cyanohydrin, the (S)-2-hydroxy-2-(3-phenoxy-phenyl) acetonitril. The (R)-cyanohydrin is an important intermediate for the chiral pool. The (S)-cyanohydrin is the precursor for deltamethrin an industrially important pyrethroid insecticide.

In the first part of this chapter, a methodology for the continuous production of the low-volatile (R)-2-hydroxypentane-nitrile was developed. Kinetic data of the enzyme suggest using a stirred tank reactor. It was demonstrated that low-volatile cyanohydrins can be removed from the reactor using pervaporation. The process must be carefully designed due to the low saturation vapor pressure of the permeating cyanohydrin. This is done through control of pervaporation temperature and downstream pressure. Furthermore, an entrainer

effect through the co-permeation of water is used to decrease to the downstream partial pressure of the cyanohydrin and by this means keeps the driving force stable for continuous separation. In a long-term experiment of about 500 hours, an excellent space-time-yield of 3.8 mole·l⁻¹·h⁻¹ at an enatiomeric excess of > 95 % ee was achieved.

In the second part of this chapter, the non-volatile (S)-2-hydroxy-2-(3-phenoxy-phenyl) acetonitril is continuously produced from a tubular reactor with laminar flow. The choice of the reactor was based on kinetic data of the enzyme and on the sensitivity of the enzyme. From the tubular reactor, an excellent space-time-yield of 0,443 mole·l⁻¹·h⁻¹ was found for the synthesis in organic media. The final product was further purified using pertraction. Using a tailored-made anion-exchange membrane with hydrogensulfite counter ions, the unreacted aldehyde is separated without any oxidation by-products. The cyanohydrin is further concentrated from the retentate without any loss in the optical activity.

List of Symbols

$[A]$	actual concentration of species A
$[A]_{0,in}$	total inlet concentration of species A
A_{spec}	specific acitivity of the enzyme $[U \cdot mg^{-1}]$
A_{vol}	specific volumetric acitivity of the enzyme solution $[U \cdot ml^{-1}]$
a_i	activity of component i
c	concentration
% ee	optical purity; enantiomeric excess $[\%]$
f_i	fugacity of component i
J_i	mass transfer or permeation rate
J_N	normalized flux density
k_{cat}	molecular acitivity (or turnover number TN) $[U \cdot mg^{-1}]$
k_C^1	forward rate constant of the non-specific chemical reaction
$k_1, k_2, ...$	elementary forward rate constant
$k_{-1}, k_{-2}, ...$	elementary reverse rate constant
k_{Des}^E	enzyme deactivation rate constant
$K_{m,A}$	Michaelis half saturation value for the aldehyde

$K_{m,P}$	Michaelis half saturation value for the cyanohydrin
$K_{i,A}$	inhibition constant relative to the aldehyde
K_S^{HCN}	apparent HCN dissociation constant $K_S^{HCN} = K_{eq}^{HCN} \cdot [H_2O]$
L	membrane thickness
N_A	Avogradro's constant
p	total pressure
p_i	partial pressure of component i
p_i^S	saturation vapour pressure of species i
P_i	permeability coefficient of species i
Q_v	volumetric flow rate
R	gas constant
$S_{i,j}^*$	ideal permeation selectivity
$S_{i,j}$	permeation selectivity
$S_{i,j}^0$	ideal selectivity
$t_{1/2}$	half time (cycle number)
T	temperature
V_{max}^*	apparent maximum reaction velocity
V_{max}^+	maximum forward reaction velocity
V_R	reactor volume
x_i	mole fraction of species i
z	coordinate in direction of transport

Greek Letters

$\alpha_{i,j}$	separation factor
$\alpha_{i,j}^{evap}$	destillation separation factor
$\alpha_{i,j}^m$	solution-diffusion membrane separation factor
β_i	enrichment factor
δ	solubility paramter
γ_i	activity coefficient
φ_i^S	fugacity coefficient
τ	residence time
λ	deactivation rate of the enzyme
μ	chemical potential
υ^*	apparent total reaction rate
υ_{out}^*	apparent total reaction rate in the outlet

υ^+	forward velocity of the enzymatic reaction
υ^-	reverse velocity of the enzymatic reaction
υ_C^+	forward velocity of the chemical reaction
υ_C^-	reverse velocity of the chemical reaction
ξ	degree of conversion, turnover

Subscripts and Superscripts:

'	value in the feed stream
' '	value in the permeate stream
0	standard reference state
*	ideal case
i	species i
m	membrane
T	temperature

Abbreviations:

Avicel®	microcrystalline cellulose, FMC Corporation, type PH-101
β-CD	β-cyclodextrine
CSTR	continuous stirred tank reactor
DIPE	di-iso-propylether
EMR	enzyme-membrane-reactor
HCN	hydrocyanic acid
LFR	tubular reactor with laminar flow
mdi	methylene-bis-diphenylisocyanate
mpba	3-phenoxybenzaldehyde
mpbac	(2)-hydroxy-2-(3-phenoxyphenyl) acetonitrile
PFR	tubular reactor with plug flow
PPO	polyphenyleneoxide
PSIS	poly(styrene-co-isoprene)sulfonic acid
SPEEK	sulfonated polyetheretherketone
TMBDA	1.4-bis-(dimethylamino)butane

References

[1]   Bailey, J.E., Ollis, D.F.
       Biochemical Engineering Fundamentals
       McGraw-Hill International Editions, 2.nd Ed., 1986

[2]   Howaldt, M.
       Reaktionstechnische Untersuchungen gekoppelter coenzymabhängiger
       Enzymsysteme in Membranreaktoren
       Dissertation Universität Stuttgart, 1988

[3]   Flaschel, E.; Wandrey, C.; Kula, M.-R.
       Ultrafiltration for the separation of biocatalysts
       in: 'Advances in Biochemical Engineering/Biotechnology', Vol. 26
       Springer Verlag, Berlin, 1983

[4]   Heath, C.A.; Belfort, G.
       Synthetic Membranes in Biotechnology: Realities and Possibilities
       Adv. Biochem. Eng. Biotech., Springer-Verlag Berlin, Vol 47, 45-88 [1992]

[5]   Wu, D.; Belfort, G.; Cramer, S.M.
       Enzymatic resolution with a multiphase membrane bioreactor: a theoretical analysis
       Ind. Eng.Chem. Res. 29(8), 1612-1621 [1990]

[6]   Schügerl, K.; Kretzmer, G.; Freitag, R.; Scheper, Th.
       Integrierte biotechnologische Produktionsprozesse
       Chem.-Ing.-Tech. 66(12), 1585-1592 [1994]

[7]   Denbigh, K.
       Chemical Reactor Theory
       University Press, Cambridge 1965

[8]   Kragl, U.; Vasic-Racki, D.; Wandrey, C.
       Kontinuierliche Reaktionsführung mit löslichen Enzymen
       Chem.-Ing.-Tech. 64(6), 499-509 [1992]

[9]   Catapano, G.; Iorio, G.; Drioli, E.; Filosa, M.
       Experimental Analysis of a cross-flow membrane bioreactor with entrapped whole cells:
       influence of transmembrane pressure and substrate feed concentration on reactor performance
       J. Membrane Sci. 35, 325-338 [1988]

[10]   Greco, G.; Alfani, F.; Iorio, G.; Cantarella, M.; Formisano, A.; Gianfreda, L.;
       Palescandolo, R.; Scardi, V.
       Theoretical and experimental analysis of a soluble enzyme membrane reactor
       Biotechnol. Bioeng. 21, 1421 [1979]

[11]   Prenosil, J.E.; Hediger, T.
       Performance of membrane fixed biocatalyst reactors: Membrane reactor systems and modelling
       Biotechnol. Bioeng. 31, 913-921 [1988]

[12]   Matson, S.L.; Quinn, J.A.
       Membrane reactors in bioprocessing
       Ann. N.Y. Acad. Sci. 469, 152-165 [1986]

[13]   Effenberger, F.; Ziegler, Th.; Förster, S.
       Degussa AG
       Verfahren zur Herstellung von optisch aktiven Cyanhydrinen
       DE 37 01 383 (28.07.1988)

[14]   Brussee, J; van der Gen; A.
         SOLVAY DUPHAR B.V.
         Method for preparing optically active cyanohydrin derivatives and their conversion products
         EP 0 322 973 (21.12.1988)

[15]   Niedermeyer, U.; Kragl, U.; Kula, M.-R.; Wandrey, C.; Makryaleas, K.; Drauz, K.
         KFA Jülich, DEGUSSA AG
         Enzymatisches Verfahren zur Herstellung von optisch aktiven Cyanhydrinen
         EP 0 326 063 (23.01.1989)

[16]   Bauer, B.; Strathmann, H.; Effenberger, F.
         Fraunhofer-Gesellschaft
         Verfahren und Vorrichtung zur enzymatischen Synthese
         DE 40 41 896 C1 (27.12.1990)

[17]   A.F.M. Barton
         Handbook of solubility parameters and other cohesion parameters
         CRC-Press 1985

[18]   J.M. Prausnitz
         The properties of gases and liquids
         McGraw-Hill book company, Fourth edition

[19]   K.W. Böddeker
         Pervaporation und ihre Anwendung zur Trennung von Flüssiggemischen
         VDI-Verlag Reihe 3: Verfahrenstechnik Nr. 129

[20]   K.W. Böddeker
         Pervaporation of low volatility aromatics from water
         J. Membrane Sci. 53 (1990) 143 - 158

[21]   R. Rautenbach
         Engineering aspects of pervaporation: Calculation of transport resistance,
         module optimization and plant design
         Pervaporation Membrane Seperation Processes, Chapter 3 (1991)

[22]   Kragl, U.; Peters, J.; Kula, M.-R.; Wandrey, C.
         KFA Jülich
         Enzym-Membran-Reaktor
         DE 39 37 892 (26.03.1991)

[23]   Acharya, H.R.; Stern, S.A.; Liu, Z.Z.; Cabasso, I.
         Separation of liquid benzene/cyclohexane mixtures by perstraction and pervaporation
         J. Membrane Sci. 37, 205-232 [1988]

[24]   R.J. Vaughan
         Membran solvent extraction process
         United States Patent, No. 4,532,347, Jul. 30, 1985

[25]   K. Luyben
         Solvent fermentation coupled with pervaporation or perstraction
         BioTechnica abstract No. 9, Biotechnology centre, BC Delft / NL

[26]   W.J. Groot
         Butanol recovery from fermentations by liquid-liquid extraction and membrane solvent extraction
         Bioprocess Enginering 5 (1990), 203-216

[27]   F. Macasek
         Membran extraction instead of solvent extraction. What does it give?
         Journal of radioanalytical and nuclear chemistry, Vol. 129, No. 2, (1989) 233-244

[28]   Black, A.
         Selective seperation of multi-ringaromatic hydrocarbons from distillates by perstraction
         UnitedStates Patent, No. 4,962,271, Oct. 9, 1990

[29]   C.G. Gerhold
         Method for the solvent extraction of aromatic hydrocarbons
         United States Patent Office, No. 3,556,991, Jan. 19.1971

[30]   K. Schneider
         Membranes and modules for transmembrane distillation
         J. Membrane Sci. 39 (1988) 25-42

[31]   J.M. Watson
         A study of organic compound pervaporation through silicone rubber
         J. Membrane Sci. 49 (1990) 171-205

[32]   G. Belfort
         An experimental study of electrodialysis hydrodynamics
         Desalination, 10 (1972) 221-262

[33]   Nii, S.; Mao, Z.G.; Takeuchi, H.
         Pervaporation with sweeping gas in polymeric hollow fiber membrane module
         J. Membrane Sci. 93, 245-253

[34]   Matsumura, M.
         Elimination of ethanol inhibition by perstraction.
         Biotechnology and bioengineering, Vol. XXVIII,(1986), 534-541

(I) CHAPTER 6

Chapter

7

CHIRAL MEMBRANES

Synopsis

The worldwide market for single-enantiomer forms of chiral drugs is greatly increasing. As a result, both industrial and fundamental research is concentrating on methods for asymmetric synthesis. From both patent literature and industrial reports it can be drawn that enzyme-catalyzed biotransformations are more often preferred than organic synthetic reactions. However, resolution of racemic mixtures is still the leading technology because often it is more economical than asymmetric synthesis.

Recent advances in chiral chromatographic technology, such as the simulated moving bed (SMB), make this the preferred technique if satisfactory separation between enantiomers can be achieved. The advantages of chromatography might be gained also by a membrane separation process using chiral membranes. Some work in this field was already done using liquid membrane technology. In this chapter, chiral membranes based on homogeneous chiral polymers are described. These functional solution-diffusion membranes are used for chiral separations using pervaporation and pertraction.

The best preliminary results in the separation of racemic cyanohydrins were obtained from homogeneous modified poly(urethane-β-cyclodextrin) membranes. In pervaporation of solutions of (R/S)-2-hydroxy-pentanenitrile in di-iso-propylether an enantiomeric excess of 22 % ee in the permeate was found. The resolution is due to a preferential sorption of one enantiomer in the chiral polymer of the membrane. The enantiomeric excess in the desorbate of the same membrane was found to be 63,2 % ee.

7.1. Introduction

The transition from the optically active form to a racemic mixture involves an increase in entropy. Therefore, this so-called racemization process is thermodynamically favourable and can occur for example just by a temperature increase of homochiral compounds. Any separation process has to work against the entropic part of the Gibb's free energy [1,2].

In gas-chromatographic separation of enantiomers [3] with cyclodextrin derivatives [4,5,6] it has been shown that a remarkable variety of chemical compounds is accessible to enantiomer separation. Chromatographic enantiomer separation is always the result of discrimination of incongruent, mirror-inverted molecules with identical constitution but different configuration by means of an aracemic or chiral stationary phase. The necessary interaction can be strong or weak and it can involve inclusion and/or other chemical interactions. For intermolecular host-guest interaction, various contributions for cyclodextrins have been discussed [7,8,9]:

- Steric adaptation by means of conformation change in the guest molecule and/or in stationary phase e.g. the cylcodextrin during induced fit
- Hydrogen bonding
- Van-der-Waals interactions
- Dipole-dipole interactions (induced and permanent dipole moment)
- Charge-transfer interactions
- Electrostatic interactions
- Hydrophobic interactions
- Release of 'enthalpy-rich' water from the cyclodextrin void with entropy production
- Breakdown of the ring strain of the macrocycle.

Molecular shape (shape selectivity and size selectivity) should play an important role in enantiomer separation by means of inclusion. In addition, chemical interactions can also be decisive for polar guest molecules (chemical functionality induced selectivity). In previous literature it was reported that molecular shape can be obviously varied to a great extent. Thus besides cyclic compounds, branched linear molecules are also separated into enantiomers. Overall molecular size does not seem to play a decisive role, but more often small structural differences in specific parts of guest molecules lead to drastic effects on chiral recognition.

In this chapter, the development of membranes will be described that allow the separation of racemic mixtures. Three routes will be described: the formation of (a) optically acitve poly-

(L)-lactic acid membranes, (b) heterogeneous membranes prepared from cyclodextrins dispersed in a silicone rubber matrix, and (c) homogeneous membranes prepared from tailor-made cyclodextrin-di-isocyanate copolymers.

These membranes can be applied in cases where the non-specific synthesis of racemic mixture is desired due to low synthesis and product recovery costs or easily accessed synthesis routes. The membranes are applied in a pervaporation process, but the technology can be easily transferred to membrane processes such as pertraction and dialysis.

7.2. Background

7.2.1. Thermodynamic Fundamentals of Enantiomer Separation

In a theoretical study on molecular recognition, Lipkowitz [10] discussed enantioselectivity in chiral chromatography. They developed a model determining which optical isomer is retained longer by a chiral chromatographic column. The separation factor α can be determined exactly by relative retention times.

$$C_R + A_R \rightleftharpoons C_R \bullet A_R \qquad (1)$$

$$C_R + A_S \rightleftharpoons C_R \bullet A_S \qquad (2)$$
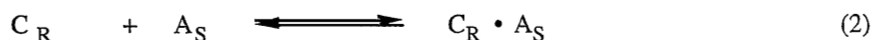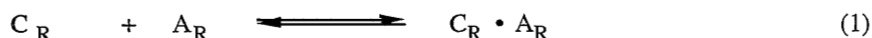
Here, C_R indicates the chiral stationary phase, and A_R and A_S the racemic analyt. Both equilibria are characterised by free enthalpy ΔG. The enantiomer, which is more strongly bonded, has a more negative ΔG value. The free enthalpy of the $C_R \bullet A_R$ complex is calculated and directly compared with the free enthalpy of the $C_R \bullet A_S$. This comparison is possible as the left side of both equilibria is chemically identical, the free enthalpy of the unbonded R form is identical to that of the S form. To allow any complex formation such as $C_R \bullet A_R$ or $C_R \bullet A_S$ the free enthalpy ΔG must be negative $\Delta G < 0$.

For the butanal cyanohydrin system chosen as the experimental system, a polymer membrane having reactive sites of (R)-Ch would show the following complexation reactions

$$(R)\text{-Ch} + (R)\text{-BuCN} \rightleftharpoons (R,R)\text{-Ch} \bullet \text{BuCN} \qquad (3)$$

$$(R)\text{-Ch}' + (S)\text{-BuCN} \rightleftharpoons (R,S)\text{-Ch} \bullet \text{BuCN} \qquad (4)$$
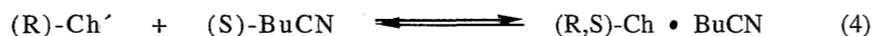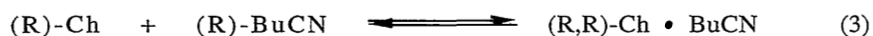
For enantiomer separation, the decrease in free enthalpy of both complexes must be different. The enantiomer, which is bonded more strongly, i.e. has a more negative ΔG value, is concentrated in the permeate assuming the same mobilty (diffusion coefficients) for the two enantiomers. As a result, the free reaction enthalpies of the complex formations β-CD–(R) enantiomer and β-CD–(S) enantiomer must be determined in order to predict successful complexation. As thermodynamic prerequisites are required for enantioselective separation, then the difference of the free enthalpy becomes

$$\Delta\Delta G^0 \ (R,S - R,R) \ < 0 \tag{5}$$

However, the entropic part of the free enthalpy counteracts the enthalpy of bonding due to associate formation. Therefore, low operation temperatures are preferred in enantioselective separation. 25 years ago, Gil-Av [11], the pioneer of gas-chromatographic enantiomer separation, was able to show that a separation of enantiomers on chiral separation phases on the basis of chiral recognition is possible as long as the formed diastereomers differ sufficiently from chiral separation phases and the enantiomers. In this case, an energy difference of $\Delta\Delta G^0 > 0.01 \ \text{kcal·mol}^{-1}$ can be sufficient for a total separation of the enantiomers in the capillary GC. A capillary separation column of 25 meters in length is equivalent to approximately 100 000 separation stages. Enantioselectivity is caused by chirality i.e. the optical activity of the chiral phase and by the concentration of optically active centres in the chiral phase [12,13,14,15]

Gas-chromatographic enantiomer separation is a suitable process for investigating the phenomenon of chiral recognition and can therefore contribute to understanding structure-properties relationships and the enantioselective interaction of chiral selectors and selectands.

7.2.2. Racemate Resolution by means of Chiral Polymers

Optically Active Polymer Films

Chromatographic material separation processes and membrane separation processes with optically active polymers are treated in a number of scientific publications and several patents. The production of polymer films from e.g. optically active poly-β-amides which are supposed to be suitable for membrane separation processes because of high mechanical stability and flexibility is described. Optical activity is also known from biopolymers. For

example Biopol®, a polyhydroxybutyrate is produced microbiologically on a large industrial scale and has good properties for film formation.

Optically Active Adsorbents

The separation performance of an optically active polymer strongly depends on the polymerisation process. Experiments with chirally substituted polyacrylamides have shown that the separation capacity of the polymer is a strong function of the degree of cross-linking. Through the inclusion of enantiomer-pure amino acids and other chiral preparations in a polystyrene matrix, the DL-mandelic acid could be concentrated by chromatography with an enantiomeric excess of 16% ee.

An optically active polymer from methacrylamides, immobilized on silica gel, for resolution of racemates of higher molecular weight by means of gel permeation chromatography (GPC) is described. Furthermore, the concentration of enantiomers of benzoin and other racemic compounds with porous poly-(N-acroyloyl-S-phenylalaninethylester) fixed on silica gel as a chromatographic separation material is mentioned. Pirkle [16] described the influence of the choice of elution agent on racemate separation by using chiral liquid membranes fixed on a silicon base. Enantiomeric purity of 75% ee was obtained for leucine butylester.

7.2.3. Cyclodextrins

As early as 1891, cyclodextrins as degradation products of starch were isolated, but it was not until 1904 that Schardinger [17] succeeded in characterising them as cyclic oligosaccharides (Schardinger dextrins). In 1948, the capacity of cyclodextrins to form molecular inclusion complexes was discovered. Cyclodextrins are a homologous series of non-reducing, cyclic oligosaccharides of at least six α-D-glucopyranose units in α-1.4-glycosidic bonding [8].

Nowadays, these cyclodextrins are produced biotechnically by means of enzymatic degradation of the α-1,4 bonded glucose units of the polysaccharide starch under the influence of the cyclodextrin glycosyltransferases of *Klebsiella pneumonia*. In this case, one ring of the helical form of the starch was cut out during cyclization. The yields and proportions of the individual cyclodextrins are enzyme-specific and can be influenced by adding organic compounds. Until now, the α-, β-, γ-, and δ-cyclodextrins with six to nine

glucose pyranose units have been isolated and characterised. The chemical structures are shown in *figure 7.1* and physical and geometric properties are listed in *table 7.1*.
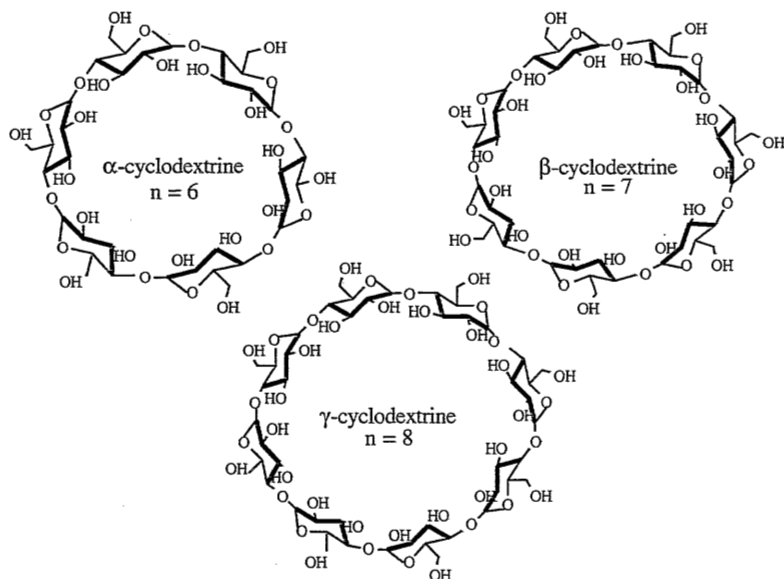
Figure 7.1 *Moleculare shape of α-, β- and γ-cyclodextrins*

The existence of cyclodextrins with up to twelve glucopyranose units has been proven, however only the α-, β-, γ-Cds are commercially available at present. Strained cyclodextrins with less than six glucopyranose units are not known to exist at the present time. Every chiral glucose unit in cyclodextrins is present in a chair-form.

The macrocyclic conformation of cyclodextrins is equivalent, in a solid and dissolved state, to a void torus. The wide opening is solely occupied with secondary hydroxy groups (C^2-OH and C^3-OH) and whose conical, narrow opening is occupied solely with primary hydroxy groups (C^6-OH). As no hydroxy groups are arranged on the inner side, the void is then hydrophobic and nonpolar.

The height of the void is constant while diameter varies. The inside of the torus is restricted by two series of CH groups (C^3 and C^5) and the intermediate series of the glycosidic ether bonds (C^1 and C^4). The free electron pairs of the oxygen atoms provide the void with high electron density.

Table 7.1 *Molecular dimensions and the physical properties of*
α-, β- and γ-cyclodextrins according to Szejtli.

cyclodextrin	α	β	γ
No. of glucose units	6	7	8
No. of chiral centres	30	35	40
Angle of rotation α_{20}^{D} (c=1 H$_2$O,dry basis)	150	163	unknown
Molecular weight [g]	972,86	1135,01	1295,15
External diameter [nm]	1,37-1,46	1,53-1,54	1,69-1,75
Internal diameter [nm]	0,47-0,52	0,60-0,65	0,75-0,85
Void volume [nm^3]	0,176	0,346	0,510
Melting and decomposition point [K]	551	572	540

Investigations on Heptakis-(2.6-di-O-methyl)-β-cyclodextrin (shown in *figure 7.2*) showed that the protection of the free hydroxy groups can enlarge the space available for a hydrophobic guest molecule. This example clearly demonstrates that the possibilities of cyclodextrins to modify conformations and to form complexes can be varied by chemical modification. The derivatisation of cyclodextrins, such as alkylation or acylation, can succeed regioselectively on the hydroxy groups.
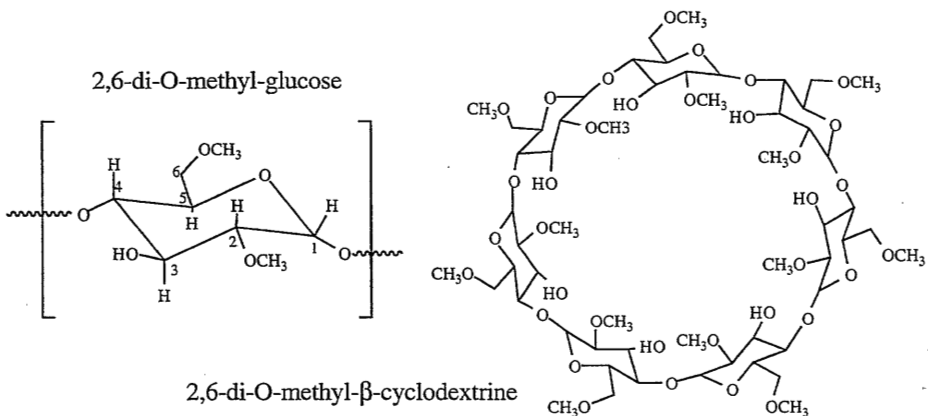

Figure 7.2 *Moleculare shape of methylated 2.6-di-O-methyl-β-cyclodextrin.*

The inherent molecular asymmetry of cyclodextrins, which is based on the presence of D-glucose units in the cyclo-oligomers, broadens the range of application considerably as the molecular inclusion of chiral guests in cyclodextrins usually proceeds on an enantioselective basis.

7.2.4. Optically Active Membranes

First experiments on chiral membranes were published by Armstrong [18] and Newcomb [19]. The work deals with the concentration of enantiomers from various racemic compounds, using liquid membranes with α-, β-, γ-cyclodextrins as chiral membrane components. They also report on the preparation of enantiomer-pure α-amino acids with immobilised optically active polyacrylic acid derivatives on which an educt for amino acid synthesis is reversibly attached. In this case, the polymer, as a chiral unit, controls the stereoselective synthesis.

Liquid membranes in general are the most intensively investigated methodology for chiral resolution using membranes. Recent publications were done by Lehn [20], Pirkle [21], Prelog [22], Bryjak [23], Ding [24], Higuchi [25,26], Keurentjes [27,28], Shinbo [29] and Yamaguchi [30,31]. Biological carriers are used by Cohen [32]. However, availability and long-term stability of those genetically engineered proteins is poor.

Homogeneous chiral membranes for optical resolution are described by Aoki [33], Maruyama [34], and Yashima [35,36]. Furthermore, Hartwig [37] describes a method to produce chiral membranes via plasma polymerisation. An innovative method is described by Linder [38]. In their patent specification, modified polysaccharide membrane and polyacrylic membranes for the concentration of enantiomers from racemic mixtures are described. Pervaporation is included as one of the membrane separation processes.

Until today however, either long-term stability or resolution power of the chiral membranes described in literature are insufficient for any practical application. Due to the fact, that the separation factor of the membranes is poor, at least 30...50, but typically 100 separation stages are necessary in order to achieve enantiomerically pure products. This is further complicated by the fact, that the separation factor typically decreases with increasing enantiomeric excess of the feed mixture. Furthermore, flux densities of the membranes are small.

7.3. Experimental

The equipment used, the synthesis of the basic chemicals as well as the test set-ups have been described in chapters 4-6. The determination of enantiomer yield was conducted by gas chromatography on a chiral separation column, which was specially prepared for this purpose and based on permethylated β-cyclodextrins on PS 086 [39]. For the analysis of the butanal cyanohydrin special care had to be taken with the cyanohydrin analysis. In order to avoid thermal decomposition, the (R/S)-butanal cyanohydrin was stabilized by acylation or silylation. Tetradecane is applied as an internal standard.

Cyclodextrins

The α-, β-, γ-cyclodextrins, which were used, are commercial products of the CycloLab Chinoin company (Budapest, Hungary). The heptakis-(2.6-di-O-methyl)-β-cyclodextrin (DIMEB) and the permethylation for heptakis-(2.3.6-tri-O-methyl)-β-cyclodextrin (TRIMEB) was produced according to Szejtli []8 in dry dimethyl sulfoxide with a sodium hydride suspension and subsequent alkylation with methyl jodide at 60°C with 88% yield. This process was also applied to the relevant α-, and γ-cyclodextrins with 83% and 59% yield.

Micro-heterogeneous polydimethylsiloxane membranes

Membranes were formed by casting a 0.3 - 1.5% solution of polymer in a suitable solvent. Firstly, polydimethylsiloxane was chosen as a polymer matrix. In general, after filtration of the polymer solution, a solution of cyclodextrin dissolved in chloroform was added to the polymer solution. Cross-linking occurred not only by hydrosilylation but also by polycondensation.

The precursors consist of the prepolymer V199A, the crosslinking agent V90 and the catalyst OL(Wacker-Chemie) with a ratio of roughly 100 : 3: 1 as a solution in toluene [40]. The crosslinking agent and the catalyst are added successively to the toluene prepolymer solution by stirring. Then the mixture is filtered by a teflon filter with a pore size of 5 μm. By using a doctors blade, the polymer solution is cast on a glass plate in the form of a 1000 μm thick film and then placed in a drying cabinet and left to react overnight at 60°C.

Also a two-component RTV silicon rubber, termed as RTV 615 (General Electrics), which has a low viscosity, pours easily into film form and hardens to a tough rubber. The mixing ratio of the basic components to the cross-linking agent was 10 : 1. To avoid imperfection in the drying film, air bubbles, which entered during the stirring process, had to be removed by a vacuum. The hardening process takes place without heat formation and with very little shrinkage (linear shrinkage <0.2%). Hardening takes approx. one hour at 100°C or eight to ten hours at room temperature.

Polyurethane-co-cyclodextrin

Polymerisation of the cyclodextrin (CD) with the methylen-bis-diphenylisocyanate (MDI) must take place in a moisture-free environment to suppress formation of urea. All CDs are highly soluble in bases, acids, DMSO, DMAc or NMP. The technical grade [diphenylmethane-4,4'-di-isocyanate] (MDI, Desmodur 44 ® Bayer AG) was purified before use by vacuum distillation up to a melting point of 39°C. The technical grade is a mixture of the 2,4'-, 2,3'- and 4,4' isomers shown in *figure 7.3*.
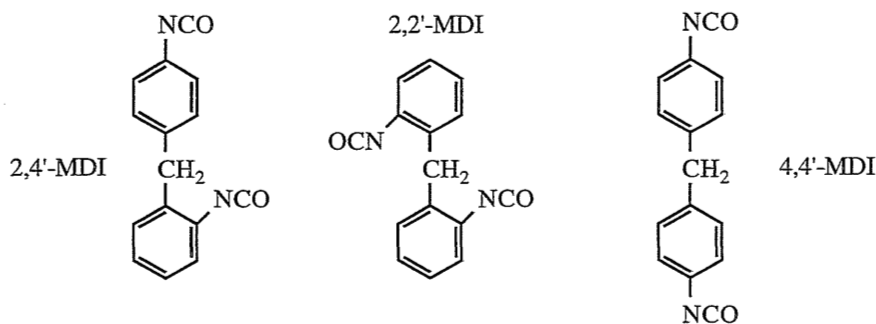
Figure 7.3 *Isomers of commercial diphenylmethane-di-isocyanate (Desmodur®)*

The cyclodextrin-copolymer membranes are produced by the polyaddition of β-cyclodextrin with the bifunctional diisocyanatodiphenylmethane (MDI). The β-cyclodextrin is dissolved and slowly added to the MDI solution in an argon atmosphere and at T= 25°C. The cross-linking density can be adjusted by the molar ratio of (OH/NCO) which was varied between 1...5. The membranes are cast by using a blade and polymerised at 90°C according to a prescribed temperature programme. Re-drying occurs at 120°C respectively. All β-CD-MDI membranes are transparent and flexible. Membranes, which have not undergone adequate polymerization, become turbid and milky when detached in deionized water.

A minimum reaction temperature of 100°C is required for the production of the heptakis (2,6-dimethly)-β-cyclodextrin polyurethane membranes. At lower temperatures crystallization of the DIMEB occurs. In this case, the cross-linking density can only be adjusted between a molar ratio of ($^{OH}/_{NCO}$) =1...1,8.

Sorption Experiments

The chiral polymer resins, used in membrane production, were additionally characterised by sorption experiments. The dry polymer was determined and then soaked in the feed mixture. After reaching equilibrium, the sorbed liquid was removed from the polymer matrix by applying a vacuum. The desorbed compounds were condensed in a cold trap and analyzed further by gas chromatography.

7.4. Results and Discussion

7.4.1. Microheterogeneous Chiral Membranes

In the simplest of cases, chiral membranes can be produced by the inclusion of optically active molecules in a non-selective polymer matrix. They should possess good film-forming properties and high mechanical stability. The chiral 'carrier molecules' should be readily soluble in the matrix and should have a high optical density. For this purpose polydimethylsiloxane with an optically active species such as β-cyclodextrins was chosen. The cyclodextrins with 35 chiral centres and an angle of rotation of $\alpha \, {}^{D}_{20}$ = 163° fulfill these requirements ideally.

In the production of chiral membranes, a specific proportion of permethylated β-cyclodextrins is dissolved in toluene, then added to the Wacker reaction resin and heterogeneously hardened during hydrosilylation. A partially covalent bonding is achieved by working the dimethylated β-cyclodextrin into the General Electric condensation resin and this is then hardened at room temperature.

From sorption measurements with pure cyclodextrins out the liquid phase it was shown that the β-cyclodextrin sorbed at 25°C approximately 46wt.% of (R/S)-butanal cyanohydrin. In contrast, the heptakis-(2.6-di-O-methly)-β-cyclodextrin sorbed only 28 wt.% approximately

of the cyanohydrin. Under the assumption of a 1 : 1 complex formation, a maximum of 8.8 wt% sorption can be expected. The excess is due to unspecific sorption in the β-cyclodextrin powder.

Membranes produced with the prepolymer V199A, could contain a maximum of 55 wt.% β-cyclodextrin. A 76 wt.% β-CD content is achieved for membranes with a matrix of RTV silicon rubber. At higher cyclodextrin concentrations, the mechanical stability of films is insufficient.

The pervaporation fluxes of the samples were used to compare permeability rates. Racemic (R/S)-butanal cyanohydrin or a 0,5 wt% mixture of butanalcyanohydrin in di-iso-propylether was chosen as a feed liquid for the characterisation of the chiral membranes by means of pervaporation.

Type of membrane	Thickness normalized flux density $[10^{-3} \text{ g·m}^{-1}\text{·h}^{-1}]$	Enantiomeric excess ee [%]	Thickness normalized flux density $[10^{-3} \text{ g·m}^{-1}\text{·h}^{-1}]$	Enantiomeric excess ee [%]
feed	(R/S)-butanalcyanohydrin		0,5 wt.% butanalcyanohydrin in di-iso-propylether	
Wacker - V 199A	4,24	0	17,76	0
+ 25 wt.% β-TMCD	1,23	0,22	12,38	1,25
+ 55 wt.% β-TMCD	0,34	0,91	2,44	3,52
GE - RTV 615	6,58	0	23,02	0
+ 50 wt.% β-DMCD	3,22	0,49	13,48	2,28
+ 76 wt.% β-DMCD	0,58	1,98	1,52	5,93

Table 7.2 *Enantioselectivity of heterogeneous 35 μm β-CD/PDMS membranes. The measurements were conducted at 40°C and $p_{permeate}$>0.01 mbar.*

The data of *table 7.2* clearly demonstrate an improvement in the enantiomeric selectivity of the membranes. However, with increasing cyclodextrin concentration the normalized flux density decreases. This particular mass transport behavior is anticipated to stem from the

morphology of the membranes which was confirmed by transmission light microscopy. The hydrophilic cyclodextrin is dispersed heterogeneously in the PDMS matrix as shown in *figure 7.4*. Transport occurs through both phases, the cyclodextrin and the PDMS. The diffusion through the PDMS phase is non selective, only the cyclodextrin establishes separation. However with increasing cyclodextrin content, the path length for the fast, non-selective transport through PDMS increases (increasing tortuosity) and the flux decreases.
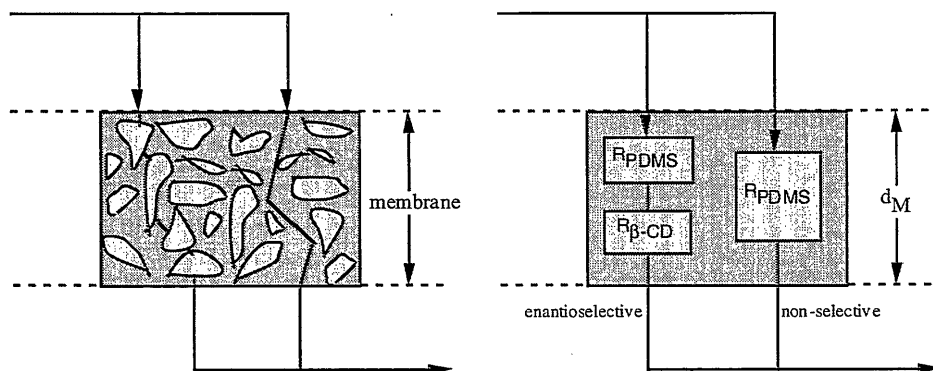
Figure 7.4 *Resistance model approach for description of transport limitations in microheterogeneous chiral membranes*

In general, the resulting resolution was rather dissappointing considering GC control experiments where the hepatkis-(2.6-di-O-methly)-β-cyclodextrin was coated on fused silica. The resolution was determined for (R/S)-butanal cyanohydrin and the chromatogram showed a clear base line separation and an exellect separation factor of α=1,18. Apparently, the fast, non-selective transport through the PDMS phase dominates the overall transport.

Another problem of the heterogeneous membranes is their long-term stability. In sorption experiment it was found that permethylated β-CD can be extracted from polydimethyl-siloxane. This leaching eventually leads to the membrane being destroyed. This was also confirmed by the so-called 'bleeding' of chiral cyclodextrin stationary phases in gas chromatography after long-term use.

By applying heterogeneous chiral membranes, it was not possible to increase the enantiomer yield to a value of at least >15% ee which could be used on a technical scale. The reason for this lies essentially in the low optical density of these membranes.

According to the equivalent circuit diagram of *figure 7.4*, the non-selective resistance of matrix material should be increased. This can be carried out by increasing the tortuosity factor or by increasing the β-cyclodextrin content. Due to reasons of mechanical stability, the maximum optical density of the membranes is limited. An improvement could be obtained by using a polystyrene-co-isoprene matrix, however the mechanical requirements for technical use were not fulfilled. Alternatively, the PDMS could be replaced by a glassy, less permeable polymer matrix. However, a solvent-stable polymer, which could be homogeneously dissolved with cyclodextrins, could not be found.

7.4.2. Homogeneous Chiral Membranes from Poly-(L) lactic acid

In 1932, Staudinger detected that all vinyl and acrylic polymers are built with a C-main-chain of chiral centres [41,42]. As these polymers show a symmetry plane vertical to the main-chain, optical activity is degraded as a meso-compound. Therefore the most important method for the production of optically active compounds is the polymerisation of monomers with optically active side groups. Another variant is polymerisation by using optically active catalysts, however the polymer, which is formed, must not exhibit a symmetry plane. The first example of this is poly(benzofurane) with a diisotactic main-chain. Another alternative is the polymerisation of an enantiomer. At present, the polymer-analogue modification of a polymer with an optically active marker is also considered as promising. A further intensely used method to introducing optical activity to homogeneous polymers results from the so-called 'molecular imprinting' [43]. In this case, a chiral molecule is placed on a monomer matrix which is ultimately polymerised. Then the chiral 'print' molecule is extracted, leaving behind a chiral void. This process seems adequate, particularly for the production of chiral chromatographic resins. However, there are no tests available concerning long-term chiral stability as a loss of optical information owing to polymer relaxation is to be expected.

In this subsection, chiral membranes are used as the general term for spatially cross-linked polymers with monomer units consisting of optically active components. The asymmetric center is not destroyed during cross-linking or polymerisation and polycondensation. Network formation occurs on a functional group of monomers. In this case, the monomers can exhibit one or several asymmetric centres and can be converted to a polymer either by direct polymerisation or by cross-linking with another component.

In the following the chiral polymer Poly-(L)-lactic acid shown in *figure 7.5.* was studied in detail

Poly-L-lactide: M_W appr. 100 000 Da
soluble in CH_2Cl_2, $CHCl_3$, HFIP
$\alpha \, _{20}^{D} = -150°$ (c=10g/L in $CHCl_3$)
T_g [°C] = 44,7
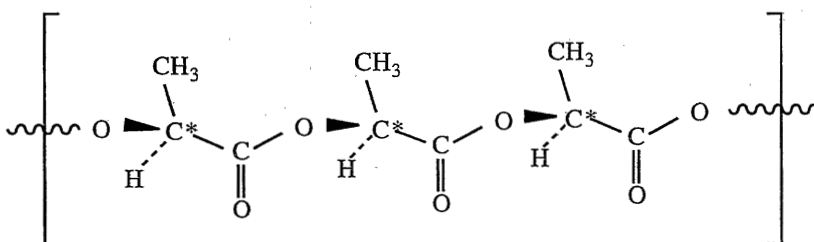
Figure 7.5 *Structural formula of Poly-L-lactide (PLLA)*

The monomer of the poly-L-lactide is [(S)-2-hydroxy-propionic acid]. Polymerisation occurs stereo-specifically with very little proportion of by-products through ring-opening condensation of the L,L-lactide in the presence of tin(II)octoate [44,45]. The polymers were produced together with the Fraunhofer Institute for Applied Polymer Chemistry. The narrow molecular-weight distribution results in very good film-forming properties.

The characterisation of homogeneous PLLA films was carried out under pervaporation conditions. As a feed solution, pure (R/S)-butanal cyanohydrin as well as a 0.5 wt.% butanal cyanohydrin solution in di-iso-propylether was specified. The thickness of the PLLA films varied between 50 μm and 8 μm.

Table 7.3 lists the enantiomeric excess and the thickness normalized flux as a function of different temperatures. In general, the separation properties of the membranes are very low. The loss in separation efficiency can be attributed to the increased effect of the entropic term influencing complex formation as well as changes in the physical state of the polymer.

The transition of the polymer can be clearly seen from the flux as a function of temperature as described in *figure 7.6.* As expected the flux through the membrane increases with increasing temperature but also a very distinct transition can be obeserverd when the

logarithmic flux is plotted vs. the inverse temperature. By applying reduced permeability versus temperature, unsteadiness could be observed at temperatures above 40°C.

Table 7.3 *Enantioselectivity of homogeneous 25 µm PLLA membranes.*
Measurements were conducted at $p_{permeate}<0.005$ mbar.

temperature [°C]	normalized flux density [10^{-6} g·m^{-1}·h^{-1}]	enantiomeric excess [%]	normalized flux density [10^{-6} g·m^{-1}·h^{-1}]	enantiomeric excess [%]
feed	(R/S)-butanalcyanhydrin		0,5 wt.% butanalcyanhydrin in di-iso-propylether	
− 10	-	≈ 0,9	0,098	10,2
± 0	-	1,45	0,501	4,8
+ 10	65	0,22	2,203	2,1
+ 20	112	0	8,706	1,7
+ 30	356	0	31,49	0,9
+ 40	409	0	82,12	0,1
+ 50	471	0	86,23	0
+ 60	593	0	90,18	0
+ 70	937	0	94,13	0

The reduction in permeability increase above 40°C results from exceeding the glass-transition temperature T_g of the polymer poly-L-lactide. This occurs at 44°C for the racemate. A change in morphology is confirmed by calculating the activation energy E_A for permeation from the slope of the logarihmic flux and the inverse temperature in *figure 7.6*. For the temperature range up to 30°C, i.e. below the glass-transition temperature, the activation energy for permeation roughly amounts to $E_A = 93.06$ kJ mol^{-1}. Above 40°C, when the glas-transition temperature is exceeded, the activation energy is reduced to $E_A = 4.05$ kJ mol^{-1}.
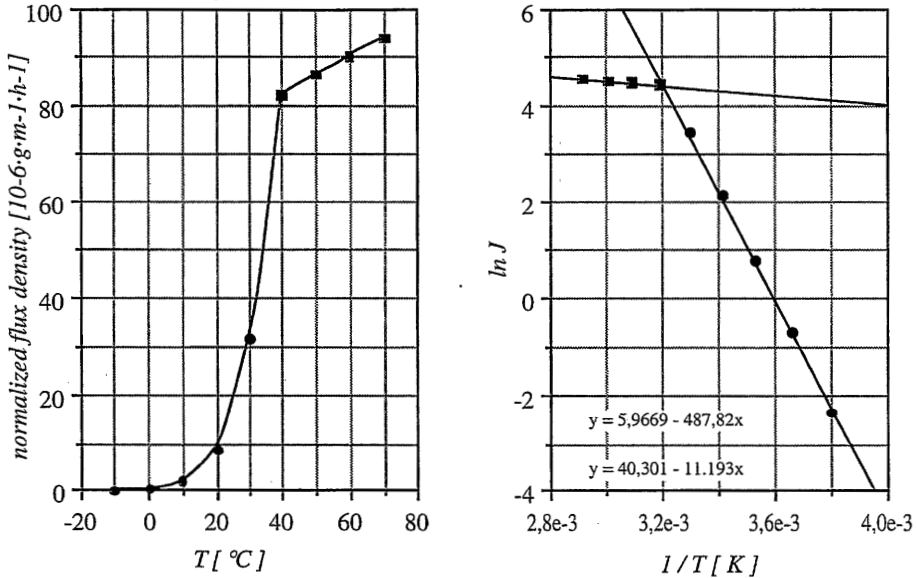
Figure 7.6 *Normalized flux density of homogeneous 25 μm PLLA membranes.*
Arrhenius plot for calculation of activation energy of permeation.

Also here, one observes that the enantiomeric excess increases by decreasing the racemate concentration by to mixing with the solvent di-iso-propylether. In literature similar results have been observed in chromatography and pervaporation. One can hypothesize that the optically active centers in the membrane are quickly occupied due to complexion, but that unselective sorption in the polymer matrix spoils the separation efficiency [46].

Reproducible membrane thicknesses can be produced with poly-L-lactide. The flexible membranes, which possess good mechanical properties, are suitable for both pervaporation and pertraction. From the results of the measurements with PLLA membranes, it became clear that the primary objective of enantiomer concentration could not be fulfilled at a technical level since the membranes show selectivity but low fluxes in the glassy state and higher fluxes but no selectivity in the rubbery state.

7.4.3. Cyclodextrin-polyurethane-copolymer membranes

The previous experiments have shown that for all the chiral membranes produced, the optical density was inadequate. Microheterogeneous membranes do not allow a further increase in the proportion of cyclodextrins owing to limited mechanical stability. Homogeneous polymer membranes exhibit, in a glassy state, permeability rates which are too low for technical application and in an elastomer state, do not exhibit sufficient enantioselectivity. In publications, a method using liquid membranes has been described as an alternative. These membranes combine high optical density and sufficiently high permeability rates. Due to the significant thickness of the membranes the flux still is low. Furthermore, liquid membranes still have disadvantages regarding their stability and reliability.

Therefore, a new route for the preparation of chiral membranes was developed: to obtain an increase in mechanical stability and in enantioselectivity by synthesizing a covalently bound network of cyclodextrins [47,48,49,50,51].

A potential crosslinking reaction is the conversion of a hydroxide group with an isocyanate group to a polyurethane. In this case, a series of various di- and triisocyanates are available as reaction partners to the cyclodextrin having the required OH-functionality. After preliminary testing, the toluidine di-isocyanate (TDI) and methlyene diphenyl di-isocyanate (MDI) were identified as potential monomers. Polyurethanes of the toluidine di-isocyanate with β-cyclodextrin are brittle with low film-forming capacity if the CD proportion is high. The membranes produced can only be used in a state of equilibrium sorption. However mechanical stability was adequate to produce test samples. In sorption measurements, an absorption of (R/S)-butanal cyanohydrin of 9.5 wt% was measured at an enantiomeric excess of 8.5% ee. This value was lower than expected and does not exceed the enantioselectivity of the unmodified cyclodextrins which was assumed to have a low selectivity due to unselective sorption. The low enantiomeric excess may also be influenced by a deformation of the β-cyclodextrin torus. The chain rigidity of the TDI possibly caused an extension or compression of the torus resulting in a reduction in interaction between the cyanohydrin and the cyclodextrin.

Cyclodextrin polyurethane membranes are successfully prepared by the polyaddition of β-CD or β-CD derivatives with the bi-functional methylene diphenyl di-isocyanate as shown in *figure 7.7*. The methylene bridge induces sufficiently free rotation and acts as a molecular spacer between the β-CD cones. During the stoichiometric conversion of the OH groups of

the β-CD with the NCO groups of the MDI, the monomers and oligomers crosslink into a three-dimensional network which does not dissolved in organic solvents.
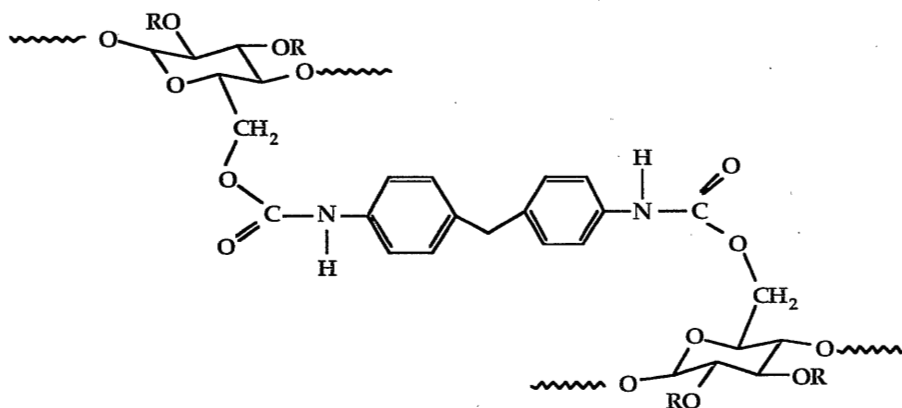
Figure 7.7 *Structural formula of Poly-{methylene-bis-(4,4'-phenyl-di-isocyanate)-co-β-Cyclodextrin}. The MDI acts as an molecular spacer.*

The material properties of the β-cyclodextrin polyurethane membranes produced are essentially determined by the ratio of β-CD to MDI. In this case, not only the network density around the β-CD molecule but also the equilibrium between the hydrophilic and hydrophobic polymer segments is specified. The hydrophilicity of the membrane increases as the proportion of MDI decreases. However, at the same time, the mechanical properties deteriorate. *Table 7.4* summarizes the effect of varying the ration of MDI and cyclodextrin.

$\left(\dfrac{OH}{NCO}\right) = 1$		$\left(\dfrac{OH}{NCO}\right) = 5$
Film forming properties	←	poor films
Hydrophilicity	→	very hydrophilic
Permeability vs. polar compounds	→	water selective
Mechanical properties	←	brittle
Flexibility	←	rigid

Table 7.4 *Properties of MDI-β-cyclodextrin membranes as a function of the ratio cyclodextran and di-isocyanate*

Poly{methylene-bis-(4,4'-phenyldi-isocyanate)-co-β-cyclodextrin}

The membranes made from MDI and the ß-CD were tested in pervaporation experiments and the results are summarized in *table 7.5*. Two types of membranes differing in the ratio of MDI and ß-CD were tested for various feed mixtures. Due to their hydrophobic character, the butanal cyanohydrin and the acetylated butanal cyanohydrin exhibits a smaller transmembrane flux density in the cyclodextrin-rich membrane. As an increase in the proportion of the polar OH groups occurs, permeability decreases, measured on the DIPE flux for aprotic solvent. The practical possibilities for the production of homogeneous flexible membranes with optimum swelling behaviour appear promising.

type of membrane	$\left(\dfrac{\beta\text{-CD / OH}}{\text{MDI / NCO}}\right) = 1$		$\left(\dfrac{\beta\text{-CD / OH}}{\text{MDI / NCO}}\right) = 3,5$	
feed	normalized flux density 10^{-3} $[\text{g·m}^{-1}\text{·h}^{-1}]$	enantiomeric excess [%]	normalized flux density 10^{-3} $[\text{g·m}^{-1}\text{·h}^{-1}]$	enantiomeric excess [%]
(R/S)-butanalcyanhydrin	1,609	0,83	21,22	2,27
(R/S)-acetyl-butanalcyanhydrin	2,867	0,22	18,97	3,13
0,5 wt.% butanalcyanhydrin in di-iso-propylether	25,36	4,91	7,34	5,34
0,5 wt.% acetyl-butanalcyanhydrin in di-iso-propylether	26,02	3,86	6,99	9,15

Table 7.5 *Enantioselectivity of homogeneous 100 μm β-CD/MDI membranes. Measurements were conducted at 25 °C and $p_{permeate} < 0.005$ mbar.*

Poly{methylene-bis-(4,4'phenyl-di-isocyanate-co-heptakis-(2,6-di-O-methyl-β-cyclodextrin}

Due to methylation, the void of the cyclodextrin becomes deeper (approx. 1000-1100 pm) and more conical. The larger opening at the end of the secondary methoxy group is extended and the small opening at the other end of the primary methoxy group is narrowed. It can be predicted that there is a great tendency for enantiomer differentiation to occur with permethylated cyclodextrins than with underivatized analogues. X-ray structure experiments have shown that hydrogen bonds between host and guest can occur with suitable guest molecules. The fact that these hydrogen bonds can also contribute decisively to enantiomer differentiation in the case of permethylated cyclodextrins, can be deduced from the crystal structures of inclusion complexes. Permethylated cyclodextrins can, in contrast to the parent compounds, only act as acceptors for hydrogen bonds with regard to compounds with protic groups. The 'classic' hydrophobic interactions can be attributed mostly to entropy effects. The formation of the guest-host complex does coincide with a decrease in entropy, however the stripping-off of the hydrate cover of the guest and the release of solvent molecules from the cyclodextrin void can lead to an increase in entropy. Although van-der-Waals forces are not very extensive, they can contribute considerably to selective inclusion, when there is close contact between host and guest.

Until now, pervaporation tests with these membranes have been less successful as the membranes are very inflexible and brittle.

Poly-{methylene-bis-(4,4'-phenyl-di-isocyanate-co-heptakis-(2,6-di-O-methyl)-β-cyclodextrin-co-β-cyclodextrin}

Mechanically stable membranes can be produced by means of copolymerisation of methylated and non-modified cyclodextrins. However, the proportion of pure β-cyclodextrin should amount to roughly 30 wt. % of the total cyclodextrin quantity in this case.

Besides the enantioselectivity with these membranes, particularly the selectivity for different polar molecules is remarkable. As has already been stated on the subject of enzymatic cyanohydrin synthesis in Chapter (I).5, these membranes are suitable for the selective separation of polar compounds from unpolar media.

Poly-{methylene-bis-(4,4'-phenyl-di-isocyanate-co-heptakis-(6-O-(+)-S-α-methoxy-α-trifluoromethyl phenylacetic acid)-β-cyclodextrin}

The cyclodextrins used have the shape of a hollow torus with a hydrophobic inner side and a hydrophilic outer side. This is confirmed by the more pronounced complex formation of the hydrophobic molecules. The smaller opening of the cyclodextrins is occupied by primary hydroxyl groups in six positions. The larger opening is surrounded by secondary hydroxyl groups which are placed clockwise in position 2 and anti-clockwise in position 3. The chiral properties of the cyclodextrins are obtained by complex formation through the molecule to be separated entering the broader part of the torus. This should allow further influencing of the complex formation properties by a chemical functionalization of the external hydroxyl groups. In this case positions 2 and 3 are preferred for modification but position 2 and 6 are more reactive.

The torus can be altered by introducing protective groups or molecular spacers but this brings about only gradual changes in intrinsic properties. Therefore attempts were made to improve enantioselective complex formation at the opening of the torus by means of chiral modification. From the gas-chromatographic analysis of cyanohydrins, the (+)-S-α-methoxy-α-trifluoromethyl phenylacetyl chloride can be recommended as a chiral agent, the so-called Mosher's reagent. In this case, a modification of the β-cyclodextrin on the secondary hydroxyl group in position 2 is desired as shown in *figure 7.8*.

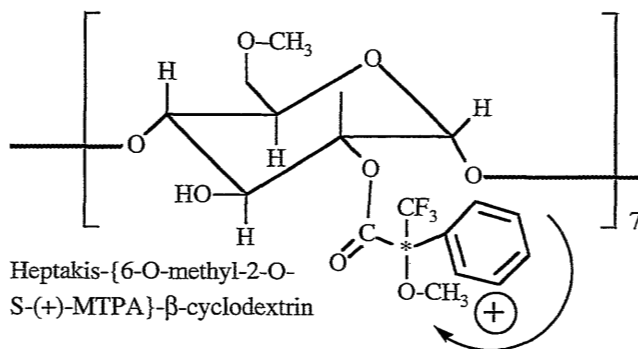Heptakis-{6-O-methyl-2-O-S-(+)-MTPA}-β-cyclodextrin

Figure 7.8 *Structure of β-CD modified at 2-position using Mosher's reagent*

However, this reaction is in competition to the conversion on the primary hydroxyl groups in position 6 as shown in *figure 7.9*, which is on the smaller opposite opening of the (+)-S-α-methoxy-α-trifluoromethyl phenylacetyl chloride torus. In equimolar alkylation, firstly

conversion is carried out accordingly with methyl jodide and then with (+)-S-α-methoxy-α-trifluoromethyl phenylacetyl chloride. Nevertheless, no structurally uniform product could be detected in the ^{1}H- and ^{13}C spectrums. The secondary hydroxyl group in position 3 is preserved completely and is therefore available to undergo further conversion to polyurethane with the isocyanate.
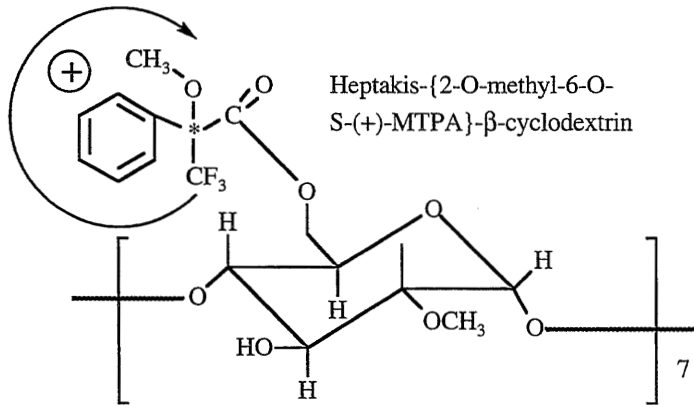
Figure 7.9 *Structure of β-CD modified at 6-position using Mosher's reagent*

Transparent, yellow polymer films with high mechanical stability can be developed by production of polyurethane from dimethyl sulfoxide. By coating microporous aluminium from AluSuisse, solvent-stable thin-film composite membranes can be produced.

In pervaporation experiments based on a model mixture of 15 wt.% butanal cyanohydrin in di-iso-propyl ether with 5 wt.% butanal, concentration of the cyanohydrin to 61 wt.% can be obtained with an enantiomeric purity of 22% ee at permeate pressure of $p_p < 0.05$ mbar and at a temperature of 15°C. The obtained selectivities were the best for all chiral membranes developed.

7.4.4. Sorption tests on homogeneous chiral membranes

The separation of enantiomers by solution-diffusion membranes can be controlled by diffusion or by sorption. Sorption experiments can provide information on selectivity-determining steps and thus on a specific increase in selectivity. This was carried out by equilibration of the membranes in a large molar excess of feed solutions. Pure (R/S)-butanal

cyanohydrin, a solution of 0.5 wt.% butanal cyanohydrin in di-iso-propyl ether as well as the hydrophobic 0.5 wt.% acetyl butanal cyanohydrin in di-iso-propyl ether were used.

type of membrane	100 wt.% (R/S)-butanalcyanhydrin	0,5 wt.% (R/S)-butanalcyanhydrin in di-i-propylether	0,5 wt.% Acetyl-butanalcyanhydrin in di-i-propylether
Wacker - V 199A + 55 wt.% β-TMCD	3,3	nn	nn
GE - RTV 615 + 76 wt.% β-DMCD	7,8	nn	nn
Poly-L-lactid	0,9	7,3	6,9
Poly(MDI-co-β-CD) 70 wt.% β-CD $\left(\dfrac{\beta\text{-CD / OH}}{\text{MDI / NCO}}\right) = 3,5$	9,7	12,1	9,75
Poly(MDI-co-β-DMCD) 75 wt.% β-DMCD $\left(\dfrac{\beta\text{-CD / OH}}{\text{MDI / NCO}}\right) = 2$	6,2	19,8	24,9
Poly(MDI-co-β-DMCD-co-β-CD) 70 wt.% β-CD$_{ges}$ $\left(\dfrac{\beta\text{-CD / OH}}{\text{MDI / NCO}}\right) = 0,5$	5,8	14,6	17,4
Poly(MDI-co-β-DMCD-co-β-(+)-MTPA-CD) 75 wt.% β-CD$_{ges}$ $\left(\dfrac{\beta\text{-CD / OH}}{\text{MDI / NCO}}\right) = 2,5$	9,1	52,7	63,2

Table 7.6 *Sorption selectivity of different microherterogeneous and homogeneous chiral membranes*

All the polyurethanes exhibit a very high sorption for cyanohydrins. With a weight fraction of approx. 70 wt.% β-cyclodextrins in the membrane phase, the sorption of cyanohydrin is

always between 15 wt.% and 22 wt.% . *Table 7.6* only shows the sorption selectivities but not the absolute sorption values.

The sorption experiments showed that an enantioselective complex formation on the chiral centres of the membrane phase occurred. Sorption selectivities are also significantly higher than permeation selectivities. This was also confirmed in chromatographic experiments with poly{methylene-bis-(4,4'phenydi-isocyanate-co-heptakis-(2,6-di-O-methly)-β-cyclodextrin. A maximum enantiomeric excess of almost 60% ee was found in liquid chromatography [52] using granules of the polymer.

One explaination for the low permeability selectivity may be a strong diastereomer formation. A second explanation could be that non-selective transport outside the active field of the optical centers still occurs although the tailor-made membranes have already a high optical density.

7.5. Conclusions

Various chiral membranes have been prepared which allows the separation of racemic mixtures. Microheterogeneous membranes prepared by dispersing cyclodextrins in a matrix polymer showed low selectivities. Improvements by dispersing higher concentrations of cyclodextrins are limited by the mechanical properties of the membranes. Homogeneous membranes from optically active Poly-(L)lactic acid also show low selectivities. Newly synthesized polyurethane-cyclodextrin copolymer membranes show promisingly high selectivities. The effect of cyclodextrin modification was studied and a modification by using Mosher's reagents yielded the best enantiomeric access of 22% ee.

List of Symbols

$\alpha_{i,j}$	separation factor
β_i	enrichment factor
A	species A or analyt
C	chiral stationary phase
R, S	stereochemical term for both enantiomers

[A]	concentration of species A
a_i	activity of component i
γ_i	activity coefficient
% ee	optical purity; enantiomeric excess [%]
E_A	activation energy
f_i	fugacity of component i
G	Gibbs free energy
J_i	mass transfer or permeation rate
J_N	normalized flux density
L	membrane thickness
p	total pressure
p_i^S	saturation vapour pressure of species i
P_i	permeability coefficient of species i
T	temperature
x_i	mole fraction of species i

Subscripts and Superscripts:

'	value in the feed stream
''	value in the permeate stream
0	standard reference state
*	ideal case
i	species i
m	membrane
T	temperature

Abbreviations:

β-CD	β-cyclodextrin
DIPE	di-iso-propylether
DIMEB	(2,6-dimethly)-β-cyclodextrin
GC	gas chromatography
mdi	methylene-bis-diphenylisocyanate
mpba	3-phenoxybenzaldehyde
mpbac	(2)-hydroxy-2-(3-phenoxyphenyl) acetonitrile
PDMS	polydimethylsiloxane

References

[1]   Pirkle, W.H.; Pochapsky, Th.C.
        Considerations of Chiral Recognition Relevant to the Liquid Chromatographic
        Separation of Enantiomers
        Chemical Reviews 89 (1989) 347-362

[2]   Pirkle, W.H.; Pochapsky, Th.C.
        Theory and Design of Chiral Stationary Phases for the Direct Chromatographic
        Separation of Enantiomers
        Chromatographic Science 47 (1990) 783-814

[3]   Rüedi, P.
        Enantiomerentrennung mittels HPLC
        Chemie für Labor und Betrieb, Nr. 40, Heft 7, (1989) 357-362

[4]   König, W. A.
        Eine neue Generation chiraler Trennphasen für die Gaschromatographie
        Nachr. Chem. Tech. Lab. 37 (1989) 471-476

[5]   König, W.A.
        Enantioselective Gas Chromatography with Modified Cyclo-Oligosaccharides
        as Chiral Stationary Phases
        Carbohydrate Research 192 (1989) 51-60

[6]   Schurig, V.; Nowotny, H. P.
        Gaschromatographische Enantiomerentrennung an Cyclodextrinderivaten
        Angewandte Chemie, Nr. 102, (1990) 969-986

[7]   Ward, J.; Armstrong, D.
        Cyclodextrin Stationary Phases
        Department of Chemistry and Biochemistry, Texas Tech. University

[8]   Szejtli, J.
        Downstream processing using cyclodextrins
        TibTech 7 (1989) 170-174

[9]   Berthod, A.; Li, W.; Armstrong, D.W.
        Multiple enantioselective retention mechanisms on derivatized cyclodextrin
        gas chromatographic chiral stationary phases
        Analytical Chemistry 64:8 (1992) 873-879

[10]   Lipkowitz, K. B.; Baker, B.; Zegarra, R.
        Theoretical Studies on Molecular Recognition: Enantioselectivity in Chiral Chromatography
        Journal of Computational Chemistry 10:5 (1989) 718-732

[11]   Gil-Av, E.
        Gas Chromatography
        Institute of Petroleum, London, (1967)

[12]   Topiol, S.
        A General Criterion for Molecular Recognition: Implications for Chiral Interactions
        Chirality 1 (1989) 69-79

[13]   Topiol, S.; Sabio, M.
        Interactions between eight centers are required for chiral recognition
        J. Am. Chem. Soc. 111 (1989) 4109-4110

[14]   Topiol, S.; Sabio, M.
Computational chemical studies of chiral stationary phase models
J. Chromatography 461 (1989) 129-137

[15]   Toda, F.
Molecular Recognition in the Solid State
Advances in Supramolecular Chemistry 2 (1992) 141-191

[16]   Pirkle, W.H.; Doherty, E.M.
Enantioselective Transport through Silicone-Supported Liquid Membrane
J. Am. Chem. Soc. 111 (1989) 4113-4114

[17]   Saenger, W.
Cyclodextrin-Einschlußverbindungen in Forschung und Industrie
Angew. Chemie 92 (1980) 343-361

[18]   Armstrong, D.W.; Jin, H.L.
Enrichment of Enatiomers and other Isomers with Aqueous Liquid Membranes
Containing Cyclodextrin Carriers
Anal. Chem. 59 (1987) 2237-2241

[19]   Newcomb, M.; Toner, J.L.; Helgeson, R.C.; Cram, D.J.
Host-Guest Complexation: 20. Chiral Recognition in Transport as a
Molecular Basis for a Catalytic Resolving Machine
J. Am. Chem. Soc. 101:17 (1979) 4941-4947

[20]   Lehn, J.M.; Moradpour, A.; Behr, J.P.
Antiport Regulation of Carrier Mediated Chiroselective Transport through a Liquid Membrane
J. Am. Chem. Soc. 97:9 (1975) 2532-2534

[21]   Pirkle, W.H.; Bowen, W.E.
Preparative separation of enantiomers using hollow-fiber membrane technology
Tetrahedron: Asymmetry 5 (1992) 773-776

[22]   Prelog, V.; Stojanac, Z.; Kovacevic, K.
Über die Enantiomerentrennung durch Verteilung zwischen flüssigen Phasen
Helv. Chim. Acta 65 (1982) 377-384

[23]   Bryjak, M.; Kozlowski, J.; Wieczorek, P.; Kafarski, P.
Enantioselective transport of amino acid through supported chiral liquid membranes
J. Membrane Sci. 85 (1993) 221-228

[24]   Ding, H.B.; Carr, P.W.; Cussler, E.L.
Racemic leucine separation by hollow-fiber extraction
AIChE J. 38 (1992) 1493-1498

[25]   Higuchi, A.; Hara, M.; Horiuchi, T.; Nakagawa, T.
Optical Resolution of Amino Acids by ultrafiltration membranes containing serum albumin
J. Membrane Sci. 93 (1994) 157-164

[26]   Higuchi, A.; Ishida, Y.; Nakagawa, T.
Surface Modified Polysulfone Membranes: Separation of Mixed Proteins and
Optical Resolution of Tryptophan
Desalination 90 (1993) 127-136

[27]   Keurentjes, J.T.F.; Nabuurs, L.J.W.M.; Vegter, E.A.
Liquid membrane technology for the separation of racemic micxtures
J. Membrane Sci. 113 (1996) 351-360

[28]   Keurentjes, J.T.F.
        Process for the separating enantiomers from a racemix mixture
        Patent Application PCT / EP 93 / 02715, 1993

[29]   Shinbo, T.; Yamaguchi, T.; Yanagishita, H.; Sakaki, K.; Kitamoto, D.; Sugiura, M.
        Supported liquid membranes for enantioselective transport of amino acid mediated by
        chiral crown ether - effect of membrane solvent on transport rate and membrane stability
        J. Membrane Sci. 84 (1993) 241-248

[30]   Yamaguchi, T.; Nishimura, K.; Shinbo, T.; Sugiura, M.
        Amino Acid Transport through Supported Liquid Membranes:
        mechanism and its application to enantiomeric resolution
        Bioelectrochemistry and Bioenergetics 20 (1988) 109-123

[31]   Yamaguchi, T.; Nishimura, K.; Shinbo, T.; Sugiura, M.
        Enantiomer resolution of amino acids by a polymer-supported liquid membrane
        containing a chiral crown ether
        Chemistry Letters (1985) 1549-1552

[32]   Cohen, C.; Dishman, R.A.; Huston, J.S.; Bratzler, R.L.; Dodds, D.R.; Zepp, C.M.
        Creative Biomolecules Inc., Sepracor Inc.
        Separation by Carrier Mediated Transport
        US Patent 5,167,824 (01.12.1992)

[33]   Aoki, T.; Shinohara, K.; Oikawa, E.
        Optical resolution through the solid membrane from
        (+)-poly{1-[dimethyl(10-pinanyl)silyl]-1-propyne}
        Makromol. Chem. Rapid Commun. 13 (1992) 565-570

[34]   Maruyama, A.; Adachi, N.; Takatsuki, T.; Torii, M.; Sanui, K.; Ogata, N.
        Enantioselective Permeation of α-Amino Acid Isomers through
        Poly(amino acid)-Derived Membranes
        Macromolecules 23:10 (1990) 2748-2752

[35]   Yashima, E.; Noguchi, J.; Okamoto, Y.
        Enantiomer Separation with Cellulose Tris(3,5-dimethylphenylcarbamate) Membrane:
        Enantioselecitve Adsorption and Desorption
        Chemistry Letters (1992) 1959-1962

[36]   Yashima, E.; Noguchi, J.; Okamoto, Y.
        Enantiomer Enrichment of Oxpropenolol through Cellulose
        Tris(3,5-dimethylphenylcarbamate) Membrane
        J. Appl. Polymer Sci. 54 (1994) 1087-1091

[37]   Hartwig, A.
        Polymerisation optisch aktiver Acrylsäureester durch Elektronenstrahl und after-glow Plasmen
        Dissertation Universität Köln, 1991

[38]   Linder, C.; Nemas, M.; Perry, M.; Kataro, R.
        Aligena AG
        Enantiomer Enrichment by Membrane Processes
        UK Pat. Appl. GB 2 233 248 A (09.01.1991)

[39]   Schurig, V.
        Gaschromatographische Enantiomerentrennung an metallkomplexfreien Stationärphasen
        Angewandte Chemie Nr. 96 (1984) 733-752

[40]   Dvornic, P.R.; Lenz, R. W.
        High Temperature Siloxane Elastomers
        Hüthig und Wepf Verlag Basel, (1990)

[41]   Wulff, G.
        Hauptkettenchiralität und optische Aktivität von Polymeren aus C-C-Ketten
        Angew. Chem. 101 (1989) 22-38

[42]   Quack, M.
        Struktur und Dynamik chiraler Moleküle
        VCH Verlagsgesellschaft, Angewandte Chemie Nr. 101, (1989)

[43]   Wulff, G.; Haarer, J.
        Enzyme-analogue built polymers, 29:
        The preparation of defined chiral cavities for the racemic resolution of free sugars
        Makromol. Chem. 192 (1991 1329-1338

[44]   Hamouchi, M.; Prud'Homme, R.E.
        Synthesis and Polymerization of Racemic and Optically Active Substituted β-Propiolactones.
        V.α-Methyl-β-Propiolactone
        J. Polymer Sci. (A): Pol. Chem. 26 (1988) 1593-1607

[45]   Jedlinski, Z.; Walach, W.; Kurcok, P.; Adamus, G.
        Polymerization of L-dilactide and L,D-dilactide in the presence of potassium methoxide
        Makromol. Chem. 192 (1991) 2051-2057

[46]   Tsuji, H.; Hyon, S.-H.; Ikada, Y.
        Stereocomplex formation between enantiomeric poly(lactic acid)s.
        3. Calorimetric studies on blend films cast from dilute solution
        Macromolecules 24 (1991) 5651-5656

[47]   Chen, Y.; Lin, J.-J.
        Optically-Active Polyurethanes containing Coumarin Dimer component:
        Synthesis, Characterization, and Chiral Recognition Ability
        J. Polymer Sci. (A): Pol.Chem. 30 (1992) 2699-2707

[48]   Kobayashi, T.; Kakimoto, M.; Imai, Y.
        Chromatographic resolution of enantiomers by HPLC chiral stationary phase
        composed of optically acitve polyurethanes
        Polymer Journal 26:6 (1994) 763-765

[49]   Lipatova, T.E.; Pkhakadze, G.A.; Snegirev, A.I.; Vorona, V.V.; Shilov, V.V.
        Supermolecular organization of some polyurethanes containing sugar derivatives in the main chain
        J. Biomedical Material Research 18 (1984) 129-136

[50]   Sreenivasan, K.
        Sorption studies in a polyurethane-b-cyclodextrin blend
        Polymer International 34, 221-223 [1994]

[51]   Wenying, X.; Wang, Y.; Sheng, S.; Li, Y.; Xia, S.; Zhang, Y.
        Studies on the polymerization of β-cyclodextrin with epichlorohydrin
        Chinese J. Polymer Sci. 7:1 (1989) 16-22

[52]   Lindner, W.
        Indirect Separation of Enantiomers by Liquid Chromatography
        Chromatographic Chiral Separations, Chapt. 4, 91-130, Marcel Dekker, 1988

Summary

Nowadays, the technical application of synthetic membranes is limited to separation problems, where the membrane simply acts as a high grade filter material. However, mass transfer in biological systems demonstrates that a membrane effectively is able to separate also on a molecular scale. In living cells, this is accomplished through self assembling systems of lipids and proteins. Specific permeation of substrates and bioproducts is done by functional biological membranes. Some aspects of non-specific transport through lipid membranes and of specific transport through selective channels might be useful in the design of special property membranes for technical separations on the molecular scale. Separations on a molecular scale typically are limited due to low selectivities of polymer membranes.

In this work, the fundamental elements for the design of natural membranes are applied to the development of different special property membranes. The work presented in this thesis deals with two separation problems:

(1)   separation of liquid mixtures

The separation of a cyanohydrine, 2-hydroxypentanenitrile, from a solution of an aldehyde, butanal, in diisopropylether using a tailored-made cation-exchange membrane is described. In contrast to this, the separation of an aldehyde, 3-phenoxybenzaldehyde, from a solution of a cyanohydrine, 2-hydroxy-2-(3-phenoxyphenyl)acetonitrile, using a tailored-made anion exchange membrane is reported in chapter 5 and 6 of this work.

(2)   separation of optical isomers

The resolution of a racemate consisting of (R)- and (S)-2-hydroxypentanenitrile through chiral membranes is shown in chapter 7 of this work.

The goal of the thesis is to develop a method for continuous production of homochiral cyanohydrins. For the synthesis of cyanohydrins, the enzyme-catalyzed addition of hydrocyanic acid to aldehydes in organic media is used. Within the work, two different enzymes, the (R)- and (S)-oxynitrilase were used for the production of a low-volatile cyanohydrin, the (R)-2-hydroxypentane-nitrile, and a non-volatile cyanohydrine, the (S)-2-hydroxy-2-(3-phenoxy-phenyl) acetonitril. The (R)-cyanohydrine is an important intermediate for the chiral pool. The (S)-cyanohydrine is the precursor for deltamethrin an industrial important pyrethroid insecticide.

In the chapter 1 and 2, the state-of-the-art in the production of homochiral compounds is summarized. It is concluded, that stereoselective enzymatic synthesis will be in almost all

cases the most important technology. Oxynitrilase-catalyzed reactions in organic media are prefered among others. In chapter 3, the kinetics of the enzymatic bi substrate reaction is derived for both a random and an ordered bi-uni mechanism. Chapter 4 describes the kinetics of the reactions. Investigations on the enzyme-stability, on immobilization procedures and on the influence of the water content are reported. Furthermore, the experimental analysis of of enzyme kinetics is compared with data obtained from a parameter identification. The experimental data satisfies with an ordered bi-uni mechanism.

In chapter 5, the development of a tailored-made functional membrane for the selective removal of cyanohydrins is described. The best results concerning the separation of cyanohydrins are observed with cation-exchange membranes. Solvent stable membranes were produced from a crosslinked membrane out of a sulfonated poly(styrene-co-isoprene) elastomer. For different counter ions of the membrane, different selectivities and permeation rates were found. This effect can be attributed to a preferential sorption of the cyanohydrin as described by using solubility parameters. For the selective removal of aldehydes, an anion exchange membrane is developed. These membranes, prepared from brominated polyphenylenoxide exhibit good selctivities for the cyanohydrine in case of sulfate counter ion. However, the selectivity reverses towards the aldehyde by an exchange of the counter ion with the hydrogensulfite. Facilitated diffusion of the aldehyde via reversible formation of bisulfite complexes might occur in this case.

In chapter 6, a methodology for the continuous production of the low-volatile (R)-2-hydroxypentane-nitrile using a stirred tank reactor is described. Pervaporation is used for the removal of the cyanohydrine. With respect to the low vapor pressure of the product, temperature, downstream pressure, and co-permeation of water are used to decrease the downstream partial pressure of the cyanohydrin and thus keeping the driving force stable for continuous separation. In a long-term experiment of about 500 hours, an excellent space-time-yield and an sufficiently high enatiomeric excess was achieved. The non-volatile (S)-2-hydroxy-2-(3-phenoxy-phenyl) acetonitril is continuously produced from a tubular reactor with laminar flow. The final product was further purified by pertraction. Using a tailored-made anion-exchange membrane with hydrogensulfite counter ions, the unreacted aldehyde is separated. A good space-time-yield was found for the synthesis in organic media using the tubular reactor hybrid process with pertraction.

In chapter 7 various chiral membranes have been prepared allowing the separation of racemic mixtures. Newly synthesized polyurethane-cyclodextrine copolymer membranes show promissingly high selectivities. The effect cyclodextrin modification is studied and a modification by using Mosher's reagents yields the best enantiomeric excess.

List of Publications

Effenberger, F.; Ziegler, T.; Schönwälder, K.-H.; Kesmarszky, T.; Bauer, B.
Acylierung von (Trimethylsilyl)enolethern mit Malonyldichlorid
Chemische Berichte 119, 3394-3404 [1986]

Bauer, B.; Gerner, F.J.; Strathmann, H.
Development of Bipolar Membranes
Desalination 68, 279-292 [1988]

Chmiel, H.; Howaldt, M.; Bauer, B.; Gudernatsch, W.
Membrantrennprozesse in der Biotechnologie
BioEngineering 3, 28-42 [1988]

Strathmann, H.; Bauer, B.; Kerres, J.
Polymer Membranes with Selective Gas and Vapor Permeation Properties
Makromol. Chem., Macromol. Symp. 33, 161-178 [1990]

Bauer, B.; Effenberger, F.; Strathmann, H.
Anion-Exchange Membranes with Improved Alkaline Stability
Desalination, 79, 125-144 [1990]

Bauer, B.; Chmiel, H.; Menzel, Th.; Strathmann, H.
Separation of Bioreactor Constituents by Electrodialysis using Bipolar Membranes
in: Biochemical Engineering Stuttgart
Gustav Fischer Verlag, Stuttgart 1991, 38-45

Bauer, B.; Menzel, Th.; Wnuk, R.; Nopper, B.
Membranverfahren im Umweltschutz
Recycling 3, 39-44 [1990]

Bauer, B.
Verminderung des Energiebedarfs von thermischen Trennverfahren mittels Membranverfahren
Programmstudie Rationelle Energieverwendung in Industrie und Kleinverbrauch,
Status-Bericht des BMFT, Essen, 11.09.1991

Strathmann, H.; Rapp, H.-J.; Bauer, B.
Entwicklung von bipolaren Membranen und ihre technische Nutzung
DECHEMA Monographien Vol. 125, 83-100 [1992]

Bauer, B.; Chmiel, H.; Krumbholz, Ch.; Menzel, Th.; Schmidt, K.-H.
Abtrennung organischer Säuren mittels Elektrodialyse
BIOFORUM 6, 202-209 [1992]

Strathmann, H.; Rapp, H.-J.; Bauer, B.; Bell, C.M.
Theoretical and practical aspects of preparing bipolar membranes
Desalination 90, 303-323 [1993]

Strathmann, H.; Rapp, H.-J.; Bauer, B.
Better bipolar membranes
CHEMTECH, 17-24, June 1993

Bauer, B.; Strathmann, H.
Oxygen separation using asymmetric microencapsulated liquid membranes
Proceedings NAMS Meeting, 22.05.-25.05.1994, Breckenridge, CO, USA

Ramírez, P.; Rapp, H.-J.; Mafé, S.; Bauer, B.
Bipolar membranes under forward and reverse bias conditions. Theory vs. experiment
Journal of Electroanalytical Chemistry, 375, 101-108 [1994]

Bauer, B.
Elektrodialyse mit bipolaren Membranen - eine Verfahrenstechnik für den Gewässerschutz
Gewässerschutz·Wasser·Abwasser GWA 143, 161-192 [1994]

Bauer, B.
Effluent free preparation of process water using electrodialysis with bipolar membranes
Electrochemical Processing - A Clean Alternantive, ICI, Toulouse [1995]

Bauer, B.
Bipolare Membrantechnologie
F&S Filtrieren und Separieren 6, 28-35 [1995]

Patents

Bauer, B.; Erlmann, W.; Strathmann, H.
Method of Continuously Removing and Obtaining Ethylene Diamine Tetraacetic Acid from the Process
Water of Electroless Copper Plating
EP 0 416 312 B1 (09.08.1990)

Strathmann, H.; Bauer, B.
Verfahren zur kontinuierlichen Entfernung und Gewinnung von Chelatbildungsmitteln aus Prozeßwässern
EP 0 415 119 A1 (03.08.1990)

Bauer, B.; Schulenberg-Schell, H.; Strathmann, H.
Stoffspezifische Trägersubstanzen enthaltende Polymermembran, Verfahren zu deren Herstellung und deren
Verwendung zur Trennung von Stoffgemischen
EP 0 597 300 B1 (22.10.1993)

Bauer, B.
N.N'-2.2-3.3-Tetramethylethylen-bis-(5-NO2-salicyliden-iminato)cobalt(II) und dessen
Verwendung als Trägersubstanz für Sauerstoff
EP 0 597 276 A1 (15.10.1993)

Bauer, B.; Strathmann, H.; Effenberger, F.
Verfahren und Vorrichtung zur enzymatischen Synthese
DE 40 41 896 C1 (27.12.1990)

Willy, A.; Bauer, B.; Stroh, N.
Vorrichtung zur Ent- und Belüftung eines Treibstofftankes
DE 40 06 465 C2 (01.03.1990)

Bauer, B.
Bipolare Mehrschichtmembranen
DE 40 26 154.C2 (17.08.1990)

Bauer, B.
Verfahren zur Herstellung von flächigen Polymergebilden mit hydrophiler Oberfläche
DE 42 11 266 A1 (03.04.1992)

Bauer, B.
Bipolare Membran und Vefahren zu deren Herstellung
EP 0 563 851 A2 (29.03.1993)

Bauer, B.; Menzel, Th.; Kehl, P.
Abstandshalter (Spacer) für Dialyse-, Elektrodialyse- oder Elektrolyse-Zellen
EP 0 645 175 A1 (09.09.1994)

Bauer, B.; Menzel, Th.; Kehl, P.
Ionenselektive Membran/Spacer-Einheiten
EP 0 645 176 A1 (09.09.1994)

Bauer, B.; Menzel, Th.
Elektrochemisches Verfahren und Vorrichtung zur Herstellung von Metallhydroxiden und/oder
Metalloxidhydroxiden
PCT / DE95 / 00643 (26.05.1994)

Naumann, D.; Olbrich, A.; Schmoll, J.; Gutknecht, W.; Bauer, B.; Menzel, Th.
Verfahren zur Herstellung von Metallhydroxiden
DE 44 18 067 C2 (24.05.1994)

Bauer, B.
Elektrodialytisches Verfahren zur Herstellung wäßriger Lösungen von Hydroxylamin oder von Hydroxylamin-
Derivaten
DE 44 28 255 A1 (11.08.1994)

Bauer, B.; Rafler, G.; Ulrich, H.-H.
Sulfonierte Polyaryletherketone
DE 195 38 025 (12.10.1995)

APPENDIX

CURRICULUM VITAE

Bernd Bauer was born on September 13, 1958 at Marbach, Germany. He graduated from Kerschensteinerschule as a Chemical Technician in 1977. In the same year he entered the Fachhochschule Aalen, studied at the department of Macromolecular Chemistry and took his engineering degree (Diplom-Ingenieur FH) in 1982. The diploma thesis was carried under Prof. Dr. G. Bauer on the modification of polydieneblock-copolymers using acrylate grafted silica gel.

During this time, he worked as a research scientist at Fa. Robert Bosch GmbH in the department of analytical chemistry, in the department of surface treatment technologies and in the department of electrochemistry. He wrote a thesis on investigations into the electrolytical deposition of aluminum from non-aqueous media.

In 1982 he entered the University of Stuttgart, studied at the department of Organic Chemistry and took his degree in chemistry (Diplom-Chemiker) in 1988. The diploma thesis was carried out under Prof. Dr. F. Effenberger on the development of an alkaline stable anion-exchange membrane.

During this time, he worked with Prof. Dr.-Ing. H. Strathmann as a research scientist at the Fraunhofer-Institut für Grenzflächen- und Bioverfahrenstechnik in the department of membrane technology. He worked on the development and characterization of porous and non-porous membranes and specialized in ion-exchange membranes.

After graduation in August 1988, he was employed at the Fraunhofer-Institut as an research chemist. He was responsible for the development of membranes and processes in the fields of electrodialysis, gas separation and pervaporation. Furthermore, he worked with Prof. Effenberger and Prof. Strathmann on the preparation of homochiral compounds and specialised in biochemical engineering within the framework of the Zentrales Schwerpunktprojekt Bioverfahrenstechnik. The research finished at the University of Twente with a Doctor's degree on October 24, 1996.

In January 1994 he left the Fraunhofer-Institut in Stuttgart and founded the Gesellschaft für funktionelle Membranen und Anlagentechnologie mbH, FuMA-Tech GmbH, in St. Ingbert (Germany) where he occupies the position of managing director.